Appendix A: Engineering
Valley Creek Flood Risk Management Study

Fiscal Years: 2018-2021

U.S. Army Corps of Engineers
Kansas City and Mobile Districts
Engineering Division

Valley Creek Basin
Jefferson County, Alabama

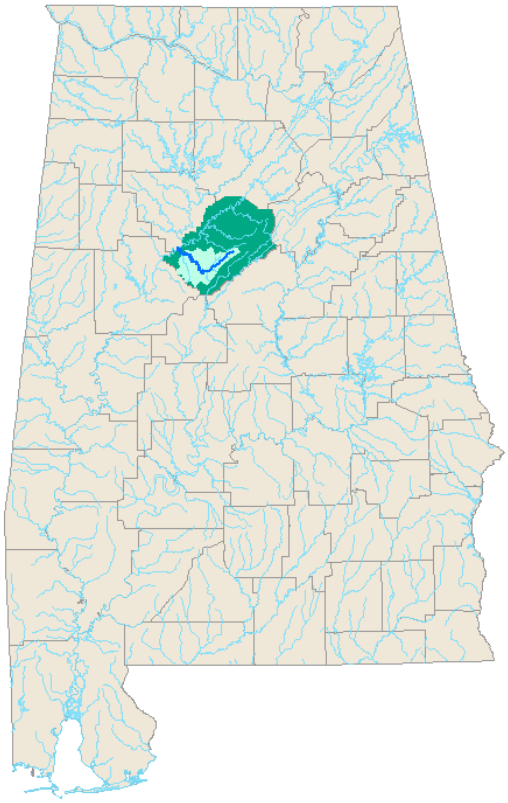

Table of Contents

List of Figures iv
List of Tables viii
Executive Summary x
1.0 Introduction 1
1.1 Location 1
1.2 Basin Characteristics 2
1.2.1 Hydrologic Characteristics 2
1.2.2 Hydraulic Characteristics 2
1.2.3 Geotechnical Characteristics 5
1.3 Flooding History 6
1.4 Data Collection 9
1.4.1 Hydrologic Data 9
1.4.2 Topographic Data 11
1.4.3 Structural Data 13
2.0 Existing Conditions Models 14
2.1 Hydrology 14
2.1.1 Hydrologic Model Background 14
2.1.2 Model Overview 14
2.1.3 Calibration and Validation 19
2.1.4 Calibration/Validation Results and Discussion 23
2.1.5 Design Rainfall 24
2.1.6 Frequency Simulation Results 26
2.2 Hydraulics 29
2.2.1 Hydraulic Model Background 29
2.2.2 Model Overview 30
2.2.3 Hydrologic Record Linkage with HEC-DSS 31
2.2.4 Calibration 33
2.2.5 Calibration Results and Discussion 37
2.2.6 Validation 37
2.2.7 Frequency Simulation Results 40
3.0 H&H Future Without Project Conditions 42

3.1 Development 42
3.1.1 Background 42
3.1.2 Storm Water Management Plan implementation 42
3.1.3 Integrated Climate and Land-Use Scenarios 42
3.2 Frequency Simulation Results 45
3.2.1 Hydrology 45
3.2.2 Hydraulics 46
4.0 Flood Risk Management Alternatives 48
4.1 Measure Development 48
4.1.1 Preliminary Screening 54
4.1.1.1 Modeling Approach 55
4.1.1.2 Results 57
4.1.1.3 Geotechnical Refinement 64
4.1.2 Refined Measures 66
4.1.2.2 Design Detail 67
4.2 Structural Alternatives 71
4.2.1 Overbank Detention Plan Formulation 71
4.2.1.1 Site Performance Assessment 71
4.2.1.2 Site Ranking 75
4.2.2 Preliminary Alternatives 75
4.2.3 Revised Overbank Detention Plan Formulation 76
4.2.4 Final Alternatives 82
4.3 Recommended Plan Details 85
4.3.1 Structural Classification 90
4.3.2 Operations and Maintenance 90
4.3.3 Phase I Geotechnical Investigation (March 2021) 91
4.3.3.1 Core Drill Investigation 91
4.3.1.2 Geophysical Investigation 96
5.0 Plan Performance 98
5.1 Plan Benefits 98
5.2 Risk Assessment 107
5.2.1 FRM Uncertainty 107
5.2.2 Recommended Plan Model Refinement 108

5.2.2.1 Model Refinement Results....111
5.2.3 Risk-Informed Planning and Design....114
5.2.4 Hazard Analysis....115
5.2.4.1 LifeSim Model Background....116
5.2.4.2 Hazard Analysis Results....117
5.2.4.3 Hazard Analysis Discussion and Conclusions....122
5.2.5 Stage Uncertainty....122
5.2.6 Cost Uncertainty....127
5.2.7 Bessemer Gardens Levee....128
6.0 Climate Change Assessment for Valley Creek....129
6.1 Introduction....129
6.2 Literature Review....129
6.2.1 Temperature....129
6.2.2 Precipitation....132
6.2.3 Hydrology....135
6.2.4. Summary....136
6.3 Nonstationarity Assessment....137
6.4 Vulnerability Assessment....145
6.5 Climate change and Impacts on Recommended Plan....149
6.6 Conclusions....151
7.0 Summary....152
References....153

List of Figures

Figure 1-1: Study location map. 3
Figure 1-2: Existing projects on Valley and Opossum Creeks. 4
Figure 1-3: Valley Creek channel in the vicinity of the Delonah Quarry. 5
Figure 1-4: Isohyetal analysis of storm rainfall, April 11-14, 1979 (from Edelen et al., 1979). 6
Figure 1-5: Precipitation gages in and near Upper Valley Creek Basin 7
Figure 1-6: Discharge at gaging stations on Valley Creek in the Black Warrior River basin in Alabama, April 2-21, 1979 (from Edelen et al., 1979). 8
Figure 1-7: Four day rainfall totals for Alabama (September 3-7, 2011; from NWS Birmingham Southeastern Forecast Office). 9
Figure 1-8: Current and historical surface water gages in Upper Valley Creek Basin. 10
Figure 1-9: Upper Valley Creek Basin DEM. 11
Figure 1-10: Channel survey extents in Valley Creek. 13

Figure 2-1: HMS subbasins.....14
Figure 2-2: Soils map of study area. 15
Figure 2-3: Dec 2015 calibration at Bessemer gage. 21
Figure 2-4: April 2017 calibration at Bessemer gage.....21
Figure 2-5: December 2018 calibration at Bessemer gage. 22
Figure 2-6: April 2014 validation at Bessemer gage.....22
Figure 2-7: September 2011 validation at Bessemer gage. 23
Figure 2-8: Rainfall distribution used for design storms compared to Type II distribution.....25
Figure 2-9: Peak flow comparisons at Princeton Parkway (near upstream model extent; USGS 02461130 location).....26
Figure 2-10: Peak flow comparisons at U.S. Route 11 (near middle of model extents).....27
Figure 2-11: Peak flow comparisons at 19th Street North (near downstream extent of measures/impacts; USGS 02461500 location). Note: LPIII = Log-Pearson Type III and is equal to weighted regression at this location.....27
Figure 2-12: Log-Pearson Type III frequency analysis results at USGS 02461500 (Valley Creek near Bessemer, AL). 28
Figure 2-13: Correlation between USGS 02461500 (y) and USGS 02462000 (x) based on 16 annual peak flow observations. 29
Figure 2-14: December 2018 calibration at USGS 02461130. 33
Figure 2-15: December 2018 calibration at USGS 02461192. 33
Figure 2-16: December 2018 calibration at USGS 02461405. 34
Figure 2-17: December 2018 calibration at USGS 02461500. 34
Figure 2-18: April 2017 calibration at USGS 02461130.....35
Figure 2-19: April 2017 calibration at USGS 02461192 (note missing flow records). 35
Figure 2-20: April 2017 calibration at USGS 02461500.....36
Figure 2-21: December 2015 calibration at USGS 02461500. 36
Figure 2-22: April 2014 validation at USGS 02461500.....38
Figure 2-23: September 2011 validation at USGS 02461500. 38
Figure 2-24: December 1983 validation at USGS 02461500 (observed stage unavailable).....39
Figure 2-25: April 1979 validation at USGS 02461500 (observed stage unavailable). 39
Figure 2-26: Profile plot of EC frequency events in the upper 1D hydraulic reach of Valley Creek (river stations and some bridges shown). 41
Figure 3-1: Total impervious area values (%) for existing and future without project conditions. 44
Figure 3-2: Profile plot of FWOP frequency events in the upper 1D hydraulic reach of Valley Creek (river stations and some bridges shown). 47
Figure 4-1: Preliminary structural FRM measure locations in the vicinity of Valley Creek headwaters, downtown Birmingham, and Fairview. 50
Figure 4-2: Preliminary structural FRM measure locations in the vicinity of Midfield. 51
Figure 4-3: Preliminary structural FRM measure locations in the vicinity of Brighton. 52
Figure 4-4: Preliminary structural FRM measure locations in the vicinity of Bessemer, Halls Creek, and Halls Tributary. Note: Two structural measures added during preliminary screening not shown on this map (VB9 [18th Ave. over Valley Creek] and UB2 [9th Ave. N over Halls Tributary]).....53
Figure 4-5: Lateral structure at VD1.....55
Figure 4-6: Preliminary storage model at VD1.....55
Figure 4-7: Example of lateral structure representation of levee at VL2. 56
Figure 4-8: Example cross section showing 120-foot bottom width channel modification terrain template and existing terrain at a location near the mid-point of the Delonah Quarry. 57
Figure 4-9: Stage hydrographs at RS 2151+54 for 0.04 AEP event with and without VD13. Vicinity of cross section to site location shown (scale = 1:6,500).....58

Figure 4-10: Profile plot of baseline (FWOP) and VD1 simulations with 0.04 AEP and 0.01 AEP events in the upper 1D hydraulic reach of Valley Creek (river stations and some bridges shown). 59
Figure 4-11: Profile plot of baseline (FWOP) 0.04 AEP event and example combinations of VD3/VD4 and VD2/VD5 in the upper 1D hydraulic reach of Valley Creek (river stations and some bridges shown). 60
Figure 4-12: Profile plot baseline (FWOP), VI1, and VI2 simulations with 0.01 AEP event in the upper 1D hydraulic reach of Valley Creek. 61
Figure 4-13: Stage and flow hydrographs over lateral structure representing RR embankment location proposed for OI1. Total flow over the lateral structure is negative due to flow direction from Opossum Creek, into Valley Creek cross sections (see Section 2.2.2 for a description of modeling approach). Note: Plan OI1 incorrectly named VI3 in the figure legend. 62
Figure 4-14: 0.002 AEP depth grid (shown in red) with VL4 in place. Structure parcel polygons from economic inventory shown in purple. Schematic notes: Scale is 1:9500; north direction is up. 62
Figure 4-15: Overview of historical borings and 2019 auger testing locations. 65
Figure 4-16: Profile plot of baseline (FWOP) and UB1/UB2 simulation during the 0.01 AEP event on Halls Tributary. 67
Figure 4-17: Net volume reduction from overbank detention sites versus design volume ratio. 71
Figure 4-18: Histogram of water surface elevation (WSE) reductions resulting from VD1. 72
Figure 4-19: Volume-benefit analysis for parcel WSE reductions between 0 and 1.00 feet. 73
Figure 4-20: Volume-benefit analysis for parcel WSE reductions between 1.0 and 3.50 feet. 73
Figure 4-21: Volume-benefit analysis for parcels removed from the 0.04 AEP floodplain. 74
Figure 4-22: Excavation and utility removal required for implementation of overbank detention sites. 74
Figure 4-23: Final overbank detention site ranks for analyzed criteria 75
Figure 4-24: Cost-benefit analysis for WSE reductions between 0 – 1.0 feet 77
Figure 4-25: Cost-benefit analysis for WSE reduction between 1.0 - 3.5 feet 77
Figure 4-26: Cost-benefit analysis for structures removed from the 0.04 AEP floodplain 78
Figure 4-27: Cost-benefit analysis for value removed from the 0.04 AEP floodplain 78
Figure 4-28: Alternatives cost-benefit analysis for value removed from the 0.04 AEP floodplain 80
Figure 4-29: Alternatives cost-benefit analysis for WSE reductions between 0 – 1.00 feet 81
Figure 4-30: Alternatives cost-benefit analysis for WSE reductions between 1.00 – 3.50 feet 81
Figure 4-31: Alternatives correlation analysis for structures and associated value removed from the 0.04 AEP floodplain 82
Figure 4-32: Conceptual plan of overbank detention basin and levee VD1. 86
Figure 4-33: Conceptual profile and section detail of basin and lateral inflow weir through levee at VD1, respectively. 87
Figure 4-34: Conceptual plan of overbank detention basin and levee VD2. 88
Figure 4-35: Conceptual profile and section detail of basin and lateral inflow weir through levee at VD2, respectively. 89
Figure 4-36: Confined and unconfined groundwater conditions. 95
Figure 4-37: Drainage swale located between boring locations VD2-1-21 and VD2-10-21. 95
Figure 5-1: D19 benefits (0.50 AEP event) in the upper extent of Valley Creek. 100
Figure 5-2: D19 benefits (0.50 AEP event) within the middle extent of Valley Creek. 101
Figure 5-3: D19 benefits (0.50 AEP event) in the lower extent of the Valley Creek study reach. 102
Figure 5-4: D19 benefits (0.04 AEP event) in the upper extent of Valley Creek. 103
Figure 5-5: D19 benefits (0.04 AEP event) within the middle extent of the Valley Creek study reach. 104
Figure 5-6: D19 benefits (0.04 AEP event) in the lower extent of the Valley Creek study reach. 105
Figure 5-7: Box plots of recommended plan WSE reductions from FWOP conditions by AEP. 106
Figure 5-8: Histograms of D19 performance by AEP. Note: frequency shows number of structures in bin (WSE reduction). 107

Figure 5-9: RAS schematic showing original modeling approach at VD1 and VD2. Structures (only) from the structure inventory are shown in white. The purple areas represent locations where profile elevations were transposed, but no actual inundation would be depicted in these areas (see Figures 5-6). Schematic notes: north is oriented up and scale is 1:8,000. 108
Figure 5-10: Original modeling approach water surface profiles (0.10, 0.04, and 0.01 AEPs shown) in the vicinity of VD1 and VD2 with cross section station names shown. Areas of increases in water surface profiles associated with the recommended plan are circled in green. 109
Figure 5-11: RAS schematic showing updated modeling approach in the vicinity of VD1 and VD2. Note that the 2D areas model both the ponds and their backflow areas. The pond berms are physically represented in the terrain. The same inflow weirs are utilized in the updated configuration; however, additional connections are used to properly transfer the left overbank flows from cross sections to the backflow areas, and vice-versa. The set-up of VD4 is similar. Schematic notes: north is oriented up and scale is 1:8,000. 110
Figure 5-12: Updated modeling approach water surface profiles (0.10, 0.04, and 0.01 AEPs shown) in the vicinity of VD1 and VD2 with cross section station names shown. Areas of increases in water surface profiles associated with the recommended plan are circled in green. Note decreased severity associated with updated profiles. The additional grey structures shown represent overbank connections required to properly transfer the left overbank flows from cross sections to the backflow areas, and vice-versa. 110
Figure 5-13: Inundation extents of original and updated D19 models as well as FWOP conditions (original, 1D-based) for the 0.04 AEP event in the vicinity of VD1 and VD2 (in Birmingham extents). Structures in the inventory as well as structures that observe an increase in WSE above their first-floor elevation with implementation of D19 are shown. 112
Figure 5-14: Inundation extents of original and updated D19 models as well as FWOP conditions (original, 1D-based) for the 0.01 AEP event in the vicinity of VD1 and VD2 (in Birmingham extents). Structures in the inventory as well as structures that observe an increase in WSE above their first-floor elevation with implementation of D19 are shown. 113
Figure 5-15: Life Safety Risk Matrix (from USACE, 2019b) 115
Figure 5-16: Total Life Risk Matrices for Minimal Warning Scenario 118
Figure 5-17: Representative 0.002 AEP LifeSim Results for D19 (left) and FWOP conditions (right). 119
Figure 5-18: Stage and flow hydrographs for 0.002 AEP at 2151+54 showing significant stage reduction for with-project condition and lack of timing differential throughout simulation. 120
Figure 5-19: Representative 0.002 AEP LifeSim Results for D19 non-breach (left) and D19 breach (right). 120
Figure 5-20: Stage and flow hydrographs for 0.002 AEP event (blue and green, respectively) and 0.02 AEP event (red and pink, respectively) at first cross section downstream of VD2 (2759+94; at 12th St. SW). Results show no change in hydraulics between non-breach, VD1 breach, VD2 breach, or combined breach simulations. 121
Figure 5-21: Stage and flow hydrographs for 0.02 AEP at 2151+54 showing no change between breach/non-breach simulations at loss location. 121
Figure 5-22: Schematic from RASMapper with plot of upstream berm hydrographs at VD1 (all analyzed AEPs shown). Profile line from which hydrographs were produced is shown in pink. Note all flow is positive; overbank flows overtop the upstream berm profile line and enter the detention basin. No outward overtopping risk associated with the analyzed berm exists. Map notes: flow is east-to-west, north is up, and scale is approximately 1:1,250. 125
Figure 5-23: Schematic from RASMapper with plot of back-berm hydrographs at VD1 (all analyzed AEPs shown). Profile line from which hydrographs were produced is shown in pink. Note flow is both positive and negative; overbank flows overtop the upstream extent of the back-berm profile line and enter the detention basin, and flows leave the basin and inundate the backflow area. Outward overtopping risk

associated with the analyzed berm exists. Greatest AEP that produces overtopping risk determined as 0.04 for this site. Map notes: flow is east-to-west, north is up, and scale is approximately 1:1,250. 126
Figure 5-24: Rating curves with hysteresis for the 0.50 AEP event at River Station 2824+43 on Valley Creek (at measure VD1). 127
Figure 5-25: Stage and flow hydrographs for 0.50, 0.02, and 0.005 AEP events at RS 2203+66 (middle extent of Bessemer Gardens Levee, approximately). 128
Figure 6-1: Annual average temperature and p-value from 1930 - 2018 130
Figure 6-2: Annual average temperature and p-value from 1970 - 2018 131
Figure 6-3: Projected changes in seasonal maximum air temperature, ºC, 2041 – 2070 vs. 1971 – 2000. The South Atlantic-Gulf Region is within the red oval (Liu et al., 2013; reprinted from USACE, 2015b). 131
Figure 6-4: Annual total precipitation and p-value from 1970 – 2018 132
Figure 6-5: Annual total precipitation and p-value from 1990 – 2018 133
Figure 6-6. (Left) change in annual number of days with precipitation greater than 3 inches in the southeast averaged over the recording locations (right) (reprinted from USGCRP, 2017). 134
Figure 6-7: Projected changes in seasonal precipitation, 2055 vs. 1985, mm. The South Atlantic-Gulf Region is within the yellow oval (Liu et al., 2013; reprinted from USACE, 2015b). 134
Figure 6-8: Summary matrix of observed and projected climate trends and literary consensus (reprinted from USACE, 2015b). 136
Figure 6-9: Study area and location of the Oak Grove gage used in this analysis 137
Figure 6-10: APF at USGS 02462000 Valley Creek Near Oak Grove, AL. 137
Figure 6-11: Results of the nonstationarity assessment for USGS 02462000 Valley Creek Near Oak Grove, AL. 139
Figure 6-12: Monotonic trend analysis for the POR before the nonstationarity. 140
Figure 6-13: Monotonic trend analysis for the POR after the nonstationarity. 140
Figure 6-14: CHAT output for USGS 02462000 Valley Creek Near Oak Grove, AL. 141
Figure 6-15: Peak 24-hour annual precipitation at the Birmingham Airport gage. 143
Figure 6-16: Peak 48-hour annual precipitation at the Birmingham Airport gage. 143
Figure 6-17: Mean projected annual maximum monthly streamflow for the Mobile-Tombigbee HUC-4. . 144
Figure 6-18: Projected hydrology for the Mobile-Tombigbee HUC-4 base on the output from 93 projections of climate changed hydrology. 145
Figure 6-19: Comparison of national vulnerability scores for CONUS HUC-4s. 147
Figure 6-20: Comparison of national vulnerability scores for South Atlantic Division HUC-4s. 147
Figure 6-21: Dominate indicators for the Flood Risk Reduction Business Line for the Dry Scenario. 148
Figure 6-22: Dominate indicators for the Flood Risk Reduction Business Line for the Wet Scenario. 149

List of Tables

Table 1-1: Summary of stream gages in the Upper Valley Creek Basin 9
Table 1-2: LiDAR Specification Summary 12
Table 2-1: Final initial loss rates for subbasins 16
Table 2-2: Final constant loss rates for subbasins 16
Table 2-3: Final transform parameters for sub-basins 17
Table 2-4: Recession baseflow parameters 18
Table 2-5: Rainfall events utilized for calibration and validation 19
Table 2-6: Summarized results of HMS calibration and validation simulations 24
Table 2-7: NOAA Atlas 14 Design Rainfall Depths with and without ARF 25
Table 2-8: HEC-DSS record linkage detail 31

Table 3-1: Differences in peak flow rates (cfs) from EC to FWOP conditions by recurrence interval at all HMS junctions 45
Table 4-1: Valley Creek FRM Study Measures 48
Table 4-2: Refined Measure Array 66
Table 4-3: Detention pond details 68
Table 4-4: Berm design summary for detention sites 68
Table 4-5: Outlet works design summary for detention sites 68
Table 4-6: Supplementary culvert data for detention sites 68
Table 4-7: Levee quantities data 69
Table 4-8: Supplementary culvert data for levees 69
Table 4-9: Bridge geometry detail 70
Table 4-10: Preliminary Structural FRM Alternatives 76
Table 4-11: Detention site performance detail 79
Table 4-12: Costs and economic performance for all HEC-FDA-modeled structural study alternatives and measures[1, 2] 82
Table 4-13: Final FRM alternatives considered for plan selection[1, 2] 84
Table 4-14: Detention basin storage details 90
Table 4-15: Summary of Boring Location Data 92
Table 5-1: Recommended Plan Structural Benefits[1] 107
Table 5-2: Breach Scenarios, Loading Parameters, and Geometric Breach Data 115
Table 5-3: Breach Erosion Rates[1] 116
Table 5-4: Stage uncertainty at critical locations[1] 124
Table 5-5: Measure performance described by AEP and LTEP 127
Table 6-1: Indicator Variables used to derive the flood risk management Vulnerability score for the Mobile-Tombigbee Basin as determined by the Vulnerability Assessment tool. 146
Table 6-2: Climate change risks and likelihood for the recommended plan measures 150

Executive Summary

A flood risk management (FRM) study for Valley Creek, a tributary to the Black Warrior River located in Jefferson County, AL, was completed to address flood risk for this system (full execution from 2018-2021) and resulted in the selection of a recommended plan for implementation following the Agency Decision Milestone (ADM) in November of 2020. Federal interest in this watershed (Valley Creek Basin) was driven by frequent, recurring flooding that induces economic and life safety risks to a densely developed corridor of the main-stem study stream as well as additional tributaries analyzed in this study. This Engineering Appendix details the engineering analysis required to support the study. Work included the development of existing conditions (EC) and future without project conditions (FWOP) hydrologic and hydraulic models as well as models to support the analysis of structural FRM measures (including levees, dams, detention basins, bridge modifications, and a channel modification). This report also documents the analysis that supported development and refinement of the array of structural measures presented to address flood risk in the study basin, and the methodology for formulation of final structural alternatives. In total, 13 final alternatives were considered for recommendation (see Table 4-13 for all final alternatives considered for plan selection), with full economic modeling and analysis completed on a total of 16 alternatives and 4 individual measures. The national economic development (NED) plan was identified to be Alternative 4 and was selected as the recommended plan (also known as D19; reference Table 4-13). This plan consists of two overbank detention basins located in Birmingham, AL at River Stations (RS; distance above Black Warrior River confluence) 2823+71 and 2783+48 on Valley Creek. The measures that make up the recommended plan, known as VD1 and VD2 were selected in combination from an overall suite of 34 structural measures, including 13 overbank detention sites. This plan was recommended on its ability to maximize NED and produce strong, uniformly distributed benefits throughout the developed length of the Valley Creek study reach. Benefits and risks associated with the performance of the selected plan were assessed, with results included in this report. Additionally, this report includes an assessment of the effects of climate change to both the study area (and its effect on modeling assumptions and uncertainties) and the performance of the recommended plan.

1.0 Introduction

This purpose of this report is to serve as documentation of the engineering analysis required to support the Valley Creek Flood Risk Management (FRM) feasibility study initiated in FY18 and executed by the U.S. Army Corps of Engineers, Kansas City and Mobile Districts. This Engineering Appendix is in accordance with ER 1110-2-115 (USACE, 1999). Federal interest in this study was driven by the recurring risk of economic damages as well as life safety risks associated with fluvial flooding along the main system of interest (Valley Creek) and analyzed tributaries. This study analyzed flood risk in the basin of interest and assessed solutions to address associated damages. Ultimately, a final plan for reducing flood risk in the study area was recommended by this study. This report details the development of existing conditions (EC) and future without project (FWOP) engineering models as well as the development, analysis, refinement, and design of structural study measures and alternative plans. Final plan performance with respect to tolerable risk guidelines (ECB 2019-15; USACE, 2019a) and underlying hydrologic uncertainty is provided as mandated by ER 1105-2-101 (USACE, 2019b), in addition to a climate change assessment of the study area and potential effects of such change on the recommended plan as mandated by ECB 2018-14 (USACE, 2018). With respect to models, spatial data, study area geography, and measure features, the vertical datum of reference is the North American Vertical Datum of 1988 (NAVD88). The horizontal datum of reference is the North American Datum of 1983, and the applicable projection is Alabama State Plane West (FIPS Zone 0102). Lastly, the frequencies of modeled flood events are described in terms of their associated annual exceedance probability (e.g., 0.5 AEP), though some figures display reference to annual chance exceedance (e.g., 1/2 ACE).

1.1 Location

This study covered an approximate 20-mile length of Valley Creek, a tributary to the Black Warrior River (River Mile 170.23) located in Jefferson County, Alabama, and within the larger Mobile-Tombigbee Basin (hydrologic unit code [HUC] 4 basin 0316). Additionally, this study covered tributaries to Valley Creek, including approximately 1 mile of Opossum Creek, 2 miles of Halls Creek, and 1.5 miles of a tributary draining to Halls Creek. Jefferson County is located in north-central Alabama and is bordered on the north by Blount and Walker Counties, on the east by Saint Clair and Shelby Counties, on the south by Bibb County, and on the west by Tuscaloosa County (Figure 1-1). Valley Creek has an overall length of about 55 miles, originating from headwater springs, but immediately passing through an underground storm drainage system before discharging to an open channel in central Birmingham near 5th Avenue and 7th Streets. From this location, Valley Creek flows southwesterly for approximately 22 miles through the cities of Birmingham, Fairfield, Midfield, Lipscomb, Brighton, Hueytown, and Bessemer. At this point, the stream turns to flow northwesterly for approximately 33 miles, before discharging into the Black Warrior River. The Valley Creek Basin drains approximately 255 square miles within the HUC-8 subbasin 03160112; the drainage area of the study-area is about 87 square miles. The basin divide crosses the channel at approximately 31 miles upstream from the mouth, bisecting the watershed into upper and lower portions. The length of

Valley Creek applicable to this study is located entirely within the upper basin, which has an average fall of 8.4 feet per mile, and a total drainage area of 96 square miles.

1.2 Basin Characteristics

1.2.1 Hydrologic Characteristics

Valley Creek portrays the distinctive characteristics of a highly developed, urban watershed. Land-cover within the basin varies but is dominated by urban use-types including industrial, commercial, and low- and high-intensity residential. High-density development produces hydrographs which are flashy in nature, whereby lag times between rainfall and runoff are short. Rising hydrograph limbs are steep, and typically, for characteristic events, falling limbs are as well. It is probable that the peak flood magnitudes observed on Valley Creek are intensified by the amount of impervious cover, floodplain grading, and artificial drainage present within the basin (CWP, 2004). Some storage can be expected during flood events, however, and is provided by unintended damming surfaces (bridges and culverts), low-lying overbank areas, and tributary floodplains and channels. This storage is ultimately ineffective at protecting the most vulnerable development (defined as that which is affected by a flood event of a given frequency) along Valley Creek.

1.2.2 Hydraulic Characteristics

The stream channel of Valley Creek varies in its conveyance capability between reaches characterized by sedimentation and vegetation growth and engineered portions that are relatively clean. Rock outcroppings (limestone) are visible throughout the majority of the study reach, and some debris has been observed at bridge crossings. Stream bank side-slopes average 1:1 (H:V) and vary in cover from dense vegetation (including small-to-mature trees) to rip-rap. Manning's n-values within the calibrated hydraulic model range from 0.038 - 0.046 for the stream channel. Overbank land-use/land-cover types range from low-to-high density urban types, to forest and pasture. Overbank Manning's n-values range from 0.022 – 0.11. Several significant tributaries draining to Valley Creek are located within the study extents. These include Nabors Branch, Opossum Creek, Halls Creek, and Fivemile Creek. The stream channel of Valley Creek was widened as part of a local effort in 1985 (USACE, 1986) in a location extending from the 19th St. N. Bridge at RS 2188+59, to a location just below the Murphys Lane Bridge (RS 2410+07; Figure 1-2). The stream bottom width in this location is approximately 120 feet; bottom widths within the total study area range from about 60 feet to 120 feet. As shown in Figure 1-2, the stream narrows drastically below this location, but widens back out to approximately 100 feet just downstream of a service bridge linking structures with the Valley Creek Water Reclamation Facility (wastewater treatment plant [WWTP] within 2D extents of hydraulic model). This portion of the channel was inspected during field work on February 26, 2019 and found to be concrete-lined (Figure 1-3). The extents of lining were estimated based on aerial imagery in Figure 1-2. Training of the channel predates 1959 and was motivated by operations in the adjacent Delonah Quarry (USACE, 1986), though more specific information regarding this effort has not been obtained.

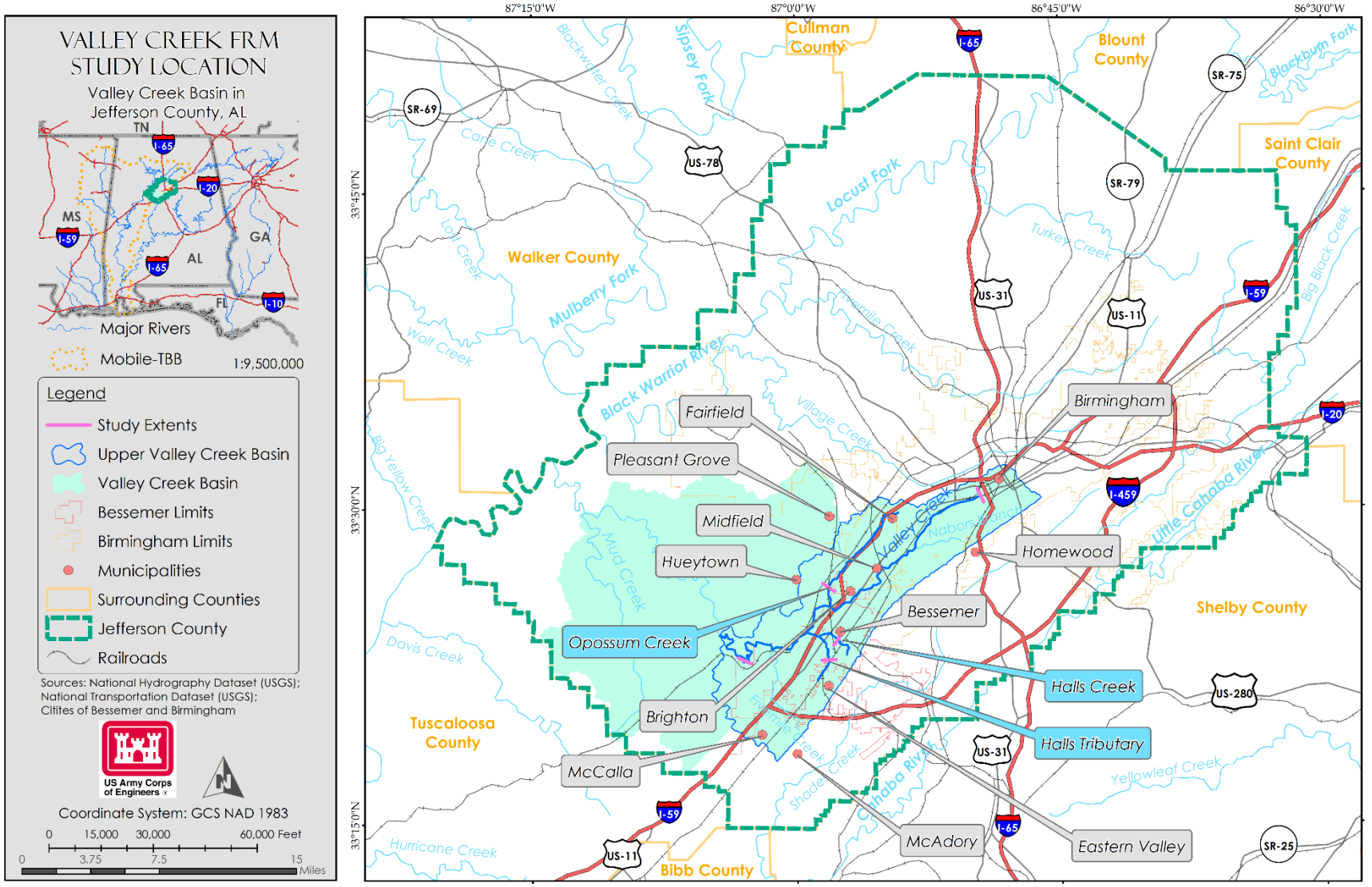

Figure 1-1: *Study location map.*

Figure 1-2: *Existing projects on Valley and Opossum Creeks.*

Conveyance within Opossum Creek was improved in an environmental remediation project to remove tar-like material and completed in April of 2018 (F. Freeman, personal communication, 6 November 2018). Large-scale excavation of tar-like material and surrounding sediments resulted in channel widening, vegetation removal, and slope protection from the Valley Creek confluence to a location approximately 1.6 miles upstream (Figure 1-2). This project also included material removal and erosion control measures (rip-rap placement) on Valley Creek; rip-rap was placed intermittently from the Opossum Creek confluence (upstream) to the 15th St N. Bridge (downstream; see Figure 1-2). Material removal resulted in widening of the Valley Creek stream channel to an approximate bottom width of 100 feet between the Opossum Creek confluence (RS 2236+94) to the 19th St. N. Bridge (RS 2188+95). No measures within the plan recommended by this study are within the vicinity of this project.

Figure 1-3: *Valley Creek channel in the vicinity of the Delonah Quarry.*

One levee exists within the study area. The project is located on the right overbank of Valley Creek, beginning at RS 2227+16, and terminating approximately 4,100 feet downstream at the 19th Street Bridge (RS 2188+95; see Figure 1-2). This project was constructed after 1999 (likely in 2000 based on design documentation) and, based modeled scenarios, provides protection up to the 0.005 AEP event, with overtopping modeled for the 0.002 AEP event. Some rip-rap protection is intermittently located along the toe of the structure. Additional, though unconfirmed, structural modifications along the stream corridor include several constructed berms. These features were most likely put in place without design, and as a method for disposal of excavated material produced from floodplain development.

1.2.3 Geotechnical Characteristics

Geology

The Valley Creek study area is located within the Birmingham-Big Canoe Valley District of the Alabama Valley and Ridge Physiographic Province. The province runs northeast to southwest, similar in orientation to the study area. Of the bedrock noted in the area, the two predominant formations are the Conasauga and Ketona Formations. The Conasauga Formation consists of a medium bluish-gray, fine-grained, thin-bedded limestone and a dark gray, interbedded shale. The Ketona Formation is characterized as a thick-bedded, coarsely crystalline dolomite that is light to medium gray in color. The Valley Creek Feasibility Report and Environmental Assessment, Supporting Documentation (USACE, 1992) details that the Conasauga Formation

was the predominant bedrock type in the previous study area, which was located along the Cahaba River. The Ketona accounted for the rest of bedrock. The upper bedrock is made of limestone and dolomite pinnacles. These pinnacles were found at ground surface where the rock outcrops, down to greater than 20.0 feet below ground surface. The current study area is in the same general location as the area detailed in the 1992 report, however, the footprint extends further beyond the banks in some cases.

General Subsurface Conditions

Geotechnical investigations were conducted in 1985 and 1989 as part of the effort to support the 1992 study. Eighty borings were sampled by auger, and four additional borings were sampled to obtain rock cores. There are no coordinates for the boring locations, but each of them has a corresponding channel stationing, suggesting they were likely sampled adjacent to the channel (estimates of sampled locations based on historical model cross sections and referenced stationing are mapped in Section 4.1.1.3). Historical borings from these investigations show that the overburden soils consist of brown sandy clays, with varying degrees of sand. Refusal was encountered in many of the borings at bedrock, however it was noted that refusal could have been due to boulders within the overburden. In general, the elevation of refusal decreased from the upstream end of the study area to the downstream end. Rock cores were obtained in the dolomite and limestone of the Conasuaga and Ketona Formations as part of the 1989 investigation. Compression testing (unconfined) was performed on the samples with strengths ranging from 285 tons/sq.ft. to 725 tons/sq.ft. reported. As such, drilling and blasting would be necessary to excavate into bedrock.

1.3 Flooding History

Flooding within the study area has been observed continuously by gaging efforts since 1975; however, some records are available prior to this time (1946-1947). A high-water mark at USGS 02461500 is available from an event that occurred in February of 1936. The high-water mark indicates that a flood elevation of 457.38 ft-NAVD88 occurred at the gage location during this event. Other notable events on record within the watershed include April 12-13, 1979, December 2-3,

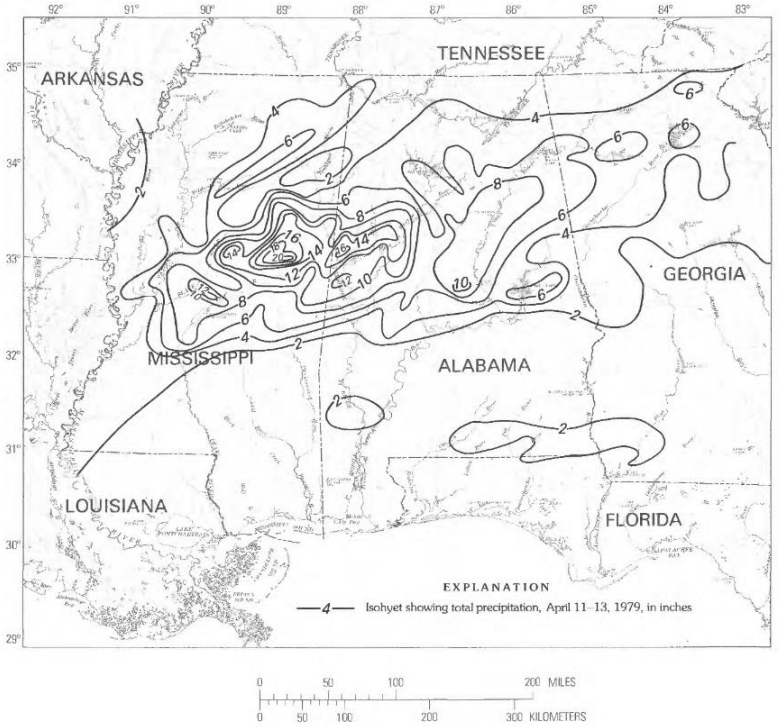

Figure 1-4: *Isohyetal analysis of storm rainfall, April 11-14, 1979 (from Edelen et al., 1979).*

1983, and September 5-6, 2011. Rainfall during April 12-13, 1979 was associated with large rainfall bands over Mississippi, Alabama, and Georgia. Birmingham experienced rainfall beginning the morning of the 12th, and lasting through the afternoon of the 13th, when intensity was greater in the upper extents of the Valley Creek Basin.

Figure 1-4 provides a historical isohyet map of the event over the southeastern United States. The National Weather Service (NWS) Forecast Office located at Oxmoor Road (relocated to Birmingham International Airport in 1990) recorded a total of 8.60 inches of rainfall during the event (see Figure 1-5 for precipitation gage locations relative to study basin). The Bessemer gage at the WWTP (coordinates estimated) recorded a total of 5.70 inches. The peak discharge at USGS 02461500 was 11,300 cfs (see Figure 1-6), which is the third largest discharge on record for the gage. This discharge is estimated as having an annual exceedance probability (AEP) between 0.10 and 0.05 (see Figure 2-12).

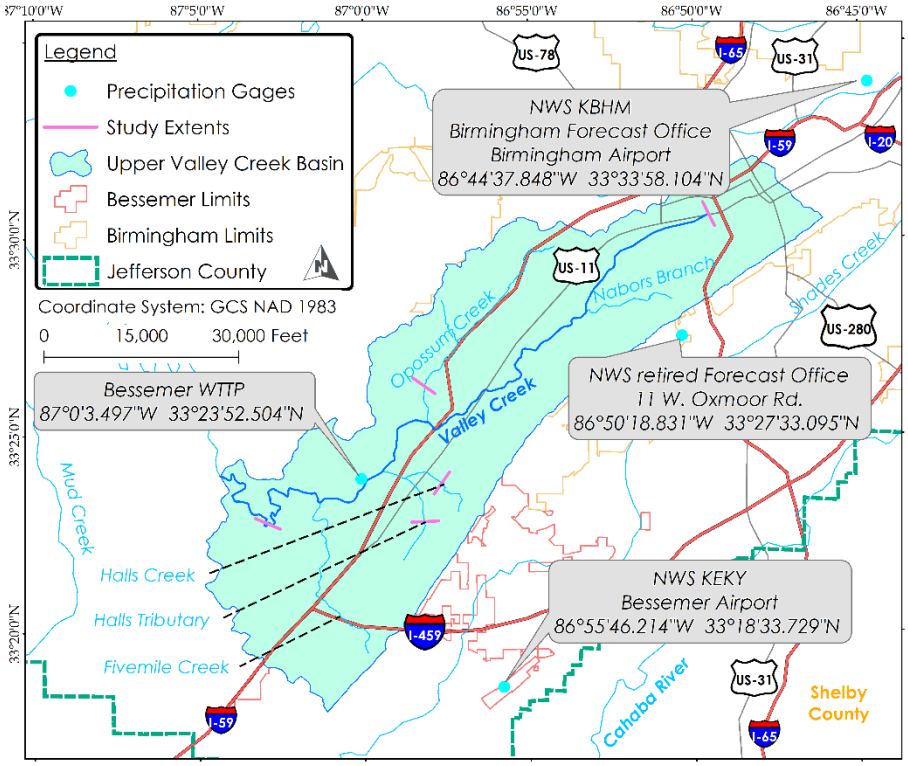

Figure 1-5: *Precipitation gages in and near Upper Valley Creek Basin*

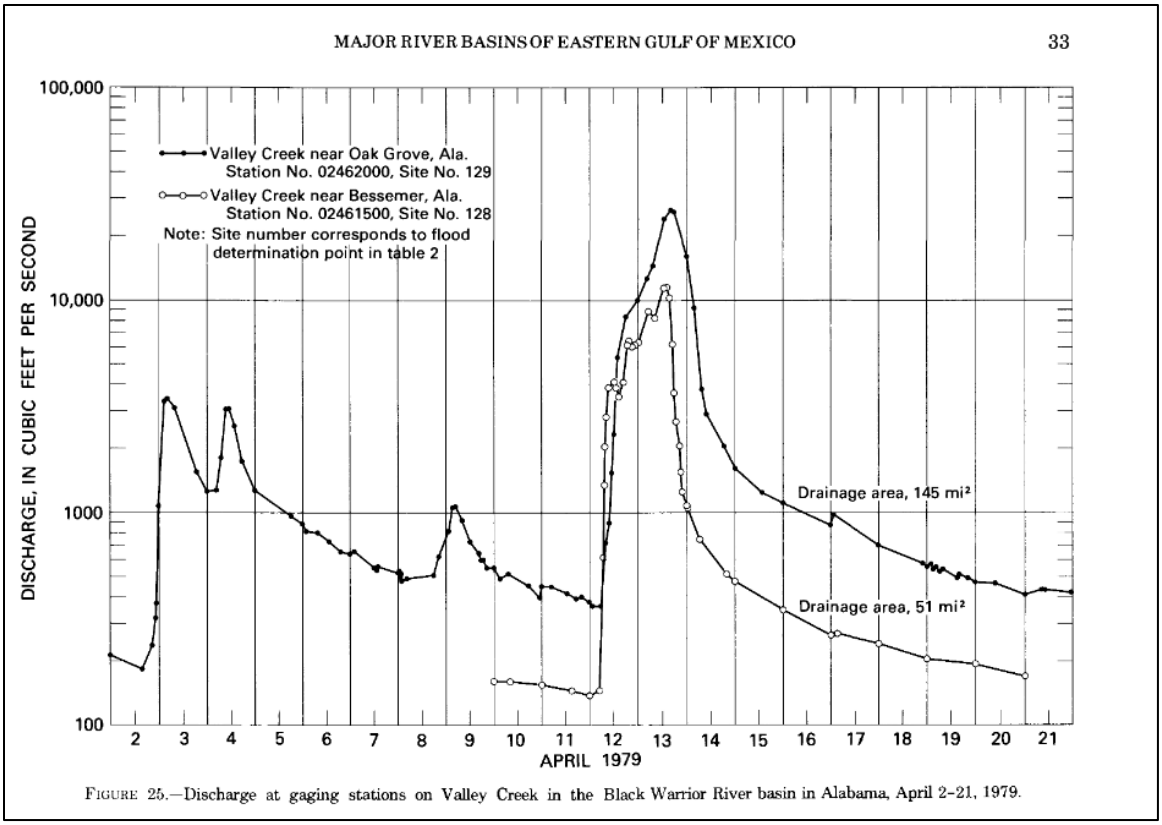

Figure 1-6: *Discharge at gaging stations on Valley Creek in the Black Warrior River basin in Alabama, April 2-21, 1979 (from Edelen et al., 1979).*

Rainfall that occurred from December 2-3, 1983 produced record flooding on Valley Creek and resulted in a Presidential Disaster Declaration (USACE, 1986). Metropolitan Birmingham received the greatest rainfall totals relative to isolated rainfall in west and central Alabama. Total precipitation was gaged from 1-to-10 inches on December 2, and additional rainfall produced flash-flooding on the morning of December 3. The Birmingham NWS Forecast Office recorded 9.22 inches of precipitation from 2200 December 2 to 2200 December 3 (24-hour period), which is presently the record high 24-hour rainfall total for the area. The peak discharge recorded at USGS 02461500 was 17,940 cfs (0.01 AEP), the highest on record for the gage station. Damage to commercial, public, and private property was estimated at $14,000,000 (USACE, 1986).

More recently, in September of 2011, the remnants of Tropical Storm Lee moved north out of the Gulf of Mexico and precipitated total rainfall depths ranging from 8-to-15 inches over Jefferson County during the four-day period of September 3-7 (Figure 1-7). Jefferson County as well as several other counties in north-central Alabama experienced flash-flooding as a result of the event. The peak flow at USGS 02461500 was 13,000 cfs (0.05 AEP), which is the second largest flow on record.

1.4 Data Collection

1.4.1 Hydrologic Data

There are several surface water gages available for Valley Creek within the study area; however, the majority have relatively short periods of record, and there is minimal length of overlap between sites. Before 2017, there were never more than two gages recording during a significant rainfall event and there was only one gage in service during two of the three highest events of record. One gage was in service on Halls Creek from 1997 – 2003, but only reported flow. Several recently installed gages are currently in service on Valley Creek, with none currently active on any of the tributaries modeled in this study (Halls Creek and Opossum Creek). Table 1-1 provides a summary of available data for both current and historical surface water gage sites within the study extents. Figure 1-8 provides a location map of sites within the study extents.

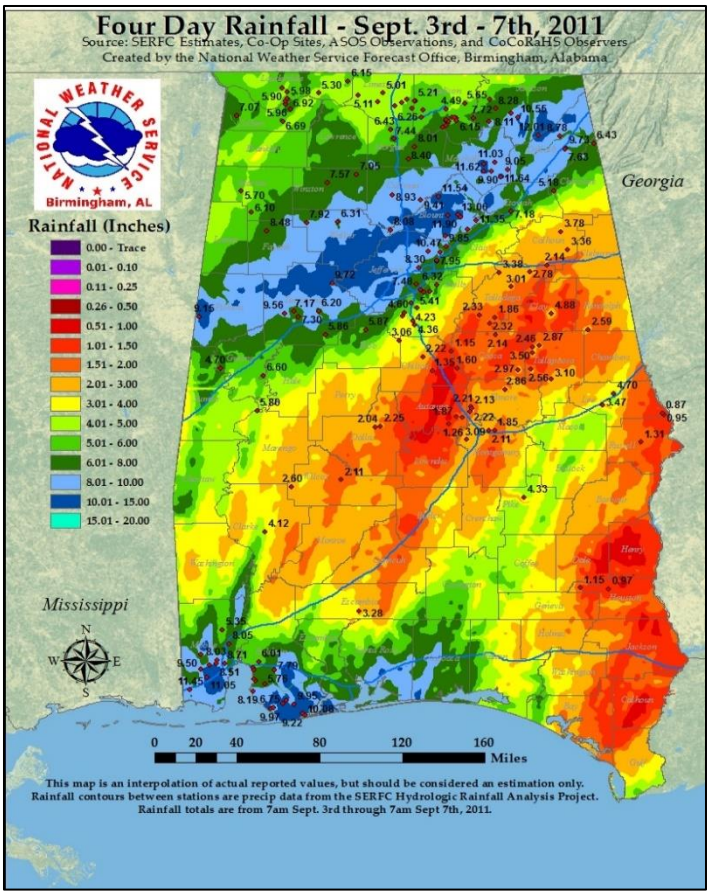

Figure 1-7: *Four day rainfall totals for Alabama (September 3-7, 2011; from NWS Birmingham Southeastern Forecast Office).*

Table 1-1: Summary of stream gages in the Upper Valley Creek Basin

Owner	Site# - Drainage Area (mi²)	Location[1, 2]	Data Type	Period of Record (per Data Type)	Datum (ft-NAVD88)
USGS	02461130 - 7.0	Valley Creek; 33°30'21"/ 86°50'11"	Discharge; Stage; Precipitation; Water Quality	2/3/2001 – 9/30/2007 (discharge); 1/4/2017 – Present (all)	545.00 (Estimate)
USGS	02461192 - 13.5	Valley Creek; 33°29'33"/ 86°52'19"	Discharge; Stage; Precipitation; Water Quality	1/4/2017 – Present (discharge and stage); 2/2/2017 – Present (all)	519.50 (Estimate)
USGS	02461405 - 34.6	Valley Creek; 33°25'32"/ 86°57'10"	Discharge; Stage; Water Quality	3/30/2018 – Present (discharge and stage); 5/14/2018 – Present (all)	456.40 (Estimate)
USGS	02461500 - 52.5	Valley Creek; 33°25'09"/ 86°58'58"	Discharge; Stage	01/1946 – 12/1947 (discharge and stage) 05/02/1974 - 05/14/1975 (discharge); 5/14/1975 – Present	438.78 (Survey)

				(discharge and stage)	
USGS	02461640 - 61.4	Valley Creek; 33°23'59"/ 86°59'36"	Discharge; Stage	10/1/1997 – 10/9/2006	429.00 (Estimate)
USGS	02461630 - 7.3	Halls Creek; 33°23'58"/ 86°59'01"	Discharge	10/1/1997 – 9/29/2003	N/A

[1]Some coordinates rounded to nearest second.
[2]Valley Creek sites ordered upstream to downstream.

From Table 1-1 it can be seen that several gage datums were estimated. The USGS-published datums for these sites were originally estimated via topographic maps (V. Stricklin, personal communication, September 21, 2018), and seemed to be highly inaccurate for some sites. For this study, datums for these locations were estimated based on channel geometry, and available USGS guidance (see, e.g., Carter and Davidian, 1968; Sauer and Turnipseed, 2010; Kenney, 2010). Because these site datums have not been formally surveyed, a high level of uncertainty is associated with their stage records. Careful work was executed in hydraulic model calibrations upstream of these gages in an effort to ensure over-parameterization did not occur. The risk associated with this uncertainty and how it relates to the performance of the recommended plan is detailed in Section 5.2.6.

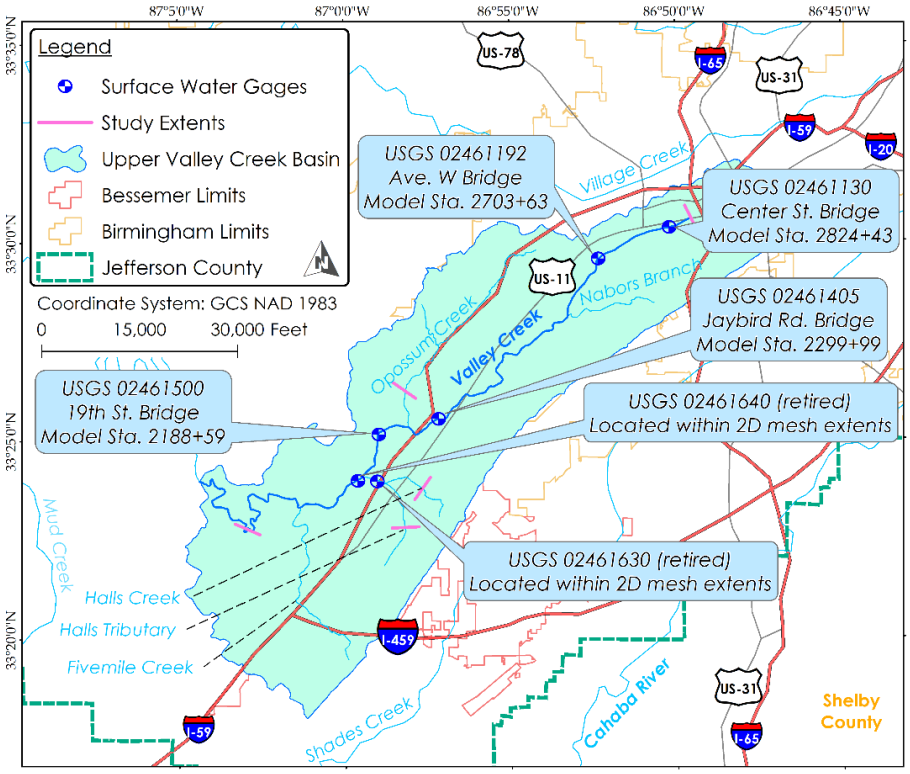

Figure 1-8: *Current and historical surface water gages in Upper Valley Creek Basin.*

Rainfall data for the events utilized for calibration and validation of the H&H models (see Section 2.1.4) were obtained from the Mobile District Water Management Server and also provided by the NWS Southeast River Forecast Center (SRFC). Data were obtained as National Oceanic and Atmospheric Administration (NOAA) Stage IV gridded precipitation in XMRG format. Stage IV is an hourly quality-controlled rainfall product available on a 4.0-kilometer (2.6-mile) grid across the United States. The hourly rainfall data in the XMRG file format was unpacked into the Standard Hydrologic Grid (SHG) format and spatially interpolated to a 500-meter grid using the

gridloadXMRG program. The gridded data was then imported into the Meteorologic Visualization Utility Engine (HEC-MetVue) program and basin average hyetographs were created from the grid for each subbasin in the hydrology model.

From Table 1-1, two precipitation gages were added within the basin in 2017; however, these gages are not included in the Stage IV gridded precipitation datasets utilized for this study as described above. The nearest applicable rainfall-recording gage supporting NOAA Stage IV precipitation is the NWS site located at the Birmingham International Airport, approximately 5 miles northeast of the basin (KBHM; see Figure 1-5). During the described historical events (1979 and 1983), this site was located at 11 Oxmoor Road (relocated in 1990). The NWS site at the Bessemer Airport (KEKY) is located approximately 4 miles southeast of the basin (see Figure 1-5). This site supported grid interpolation for calibration/validation events (see Section 2.1.4) after 7/14/2016 (in-service date). The Interim Reconnaissance Report (USACE, 1986) describes the WWTP site as non-recording; however, the report does provide rainfall depths for the April 1979 event as described in Section 1.3. No other information for this site has been obtained, and therefore, this gage only served to support model validations with the April 1979 event.

1.4.2 Topographic Data

Between March 13, and April 7, 2013, The Atlantic Group, LLC conducted a Light Detection and Ranging (LiDAR) survey encompassing Jefferson County, AL. Data collected during this flight period were supplemented with an additional flight on August 27, 2013. The final area of coverage from 63 flight lines was 1,124 square miles (Atlantic, 2013). Upon the conclusion of post-processing, a digital elevation model (DEM) of last-return points was produced (bare-earth model). The data are referenced vertically to the North American Vertical Datum of 1988 (NAVD88), and horizontally to the North American Datum of 1983 (NAD83). The DEMs were provided as tiles in .tif format from Jefferson County. Tiles covering the extent of the upper Valley Creek Basin were mosaicked to form a continuous DEM for use in modeling and mapping (Figure 1-9). Table 1-2 provides an

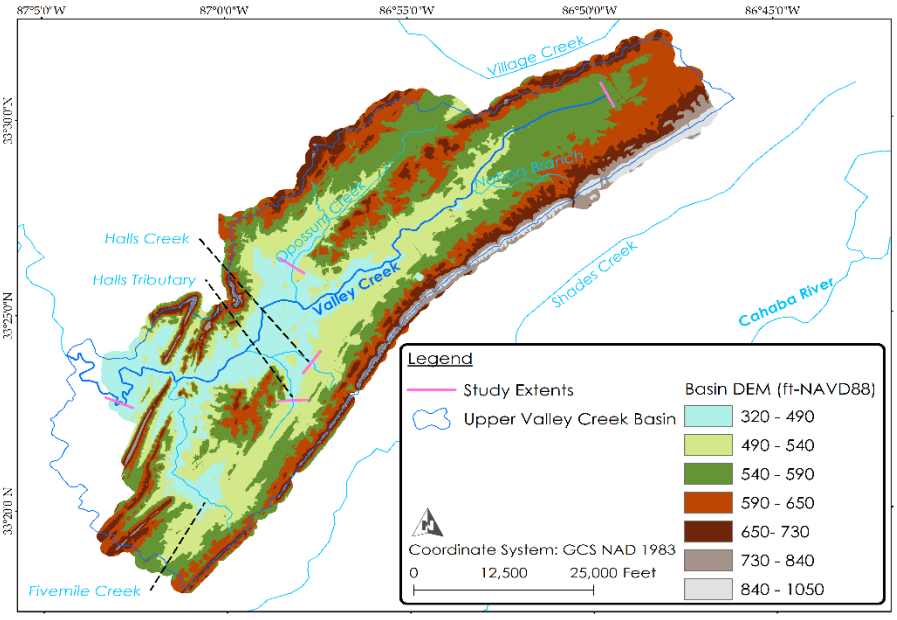

Figure 1-9: *Upper Valley Creek Basin DEM.*

accuracy specification summary of the dataset based on the dataset's classification as USGS Quality Level 2 (Heidemann, 2018) as provided in the LiDAR metadata (Atlantic, 2013).

Table 1-2: LiDAR Specification Summary

Parameter	Value
Nominal Pulse Spacing	< 1 m
Point Density	2.6/m^2
Horizontal Projection	SPAW (FIPS 0102)
Horizontal Accuracy	< 1 m
Vertical Projection	NAVD 88
Fundamental Vertical Accuracy	16.43 cm
$RMSE_z$	≤ 8.4 cm
Equivalent Contour Accuracy	2-ft
Format and Grid Cell Size	TIFF; 2 ft. grid cells
Horizontal and Vertical Units	ft/ft

The project DEM was supplemented with channel surveys to refine model geometry within the stream banks for the majority of the study reach. Cross-sectional topographic surveys were obtained sometime prior to the initiation of the present study and encompassed a length of Valley Creek from the headwaters (RS 2859+15) to the 19 Street North Bridge (RS 2188+95; Figure 1-10). A DEM was produced from the survey data and was included with the existing model package from which the present study-model was built. Additional metadata including accuracy and acquisition dates have not been obtained. Cross sections downstream of the channel survey extents reflect topography/bathymetry captured by the LiDAR only. As base-flow depths are very small, it is assumed that the DEM is accurately representing the channel geometry in this location (as well as upstream, surveyed areas), despite applied hydrologic corrections (i.e., channel smoothing and grading) during DEM creation. Additionally, strong agreement between surveyed cross sections and the basin DEM helped to certify the accuracy of channel data in this portion of the model.

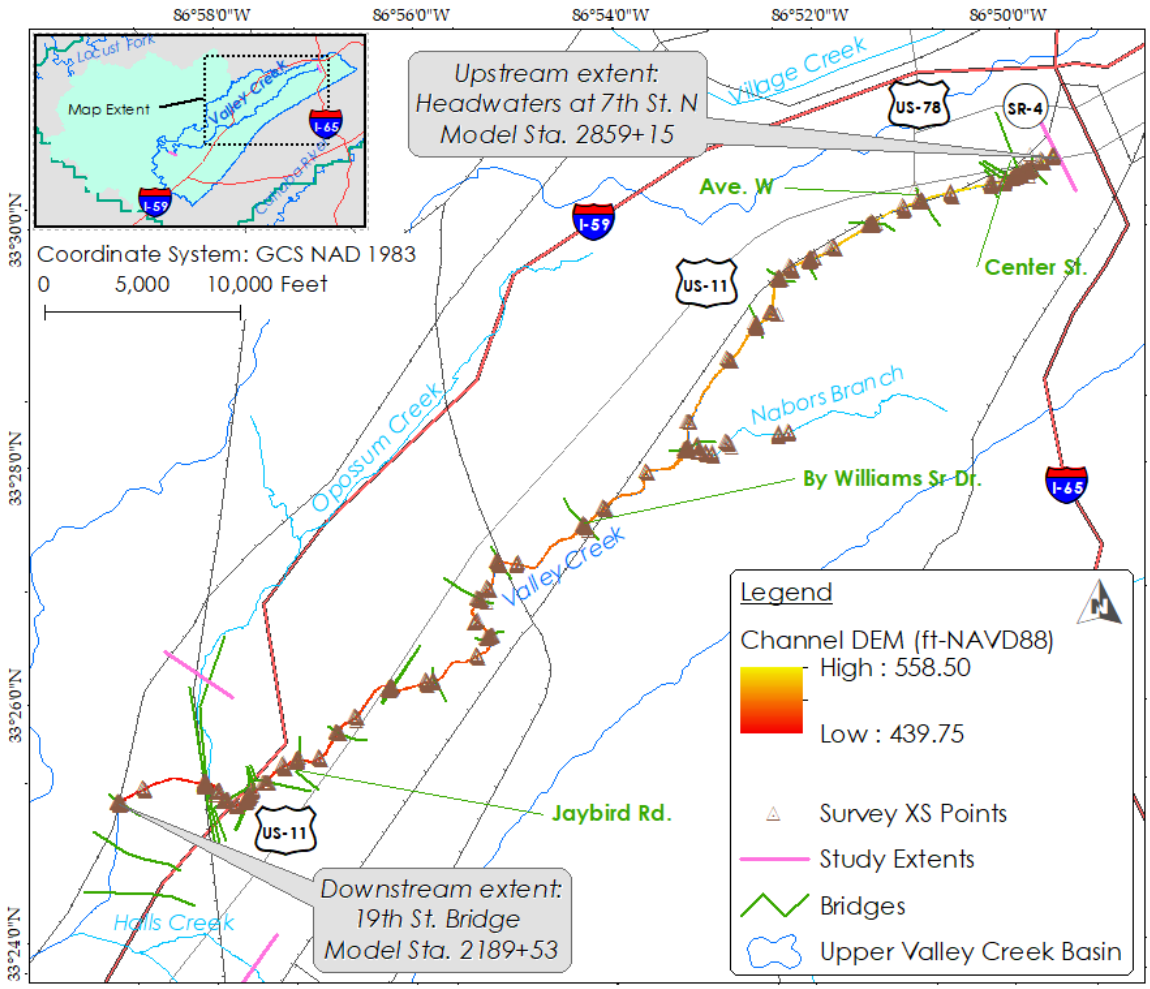

Figure 1-10: *Channel survey extents in Valley Creek.*

1.4.3 Structural Data

The majority of hydraulic structures within the Valley Creek study extents were present in the previous hydraulic model that the existing conditions geometry was developed from (see Section 2.3.1). The abutments of several structures were modified from their original state to better reflect the terrain of the overbank approach ramps/roadways. The City of Bessemer provided as-builts for several structures and these geometries were confirmed with the provided data (R. Gilbert, personal communication, 6 December 2018). Three structures, including a service bridge within the Valley Creek Water Reclamation facility (within 2D mesh extents) and two abandoned railroad crossings were not present in the old geometry. As-builts for the WWTP structure were provided and it was added to the model geometry. Geometry for the abandoned railroad crossings were estimated via LiDAR and photographs provided by the City of Bessemer (J. Champion, personal communication, 28 May 2019). As-builts for the existing levee along Valley Creek were provided; however, adjustment to the model geometry to reflect this feature was not necessary due to its accurate representation within the LiDAR data. Data for bridges located within the model extents of included tributaries were added to the model after data collection via field-survey from February 25-26, 2019.

2.0 Existing Conditions Models

2.1 Hydrology

2.1.1 Hydrologic Model Background

A planning level hydrologic model was developed within the Hydrologic Engineering Center Hydrologic Modeling System (HEC-HMS), version 4.3 for the 87 square mile study area. Construction of the hydrologic model for this study began from an existing HEC-HMS model for Valley Creek. This model was initially produced for a joint effort between the Mobile District and the City of Birmingham originally in support of the Silver Jackets Flood Forecasting and Inundation Mapping (FFIM) program in 2017. For various reasons, this effort was discontinued. The updated model was extended further downstream, and the delineation was refined to match potential measures to be investigated as part of the alternative screening. Additionally, methods for loss, transform, routing, and precipitation modeling were updated.

2.1.2 Model Overview

<u>Basin Delineation</u>

Sub-basins were verified and manually re-delineated from the existing model using HEC-GeoHMS program and using the Hydrologic Unit Code 10 (HUC-10) sub-basins. The watershed was divided into 52 sub-basins (shown in Figure 2-1) at selected critical locations along the stream to account for significant hydrologic changes due to confluences with other streams or flow attenuation locations. Flow change locations were also added at gaged locations along the reaches to allow for comparison during model calibration. Additionally, basin breaks were placed at potential measure locations identified by the Project Delivery Team (PDT).

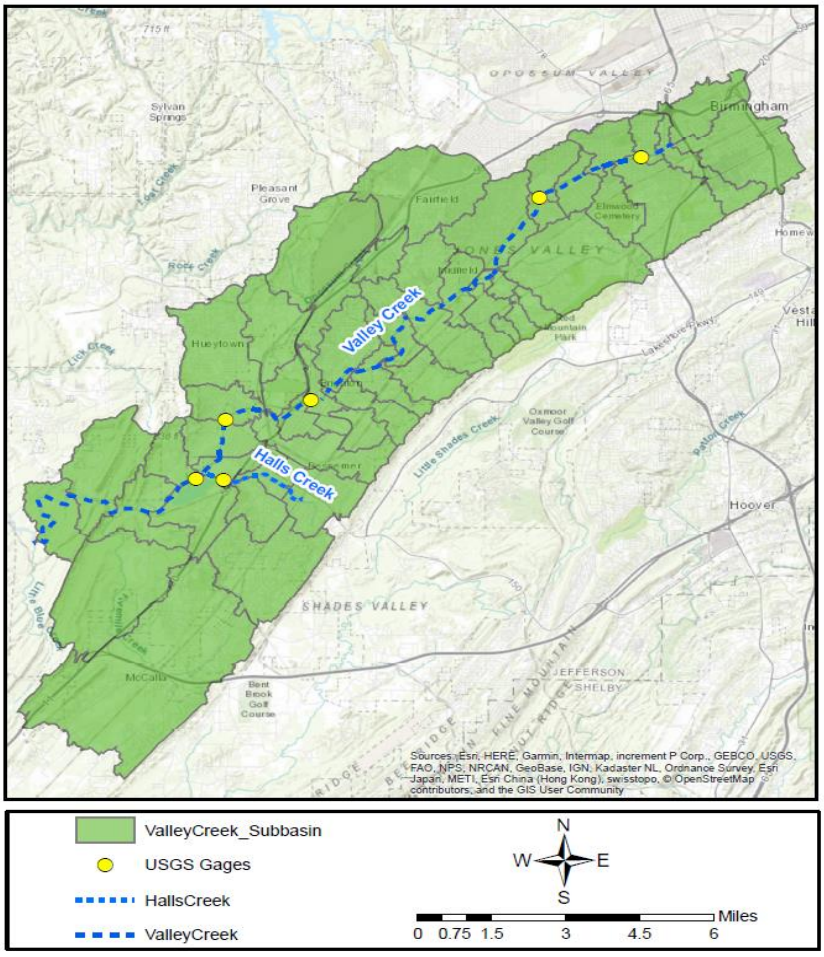

Figure 2-1: *HMS subbasins.*

Rainfall Losses

The deficit and constant loss methodology was used to estimate the losses from a precipitation event occurring over the study area. Initial deficit values were estimated through trial and error and calibration (Table 2-1). Constant loss rates were based on data from the Soil Survey Geographic (SSURGO) Database (Soil Survey Staff, 2019; Figure 2-2), by assigning a range of loss rates based on soil types within each sub-basin, and then varying during model calibration (Table 2-2). Impervious surface area is also a parameter in deficit and constant loss modeling. Impervious areas were estimated with an impervious surface area dataset (referenced to 2006) available within the National Land Cover Database (NLCD; Xian et al., 2011). Sub-basin averages from this dataset were adjusted to account for connected and non-connected impervious areas utilizing empirical relations provided by Sutherland (1995) as recommended by the Environmental Protection Agency (EPA, 2014). In the model, effective impervious area was determined for sub-basins assumed to have significant ineffective (or disconnected) impervious area with the following equation:

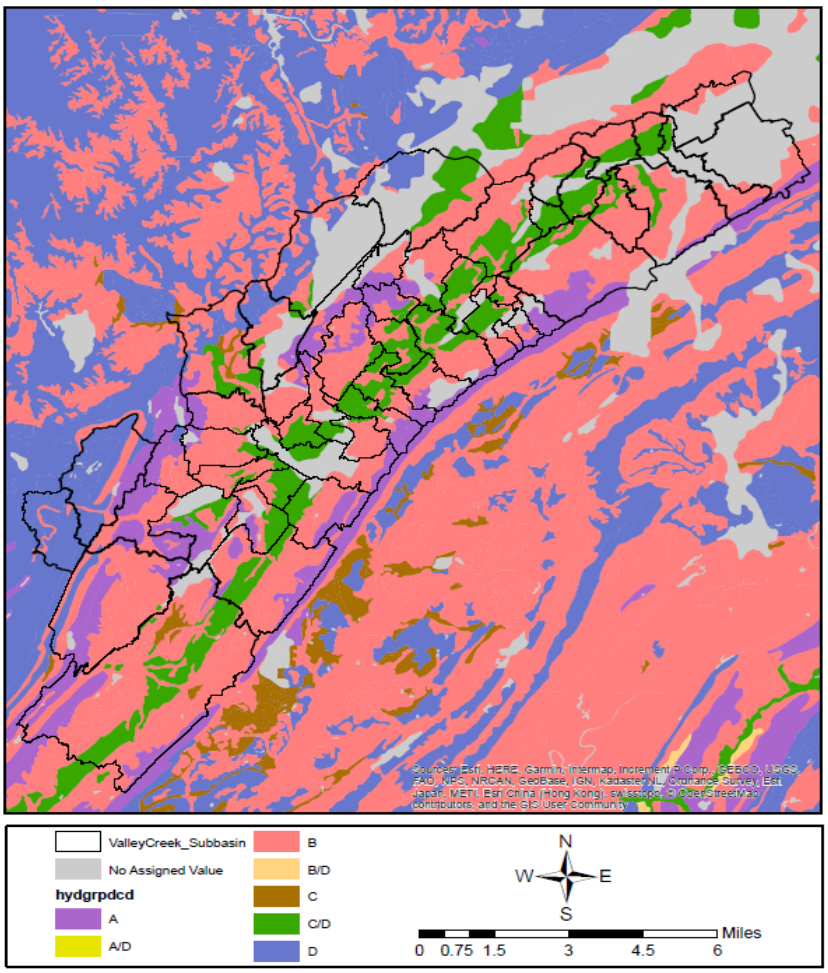

Figure 2-2: *Soils map of study area.*

$$EIA = 0.1(TIA)^{1.5}, \qquad TIA \geq 1 \qquad \text{Equation 1}$$

where EIA is the effective impervious area, and TIA is the total impervious area.

Table 2-1: Final initial loss rates for subbasins

Subbasin	Initial Loss (in.)	Subbasin	Initial Loss (in.)	Subbasin	Initial Loss (in.)	Subbasin	Initial Loss (in.)
SB_VC2	0	SB_TR1_2	1.95	SB_VC22	1.95	SB_VC28	1.95
SB_VC1	0	SB_TR1_3	1.95	SB_VC23	1.95	SB_HT1	1.95
SB_VC3	1.5	SB_TR2_1	1.95	SB_VC24	1.95	SB_HC1	1.95
SB_VC4	1.5	SB_TR2_2	1.95	SB_OC1	1.95	SB_HT2	1.95
SB_VC5	1.5	SB_VC13	1.95	SB_OC2	1.95	SB_HC2	1.95
SB_VC6	1.5	SB_VC15	1.95	SB_OC4	1.95	SB_VC29	1.95
SB_VC7	1.5	SB_VC14	1.95	SB_OC3	1.95	SB_VC30	1.95
SB_VC8	1.5	SB_VC16	1.95	SB_OC6	1.95	SB_VC31	1.95
SB_VC9	1.5	SB_VC17	1.95	SB_OC5	1.95	SB_TR4_1	1.95
SB_VC10	1.95	SB_VC19	1.95	SB_VC25	1.95	SB_TR4_2	1.95
SB_VC11	1.95	SB_VC18	1.95	SB_OC7	1.95	SB_VC32	1.95
SB_VC12	1.95	SB_VC20	1.95	SB_VC26	1.95	SB_VC33	1.95
SB_TR1_1	1.95	SB_VC21	1.95	SB_VC27	1.95	SB_VC34	1.95

Table 2-2: Final constant loss rates for subbasins

Subbasin	Constant Loss Rate (in./hr.)	Subbasin	Constant Loss Rate (in./hr.)	Subbasin	Constant Loss Rate (in./hr.)	Subbasin	Constant Loss Rate (in./hr.)
SB_VC2	0.01	SB_TR1_2	0.20	SB_VC22	0.22	SB_VC28	0.29
SB_VC1	0.01	SB_TR1_3	0.21	SB_VC23	0.20	SB_HT1	0.29
SB_VC3	0.24	SB_TR2_1	0.15	SB_VC24	0.15	SB_HC1	0.16
SB_VC4	0.17	SB_TR2_2	0.14	SB_OC1	0.14	SB_HT2	0.2
SB_VC5	0.22	SB_VC13	0.20	SB_OC2	0.31	SB_HC2	0.16
SB_VC6	0.26	SB_VC15	0.18	SB_OC4	0.32	SB_VC29	0.25
SB_VC7	0.20	SB_VC14	0.10	SB_OC3	0.35	SB_VC30	0.35
SB_VC8	0.11	SB_VC16	0.17	SB_OC6	0.30	SB_VC31	0.36
SB_VC9	0.20	SB_VC17	0.31	SB_OC5	0.23	SB_TR4_1	0.27
SB_VC10	0.06	SB_VC19	0.17	SB_VC25	0.31	SB_TR4_2	0.32
SB_VC11	0.16	SB_VC18	0.16	SB_OC7	0.29	SB_VC32	0.38
SB_VC12	0.22	SB_VC20	0.18	SB_VC26	0.15	SB_VC33	0.16
SB_TR1_1	0.27	SB_VC21	0.26	SB_VC27	0.34	SB_VC34	0.08

Subbasin Response

The Clark transform method was used for this study. The initial time of concentration values for each sub-basin were calculated following the methodology in TR-55 (NCRS, 1986), and were adjusted to match the observed hydrographs at gaged locations. Final times of concentration and storage coefficients based on the average of calibrated values for each subbasin are shown in Table 2-3.

Table 2-3: Final transform parameters for sub-basins

Subbasin	Time of Conc. (Tc; hr.)	Storage Coefficient (R)	Subbasin	Time of Conc. (Tc; hr.)	Storage Coefficient (R)
SB_VC2	1	0.1	SB_VC22	1.61	2.22
SB_VC1	0.8	0.05	SB_VC23	1.21	1.67
SB_VC3	1.2	1.12	SB_VC24	1.26	1.74
SB_VC4	0.8	0.8	SB_OC1	2.23	2.37
SB_VC5	1.64	0.64	SB_OC2	0.89	0.94
SB_VC6	1.9	0.8	SB_OC4	2.02	2.14
SB_VC7	0.45	0.16	SB_OC3	1.11	1.18
SB_VC8	1	0.48	SB_OC6	2.04	2.16
SB_VC9	0.22	0.22	SB_OC5	2.05	2.18
SB_VC10	1.01	1.4	SB_VC25	1.44	1.53
SB_VC11	2.1	2.9	SB_OC7	1.66	1.77
SB_VC12	3	4.14	SB_VC26	2.09	2.22
SB_TR1_1	0.85	1.18	SB_VC27	1.33	1.42
SB_TR1_2	0.96	1.33	SB_VC28	1.34	1.34
SB_TR1_3	1.03	1.43	SB_HT1	1.67	1.67
SB_TR2_1	0.67	0.93	SB_HC1	1.59	1.59
SB_TR2_2	1.56	2.15	SB_HT2	1.17	1.17
SB_VC13	0.98	1.36	SB_HC2	1.55	1.55
SB_VC15	1.51	2.1	SB_VC29	2.05	2.05
SB_VC14	1.43	1.97	SB_VC30	1.44	1.44
SB_VC16	1.79	2.47	SB_VC31	1.43	1.43
SB_VC17	1.07	1.47	SB_TR4_1	2.95	2.95
SB_VC19	1.53	2.11	SB_TR4_2	2.84	2.84
SB_VC18	1.67	2.31	SB_VC32	1.15	1.15
SB_VC20	1.83	2.54	SB_VC33	0.69	0.69
SB_VC21	1.79	2.47	SB_VC34	0.62	0.62

Baseflow

The Recession Baseflow method was used as the baseflow method for all subbasins. Before calibration, all subbasins were set to an initial discharge of 1 cfs/mi^2, a recession constant of 0.9 and a ratio to peak of 0.1. These where set based on knowledge of typical values for these parameters for urban watersheds in the area. Each parameter was then adjusted to best fit the hydrographs at calibration points in the model. The parameters are provided in Table 2-4 are the final parameters used in validation and the final existing conditions and future without project conditions models.

Table 2-4: Recession baseflow parameters

Subbasin	Initial Discharge (cfs/mi^2)	Recession Constant	Ratio to Peak	Subbasin	Initial Discharge (cfs/mi^2)	Recession Constant	Ratio to Peak
SB_VC2	1.57	0.9	0.03	SB_VC22	1.57	0.9	0.09
SB_VC1	1.57	0.9	0.03	SB_VC23	1.57	0.9	0.09
SB_VC3	1.57	0.9	0.03	SB_VC24	1.57	0.9	0.09
SB_VC4	1.57	0.9	0.03	SB_OC1	1.57	0.9	0.09
SB_VC5	1.57	0.9	0.03	SB_OC2	1.57	0.9	0.09
SB_VC6	1.57	0.9	0.03	SB_OC4	1.57	0.9	0.09
SB_VC7	1.57	0.9	0.03	SB_OC3	1.57	0.9	0.09
SB_VC8	1.57	0.9	0.03	SB_OC6	1.57	0.9	0.09
SB_VC9	1.57	0.9	0.03	SB_OC5	1.57	0.9	0.09
SB_VC10	1.57	0.9	0.09	SB_VC25	1.57	0.9	0.09
SB_VC11	1.57	0.9	0.09	SB_OC7	1.57	0.9	0.09
SB_VC12	1.57	0.9	0.09	SB_VC26	1.57	0.9	0.09
SB_TR1_1	1.57	0.9	0.09	SB_VC27	1.57	0.9	0.09
SB_TR1_2	1.57	0.9	0.09	SB_VC28	1.57	0.9	0.09
SB_TR1_3	1.57	0.9	0.09	SB_HT1	1.57	0.9	0.09
SB_TR2_1	1.57	0.9	0.09	SB_HC1	1.57	0.9	0.09
SB_TR2_2	1.57	0.9	0.09	SB_HT2	1.57	0.9	0.09
SB_VC13	1.57	0.9	0.09	SB_HC2	1.57	0.9	0.09
SB_VC15	1.57	0.9	0.09	SB_VC29	1.57	0.9	0.09
SB_VC14	1.57	0.9	0.09	SB_VC30	1.57	0.9	0.09
SB_VC16	1.57	0.9	0.09	SB_VC31	1.57	0.9	0.09
SB_VC17	1.57	0.9	0.09	SB_TR4_1	1.57	0.9	0.09
SB_VC19	1.57	0.9	0.09	SB_TR4_2	1.57	0.9	0.09
SB_VC18	1.57	0.9	0.09	SB_VC32	1.57	0.9	0.09
SB_VC20	1.57	0.9	0.09	SB_VC33	1.57	0.9	0.09
SB_VC21	1.57	0.9	0.09	SB_VC34	1.57	0.9	0.09

Reach Routing

For the main reach of Valley Creek, Modified-Puls reach routing was applied utilizing the discharge-storage curves generated by the HEC-RAS Silver Jackets (steady flow) model (see Section 2.3.1). For Halls Creek, Halls tributary, and Opossum Creek, reaches from the present study model were used to generate discharge-storage curves. Cross sections were added through the mesh for Halls Creek to produce curves for the entire modeled length of the system. The storage-outflow tables for all reaches (Valley Creek, Halls Creek, unnamed tributary, and Opossum Creek) were updated iteratively as the HEC-RAS model was better calibrated. For

hydrology-only reaches along downstream portions of Valley Creek and upstream portions of Opossum Creek that did not have HEC-RAS models available, sub-basin reach routings were estimated using the Muskingum-Cunge method with eight-point cross sections. The seamless terrain data was used to determine cross section geometry, slope, and length of the reaches for the studied streams. Aerial imagery was used to estimate the Manning's n-value for the reach routing.

2.1.3 Calibration and Validation

To support the development of a calibrated hydrology model, five rainfall events were chosen for analysis. Calibration events were selected on the basis of data availability, maximization of observation sites, accurate representation of land-use within the watershed, and normality of antecedent conditions. Three events were used to support calibration of the model and two more events were used to validate the model parameterization. Table 2-5 summarizes the events used for calibration and validation.

Table 2-5: Rainfall events utilized for calibration and validation

Event	Precipitation Source	Event Start	Event End	Avg. Rainfall Depth (inches)	Event Classification
December 25-26, 2015	NOAA XMRG	12:00	12:00	3.21	Calibration
April 2-3, 2017	NOAA XMRG	18:00	18:00	3.51	Calibration
December 27-29, 2018	NOAA XMRG	00:00	00:00	4.58	Calibration
September 5-6, 2011	NOAA XMRG	18:00	18:00	9.29	Validation
April 6-8, 2014	NOAA XMRG	00:00	12:00	4.14	Validation
April 12-13, 1979	Gage	06:00	18:00	8.6	Historical Event
December 2-3, 1983	Gage	20:00	20:00	8.6	Historical Event

Rainfall data for the basin were taken from two sources. For events before 2009, land-based gages were used for calibration. After 2009, NEXRAD Stage IV hourly gridded precipitation data from the National Weather Service were used for calibration. All selected calibration events occurred during the wet season of early winter to spring, and were most likely the result of slow-moving, frontal-type storms - those characteristic of extreme rainfall events in the southern Valley and Ridge and surrounding southeastern physiographic provinces of the study area - and those considered most-likely risk drivers for flooding in the study location. Seasonal variation in weather systems does exist within the study basin, however, and flash-flooding can occur throughout the year as the result of alternate storm types including isolated thunderstorms (convective) and dissipating tropical cyclones and their associated frontal systems (Konrad and Perry, 2010).

While other rainfall events with more significant flooding have been observed as documented by USGS gage annual maximum discharge records, more recent events were selected due primarily to the availability of more detailed rainfall observations through a combination of ground-based precipitation gages, and NOAA Stage IV Radar. Additionally, there have been significant changes to the basin since the extreme storms in the 1970s and 1980s including a

major increase in urbanization, implementation of stormwater management plans, channel modifications to reduce flooding, and bridge additions that have created constrictions in the channel. Such drastic changes suggest that these historical events are an inaccurate representation of existing conditions within the study area. Reference Chapter 6 of this appendix for a detailed climate change assessment of the study area including a nonstationarity assessment of peak streamflow (Section 6.3).

Calibration to observed events was performed on three fairly recent storm events. Ideally, larger (out-of-bank) events would be utilized; however, there were several limitations to this. First, stream gage and rain gage data are sporadic through the longest available period of record and availability of data does not line up with larger events. Also, the largest events in this basin occurred over 35 years ago, and since that time, there have been changes in urbanization, implementation of storm water management plans, channel modifications to reduce flooding, and numerous bridges added to the reach. All of these factors affect time and flow in the system. Therefore, more recent events were used to calibrate and validate models. However, the previously discussed historical events in the basin (1979 and 1983) were included in the hydrology model for comparison purposes. Events chosen for calibration occurred after 2009, the earliest year reasonable gridded precipitation data was available for the area. Below, in Figures 2-3 through 2-7, are the results for all calibration and validation events at USGS 02461500. Other locations used for calibration are available in the model.

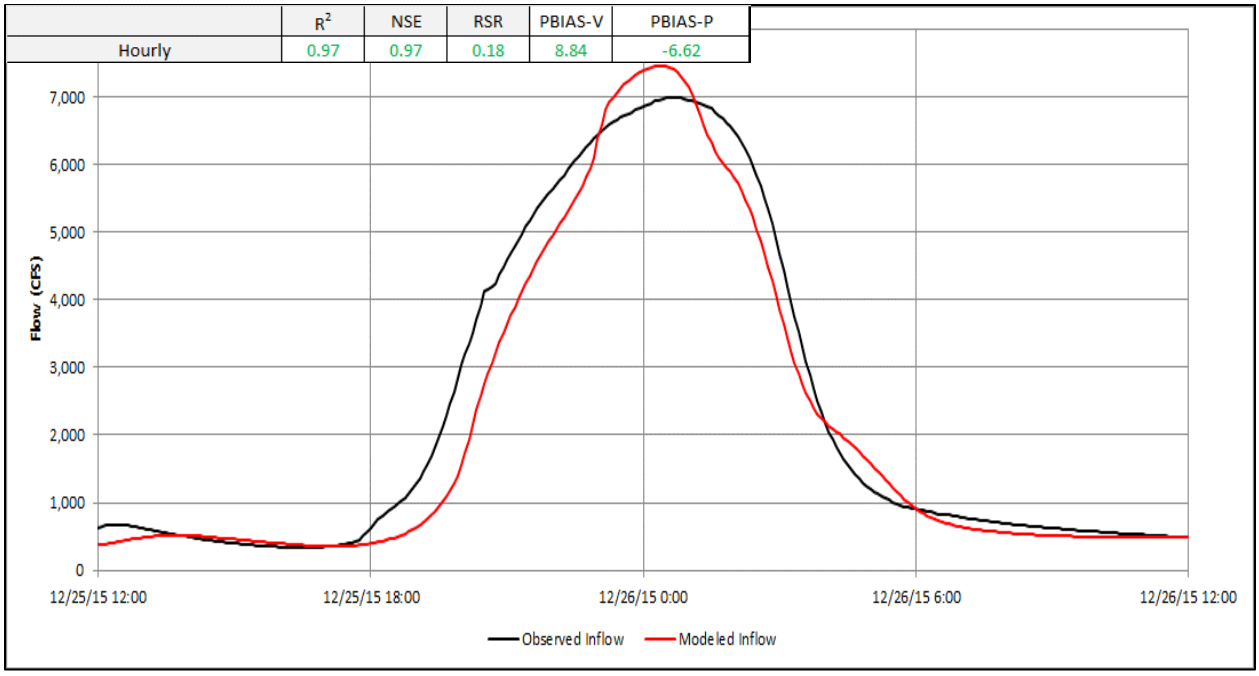

Figure 2-3: *Dec 2015 calibration at Bessemer gage.*

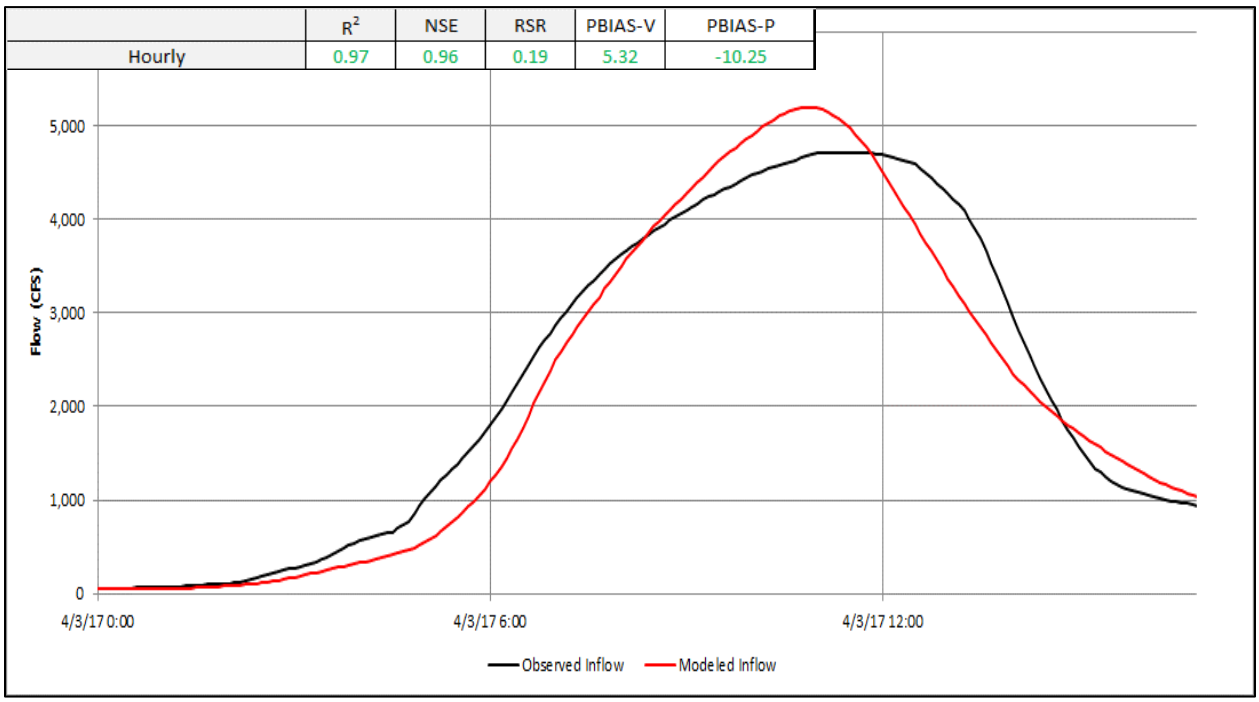

Figure 2-4: *April 2017 calibration at Bessemer gage.*

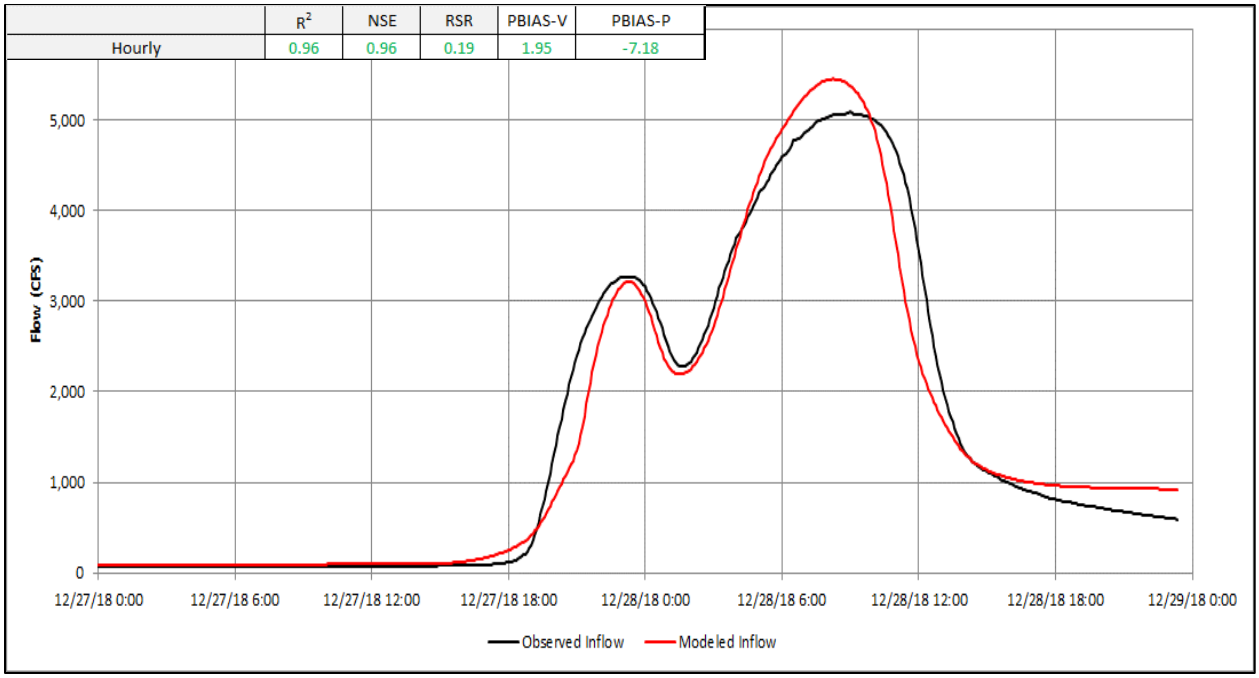

Figure 2-5: *December 2018 calibration at Bessemer gage.*

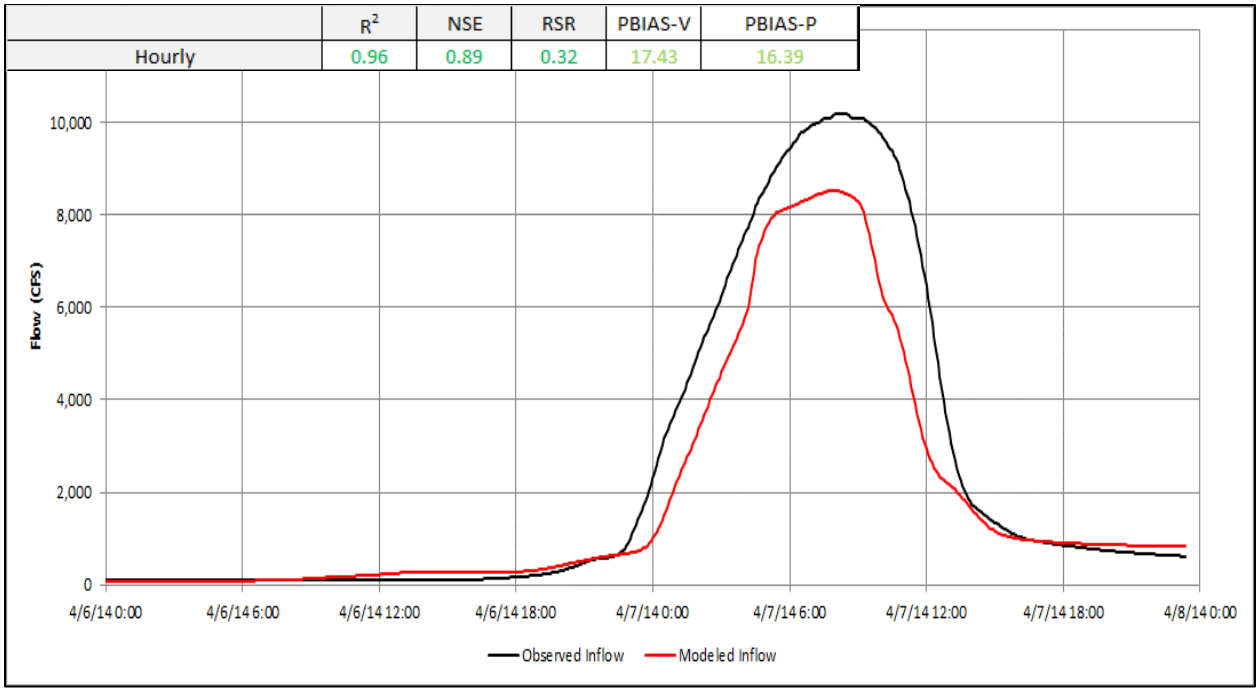

Figure 2-6: *April 2014 validation at Bessemer gage.*

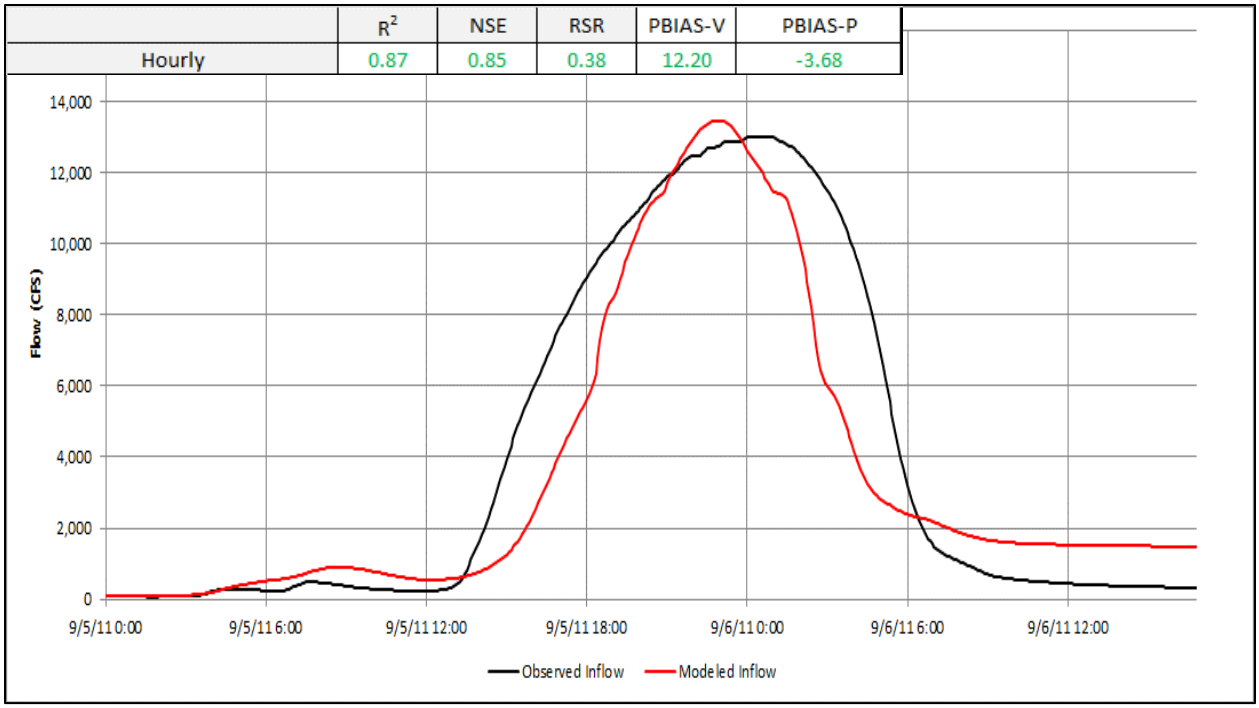

Figure 2-7: *September 2011 validation at Bessemer gage.*

2.1.4 Calibration/Validation Results and Discussion

For this study, it was important to consider both peak flow and volume to accurately screen the array of alternatives being considered. Therefore, efforts were made to balance both peak flow and peak volume at every calibration point. Calibration is within acceptable ranges for the selected events for both peak and volume. The model simulates a peak flow of 7,463 cfs for the December 2015 event, while the observed peak was 7,000 cfs. Timing for this event was good, with a flood wave peak discrepancy of 15 minutes. A high Nash-Sutcliffe value of 0.96 indicates that the simulated hydrograph is in strong agreement with the observed. The peak flow was allowed to remain slightly high to conserve volume. The model is also considered well-calibrated to April 2017 and December 2018 events (Nash-Sutcliffe values of 0.96 and 0.95, respectively). Peak timing discrepancy for April 2017 was 15 minutes, while peak flows were 5,186 cfs (simulated) and 4,720 cfs (observed). December 2018 timing was somewhat less accurate than other events, with a peak arrival discrepancy of 1 hour; however, peak flows were well-calibrated (5,455 cfs simulated and 5,090 cfs observed).

Validation of the model was done using the average parameters from calibration for the transform, losses, and baseflow parameters. Mod-Puls subreaches where consistent throughout the calibrations and carried forward through the validation runs. The existing conditions basin model utilized the same parameters as the validation runs. The future without project conditions basin model also utilized the same parameters as the validation runs with the impervious areas adjusted to account for changes in future land use (see Section 3.0 of this report for more detail on development).

The model was less accurate in validating the peak of the April 2014 event (8,528 cfs simulated vs. 10,200 cfs), while validation was moderately accurate for September 2011. Timing of the April 2014 event was good, whereby a peak wave discrepancy of 15 minutes was observed. It was impossible to reach the total volume of the flow hydrograph for this event. This is likely due to some missing rainfall volume in the precipitation data as loss rates required to reach that peak would be unreasonably low. Peak flow during September 2011 was overestimated (13,478 cfs simulated vs. 13,000 cfs observed), although the volume discrepancy was limited to about 2%. As seen in the model, validation with April 1979 shows a severe underestimation of flow throughout the simulation (volume discrepancy of about 34%). Improved results can be observed for validation with December 1983, which is summarized by a peak flow difference of approximately 200 cfs, a volume discrepancy of 28.1%, and time discrepancy of 160 minutes.

Table 2-6: Summarized results of HMS calibration and validation simulations

Event	Calibration/ Validation	Computed Peak Flow (cfs)	Observed Peak Flow (cfs)	Computed Volume (ac-ft)	Observed Volume (ac-ft)
December 2015	Calibration	7463	7000	4449	4880
April 2017	Calibration	5186	4720	3119	3298
December 2018	Calibration	5391	5090	4137	6130
April 2014	Validation	8433	10200	8288	10040
September 2011	Validation	13214	13000	12063	13744

It should be noted that most events selected for calibration and validation have recurrence intervals of approximately 10 years or less (≤ 0.10 AEP) based on frequency analysis at USGS 02461500 (see Section 2.1.6), while the AEP of September 2011 is estimated between 0.10 and 0.04. This was due to the limited availability of data for larger events. The largest events on record (1979 and 1983) are included in the model, although they could not be reasonably used for calibration. There have been major channel improvements as well changes to urbanization and the implementation of storm water management plans since there occurrence. Therefore, these events are only included in the model as examples. Because of the limited data on recent, large events reflective of current basin conditions, there is a fair amount of uncertainty for the less frequent storms.

2.1.5 Design Rainfall

Because each heavy rainfall event is unique with high variability across even a small area, a “design storm” is used to create a more objective and homogenous rainfall pattern that can be used for engineering purposes. NOAA Atlas 14 (NOAA, 2013) was used to develop design storms for the following annual exceedance probabilities: 50%, 20%, 10%, 4%, 2%, 1%, 0.5%, and 0.2%. Due to the relatively small area covered by this study (87 sq. mi.), a single precipitation value was used over the full basin (it was confirmed that there is negligible variability in Atlas 14 guidance across the basin). Because Atlas 14 estimates are “point-specific”, an Areal Reduction Factor (ARF) is required in order to reduce the value by accounting for increasing basin area size. The following ARF equation, obtained from Allen and Degaetno (2005), was used:

$$\mathrm{ARF} = 1 - \exp\left(at^b\right) + \exp\left(at^b - cA\right) \quad \text{Equation 2}$$

where t is event duration (hour) and A is area (km^2). The coefficients a and c as well as the exponent b are empirically fit where a = -1.1, c = 2.59490 x 10^2 and b = 0.25. With t = 24 hours and A = 225 km^2, an ARF of 0.91 was obtained. Table 2-7 shows the design rainfall values, before and after applying the ARF, used for the 24-hour design storms.

Table 2-7: NOAA Atlas 14 Design Rainfall Depths with and without ARF

AEP	Atlas 14	Atlas 14 with ARF
50%	4.09	3.72*
20%	4.97	4.52*
10%	5.82	5.29*
4%	7.18	6.53
2%	8.38	7.63
1%	9.71	8.84
0.5%	11.20	10.19
0.2%	13.30	12.10

**Additional reduction made to account for partial duration to annual duration conversion.*

The temporal distribution of the design storm was based on a site-specific distribution developed from NOAA Atlas 14 precipitation (NOAA, 2013) and using the Natural Resources Conservation Service (NRCS) procedure for development of rainfall distributions (Merkel, Moody, and Quan, 2015). The goal was to include all of the rainfall amounts at the shorter durations, such as the 5-minute, 10-minute, and 1-hour, rainfall provided within NOAA Atlas 14 for the 24-hour rainfall distribution. The Valley Creek study area is categorized under the Midwest-Southeast (MSE) Type 5 distribution, where the ratio of the 60-minute to 24-hour rainfall intensity is typically between 0.38 and 0.43. The 0.04 AEP site specific storm distribution was chosen as the distribution for all frequency storms. This distribution contains a ratio of 60-minute to 24-hour rainfall intensity of 0.40. Figure 2-8 shows the site-specific distribution compared to the NRCS TP-40 Type II distribution used for this area.

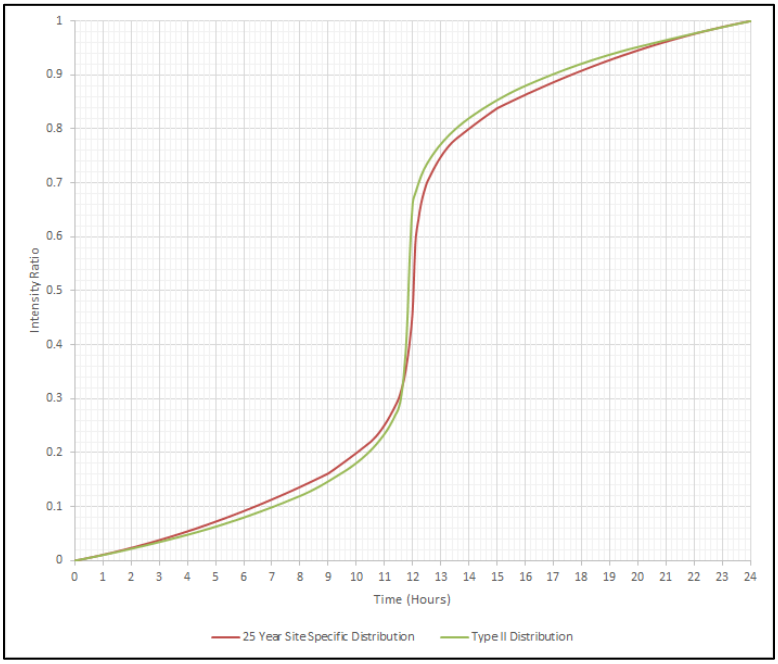

Figure 2-8: *Rainfall distribution used for design storms compared to Type II distribution.*

2.1.6 Frequency Simulation Results

Design storms were applied to the existing hydrologic conditions basin model and used to produce flow estimates for 0.50, 0.20, 0.10, 0.04, 0.02, 0.01, 0.005, and 0.002 AEP events. Peak computed flows were compared to other data sources including the current, effective flood insurance study (FIS; FEMA, 2019) and regional information (Figures 2-9 through 2-11). Hydrology supporting the effective FIS (FEMA, 2019) is based on regional regression (Hains, 1973 and Sauer, 1986), and aligns very closely with weighted regression estimates at Princeton Parkway and U.S. Route 11 (Figures 2-9 and 2-10).

Regional data were derived from regression models applicable to the study basin (i.e., Hedgecock and Lee, 2010) and computed via StreamStats (USGS, 2018). The derivation of updated regression models is important to note as gages within the study basin, or surrounding watersheds within Jefferson County, were not utilized in their development due to concerns with excessive urbanization (Hedgecock and Lee, 2010). The regression values are plotted with their associated margin of error (+/- 31%). Additionally, results were compared to flow frequencies computed for the appropriate gage on Valley Creek (Figure 2-12). Frequency flow estimates from regression models were weighted with estimates from the gage frequency analysis at USGS 02461500 using methods provided by Hedgecock and Feaster (2007). The weighted estimates were transferred upstream and downstream to the study inflow locations for comparison with other datasets.

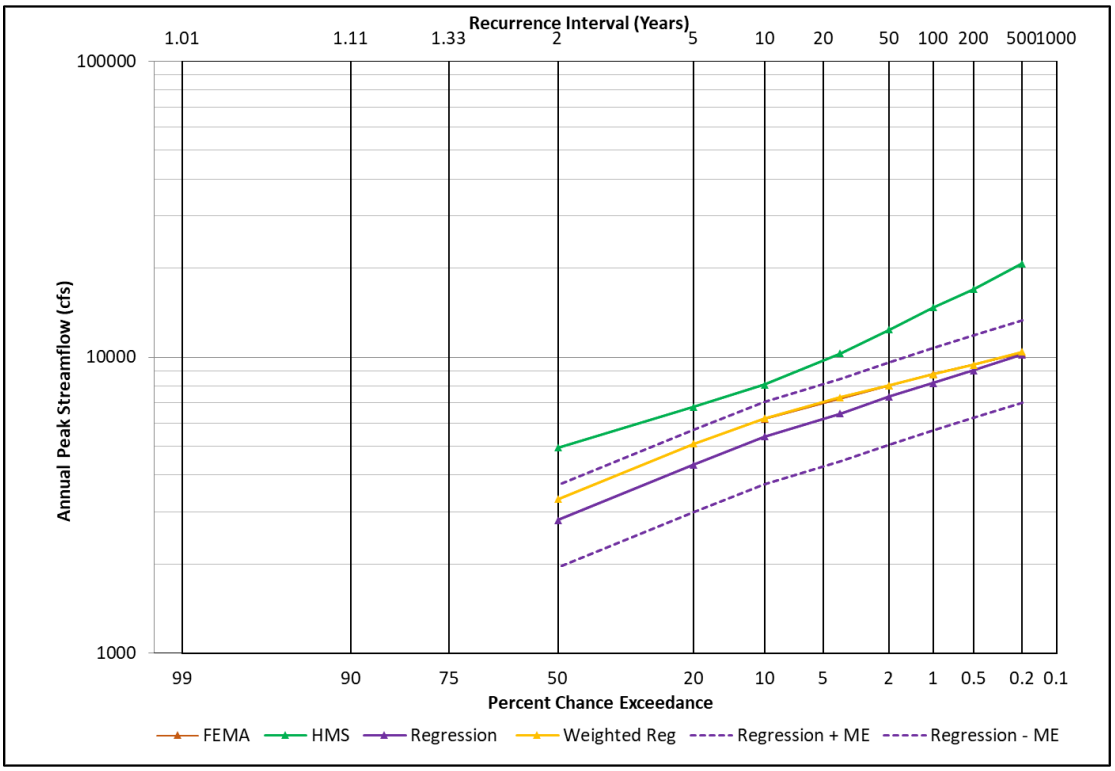

Figure 2-9: *Peak flow comparisons at Princeton Parkway (near upstream model extent; USGS 02461130 location).*

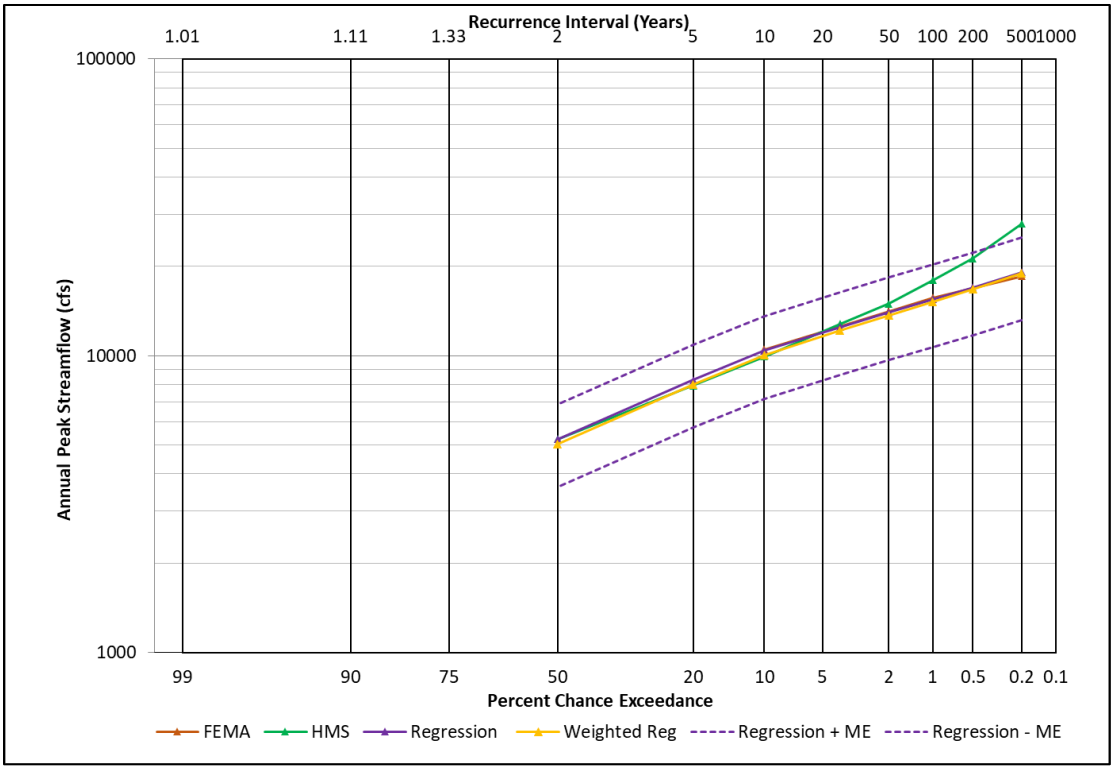

Figure 2-10: *Peak flow comparisons at U.S. Route 11 (near middle of model extents).*

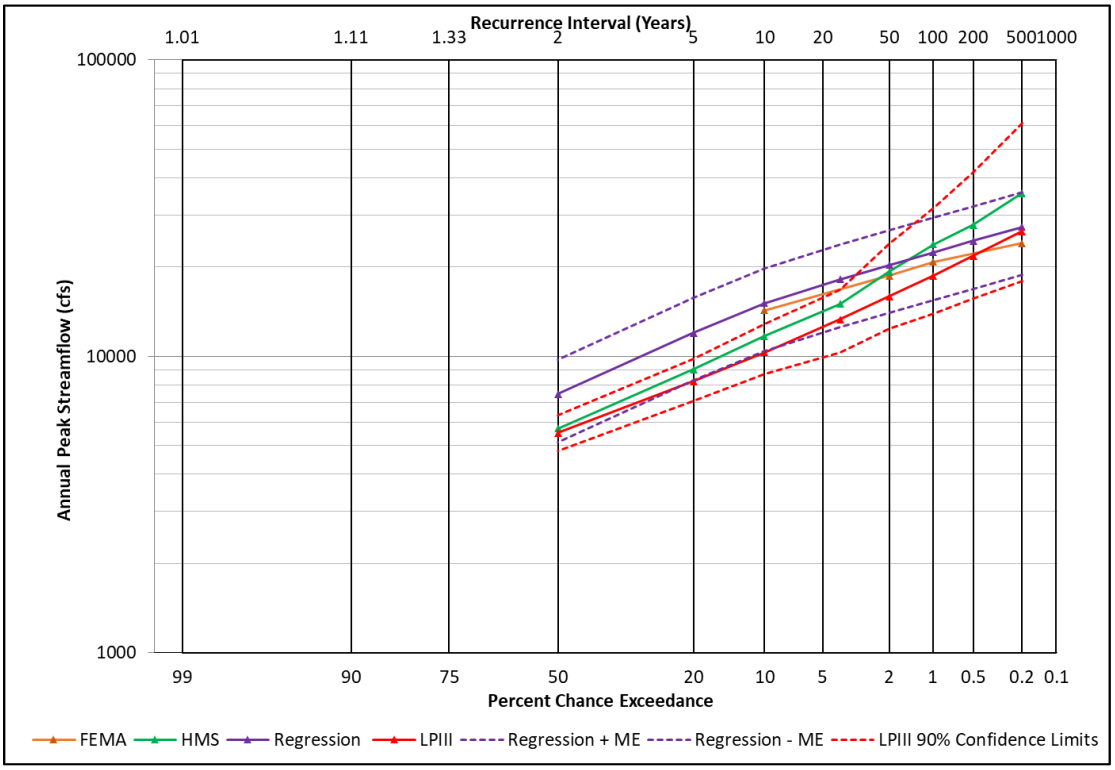

Figure 2-11: *Peak flow comparisons at 19th Street North (near downstream extent of measures/impacts; USGS 02461500 location). Note: LPIII = Log-Pearson Type III and is equal to weighted regression at this location.*

Overall, the peak frequency flow rates simulated in HMS have a reasonable agreement with regional and other published datasets. At USGS 02461500 (19th St. North), HMS produced similar peak flows to other datasets through the range of simulated frequencies. At this location, the most valuable dataset for comparison with HMS results is the gage frequency analysis developed from records at this site (Figure 2-10; 90% confidence limits shown). Discrepancies were larger for less frequent events (i.e., < 0.04 AEP). The average difference between the peaks from these datasets was 3,455 cfs. At U.S. 11, HMS is in strong agreement with compared datasets for most events. A peak discrepancy of 8,904 cfs exists between the model and the weighted regression estimate for the 0.002 AEP event; however, this value is near the upper limit of the regression model margin of error (25,021 cfs). At Princeton Parkway, the largest peak flow discrepancies (between weighted regression and HMS) occurred; results averaged 4,545 cfs.

The gage frequency analysis was completed by standard methods (Bulletin 17C; England et al., 2017), whereby a Pearson Type III distribution (and corresponding 90% confidence interval) was fit to the logarithm of observed annual peak flows at the site. One historical data point was derived from available gage information that provided a flood stage of 18.6 feet for an event in February of 1936. The published rating curve for the gage-site was extrapolated to obtain an estimate of flow associated with the provided stage value. The inclusion of this data point extended the historic period to 83 years, while a total of 35 systematic events were utilized for the analysis.

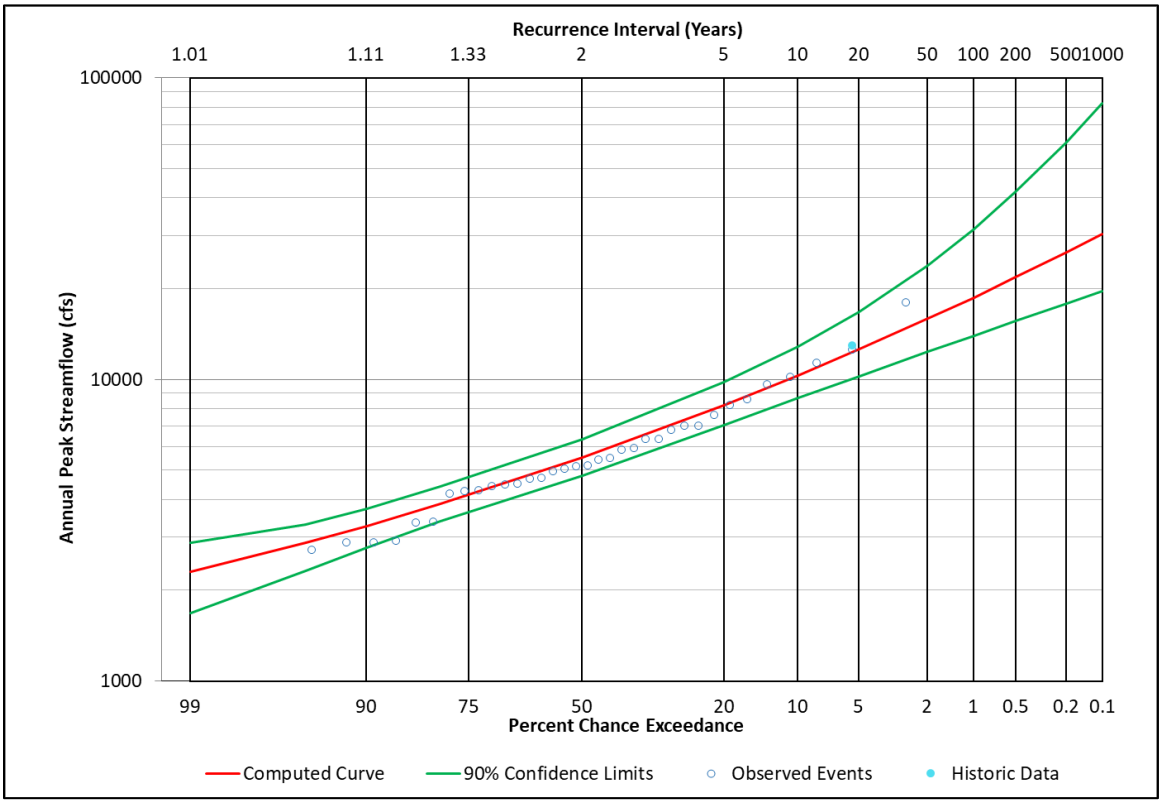

Figure 2-12: *Log-Pearson Type III frequency analysis results at USGS 02461500 (Valley Creek near Bessemer, AL).*

Consideration was made to include additional historical information from a nearby gage, USGS 02462000, which is located approximately 28 miles downstream of USGS 02461500. Data at USGS 02462000 (148.0 square-mile drainage area) includes peak records for both a 1935 and 1916 event. It is feasible to assume that such events would have also produced significant flows at 02461500, so analysis was completed to analyze the correlation between the two gage sites. Based on 16 shared events, only a weak, positive correlation could be established (Figure 2-13). Moreover, for some shared events, higher peak flow rates were observed at the site of interest (02461500), where the contributing drainage area (52.5 square miles) is significantly less than the target site (148.0 square miles). For these reasons, it was determined that strong estimates of peak flows at 02461500 for these events could not be made.

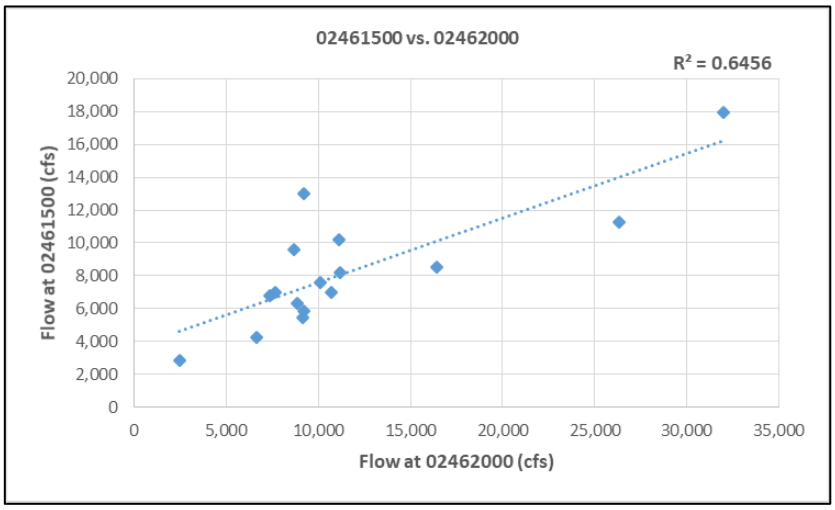

Figure 2-13: *Correlation between USGS 02461500 (y) and USGS 02462000 (x) based on 16 annual peak flow observations.*

2.2 Hydraulics

2.2.1 Hydraulic Model Background

The existing conditions (EC) hydraulic model was developed from an existing model previously constructed by a contractor and the Mobile District. This model was produced for a joint effort originally in support of the Silver Jackets Flood Forecasting and Inundation Mapping (FFIM) program. For various reasons, this effort was discontinued; however, a flood mapping effort for Valley Creek was undertaken by the Mobile district for the City of Birmingham beginning in August of 2018. This effort was postponed due to the initiation of the FRM study for Valley Creek. The previously developed model was heavily modified to better represent the existing conditions of the study area. Modifications included bridge additions and modifications along Valley Creek, the addition of reaches for detailed modeling of Opossum Creek, Halls Creek, and the unnamed tributary draining to Halls Creek, addition of new cross sections, reconfiguration of existing sections, addition of 2-D flow areas (with corresponding connecting structures) on Valley Creek, addition of storage areas on Valley Creek, and geometry parameter adjustments.

2.2.2 Model Overview

Valley Creek

The hydraulic model was developed in the Hydrologic Engineering Center's River Analysis System (HEC-RAS), version 5.0.7. The model consists of both 1D and 2D components. Valley Creek is modeled as a 1D reach from its headwaters near downtown Birmingham at RS 2859+15, to a location just downstream of the Murphys Lane Bridge in Bessemer (RS 2140+07). At this location, the 1D reach transitions into a 2D mesh. Further downstream, just upstream of Powder Plant Road, the model transitions back into a 1D reach, and continues as such to the downstream extent of the study extent (RS 1788+76). The total length of model along Valley Creek is approximately 20.3 miles. This length features 2 storage areas (Fivemile Creek and leveed area), and a total of 35 hydraulic structures including two lateral weirs (one levee and one railroad embankment), 28 bridges, and 5 culverts. One bridge is modeled as a culvert to comply with 2D modeling limitations (WWTP bridge at Valley Creek Water Reclamation).

Opossum Creek

Opossum Creek was initially added into the model for analysis of a measure on this system; however, it became apparent that its inclusion was also necessary for accurate modeling of flow contributions from this tributary. The presence of a large railroad embankment and narrow bridge crossing the Opossum Creek floodplain approximately 700 feet above the stream's confluence with Valley Creek greatly reduces peak flows into the system. It was considered highly important to capture this both hydrologically and hydraulically given the substantial flows that Opossum Creek contributes, and its proximity to several measures and areas of concern on Valley Creek.

Several alternative configurations of Opossum Creek beginning approximately 2,400 feet above Davey Allison Boulevard were modeled, including 1D/2D and 1D only types. The final configuration, however, features a simplified approach by utilizing only a 2D mesh that extends from a location just below Davey Allison Boulevard, to the aforementioned railroad embankment above the Valley Creek confluence. Simplification was made based on an understanding that suitable analysis of benefits and impacts would not require unique modeling of this reach to the previous extent. Early modeling showed that the measure would not be likely to cause impacts on the reach, and, because the measure is located just upstream of the Valley Creek confluence, the benefits would be observed on Valley Creek only.

Halls Creek and Tributary

Halls Creek and the unnamed tributary draining to it are both 1D reaches that combine at a junction, flow into a short combined 1D reach, and transition into a 2D mesh. Stationing on the streams is based on distance above the Halls Creek-Valley Creek confluence. The 2D mesh is the same mesh that serves as an inline connection on Valley Creek. Thus, this mesh ("Halls &

Quarry") converts 1D flow from two inline connections. This modeling approach was pursued as a most accurate method of portraying the characteristics of floodplain hydraulics in and around the overbanks of Valley Creek and Halls Creek, the confluence of the two stream channels, and flow into and around a retired quarry in the vicinity of the confluence location. Halls Creek includes a total of 4 bridges and 2 culverts. The tributary reach includes 7 bridges and 2 culverts. A lateral structure links cross sections of the streams in a location of shared floodplain near the downstream confluence (above 14th Ave.).

2.2.3 Hydrologic Record Linkage with HEC-DSS

The Hydrologic Engineering Center Data Storage System (DSS) version 7 was utilized to transfer hydrologic records between the hydrologic and hydraulic models. Additionally, DSS was utilized for collection of observed flow records from USGS gages. Appropriate linkage between these models was certified using the following methodology:

- apply "combined" flow records at all headwater cross sections (RS 2859+15 on Valley Creek, RS 106+48 on Halls Creek, and RS on 123+17 Halls Tributary) and the external boundary condition line of the Opossum Creek mesh;
- apply "local" flow records at all cross sections corresponding to subbasin outfall locations without incoming reach flow; and
- apply computed flow records at sub-basin outfall locations with incoming reach flow.

The computations applied to all DSS records (including calibration, validation, and frequency events) combined reach outflow with the "local," or subbasin, outflow at Junction 11, Junction 12, Junction 21, and Junction 29 from the HMS model. Computations at Junctions 11 and 12 combine HMS reach flow from unnamed tributaries, and the computation at Junction 29 combines reach flow from Fivemile Creek. Main stem flow from Opossum Creek is routed through the 2D mesh as described, whereby the "combined" outflow record from Junction 21_5 is applied to the mesh boundary condition line. As a result, there is no need to combine reach flow from Reach OC4 at the Valley Creek junction. The computation at Junction 21, however, combines "local" outflow from subbasins VC25 and OC7 to more accurately define the outflow location of these adjoining subbasins at the Opossum Creek confluence. Table 2-8 summarizes the HMS-RAS model linkage. In the table, boundary condition (BC) lines correspond to 2D area inflow locations.

Table 2-8: HEC-DSS record linkage detail

HMS Junction	RAS River	RAS Reach	RAS Cross Section/BC Line (2D only)	Boundary Condition
J26_2_5TH AVE. N	Halls Creek	Main Reach	10648.00	Flow Hydrograph
J26_4_SR 59	Halls Creek	Main Reach 2	3902.34	Lateral Inflow Hydrograph
J26_3_EASTERN VALLEY RD.	Unnamed Trib	Main Reach	12317.17	Flow Hydrograph
J1_5TH AVE. AT 7TH ST. N	Valley Creek	Main Reach	285915	Flow Hydrograph

J2_4TH AVE AT 4TH ST.	Valley Creek	Main Reach	285000	Lateral Inflow Hydrograph
J3_CENTER ST	Valley Creek	Main Reach	282629	Lateral Inflow Hydrograph
J4_PRINCETON PARKWAY_8TH	Valley Creek	Main Reach	279016	Lateral Inflow Hydrograph
J5	Valley Creek	Main Reach	278348	Lateral Inflow Hydrograph
J6_12TH ST. W AT LOMB AVE.	Valley Creek	Main Reach	276356	Lateral Inflow Hydrograph
J7_FAYETTE AVE. SW	Valley Creek	Main Reach	272665	Lateral Inflow Hydrograph
J8_AVENUE W	Valley Creek	Main Reach	270826	Lateral Inflow Hydrograph
J9_SOUTH PARK RD.	Valley Creek	Main Reach	267785	Lateral Inflow Hydrograph
J10_CLEBURN AVE	Valley Creek	Main Reach	259854	Lateral Inflow Hydrograph
RAS AT J11*	Valley Creek	Main Reach	259181	Lateral Inflow Hydrograph
RAS AT J12*	Valley Creek	Main Reach	255814	Lateral Inflow Hydrograph
J13	Valley Creek	Main Reach	251745	Lateral Inflow Hydrograph
J14_WHATTEY ST.	Valley Creek	Main Reach	247936	Lateral Inflow Hydrograph
J15	Valley Creek	Main Reach	239419	Lateral Inflow Hydrograph
J16_9TH AVE. N, ROUTE 11	Valley Creek	Main Reach	236455	Lateral Inflow Hydrograph
J17_HARMER ST.	Valley Creek	Main Reach	233059	Lateral Inflow Hydrograph
J18_OLD WOODWARD IRON RR	Valley Creek	Main Reach	231881	Lateral Inflow Hydrograph
R_TR3_1	Valley Creek	Main Reach	231160	Lateral Inflow Hydrograph
J20_JAYBIRD RD.	Valley Creek	Main Reach	230070	Lateral Inflow Hydrograph
RAS AT OPOSSUM MOD*	Valley Creek	Main Reach	223694	Lateral Inflow Hydrograph
J23	Valley Creek	Main Reach	223351	Lateral Inflow Hydrograph
J24_BESSEMER GAGE 19THST	Valley Creek	Main Reach	219065	Lateral Inflow Hydrograph
J25_13TH STREET	Valley Creek	Main Reach	214454	Lateral Inflow Hydrograph
J28_POWER PLANT RD	Valley Creek	Main Reach 2	202960	Lateral Inflow Hydrograph
RAS AT FIVEMILE CREEK*	Valley Creek	Main Reach 2	199083	Lateral Inflow Hydrograph
J30	Valley Creek	Main Reach 2	194221.	Lateral Inflow Hydrograph
SB_VC34**	Valley Creek	Main Reach 2	179662	Lateral Inflow Hydrograph
N/A	Valley Creek	Main Reach 2	178875.7	Normal Depth
J26_DOWNSTREAM HALL CREEK	Valley Creek	2D Flow Area	Halls & Quarry BC Line: DS Halls Creek	Flow Hydrograph
J27	Valley Creek	2D Flow Area	Halls & Quarry BC Line: J2040	Flow Hydrograph
J21_5	Opossum Creek	2D Flow Area	Opossum Creek BC Line: Opossum Creek	Flow Hydrograph

2.2.4 Calibration

As mentioned, the existing conditions model was developed from a previous Silver Jackets model. Base roughness coefficients for this model were selected utilizing aerial imagery, field reconnaissance, and standard guidance (see, e.g., Cowan, 1956 Chow, 1959; Rouse, 1965; FHWA, 1979; Yen, 1991; and Hicks and Mason, 1991). This steady flow model was initially calibrated to both rating curves available within the study extents (USGS 02461130 and USGS 02461500). The final existing conditions model was calibrated to the hydrographs of the selected calibration events. The availability of observed data fluctuated with each event (see Table 1-1). Figures 2-14 through 2-17 provide stage and flow hydrographs for December 27-28, 2018. Figures 2-18 through 2-20 provide stage and flow hydrographs for April 2-3, 2017. Finally, Figure 2-21 provides stage and flow hydrographs for December 25-26, 2015.

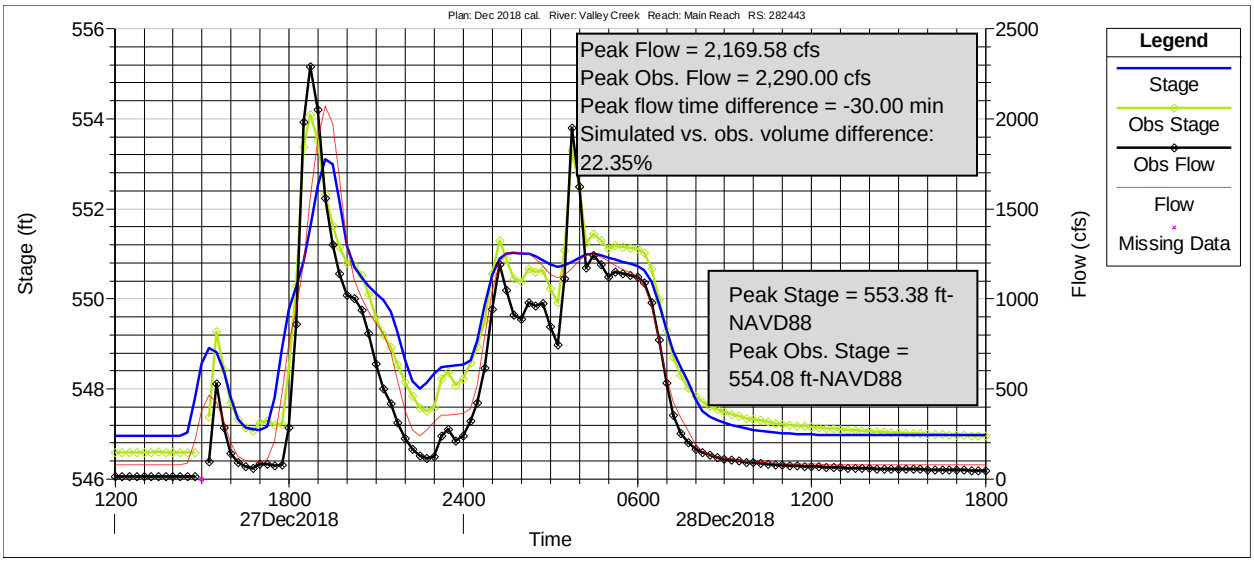

Figure 2-14: *December 2018 calibration at USGS 02461130.*

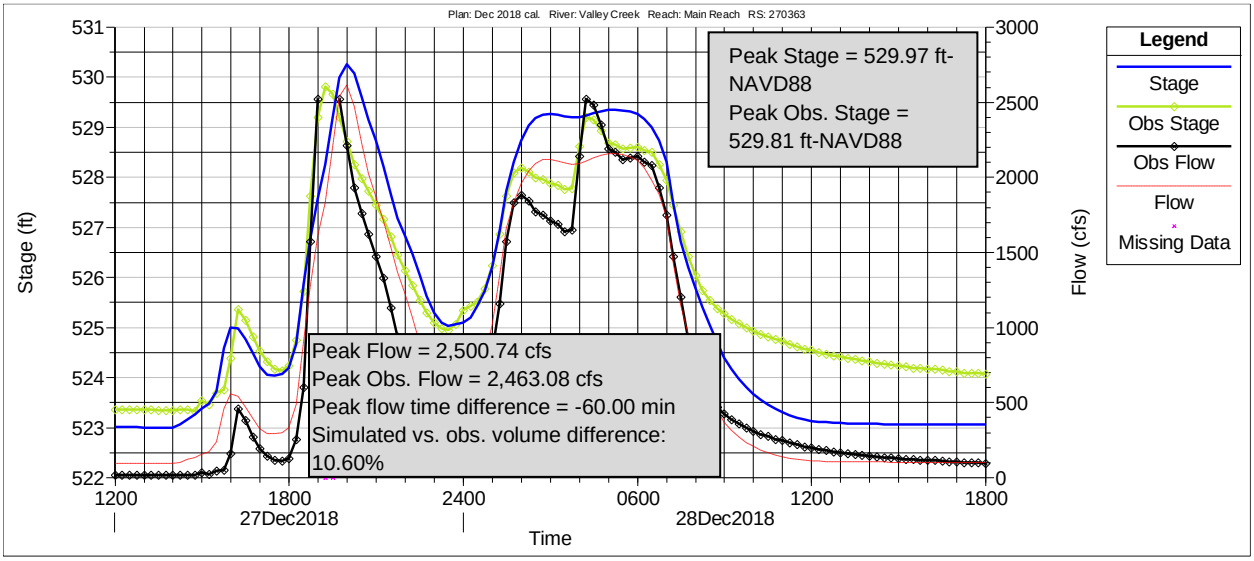

Figure 2-15: *December 2018 calibration at USGS 02461192.*

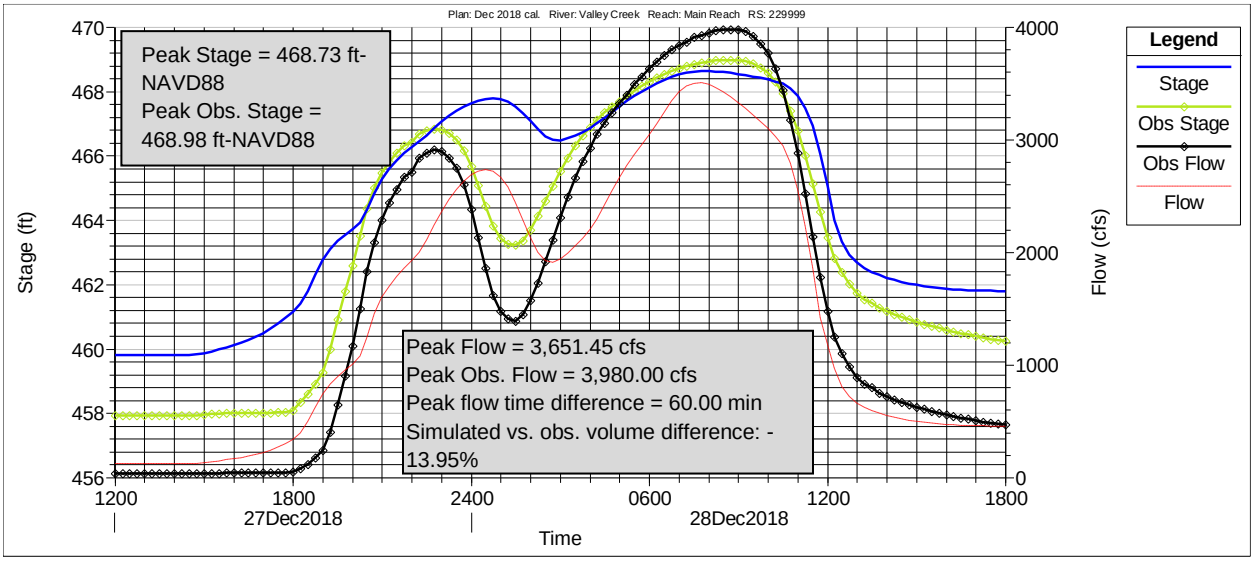

Figure 2-16: *December 2018 calibration at USGS 02461405.*

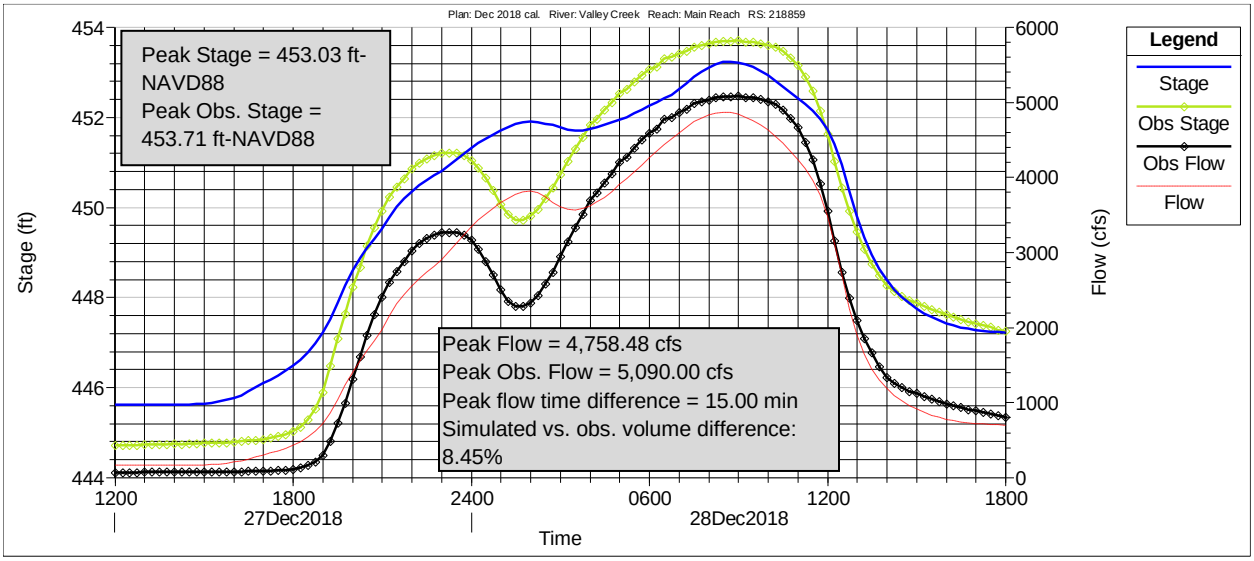

Figure 2-17: *December 2018 calibration at USGS 02461500.*

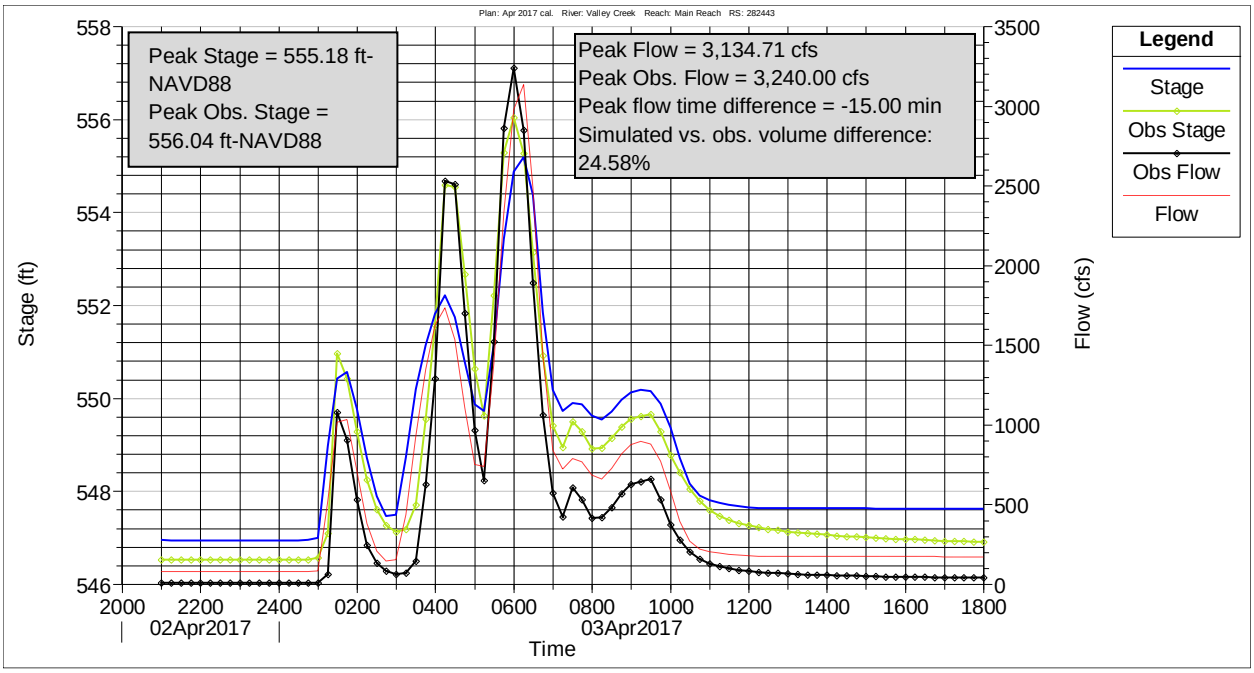

Figure 2-18: *April 2017 calibration at USGS 02461130*

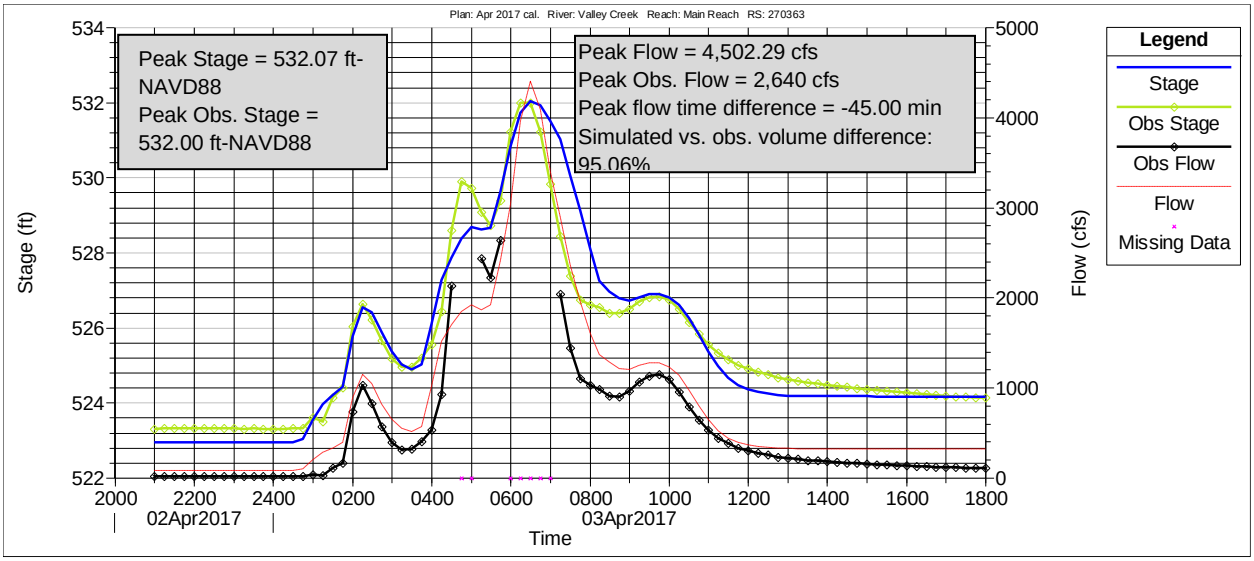

Figure 2-19: *April 2017 calibration at USGS 02461192 (note missing flow records).*

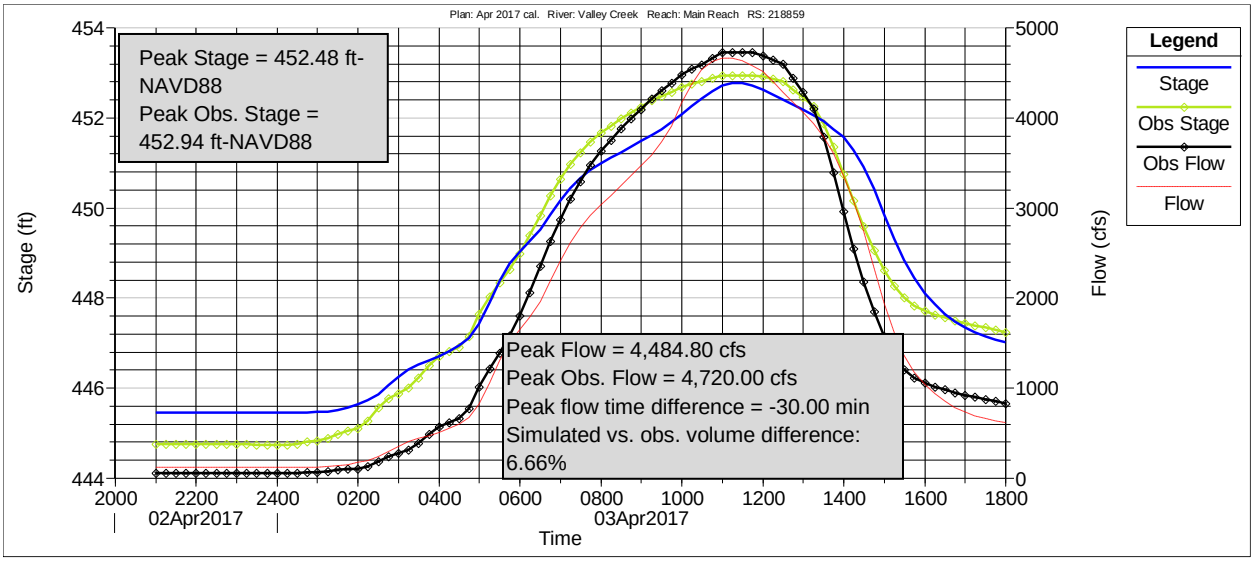

Figure 2-20: *April 2017 calibration at USGS 02461500.*

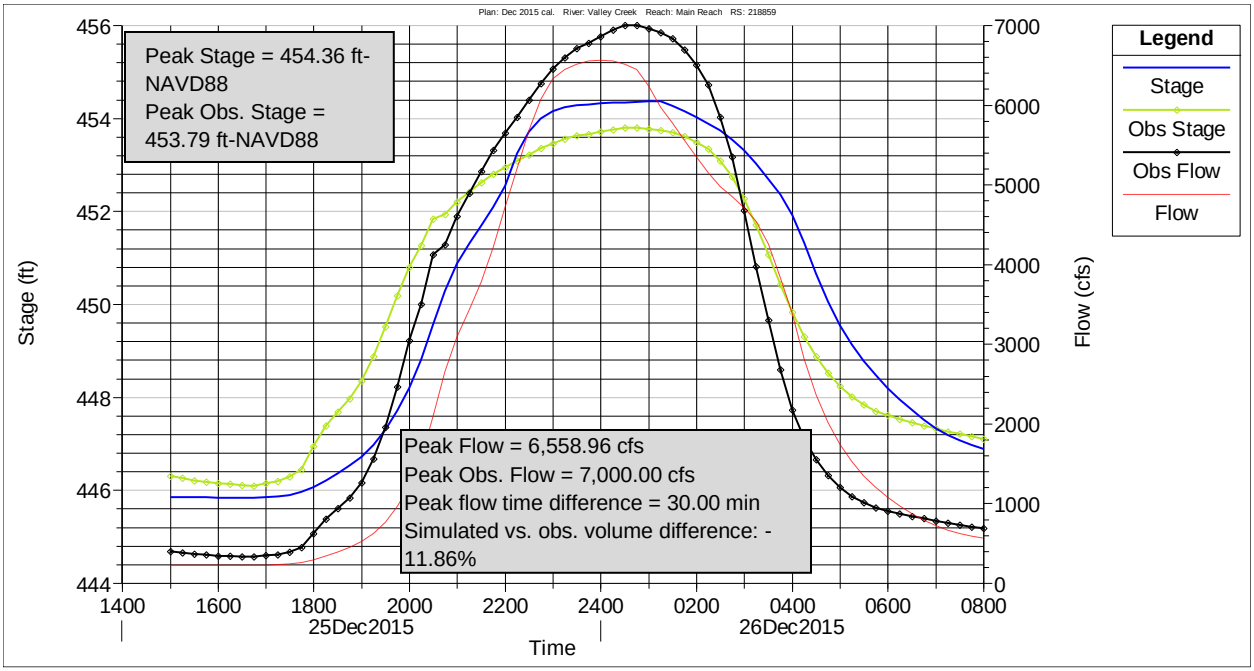

Figure 2-21: *December 2015 calibration at USGS 02461500.*

2.2.5 Calibration Results and Discussion

December 2018

Upon completion of calibration, the model is considered accurate in simulating the characteristics of the flood wave observed during the December 2018 event. Timing of the hydrograph peak is within 60 minutes for all locations. The volume difference between observed and simulated results was greatest at USGS 02461130 (22.35%). Additionally, the largest peak flow difference was approximately 332 cfs at USGS 02461500, while a maximum difference of 0.70 feet was computed from simulated and observed stages (USGS 02461130). The largest peak stage value is outside of calibration ranges typically employed for modeling practice; however, it occurs at one of the previously described stations where a high-level of uncertainty is associated with the gage datum.

April 2017

Calibration between the model and observed data for the April 2017 event was completed with the largest volume discrepancy occurring at USGS 02461130 (24.58%). A larger volume difference is shown for USGS 02461192; however, this value is in error due to missing data at this station. The largest stage discrepancy occurred at USGS 02461130 (estimated datum) and was computed as 0.86 feet. The maximum difference in peak flow rate was about 236 cfs, which occurred at USGS 02461500 (omitting results from 02461192 based on missing data). The maximum difference in peak flow timing was computed as -45.00 minutes and located at USGS 02461192 where missing data is applicable. Despite this, timing is considered to be strong based on the locations of the rising and falling limbs of the hydrographs.

December 2015

Calibration for this event is moderately strong with a peak flow discrepancy of approximately 441 cfs, peak stage discrepancy of 0.57 feet, and volume difference of -11.86%. Timing of the flood wave peak was within 30 minutes of the observed.

2.2.6 Validation

In order to gage the accuracy of model calibrations and performance, validation events were selected. Model simulations with April 2014, September 2011, and the previously discussed historic flood events of April 1979 and December 1983 (stage records unavailable) were run as validations. Results from these simulations are limited to USGS 02461500 and are provided in Figures 2-22 through 2-25.

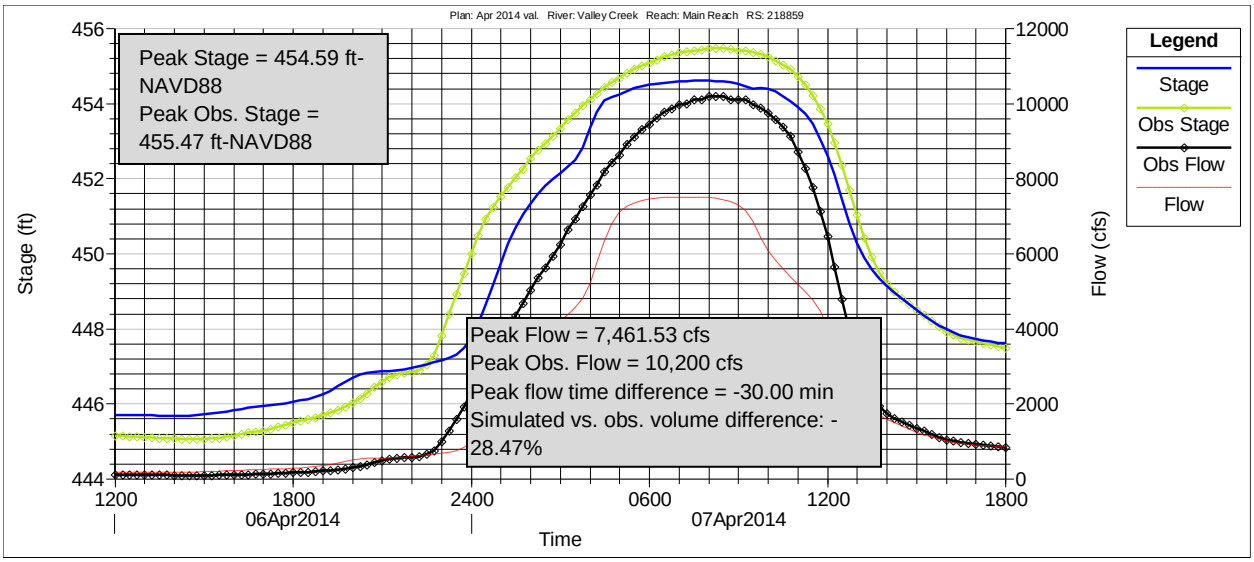

Figure 2-22: *April 2014 validation at USGS 02461500.*

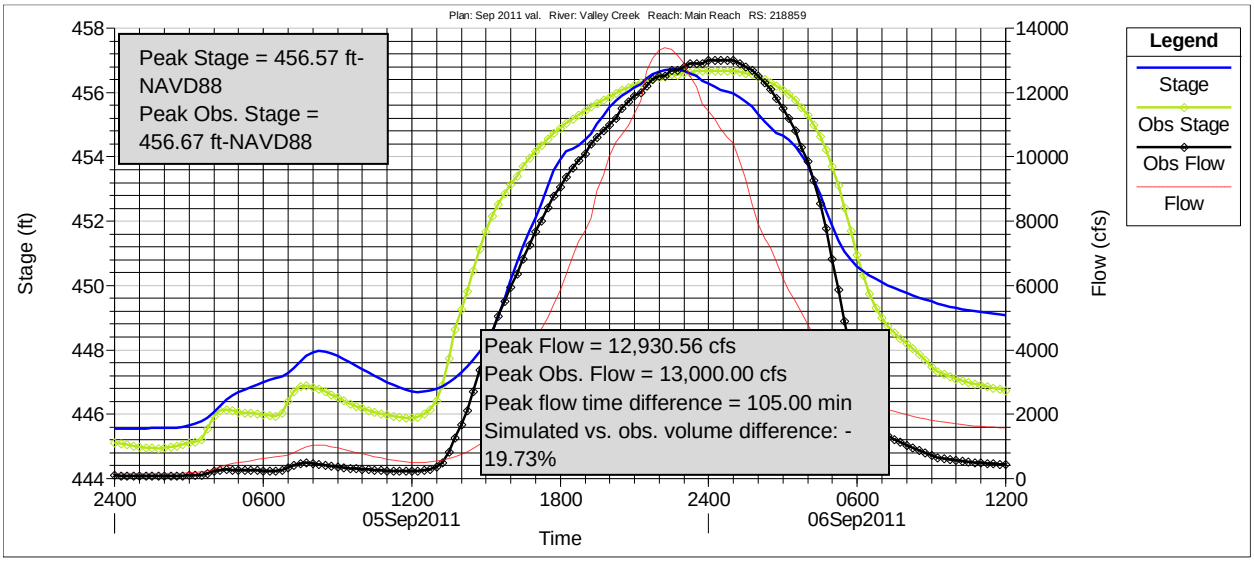

Figure 2-23: *September 2011 validation at USGS 02461500.*

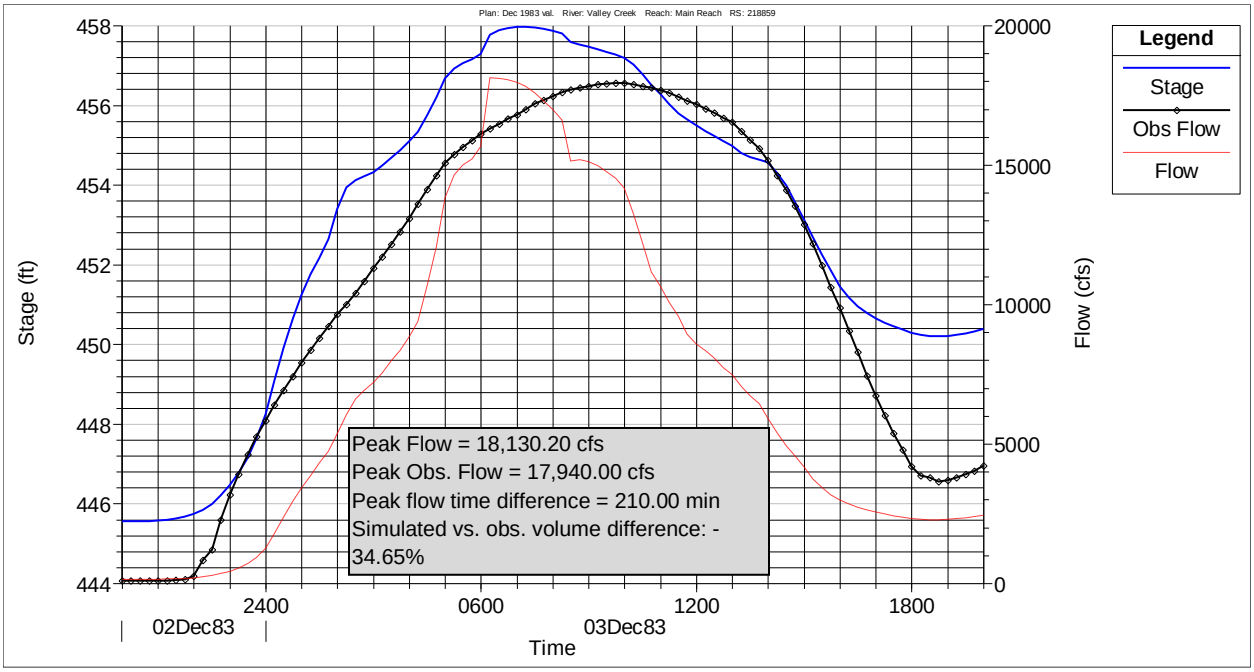

Figure 2-24: *December 1983 validation at USGS 02461500 (observed stage unavailable).*

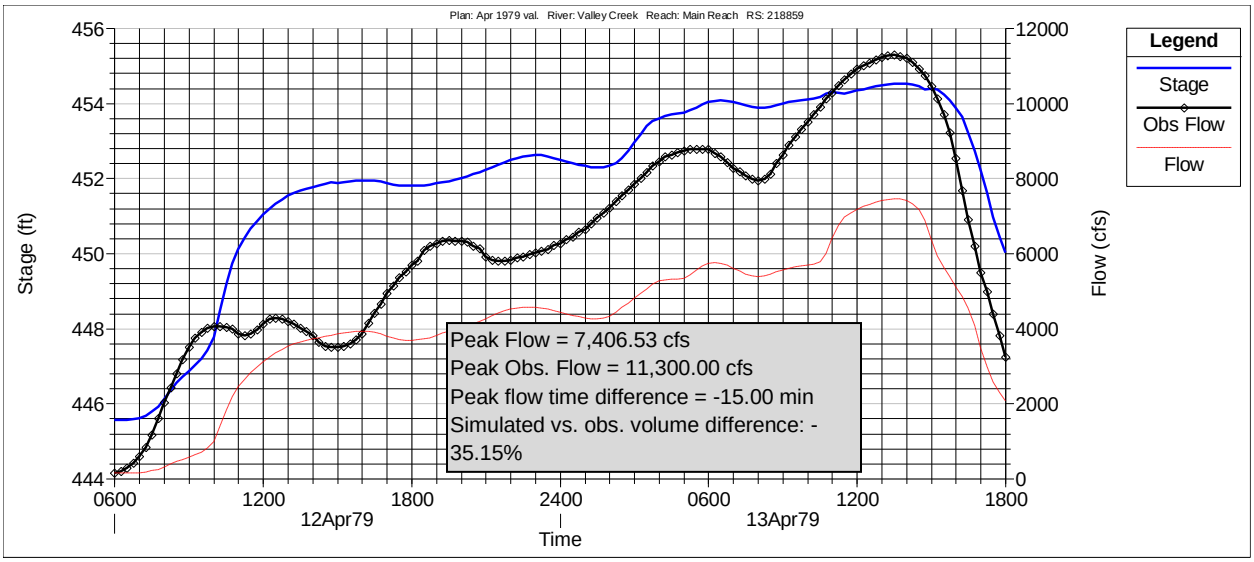

Figure 2-25: *April 1979 validation at USGS 02461500 (observed stage unavailable).*

The existing conditions model does not accurately simulate the April 1979 event; the model does somewhat accurately simulate the September 2011 event. For April 2014, the timing of the model appears to be very good; however, the discrepancy in peak flow and volume is considered high (approximately 2,738 cfs and 28.47%, respectively). For this event, however, a high level of confidence was not associated with the rainfall data. The poor results from April 1979 are not considered critical due to the previously described differences in basin conditions between existing conditions and those during the analyzed historic flood events. The main factors contributing to the substantial difference in peak flow rates are most likely channel modifications to Valley Creek that occurred upstream and in the vicinity of the gage, and construction of bridges upstream. Additionally, it is possible that the railroad embankment near the Valley-Opossum confluence (described previously) was not yet in place for this event. If the railroad embankment was not constructed, the modeling approach employed for Opossum Creek is inaccurately detaining flows from this system, which may help to explain the substantial loss in volume for this validation event as well as December 1983. The simulated, early arrival of the hydrograph for this event is likely the result of urbanization.

2.2.7 Frequency Simulation Results

Simulation of the 0.50, 0.20, 0.10, 0.04, 0.02, 0.01, 0.005, and 0.002 AEP events produced profiles representative of the flooding potential for current floodplain conditions. Profile plots of water surface elevations along the upper 1D reach of Valley Creek (“Main Reach”) resulting from simulated flows are provided in Figure 2-26. Plots of the lower, 1D reach (“Main Reach 2”) are available in the model as well as profile information for the 2D mesh connecting the reaches. Similarly, profile plots of the modeled tributaries are not provided here.

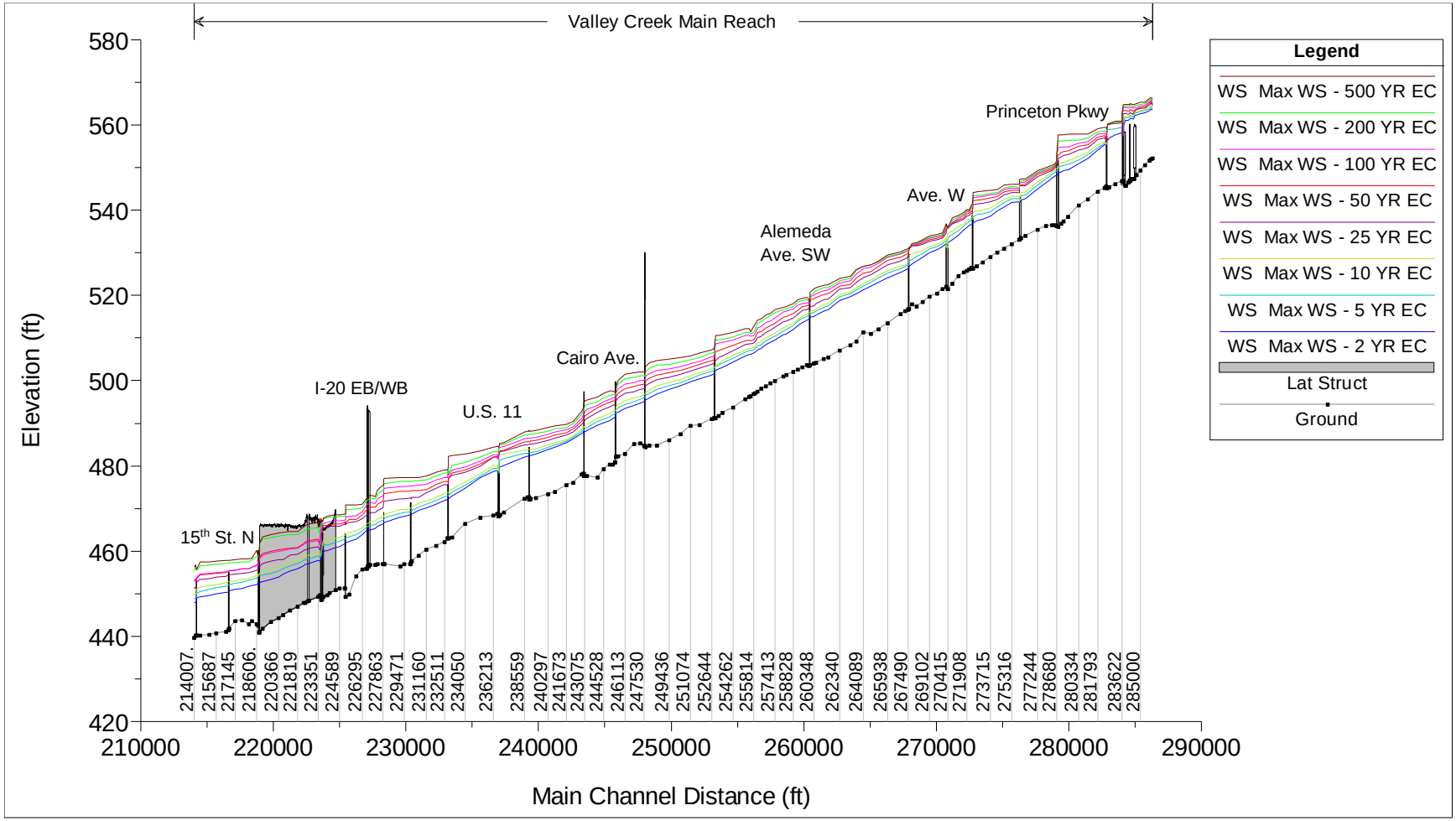

Figure 2-26: *Profile plot of EC frequency events in the upper 1D hydraulic reach of Valley Creek (river stations and some bridges shown).*

3.0 H&H Future Without Project Conditions

3.1 Development

3.1.1 Background

Future without project (FWOP) conditions flow rates were based on changes to impervious surface area within the watershed and estimated with a forecasted land-use dataset for the City of Birmingham, municipality-provided stormwater management plans, and a forecasted land use dataset provided within the Integrated Climate and Land-Use Scenarios (ICLUS) datasets available from the EPA (ICLUS, 2017a). Locally provided data were prioritized in the development of future hydrologic conditions, whereby SWMPs were consulted and used to over-ride land-use changes in applicable sub-basins. The locally provided future land-use data for the Birmingham area were analyzed for estimating changes in impervious surface area for applicable sub-basins; however, it was ultimately found that land-use within these sub-basins did not vary significantly from existing land-use (determined from National Land Cover Database [NLCD] of 2011 [Homer et al., 2015]), forecasted land-use datasets from ICLUS (2017a), and the dataset provided by the City of Birmingham. Additionally, it was found that, due to the level of existing cover, impervious surface area in these applicable sub-basins does not change from current (NLCD 2011) land-use to forecasted (ICLUS, 2017a).

3.1.2 Storm Water Management Plan implementation

SWMPs were provided for Bessemer, Birmingham, Brighton, Hueytown, Midfield, and Jefferson County. The total area of these municipalities covers the majority of the study area. The core regulation within the SWMPs is shared by the communities – post-construction hydrology shall mimic (i.e., be less than or equal to) pre-construction hydrology for 0.50, 0.20, 0.10, and 0.04 AEP rainfall events as determined from Atlas 14, Vol. 9, Version 2 (NOAA, 2013). A small portion of the drainage area within the study basin is covered by district boundaries of the McCalla, McAdory, and Eastern Valley areas. For these locations, the core regulation from the SWMPs was carried forward, due in part to their location downstream (mostly) of infrastructure analysis locations, and their very small area of coverage in comparison to the subbasins by which they are encompassed.

3.1.3 Integrated Climate and Land-Use Scenarios

The land-use datasets available from EPA are based on the 2010 U.S. Census and demographic components of mortality, fertility, and immigration as well as climate-influenced county-to-county migration to project population to 2100, and results from a spatial allocation model (Spatially Explicit Regional Growth Model [SERGoM v2]) used to project future increases in housing density (see EPA, 2017). Two datasets (per decade) consisting of forecasted land-use were available from the EPA and correspond to Socioeconomic Pathways (SSPs) 2 and 5 (SSP2 and SSP5) as described by O'Neill and others (2016). The 2070 datasets (i.e., 50-year

forecast) were initially selected from the decadal series to determine the change in urban development from existing (based on NLCD 2011) to FWOP conditions.

Forecasted impervious surface datasets were also available within the ICLUS database (EPA, 2017b). These were desirable for analysis of FWOP conditions because loss modeling via initial and constant deficit loss rates includes an allocation of impervious area per sub-basin as a model parameter. However, the forecasted impervious datasets are extremely coarse (1 km^2 resolution) and were thought to be grossly underestimating increases in impervious cover within study sub-basins. For this reason, the initially selected forecasted land-use datasets were utilized, and a relationship with impervious area was established on a subbasin scale as follows:

$$PI_{FWOP} = PU_{FWOP} \frac{PI_{EC}}{PU_{EC}} \qquad \text{Equation 3}$$

where PI_{FWOP} is the percentage of impervious area for a given sub-basin in 2070, PU_{FWOP} is the percentage of urban land-use in a given sub-basin in 2070, PI_{EC} is the percentage of impervious area in for a given sub-basin in 2020, and PU_{EC} is the percentage of urban land-use in a given sub-basin in 2020. Impervious surface area totals for each study subbasin are provided for both existing and future without project conditions in Figure 3-1. In subbasins where impervious cover was projected to decrease by 2070, the existing conditions impervious value was utilized as a conservative approach.

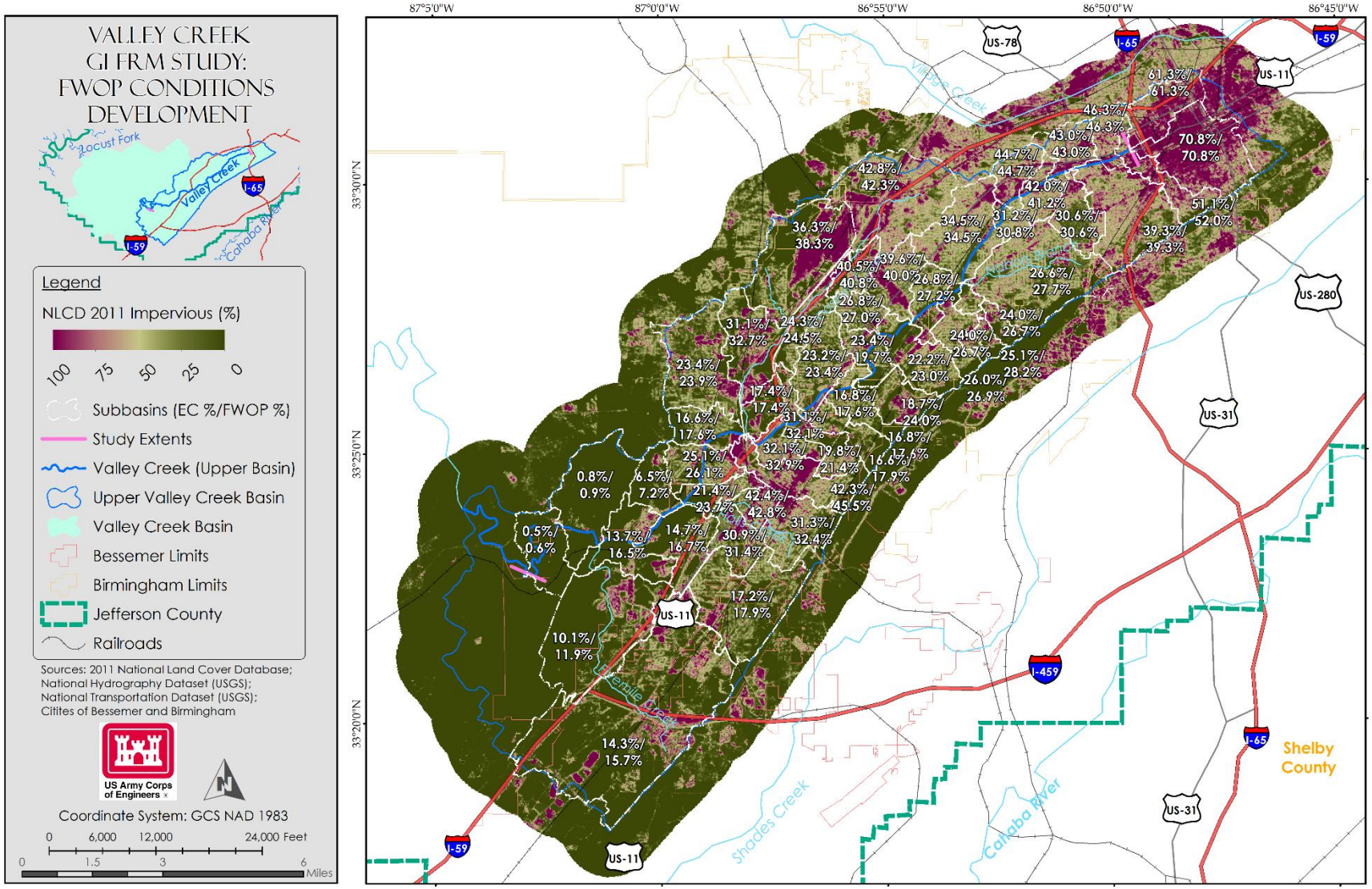

Figure 3-1: *Total impervious area values (%) for existing and future without project conditions.*

3.2 Frequency Simulation Results

3.2.1 Hydrology

The implementation of FWOP hydrologic conditions produced flow rates slightly larger than existing conditions for 0.02, 0.01, 0.005, and 0.002 AEP events at the HMS model junctions. Differences (FWOP minus EC) between peak flow rates for the study conditions were computed for all HMS model junctions and are provided in Table 3-1.

Table 3-1: Differences in peak flow rates (cfs) from EC to FWOP conditions by recurrence interval at all HMS junctions

Location	Drainage Area (mi^2)	0.50 AEP	0.20 AEP	0.10 AEP	0.04 AEP	0.02 AEP	0.01 AEP	0.005 AEP	0.002 AEP
J1_5th Ave. at 7th St. N	4.49	0	0	0	0	0	0	0	0
J2_4th Ave at 4th St.	5.67	0	0	0	0	1.2	1.2	1.2	1.2
J3_Center St	6.28	0	0	0	0	1.1	1.4	13.8	2.3
J4_Princeton Parkway/8th	9.37	0	0	0	0	3	1.3	1.1	3.1
J5	10.53	0	0	0	0	2.4	1.7	1.1	2.6
J6_12th St. W at Lomb Ave.	11.55	0	0	0	0	1.9	1.8	1.3	2.5
J7_fayette Ave. SW	12.38	0	0	0	0	1.7	1.5	1.6	2.3
J8_Avenue W	13.27	0	0	0	0	1.7	1.4	1.6	3.4
J9_South Park Rd.	13.67	0	0	0	0	1.6	1.4	1.1	2.6
J10_Cleburn Ave	16.15	0	0	0	0	1.9	1.6	4.1	2.6
JCT Nabors Branch	20.27	0	0	0	0	5.3	4.8	7.5	5.9
J11_2	0.75	0	0	0	0	1.9	1.7	1.7	1.6
J11	21.28	0	0	0	0	5.4	8.7	3.7	7
J12_2	0.19	0	0	0	0	0.2	0.1	0.1	0.1
J12_ Seaboard RR Upstream	22.48	0	0	0	0	6.1	9.2	4.7	18.6
J13	24.72	0	0	0	0	7	6.7	7.9	5.5
J14_Whattey St.	27.09	0	0	0	0	7	-31.6	8.8	8.5
J15	29.04	0	0	0	0	10.3	10.9	7.5	6
J16_9th Ave. N, Route 11	30.04	0	0	0	0	9.3	7.7	13.5	4.6
J17_Harmer St.	31.76	0	0	0	0	10.5	8	13.8	4.6
J18_Old Woodward Iron RR	32.75	0	0	0	0	11.3	10.6	13.3	11.2
J19_2	0.69	0	0	0	0	0.8	0.7	0.7	0.7

J19	33.44	0	0	0	0	12.2	11.1	13.3	13
J20_Jaybird Rd.	34.25	0	0	0	0	12.6	18.7	14.3	12.9
J21_2_South of U.S. Steel Pk	4.01	0	0	0	0	0	0	0	0
J21_3	4.8	0	0	0	0	0.2	0.2	0.2	0.3
J21_4	9.42	0	0	0	0	8.9	8.7	8.9	8.9
J21_5	14.4	0	0	0	0	13.9	11.6	11.4	109.9
J21	49.28	0	0	0	0	15.4	30.9	30.9	32.2
J22_CSX RR	50.07	0	0	0	0	28.3	19.9	24.5	27.5
J23	51.94	0	0	0	0	34.2	21.8	27.9	32.9
J24_Bessemer Gage 19thSt	53.07	0	0	0	0	35	25.9	28.5	27.8
J25_13th Street	54.31	0	0	0	0	25.7	29.7	28.7	31.5
J26_3_Eastern Valley Rd.	3.59	0	0	0	0	2.2	2.1	2.1	2.1
J26_2_5th Ave. N	1.66	0	0	0	0	1.4	1.2	1.1	1.1
J26_4_SR 59	6.98	0	0	0	0	3.5	2.9	4.1	3.2
J26_Downstream Halls Creek	62.06	0	0	0	0	19.5	35.8	34.2	67.7
J27	63.08	0	0	0	0	41.1	37.5	34.4	31.7
J28_Power Plant Rd	64.83	0	0	0	0	46.7	35.5	34	19.4
J29_2	11.05	0	0	0	0	10.2	10.1	10.2	10.2
J29_3	15.88	0	0	0	0	15.8	15.7	15.8	16
J29	82.52	0	0	0	0	58.7	47.8	48.7	59.1
J30	85.44	0	0	0	0	58.6	47.9	48.9	70.2
Outlet	86.99	0	0	0	0	58	49.3	48.5	73

3.2.2 Hydraulics

Simulation of the 0.50, 0.20, 0.10, 0.04, 0.02, 0.01, 0.005, and 0.002 AEP events with updated (FWOP) hydrology produced profiles representative of the flooding potential for floodplain conditions estimated for the year 2070. Profile plots of water surface elevations on Valley Creek resulting from simulated flows are provided in Figure 3-2.

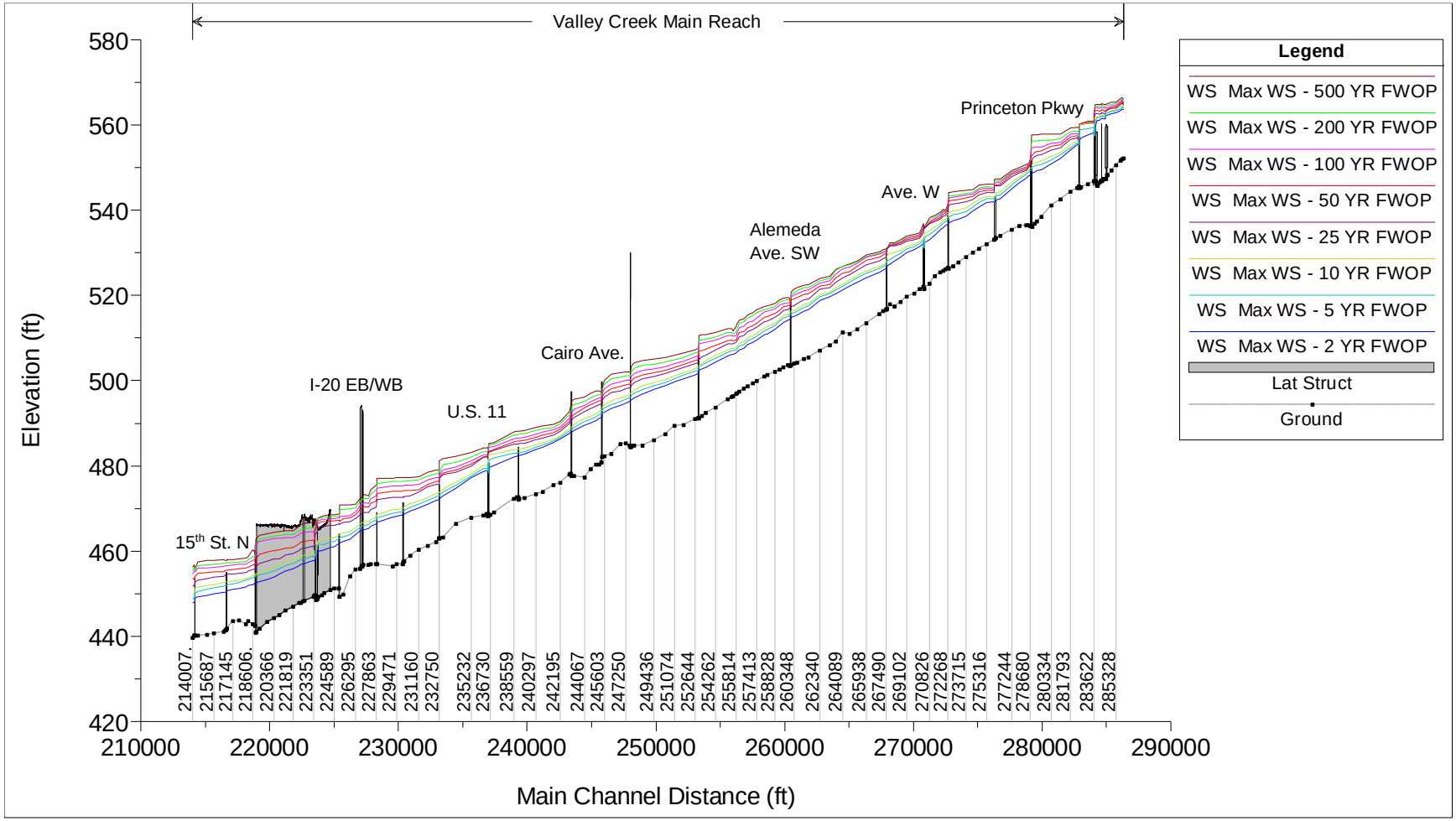

Figure 3-2: *Profile plot of FWOP frequency events in the upper 1D hydraulic reach of Valley Creek (river stations and some bridges shown).*

4.0 Flood Risk Management Alternatives

This section details the development and performance of the alternative structural plans designed for mitigation of flood risk in the Valley Creek basin. A total of 35 structural measures were identified and analyzed, from which a refined set of 18 tested measures were carried forward to alternatives formulation. A total of 17 structural alternatives were produced from these measures for which costs and national economic benefits were derived. Thorough preliminary analysis of the structural measures insured that all final alternatives were effective at producing hydraulic benefits with reduced risk and minimal impacts.

4.1 Measure Development

Structural flood risk management measures were developed based on an in-depth flood risk analysis of the study area and engineering judgment of structure-type performance. The measures were located throughout the majority of the Valley Creek study length (approximately from RS 2840+58 to 2034+67), in addition to Halls Creek and the Halls Tributary. The scope of investigation was expanded to explore FRM opportunities in these tributaries based on repetitive loss areas (data provided by the City of Bessemer [F. Freeman, personal correspondence, 16 October 2018]. The extents of exploration are in accordance with guidance (ER 1165-2-21; USACE, 1980). Measures identified for this study included overbank detention sites, dams, levees, bridge modifications, and a channel modification. A naming convention was derived for organizational purposes and is shown with details of the measures in Table 4-1. Locations of the measures are shown in Figures 4-1 through 4-4. In the figures, preliminary cross sections from the hydraulic model utilized for the Birmingham mapping effort described in Section 2.1.1 are shown.

Table 4-1: Valley Creek FRM Study Measures

Type	Name	Description
Overbank Detention	VD1	10.0 acres on left overbank downstream of Center St. One home on property and minor roadways.
	VD2	13.6 acres on left overbank downstream of Princeton Pkwy. Note: 2 sizes initially considered with largest moving forward. This area includes 3 homes and minor roadways. Size updated again through refinement phase.
	VD3	22.2 acres on left overbank at Fayette Ave. SW. Previous buyout area with minor roadways and slab foundations.
	VD4	16.4 acres on left overbank at Lincoln Ave.
	VD5	55.6 acres on left overbank downstream of Alemeda Ave. SW. Clear area but contains Land Trust.
	VD6	27.9 acres on left overbank at Hartman Industrial Blvd. Site uses existing quarry.
	VD7	38.6 acres at By Williams Sr Dr. Site uses existing, ponded quarry.
	VD8	54.5 acres on left overbank immediately downstream of By Williams Sr Dr. Area is clear of development but contains Land Trust.
	VD9	24.8 acres on right overbank immediately downstream of By Williams Sr Dr. Both areas clear of development; however, VD8 contains Land Trust.

	VD10	85.6 acres on left overbank immediately downstream of Martin Luther Ave. Area is clear of development but contains Land Trust.
	VD11	39.6 acres on left overbank just upstream of Jaybird Rd. Area is clear of development other than roadways.
	VD11b	Additional 8.5 acres on right overbank added to VD11. Open area.
	VD12	33.4 acres on left overbank just upstream of 19th St. Area is clear of development but may have HTRW issues.
	VD13	26.5 acres on left overbank just downstream of 19th St. Area is clear of development but contains Land Trust area.
Levee	VL1	Berm repair of existing RR embankment on right overbank near Quincy Ave. (745 feet).
	VL2	Levee on right overbank extending from a location just upstream of Martin Luther Ave. and tying into a point near Sugar Ray Dr. downstream (3265 feet).
	VL3	Levee on right overbank extending from Sugar Ray Dr. upstream and tying into a location due east of 47th St. (3765 feet).
	VL4	Ring levee on left embankment extending from 19th St. N upstream and tying in to I-20 embankment (8740 feet).
Bridge Modification	VB1	3rd Ave. N over Valley Creek.
	VB2	RR DS 3rd Ave. N over Valley Creek.
	VB3	Fayette Ave. SW over Valley Creek.
	VB4	By Williams Sr. Dr. over Valley Creek.
	VB5	RR DS Jaybird Rd. over Valley Creek.
	VB6	RR at Opossum Creek over Valley Creek.
	VB7	2nd RR at Opposum Creek over Valley Creek.
	VB8	Murphys Ln. over Valley Creek
	VB9[1]	18th Ave. over Valley Creek.
	HB1	8th Ave. N over Halls Creek.
	HB2	9th Ave. N/Bessemer Hwy. over Halls Creek.
	UB1	5th St. N over Halls Tributary.
	UB2[1]	9th Ave. N/Bessemer Hwy. over Halls Tributary.
Channel Modification	VC1	120-ft. channel from Murphys Ln to WWTP service bridge (approximately).
Dam	VI1	Dam as appurtenant structure to RR embankments (bridge removed) near central basin quarries with crest elevation at 516.5 ft-NAVD88.
	VI2	Dam as appurtenant structure to RR embankments (bridge converted to pedestrian) just downstream of Midfield High School with crest elevation at 505.0 ft-NAVD88.
	OI1	Dam as appurtenant structure to active RR embankments on Opossum Creek near Valley Creek confluence. Crest elevation at 465.0 ft-NAVD88.

[1]*Indicates measures that were added during the preliminary screening phase.*

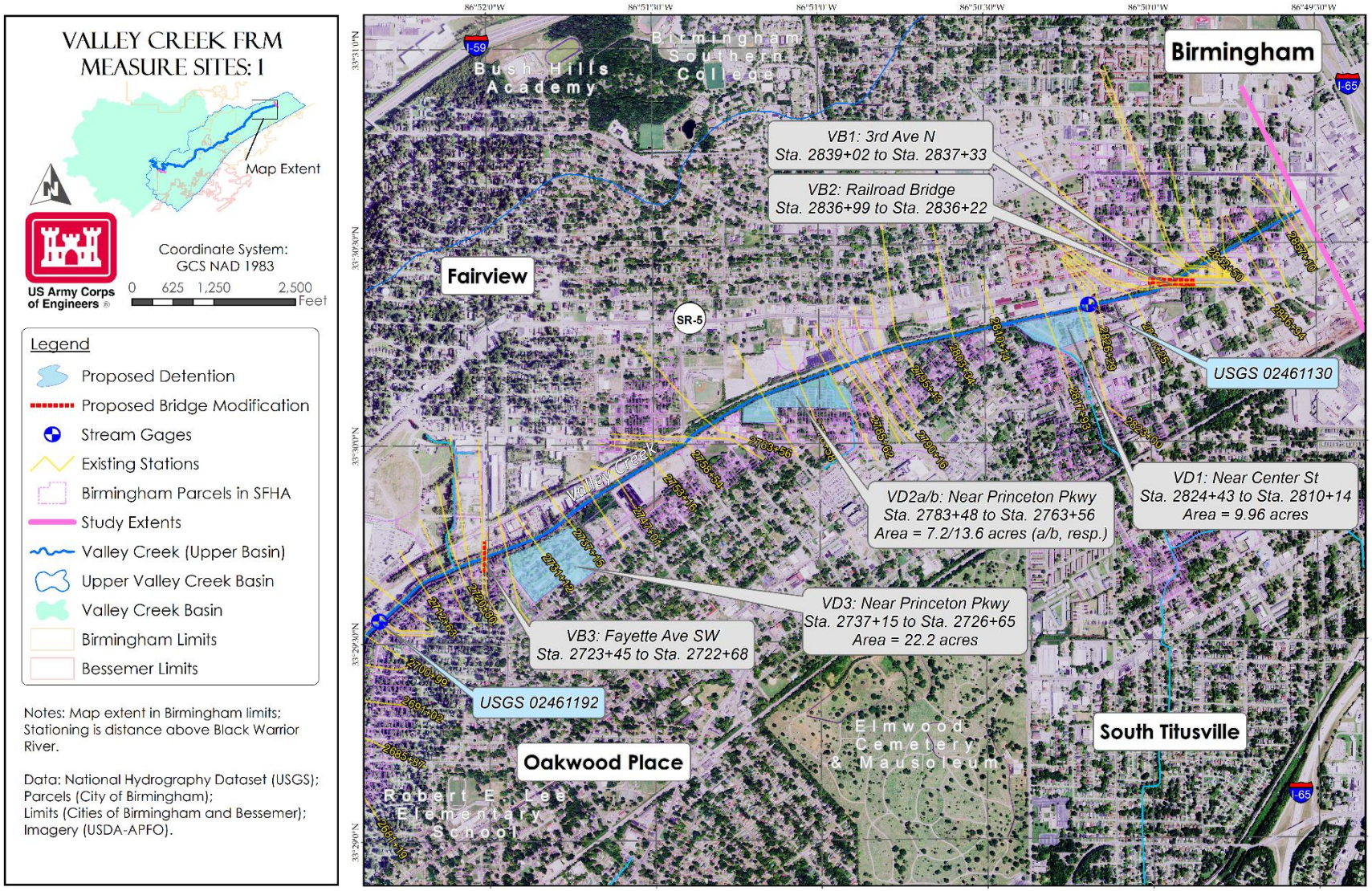

Figure 4-1: *Preliminary structural FRM measure locations in the vicinity of Valley Creek headwaters, downtown Birmingham, and Fairview.*

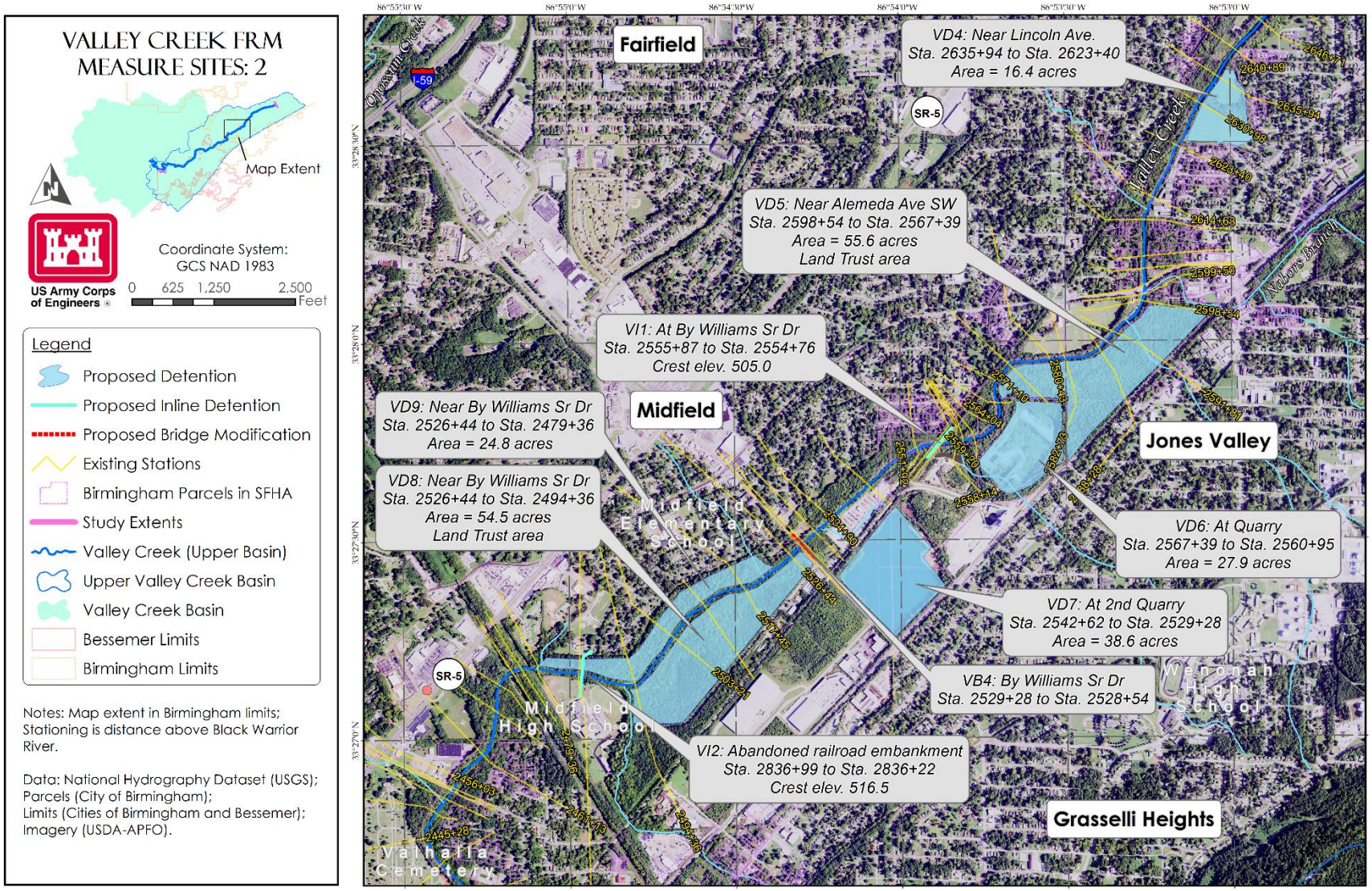

Figure 4-2: *Preliminary structural FRM measure locations in the vicinity of Midfield.*

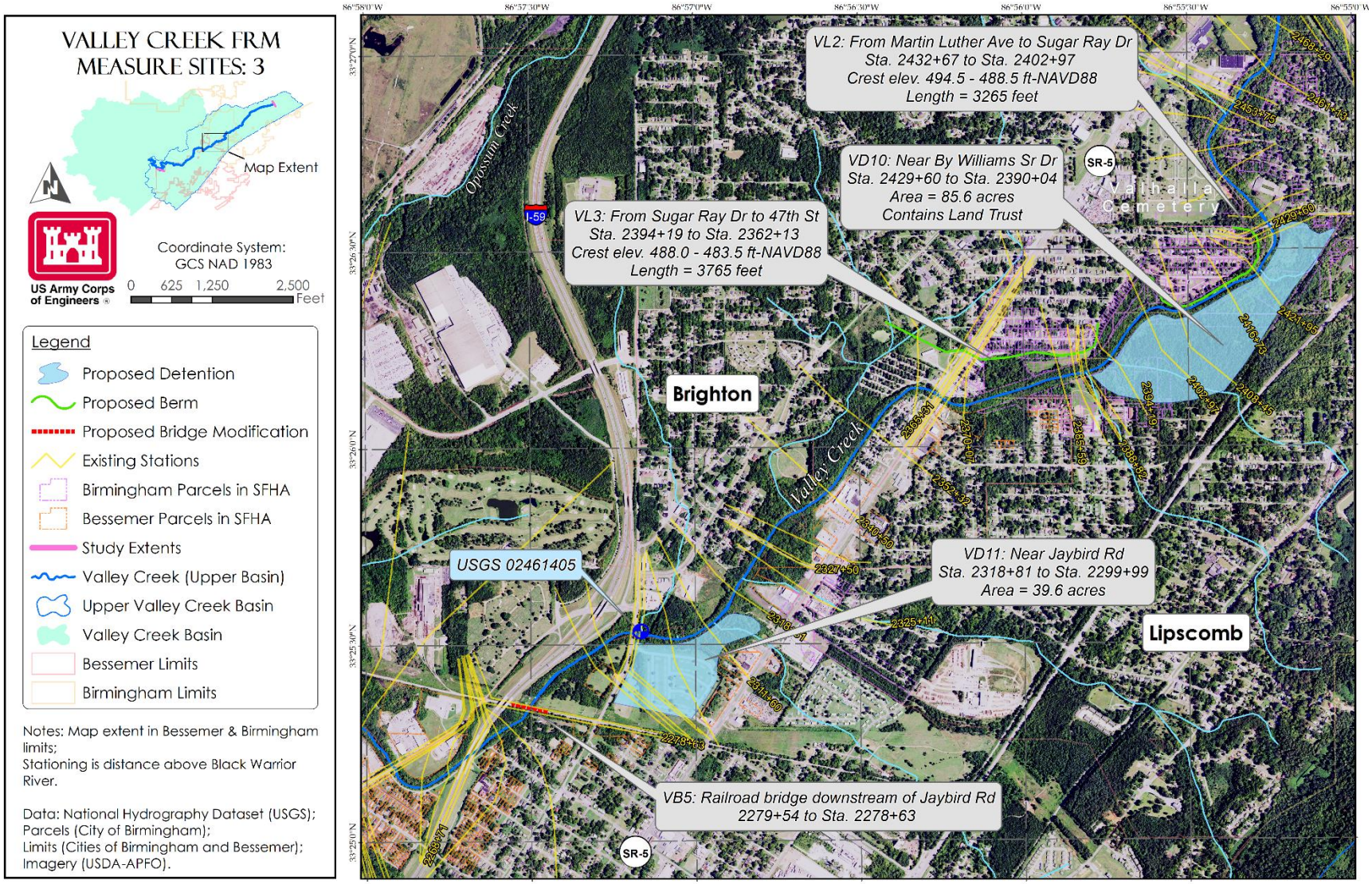

Figure 4-3: *Preliminary structural FRM measure locations in the vicinity of Brighton.*

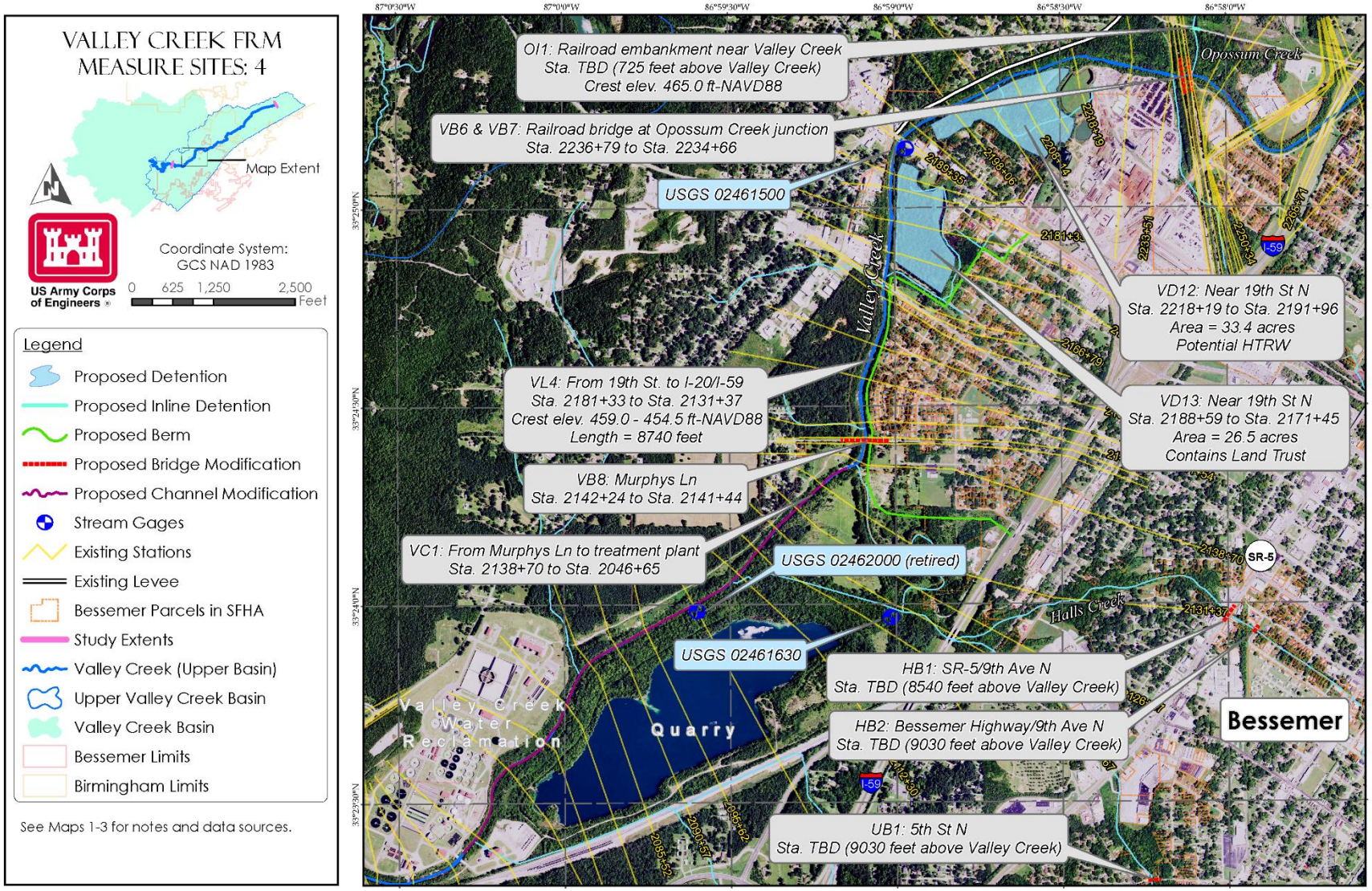

Figure 4-4: *Preliminary structural FRM measure locations in the vicinity of Bessemer, Halls Creek, and Halls Tributary. Note: Two structural measures added during preliminary screening not shown on this map (VB9 [18th Ave. over Valley Creek] and UB2 [9th Ave. N over Halls Tributary]).*

Overbank detention sites were selected based on open space availability. Due to the number of open sites available, no developed locations were considered for utilization. Bridges were initially selected for modification based on their hydraulic performance as indicated in the preliminary model discussed in Section 2.2.1. Bridges that acted as constrictions significant enough to induce backwater flooding were noted and those whose negative effects coincided with inundated structures/developed areas were selected for analysis. Inline detention sites were selected based on basin topography and hydrology as well as proximity to developed areas. Levee sites were selected based on existing flood risk in the basin, and alignments were directed by site topography and adjacent development. Finally, the channel modification measure was conceptualized based on changes to the stream geometry in its location and attributed upstream flood risk.

4.1.1 Preliminary Screening

Measures were analyzed for performance in the hydraulic model. Additionally, measures were assessed by the entire PDT on site constraints and associated risks including environmental hazards such as hazardous, toxic, and radioactive waste sites (HTRW), land-use feasibility, and real-estate restrictions. Overall, hydraulic performance was the key criteria used for measure refinement, although a small number of sites were screened based on site constraints alone. Approaches to geometry construction and the choice of frequency events simulated for screening varied based on measure-type; however, performance was consistently based on (1) a measure's ability to reduce flood risk to areas of development across the range of analyzed frequency events, and (2) the impacts associated with implementation of the measure.

Some measure testing began during the targeted Agency Technical Review (ATR) associated with this study (April – June 2019), and therefore, this initial testing occurred prior to some baseline H&H model revisions. During this time, hydrology was updated several times, and some geometric modifications were made to the RAS model. Some geometric parameters of measures were based on early hydrology and RAS geometry versions, and these are noted in the details that follow (see Section 4.1.1.1). For those measures that remained after preliminary screening, basic design parameters were updated with the final FWOP profile elevations and characteristics, and performance was verified. Those measures that were removed in preliminary screening were not analyzed with updated FWOP conditions; however, it is considered highly unlikely that their performance would differ as a result of these updates.

To execute preliminary testing, stand-alone and/or combined measure geometries were developed in the hydraulic model. For some measures, limited-detail geometries were constructed to expedite the screening process. For example, in analyzing the selected bridges for modification (i.e., lengthening spans with and without widening the stream channel), structures were removed from the geometry and a test simulation was run. For bridge modifications, effectiveness was first tested with the 0.01 AEP event, followed by the 0.04 AEP event. In cases where results of performance were not definitively obvious, additional frequency simulations were run in order to fully-illustrate the measure's performance. For other measures, more detailed geometries were constructed for preliminary screening, and alternate frequencies

were targeted for optimization. The model set-up and screening process for each measure-type are detailed in the sections that follow.

4.1.1.1 Modeling Approach

Overbank Detention

A consistent design approach was developed for modeling the detention sites remaining after preliminary screening. The measures were modeled as storage areas and connected to model cross sections via lateral structures. The lateral structures reflected a constructed berm with an inflow weir (Figure 4-5). For consistency, all berm heights were set to the 0.01 AEP FWOP water surface elevations (based on preliminary modeling) at the upstream extents of the pond locations. The storage model of each pond (Figure 4-6) was developed from the design invert elevation, projected storage capacity, and the pond berm height. The projected storage capacities of each site were based on available areas, design invert elevations, and an applied 30% reduction to account for side slopes and site grading.

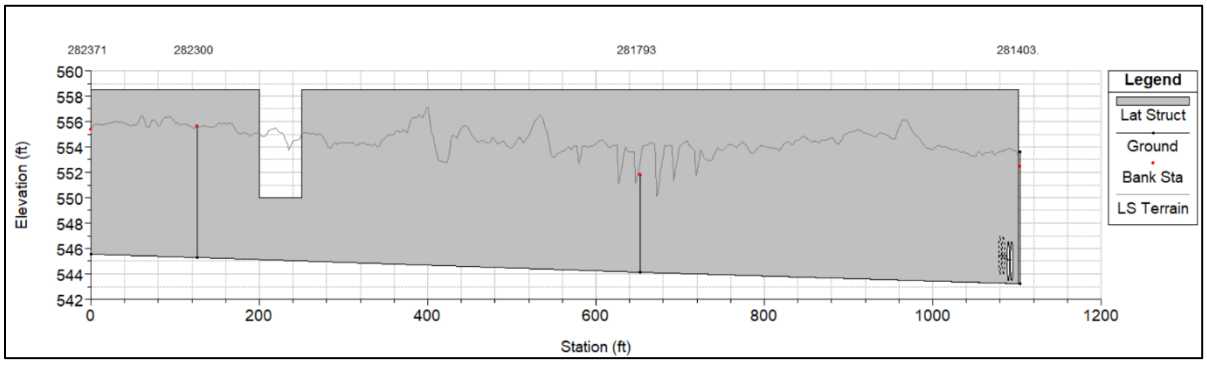

Figure 4-5: *Lateral structure at VD1*

Weir lengths and elevations were chosen as optimization parameters, with optimization directed at maximizing storage during the 0.04 AEP event. Initial weir elevations were set at approximately 2 feet below the preliminary 0.50 AEP FWOP WSE at their locations, and initial weir lengths were estimated based on judgement. This methodology was followed based on results obtained during a previous study (Village Creek FRM Resumption Study, Mobile District; USACE, 2017) located in a bordering watershed that shares many characteristics with the study basin.

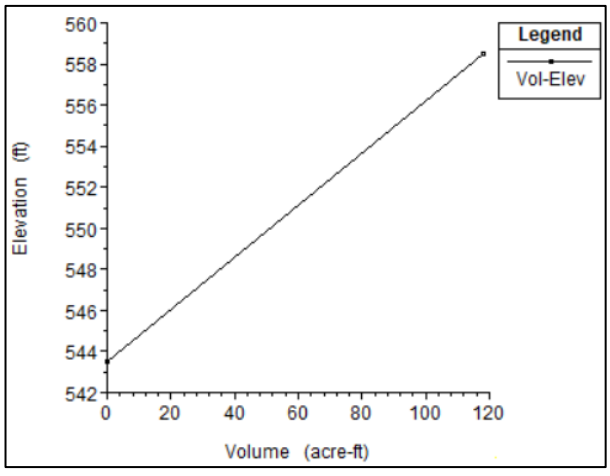

Figure 4-6: *Preliminary storage model at VD1*

Dams

Dams were modeled as inline structures with crest elevations above the current (at the time of preliminary screening) 0.002 AEP WSE at their location. A simplified target elevation (as opposed to a risk tolerability-based elevation [see USACE, 2019b]) that offered protection for all analyzed event frequencies was considered appropriate for early measure screening. Sites VI1 and VI2 were configured with slot-weir spillways, while OI1 was simply represented as a reduction in the existing area of the bridge to which it would connect (RR bridge just upstream of Opossum-Valley confluence). Their effectiveness was first tested with the 0.01 AEP event. Resulting profile plots, changes to inundation extents, and reductions in downstream water surface elevations were analyzed to understand the effects of the measures. Additional frequency events were simulated for all chosen sites, including the 0.20, 0.04, and 0.002 AEP events.

Levees

Levees were represented as lateral structures in the hydraulic model. Backwater areas were constructed as storage areas. Similar to dams, initial levee crest elevations were based on exceeding the preliminary 0.002 AEP flood elevations at the upstream extent of the measure locations for screening purposes. All levee elevations were reduced from upstream to downstream to mimic the slope of the energy grade line in their locations (Figure 4-7).

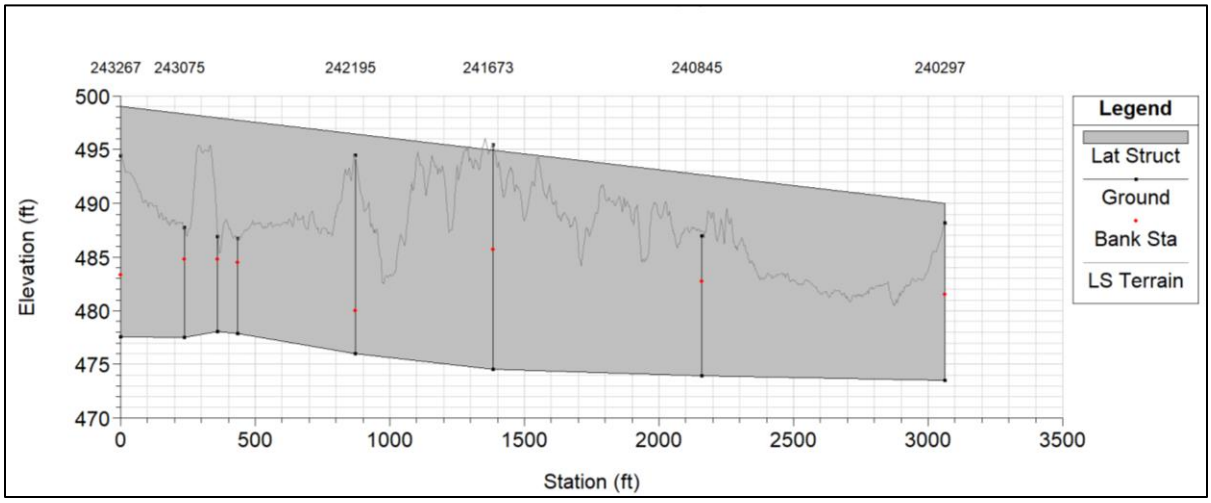

Figure 4-7: *Example of lateral structure representation of levee at VL2.*

Bridge Modifications

As mentioned, these measures were modeled by removing the selected structures from the geometry. Only one chosen location included raised embankments for the bridge approaches, and this location passed preliminary screening. Therefore, a more detailed geometry applicable to the site conditions was developed for this structure. The simplistic modeling approach for the other locations was considered appropriate for efficient analysis of performance. In testing,

iterative modeling with combinations of closely located and adjacent sites was completed to understand performance dependencies between sites.

Channel Modification

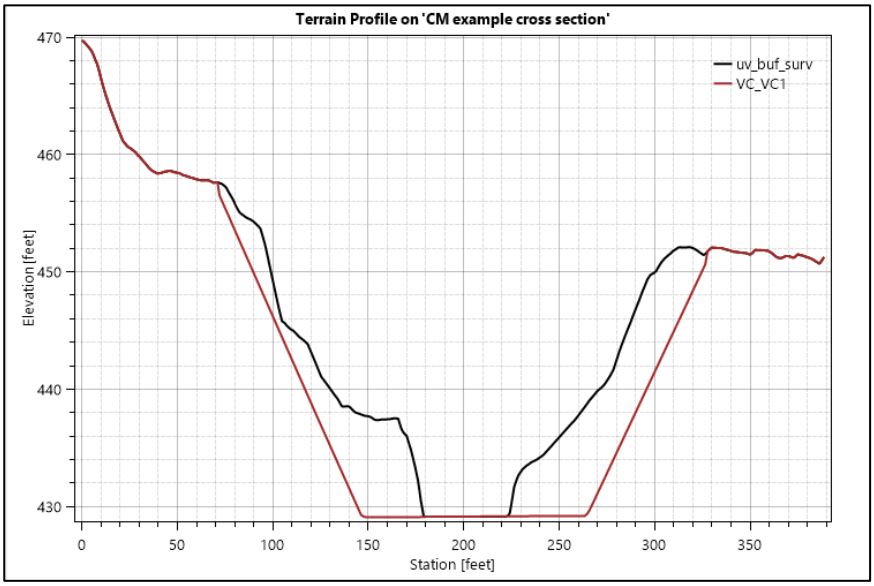

Figure 4-8: *Example cross section showing 120-foot bottom width channel modification terrain template and existing terrain at a location near the mid-point of the Delonah Quarry.*

The proposed channel modification is located within the Valley Creek 2D mesh extents. In the initially proposed location, the channel narrows from approximately 120 feet (bottom width) to 45 feet (just below Murphys Ln. [RS 2141+84]) and widens back out to 120 feet just downstream of the WWTP service bridge (in 2D mesh extents, approximately 1,480 feet upstream of 2034+67). The measure was represented by modifying the existing terrain to reflect the proposed channel geometry. Three alternative channel templates were produced with differing bottom widths including 100', 120', and 140'. Side-slopes of 1:3 (V:H) were utilized for bank grading (example shown in Figure 4-8). A raster surface was created from points and mosaicked with the existing terrain for modeling. The existing conditions geometry was associated with the modified terrains for test simulations.

4.1.1.2 Results

Overbank Detention

The PDT was able to eliminate 3 detention sites on the basis of site constraints alone. Real Estate informed the team that VD6 serves as a dump site for the City of Midfield. Based on the availability of surrounding sites (VD5, VD7, VD8, and VD9) and the environmental hazards associated with this site, it was removed from the study. VD7 was removed from the study on the basis of constraints and costs related to additional construction required for use of this site. Utilization would require floodwater routing underneath an industrial boulevard servicing the nearby dump (VD6) as well as a major railroad next to the roadway. These requirements were unique to this site, and nearby sites provided similar storage potential. The presence of HTRW was identified in VD12, and the sponsor indicated that mitigation responsibility was not possible. Additionally, modeling at nearby sites (VD11 and VD13) showed that detention would likely be ineffective at reducing flood risk for infrastructure downstream of this location.

Site VD11b was developed as a supplemented configuration of VD11 to include a small area of additional open space on the right overbank. This option of the measure was eliminated based on-site performance. No significant reduction in flood risk was realized when compared to VD11. Site VD13 was eliminated based on performance; only negligible changes to flood elevations for a range of frequency events were observed in the densely developed residential areas located immediately downstream. These areas were critical for analyzing effectiveness of this site because they represent the only development subjected to flood risk and located downstream of this measure. For the optimized 0.04 AEP event, peak stages were nearly identical (see Figure 4-9), which was likely the result of this location's close proximity to the target benefit area, and the presence of a bridge (15th St. N) immediately downstream of the pond location. Sensitivity testing was completed to analyze this site's benefits in conjunction with others. Simulations revealed similar results to the stand-alone configuration – no significant benefits driven by the site were observed.

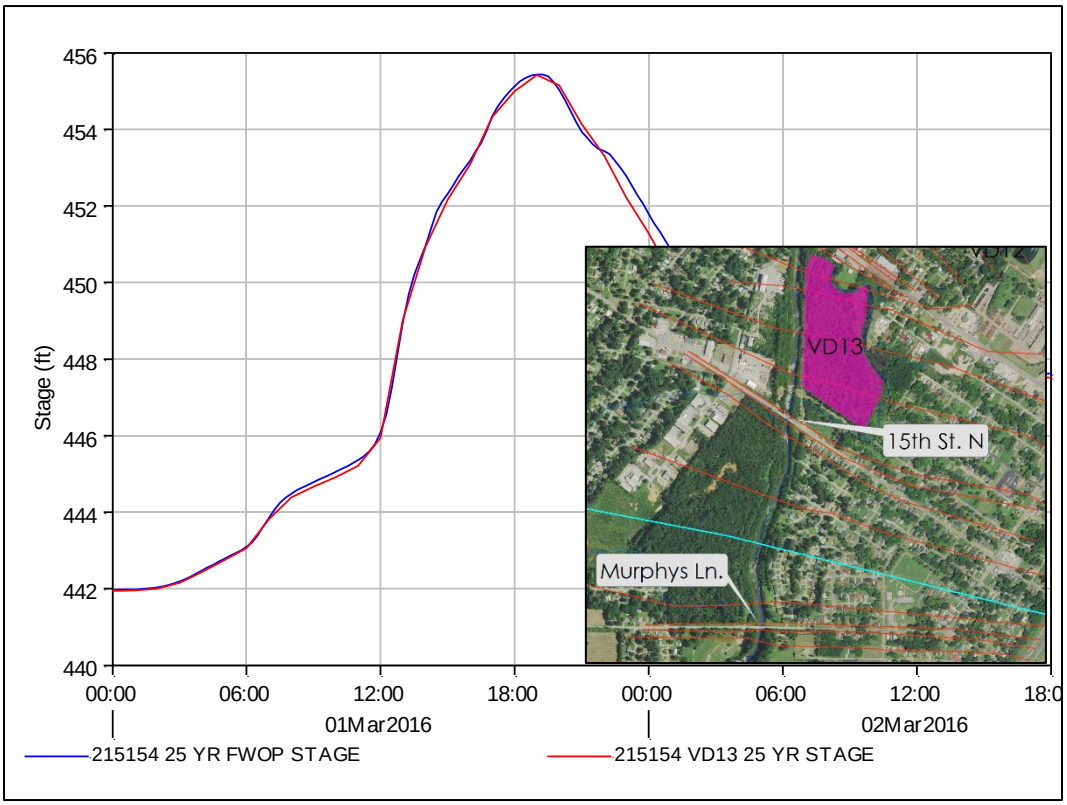

Figure 4-9: *Stage hydrographs at RS 2151+54 for 0.04 AEP event with and without VD13. Vicinity of cross section to site location shown (scale = 1:6,500).*

In general, all other sites were considered effective in reducing downstream flood elevations (example profiles provided in Figures 4-10 and 4-11) and were carried forward to the refined measure array. Individual geometries were constructed for each site, and combination-geometries were also constructed for sensitivity testing of interdependence. The previously described storage models (see Section 4.1.1.1) for each site were improved with storage capacity curves obtained from a modified terrain that featured representation of design templates for all pond and berm geometries.

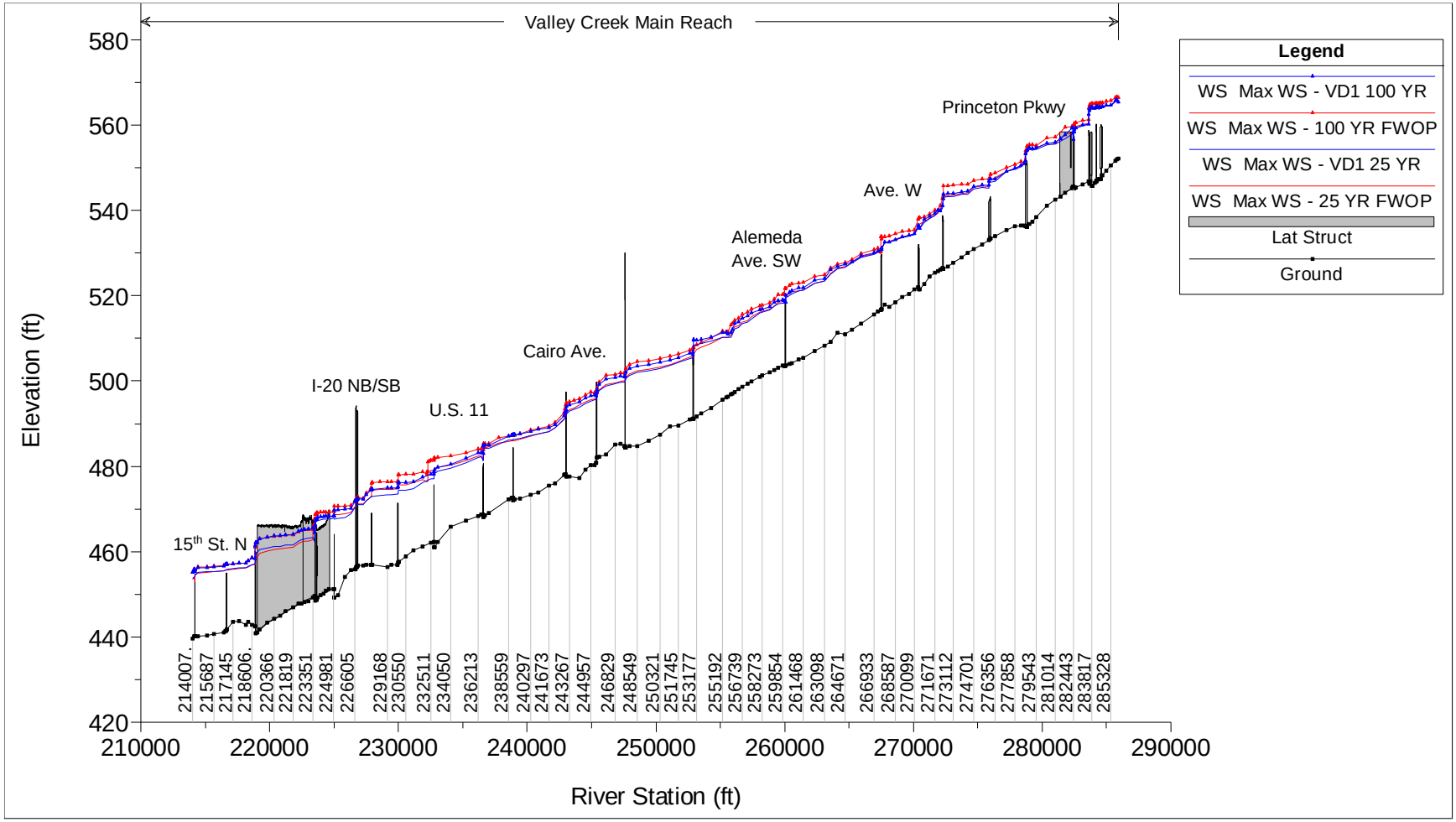

Figure 4-10: *Profile plot of baseline (FWOP) and VD1 simulations with 0.04 AEP and 0.01 AEP events in the upper 1D hydraulic reach of Valley Creek (river stations and some bridges shown).*

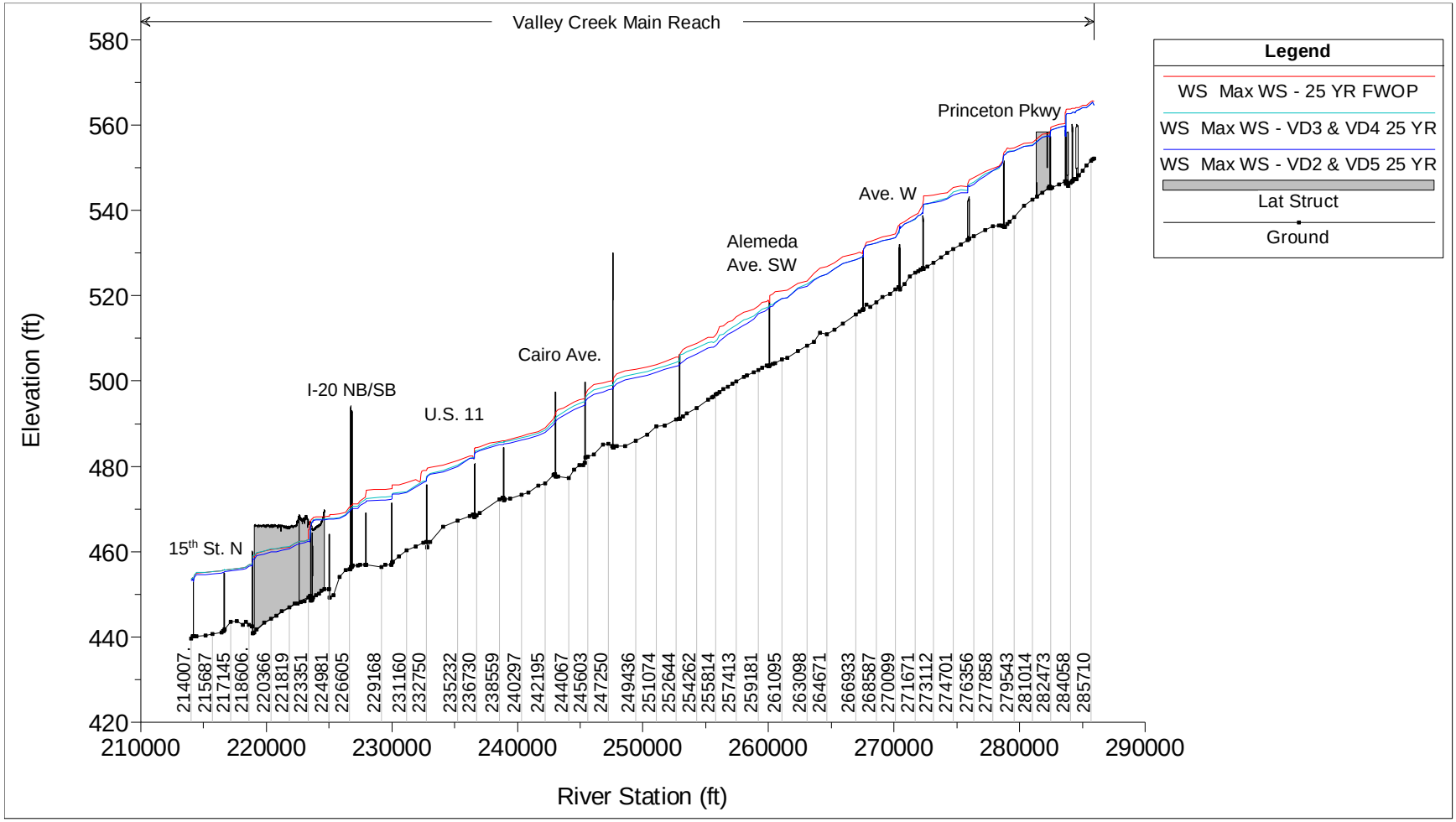

Figure 4-11: *Profile plot of baseline (FWOP) 0.04 AEP event and example combinations of VD3/VD4 and VD2/VD5 in the upper 1D hydraulic reach of Valley Creek (river stations and some bridges shown).*

Dams

From the results of simulations with dam measures, it was determined that for all of the sites, either reductions of downstream flood elevations were nearly negligible, or the upstream impacts outweighed the benefits produced. Based on test results, all dam-sites were removed from analysis. VI1 was ineffective at reducing downstream flood elevations through the range of simulated frequency events without inducing significant upstream impacts. Multiple iterations of the slot-weir geometry at this location were modeled to encompass a range of conveyance areas. Limiting the conveyance through the slot weir to the point of overtopping (during a 0.002 AEP event) improved results downstream; however, significant induced flooding on upstream residential areas (30+ structures with associated impacts) was observed. Results were sensitive to the structure geometry, but a beneficial measure with minimal upstream impacts could not be established. VI2 performed well overall, but, similar to VI1, upstream impacts could not be minimalized. Because results could be matched or improved with overbank detention upstream or near this site, this measure was removed from analysis. OI1 was likely ineffective due to the significance of the existing constriction that the targeted overpass places on the floodplain of Opossum Creek. The results of 0.01 AEP simulations with final configurations of VI1 and VI2 are provided in Figure 4-12. Figure 4-13 provides stage and flow hydrographs over OI1 (RR overpass) showing the negligible changes to peak stage as a result of implementing the measure.

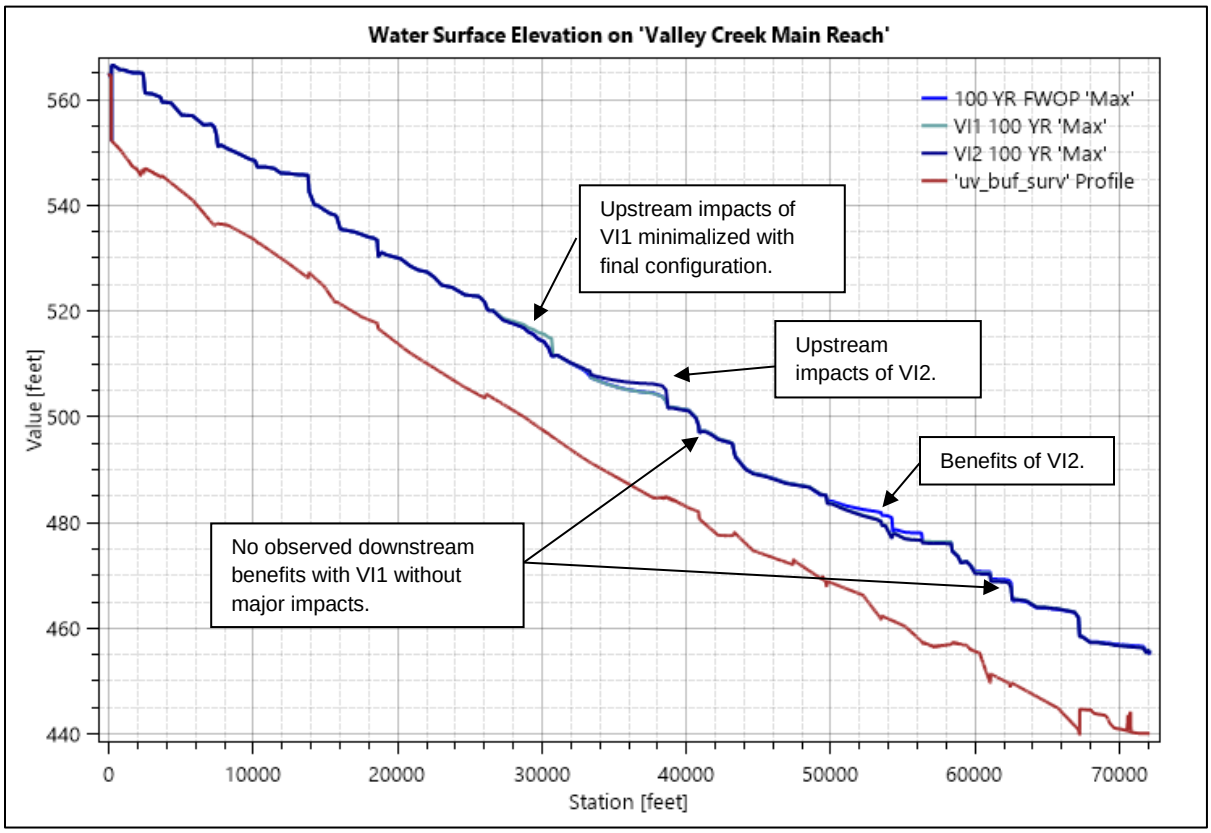

Figure 4-12: *Profile plot baseline (FWOP), VI1, and VI2 simulations with 0.01 AEP event in the upper 1D hydraulic reach of Valley Creek.*

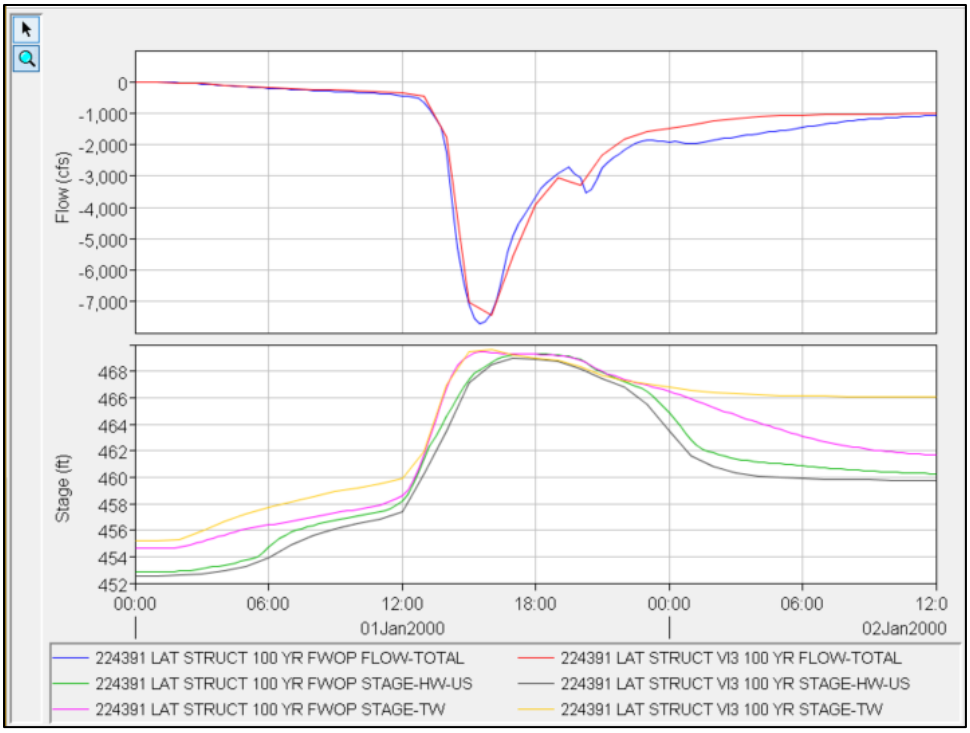

Figure 4-13: *Stage and flow hydrographs over lateral structure representing RR embankment location proposed for OI1. Total flow over the lateral structure is negative due to flow direction from Opossum Creek, into Valley Creek cross sections (see Section 2.2.2 for a description of modeling approach). Note: Plan OI1 incorrectly named VI3 in the figure legend.*

Levees

Sites VL2 and VL3 performed well with minimal impacts to upstream or adjacent structures; however, site VL4 worsened flood conditions in several upstream locations. An estimated 30 structures located at the upstream extent of the feature observed a 4-foot rise in water surface elevation during the 0.002 AEP event. These same structures observed increases of approximately 2 feet and 3 feet for the 0.04 AEP

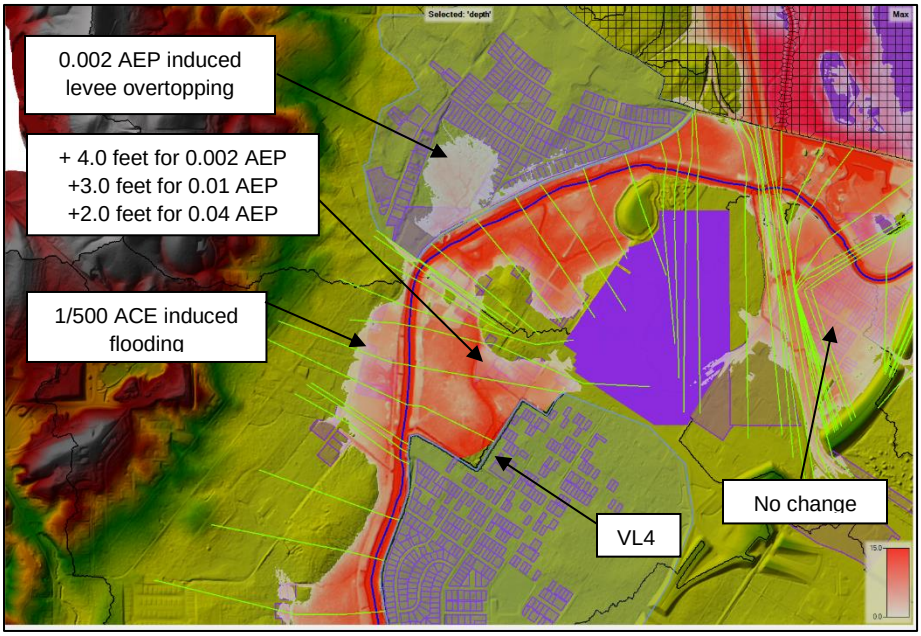

Figure 4-14: *0.002 AEP depth grid (shown in red) with VL4 in place. Structure parcel polygons from economic inventory shown in purple. Schematic notes: Scale is 1:9500; north direction is up.*

and 0.01 AEP events, respectively. Additionally, VL4 induced new flood risk on approximately 20 structures from overtopping of the existing Bessemer Gardens levee upstream, and those on the right overbank, adjacent to the measure's location (see Figure 4-14). Impacts within the proposed protected area of VL2 were observed during simulations with VL3 alone. For this reason, it was decided that either VL2 should be carried forward as a stand-alone measure, or VL2 and VL3 should be carried forward in combination.

Bridge Modifications

The effects of bridge modifications were analyzed with profile plots, inundation extents, and spatial observation of flood elevation changes. The following sites were removed from the study based on performance: VB3, VB4, VB5, VB6, VB7, HB1, and HB2. Upstream impacts in existing conditions were not improved by the removal of these structures. In some cases, insignificant (i.e., < 0.2 feet) upstream flood elevation reductions were coupled with increases of the same magnitude downstream. The elimination of the Halls Creek sites (HB1 and HB2) removed all structural measures from this system (only bridge modifications originally identified). Elimination of HB2 decreased flood elevations during the 0.01 AEP event by approximately 2.5 feet; however, only 2 structures were located within the upstream inundation extents where the change occurred (results were limited to 8th Ave. N approximately 425 feet upstream).

It was not considered advantageous to pursue further analysis at this site considering the probable costs applicable to modification of the culverts under the four-lane divided highway. During fieldwork for bridge data collection on the tributaries from 2/25/2019 – 2/26/2019, it was observed that site HB1 (8th Ave. N over Halls Creek) was recently modified. Simulations with the modified geometry showed that the structure was no longer acting as a constriction. Thus, flood risk in the repetitive loss area upstream of this structure was addressed and is reflected in the existing conditions geometry. The City of Bessemer confirmed that the bridge was updated in 2017 and provided plans for the structure (J. Champion, personal communication, 21 March 2019).

Channel Modification

Preliminary testing showed that a 120-ft. bottom width was the best alternative for the channel modification template. Results between 120-ft. and 140-ft. templates were nearly identical, with the 140-ft. template requiring additional earthwork. The 100-ft. template was less effective at lowering upstream flood elevations than the 120-ft. template through the range of tested frequency events. Additionally, the existing channel upstream of the proposed location for widening has a bottom width near 120 feet. The length of channel work was also updated, whereby the total project length was shortened from approximately 8,980 feet to 3,300 feet. This change was based on model testing which showed that the initially proposed length was not required to produce the same upstream profile reductions. The terminus of the modified channel template is located just below the Halls Creek-Valley Creek confluence.

4.1.1.3 Geotechnical Refinement

Geology

The Valley Creek study area is located within the Birmingham-Big Canoe Valley District of the Alabama Valley and Ridge Physiographic Province. The province runs northeast to southwest, similar in orientation to the study area. Of the bedrock noted in the area, the two predominant formations are the Conasauga and Ketona Formations. The Conasauga Formation consists of a medium bluish-gray, fine-grained, thin-bedded limestone and a dark gray, interbedded shale. The Ketona Formation is characterized as a thick bedded, coarsely crystalline dolomite that is light to medium gray in color. The Valley Creek Feasibility Report and Environmental Assessment, Supporting Documentation (USACE, 1992) details that the Conasauga Formation was the predominant bedrock type in the previous study area, which was located along the Cahaba River. The Ketona accounted for the rest of bedrock. The upper bedrock is made of limestone and dolomite pinnacles. These pinnacles were found at ground surface where the rock outcrops, down to greater than 20.0 feet below ground surface. The current study area is in the same general location as the area detailed in the 1992 report, however, the footprint extends further beyond the banks in some cases.

1985 and 1989 Investigations

Geotechnical investigations were conducted in 1985 and 1989 as part of the effort to support the 1992 study. Eighty borings were sampled by auger, and four additional borings were sampled to obtain rock cores. There are no coordinates for the boring locations, but each of them has a corresponding channel stationing, suggesting they were likely sampled adjacent to the channel (estimates of sampled locations based on historical model cross sections and referenced stationing are mapped in Section 4.1.1.3). Historical borings from these investigations show that the overburden soils consist of brown sandy clays, with varying degrees of sand. Refusal was encountered in many of the borings at bedrock, however it was noted that refusal could have been due to boulders within the overburden. In general, the elevation of refusal decreased from the upstream end of the study area to the downstream end. Rock cores were obtained in the dolomite and limestone of the Conasuaga and Ketona Formations as part of the 1989 investigation. Compression testing (unconfined) was performed on the samples with strengths ranging from 285 tons/sq.ft. to 725 tons/sq.ft. reported.

2019 Investigation

Twenty-four manual auger borings were performed in August and September of 2019. Borings were taken at the potential pond locations, primarily to delineate the elevation of bedrock. The sample number per site varied (locations summarized in Figure 4-15). All soil samples were visually classified; no lab samples were conducted as part of this investigation. The overburden soil types are commensurate with the subsurface soil conditions detailed in the 1992 study report. The overburden consists of primarily brown, clayey sand (SC) to sandy lean clay (CL) with some gravel. Fat clays (CH) were also encountered above top-of-rock in a few locations.

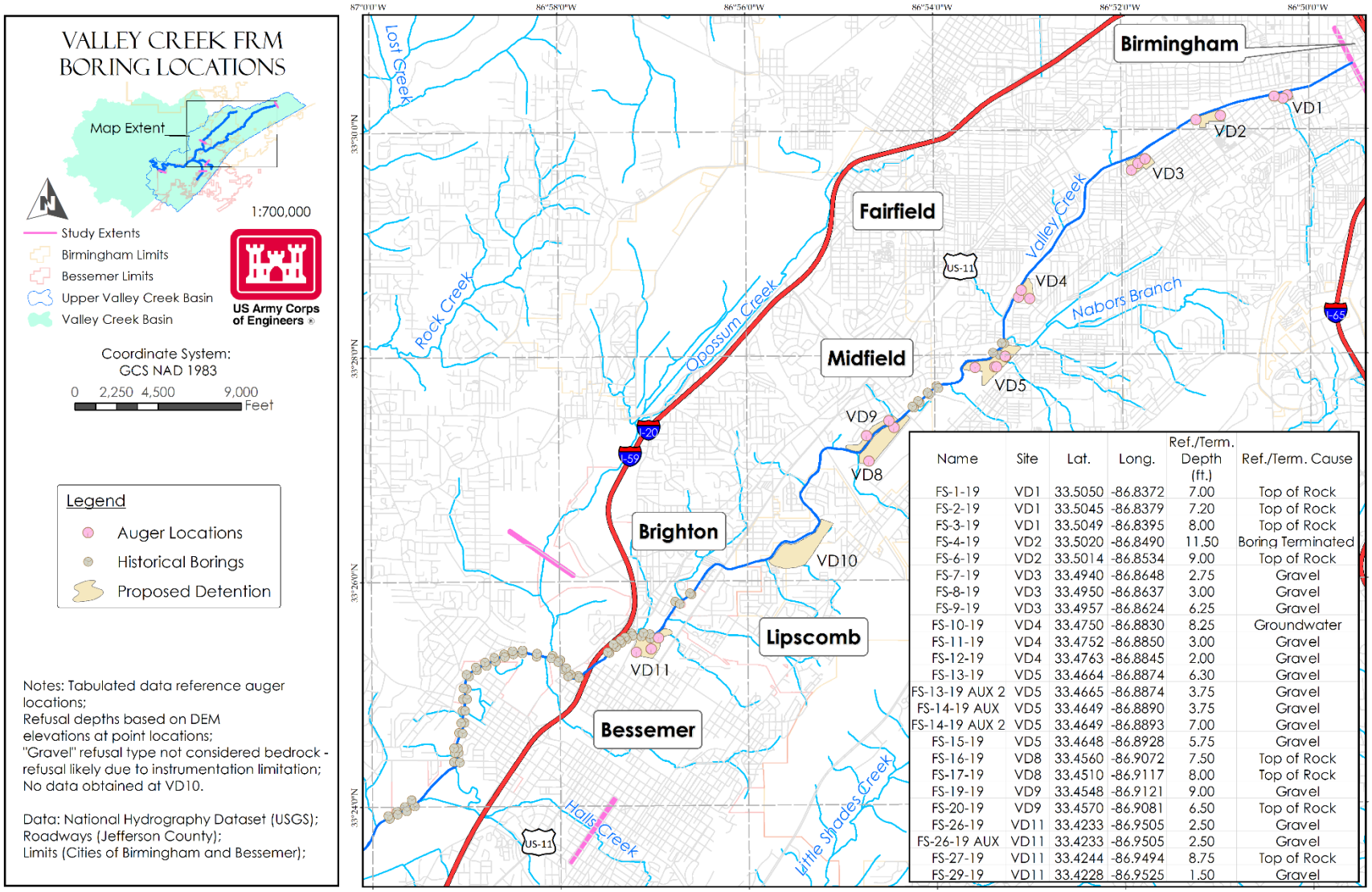

Name	Site	Lat.	Long.	Ref./Term. Depth (ft.)	Ref./Term. Cause
FS-1-19	VD1	33.5050	-86.8372	7.00	Top of Rock
FS-2-19	VD1	33.5045	-86.8379	7.20	Top of Rock
FS-3-19	VD1	33.5049	-86.8395	8.00	Top of Rock
FS-4-19	VD2	33.5020	-86.8490	11.50	Boring Terminated
FS-6-19	VD2	33.5014	-86.8534	9.00	Top of Rock
FS-7-19	VD3	33.4940	-86.8648	2.75	Gravel
FS-8-19	VD3	33.4950	-86.8637	3.00	Gravel
FS-9-19	VD3	33.4957	-86.8624	6.25	Gravel
FS-10-19	VD4	33.4750	-86.8830	8.25	Groundwater
FS-11-19	VD4	33.4752	-86.8850	3.00	Gravel
FS-12-19	VD4	33.4763	-86.8845	2.00	Gravel
FS-13-19	VD5	33.4664	-86.8874	6.30	Gravel
FS-13-19 AUX 2	VD5	33.4665	-86.8874	3.75	Gravel
FS-14-19 AUX	VD5	33.4649	-86.8890	3.75	Gravel
FS-14-19 AUX 2	VD5	33.4649	-86.8893	7.00	Gravel
FS-15-19	VD5	33.4648	-86.8928	5.75	Gravel
FS-16-19	VD8	33.4560	-86.9072	7.50	Top of Rock
FS-17-19	VD8	33.4510	-86.9117	8.00	Top of Rock
FS-19-19	VD9	33.4548	-86.9121	9.00	Gravel
FS-20-19	VD9	33.4570	-86.9081	6.50	Top of Rock
FS-26-19	VD11	33.4233	-86.9505	2.50	Gravel
FS-26-19 AUX	VD11	33.4233	-86.9505	2.50	Gravel
FS-27-19	VD11	33.4244	-86.9494	8.75	Top of Rock
FS-29-19	VD11	33.4228	-86.9525	1.50	Gravel

Figure 4-15: *Overview of historical borings and 2019 auger testing locations.*

Groundwater was encountered in five different boreholes, all within 0.5 feet of bedrock. Bedrock was encountered in eight of the borings in pond sites VD-1, VD-2, VD-8, VD- 9, and VD-11. Generally, the top-of-rock decreased in elevation as the pond sites progressed downstream. Borings from the investigation are provided in Appendix A-2 of this report.

4.1.2 Refined Measures

The measures that remained at the conclusion of preliminary screening included overbank detention, levee, bridge modification, and channel modification types. The refined measure set is summarized in Table 4-2. Two additional opportunities for bridge modifications were identified during the screening process (UB2 and VB9). As the ATR was being conducted on EC and FWOP models during the preliminary screening process, hydrology was being updated, and therefore, the performance of some hydraulic structures within the RAS model changed. UB2 (Bessemer Hwy. over Halls Tributary) appeared to be acting as a significant hydraulic control in existing conditions, in addition to when UB1 was modified (with channel widening). The existing culverts were shown to create upstream backwater, placing flood risk on homes on both overbanks upstream (see Figure 4-17). Additionally, the residential area on the left overbank upstream of VB9 was shown to be at risk from backwater created by the existing bridge (18th Ave. over Valley Creek). These measures were added to the final array and contributed to the structural alternatives analyzed in this study.

Table 4-2: Refined Measure Array

Type	Name	Description	Initial Screening Status[1]
Detention	VD1	10.0 acres on left overbank downstream of Center St. One home on property and minor roadways.	Final measure
	VD2	13.6 acres on left overbank downstream of Princeton Pkwy. Note: 2 sizes initially considered with largest moving forward. This area includes 3 homes and minor roadways. Size updated again through refinement phase.	Final measure
	VD3	22.2 acres on left overbank at Fayette Ave. SW. Previous buyout area with minor roadways and slab foundations.	Final measure
	VD4	16.4 acres on left overbank at Lincoln Ave.	Final measure
	VD5	55.6 acres on left overbank downstream of Alemeda Ave. SW. Clear area but contains Land Trust.	Final measure
	VD8	54.5 acres on left overbank immediately downstream of By Williams Sr Dr. Area is clear of development but contains Land Trust.	Final measure
	VD8 & VD9	79.3 acres on left and right overbank immediately downstream of By Williams Sr Dr. Both areas clear of development; however, VD8 contains Land Trust.	Final measure
	VD10	85.6 acres on left overbank immediately downstream of Martin Luther Ave. Area is clear of development but contains Land Trust.	Final measure
	VD11	39.6 acres on left overbank just upstream of Jaybird Rd. Area is clear of development other than roadways.	Final measure
Levee	VL2	Levee on right overbank extending from a location just upstream of Martin Luther Ave. and tying into a point near Sugar Ray Dr. downstream (3265 feet).	Final measure

	VL3	Levee on right overbank extending from Sugar Ray Dr. upstream and tying into a location due east of 47th St. (3765 feet).	Final measure - conditional
Bridge Modification	VB1	3rd Ave. N over Valley Creek.	Final measure - conditional
	VB2	RR DS 3rd Ave. N over Valley Creek.	Final measure - conditional
	VB8	Murphys Ln. over Valley Creek	Final measure - conditional
	VB9	18th Ave. over Valley Creek.	Final measure
	UB1	5th St. N over Halls Tributary.	Final measure
	UB2	9th Ave. N/Bessemer Hwy. over Halls Tributary.	Final measure
Channel Modification	VC1	120-ft. channel from Murphys Ln. to WWTP service bridge (approximately).	Final measure

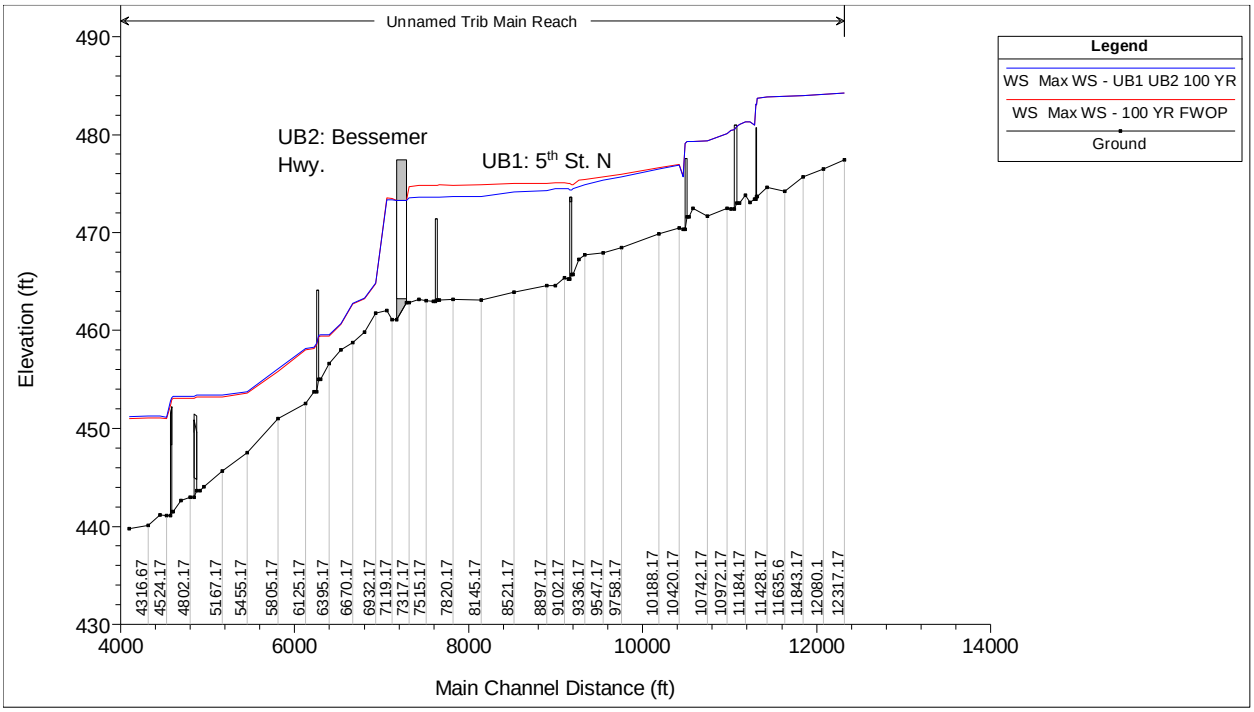

Figure 4-16: *Profile plot of baseline (FWOP) and UB1/UB2 simulation during the 0.01 AEP event on Halls Tributary.*

4.1.2.2 Design Detail

Overbank Detention

Conceptual-level designs of the refined measures were improved/formulated after preliminary screening in order to provide quantities for rough-order-of-magnitude (ROM) cost calculations (details summarized in Table 4-3; values rounded as appropriate). Final configurations of all detention sites feature 1:2 (V:H) side slopes and 0.5% bottom grading increasing in the upstream direction from the invert elevation to allow for gravity drainage (reinforced concrete pipe [RCP] culverts with flap gates selected for drainage). Armoring of the surrounding embankment was included in the cost formulation for these measures due to configuration with

1:2 side slopes, and overtopping potential. Ponds were initially drafted with milder side slopes (1:3); however, storage capacity was greatly reduced with this configuration. Additional protection was also designed for the spillways of each site, whereby additional armor, choke, and filter stone were sized and quantified (Table 4-4). Design details for outlet works and supplementary drainage structures are provided in Tables 4-5 and 4-6, respectively.

Table 4-3: Detention pond details

Name	Design Volume (ac-ft.)	Area (acres)	Invert Elevation (ft-NAVD88)	Berm Elevation (ft-NAVD88)	Weir Elevation (ft-NAVD88)	Required Excavation ($yd.^3$)	Required Fill ($yd.^3$)
VD1	94	9.5	543.5	558.5	550.0	99,062	6,181
VD2	191	18.9	534.5	550.5	544.0	227,485	7,380
VD3	283	21.6	527.0	545.0	535.5	382,203	8,800
VD4	163	15.9	508.0	527.0	516.0	267,850	11,151
VD5	536	53.2	499.5	519.5	510.0	480,223	33,196
VD8	598	21.1	486.5	507.0	500.0	440,099	41,890
VD9	193	52.7	485.5	506.0	502.0	133,508	47,075
VD10	773	80.3	473.5	492.5	483.5	764,120	143,860
VD11	519	38.3	458.5	478.0	469.0	427,673	38,699

Table 4-4: Berm design summary for detention sites

Site	Armor Area ($ft.^2$)	Class V Toe Stone ($yd.^3$)	Class II Choke Stone ($yd.^3$)	Toe Filter ($yd.^3$)	Spillway Length (ft.)
VD1	118,959	74	19	19	50
VD2	198,261	185	46	46	125
VD3	205,172	444	111	111	300
VD4	192,533	296	74	74	200
VD5	393,734	444	111	111	300
VD8	368,768	370	93	93	250
VD9	360,297	296	74	74	200
VD10	439,537	593	148	148	400
VD11	354,251	519	130	130	350

Table 4-5: Outlet works design summary for detention sites

Site	Culvert type and size	Length (ft.)	Inlet/outlet protection ($yd.^3$)
VD1	RCP – 36”	200	100
VD2	RCP – 36”	140	100
VD3	RCP – 36”	240	100
VD4	RCP – 36”	240	100
VD5	RCP – 2 @ 36”	280	200
VD8	RCP – 2 @ 36”	580	200
VD9	RCP – 36”	180	100
VD10	RCP – 2 @ 36”	250	200
VD11	RCP – 36”	240	100

Table 4-6: Supplementary culvert data for detention sites

Site	Existing flow area estimate ($ft.^2$)	Box culvert size (span x rise)	Length (ft.)
VD1	N/A	N/A	N/A
VD2	50	2 @ 5’ x 5’	30

VD3	N/A	N/A	N/A
VD4	50	2 @ 5’ x 5’	180
VD5	188	2 @ 8’ X 12’	40
VD8	N/A	N/A	N/A
VD9	N/A	N/A	N/A
VD10	192	2 @ 11’ x 10’	25
	280	2 @ 12’ x 12’	30
	384	3 @ 12’ x 12’	100
VD11	225	2 @ 12’ x 10’	75
	60	2 @ 6’ x 6’	65

Armoring was based on the surface area of the embankments (or berms) for each site. The armoring suggested is of the articulated concrete block (ACB) or articulated concrete mat (ACM) type. The volume of stone required for tailwater toe protection at each site was based on a common assumption of a set width (away from toe) of 10 feet, a set depth of 4 feet (2 lifts), and a unique (per site) spillway length, although many of these lengths are equivalent between sites. The stone applicable for these sites (based on overtopping velocities at the spillway) is Alabama Department of Transportation (ALDOT) Class V riprap (D_{50} = 1000 pounds). Quantities also included a Class II choke stone. A cursory estimate for the filter material was included in the quantities. This would be in the form of a poorly graded gravel layer, topped with an AASHTO #57 stone or similar. A filter fabric may also be required below the base (filter) layer, though no detail has been formulated for this component.

Levees

A major assumption applicable to the levees was that excavated material from detention sites would be suitable and utilized for their construction. This assumption only applied to plans that included both measure-types. VL2 requires 1:2 (V:H) side slopes, and thus, will require armoring. An ACB or ACM from manufacturers provided in the detention site detail is recommended for scour and overtopping protection. A total area of 143,791 square feet would be required to support both VL2 and VL3. Additionally, flood gates are required at both sites for roadway crossings (2.25 ft. by 30 ft. at VL2 and 8 ft. by 100 ft. at VL3). Table 4-7 provides the earthwork and armoring quantities for the levee sites. Conveyance requirements for existing drainage channels running through the levee footprints have been estimated (Table 4-8). These were based on the methodology described for detention site quantities development.

Table 4-7: Levee quantities data

Site	Cut (yd.^{3})	Fill (yd.^{3})	Side Slopes (V:H)	Armor Area (ft.^{2})
VL2	90	23603	1:2	143791
VL3	213	1179201	1:3	N/A

Table 4-8: Supplementary culvert data for levees

Site	Existing flow area estimate (ft.^{2})	Box culvert size (span x rise)[1]	Length (ft.)
VL2	100	2 @ 10’ x 6’	60
VL3	20	1 @ 6’ x 6’	95
	100	2 @ 10’ x 6’	100

[1]*Culvert dimensions provided as span x rise.*

Bridge Modifications

The bridge quantities have been developed from modeling various configurations at the chosen sites to reflect a “no-bridge” condition. This metric was selected as the threshold because widening to reduce flood elevations below these levels would move beyond a simple bridge modification and would require an unrealistic channel modification measure to support. Furthermore, the sites of interest did not present widening opportunities beyond this threshold based on surrounding development and other constraints. At most locations, existing bridge spans were repeated as needed, and as allowable based on-site constrictions, to achieve the desired result. For other locations, configurations were changed based on-site feasibility (i.e., culvert changed to bridge).

The existing and modified structure geometries are detailed in Table 4-9. The modified piers are assumed to be the same type/configuration as those currently in place at all of the applicable structures. These are usually capped-pile or solid wall types; however, a trestle-type bent is applicable to the railroad bridge. While basic model geometric inputs for bridge piers are known, the configuration (i.e., wall versus capped-pile) is not known at every measure locations. The pier geometry helps to suggest the type, however, whereby a semi-circular geometry is usually representative of a pier wall, and square piers usually represent a capped-pile configuration (reported in Table 4-10). Channel widening through modified bridges to match the increased span lengths is proposed for all locations. In all cases, channel side-slopes were set at 1:3 (V:H). In addition to the described data, spatially based quantities for earthwork were provided to cost for formulation.

Table 4-9: Bridge geometry detail

Site	Street	Existing span length (ft.)	Existing pier/culvert detail[1]	Modified span length (ft.)	Modified pier/culvert detail
VB1	3rd Ave. N	N/A – culverts	2 box culverts @ 17.5’ x 10’	150.0	4 piers @ 2’ (square)
VB2	RR DS VB1	78.0	1 pier @ 5.5’ (circular trestle)	155.5	2 piers @ 5.5’ (circular trestle)
VB8	Murphys Ln.	160.0	2 piers @ 2’ (square)	310.0	5 piers @ 2’ (square)
VB9	18th St. N	126.6	3 piers @ 2’ (semi-circular)	192.0	5 piers at 2’ (semi-circular)
UB1	5th St. N	38.0	N/A – clear span	76.0	1 pier @ 2’ (square)
UB2	Bessemer Hwy.	N/A - culverts	3 box culverts @ 12’ x 10’	N/A - culverts	7 box culverts @ 12’ x 10’

[1]*Culvert dimensions provided as span x rise.*

4.2 Structural Alternatives

4.2.1 Overbank Detention Plan Formulation

Formulation of stand-alone detention plans (and subsequent determination of sites to be used for combination plans) required quantitative analyses of individual sites to better understand their effectiveness. Work was completed to rank sites on the basis of performance and constructability, which required estimation of expected costs and benefits associated with individual sites. This analysis was considered necessary due to the strong performance associated with all remaining sites, and the understanding (based on prior study knowledge; USACE, 2017) that this measure type would likely be a key component to the recommended plan. Furthermore, this analysis sought to reduce the risks associated with over- or under-designing a plan featuring these measure-types or prolonging the study schedule with excessive economic modeling of individual sites and/or possible combinations. All analyses described in this section include VD11 as they were completed prior to reception of geotechnical site data described in Section 4.1.1.3. Additionally, the analysis presented in following Section 4.2.1.1 was completed prior to development of design templates, quantities, or costs for the detention sites.

4.2.1.1 Site Performance Assessment

In order to forecast economic benefits associated with a particular site, it was necessary to analyze benefits on a structure-by-structure basis. A first attempt for site performance quantification involved regression of a design volume-to-0.04 AEP (FWOP) hydrograph volume with the net volume reduction produced by each site (see Figure 4-17). This approach was pursued to define a transferrable system for rapid site assessment of feasibility for overbank detention. Net volume reduction was achieved with cut-fill analyses on baseline and with-project 0.04 WSE AEP rasters for each site. The 0.04 AEP hydrograph volume was selected for analysis based on selection of this event for optimization of this measure-type. Figure 4-17 presents a fairly strong correlation (R^2 = 0.7391), which suggests that the chosen parameter can serve as an indicator for overall performance. However, the

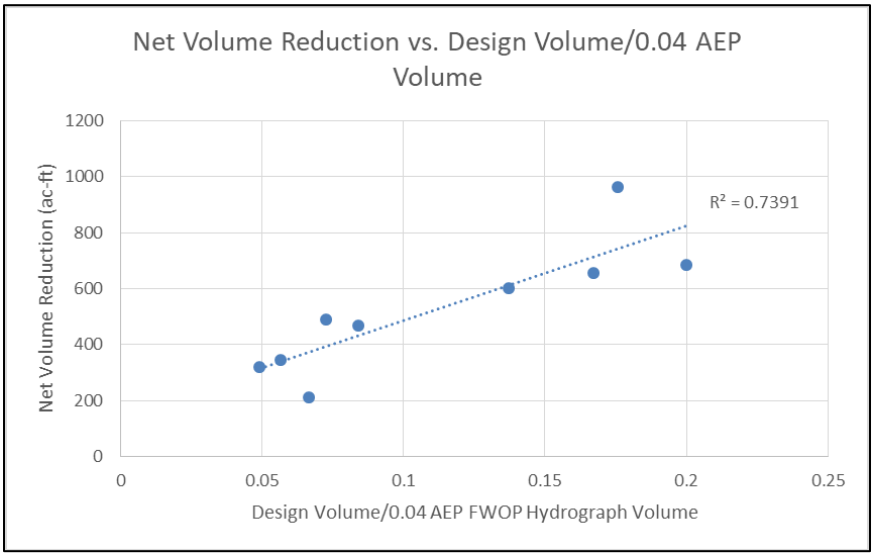

Figure 4-17: *Net volume reduction from overbank detention sites versus design volume ratio.*

downfall of this approach is that net volume reduced cannot be translated as economic benefit unless the assumption that development is universally distributed downstream of a project site is made. This assumption is most often invalid, and as a result, overall site performance should not be interpreted from the approach. Thus, quantification of site-specific benefits was required.

To support, bin statistics were generated from the economic structure inventory based on reductions in flood elevations observed during the 1/25 ACE event for each site (Figure 4-18). These "reduction frequency" analyses utilized the 0.04 AEP event because it served as the basis for site optimization. Data for all sites were compiled and selected bin ranges were plotted with design volumes, which served as an indicator of earthwork costs (analyses completed prior to production of design templates and derivation of quantities and costs; however, see Section 4.2.3 for revised analysis). Multiple bin ranges were analyzed, which revealed differences in overall trend direction; however, only the bin ranges utilized for final rank assessment are provided here (Figures 4-19 and 4-20). These bins were considered the best ranges for representation of performance based on the distributions of individual reduction frequency analyses. Volume-benefit analysis was also completed for structures removed from the 1/25 ACE floodplain (see Figure 4-21). Correlations in the plots are not pertinent; trends were analyzed for informational purposes only. The plotting positions are considered the most critical aspect of the plot, as they speak specifically to a site's overall efficiency (i.e., an estimate of associated economic benefit versus volume of excavation required). In the figures, VD8 and VD9 are plotted in combination due to an early idea of also analyzing these locations as a single measure; it was later decided to analyze these sites as separate measures.

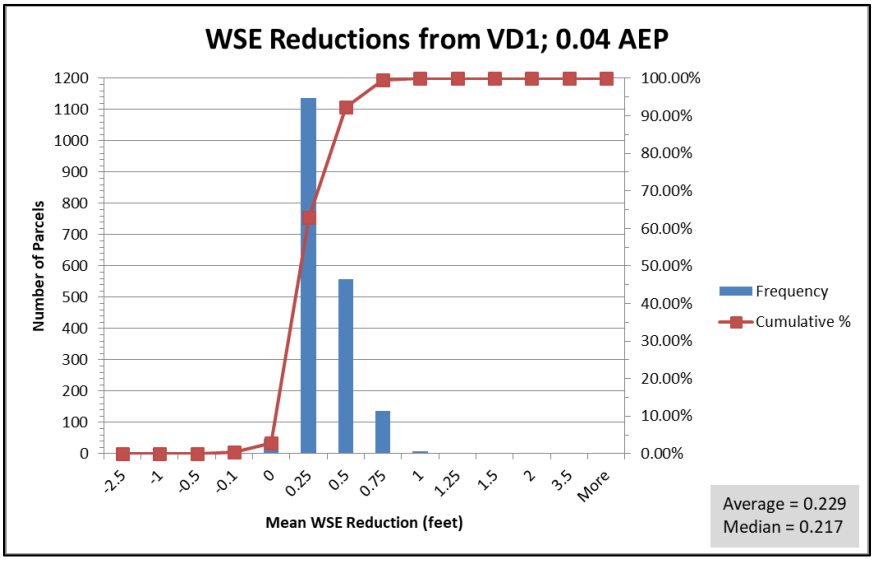

Figure 4-18: *Histogram of water surface elevation (WSE) reductions resulting from VD1.*

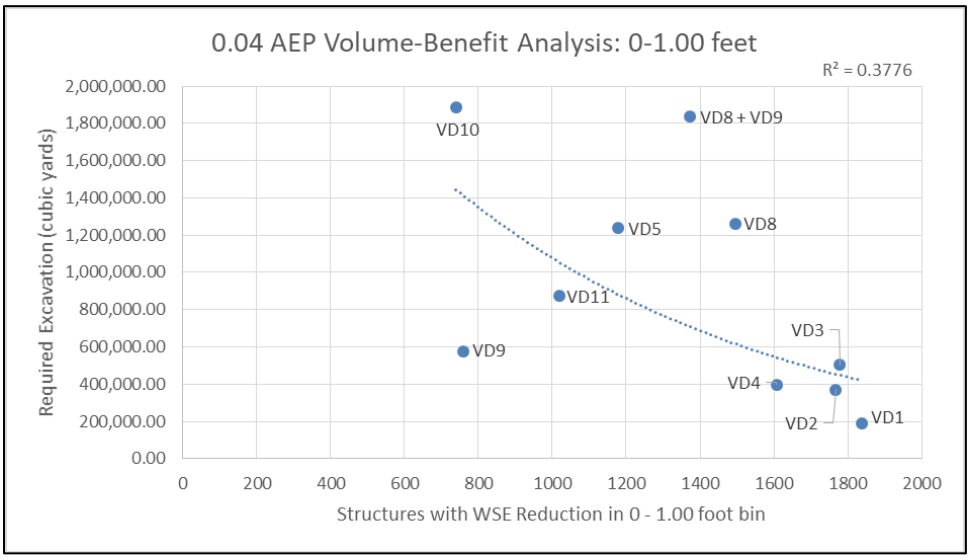

Figure 4-19: *Volume-benefit analysis for parcel WSE reductions between 0 and 1.00 feet.*

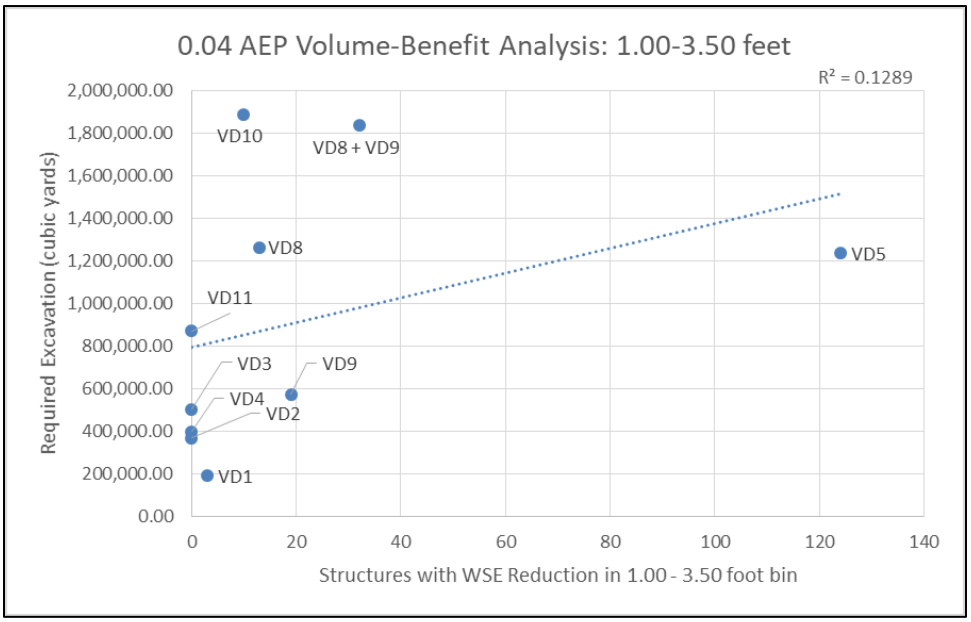

Figure 4-20: *Volume-benefit analysis for parcel WSE reductions between 1.0 and 3.50 feet.*

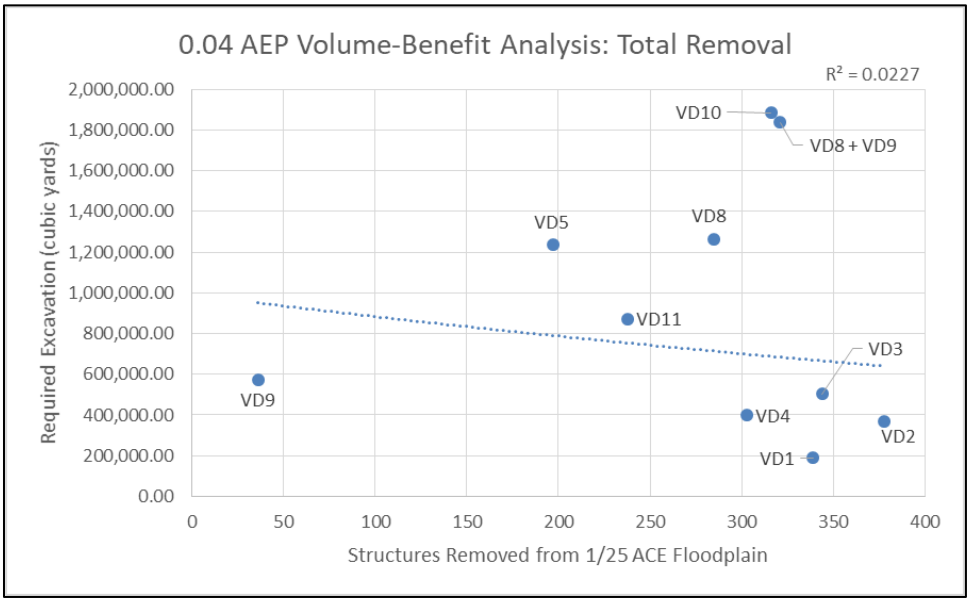

Figure 4-21: *Volume-benefit analysis for parcels removed from the 0.04 AEP floodplain.*

Constructability of each site was analyzed on the basis of required excavation and utility removal. Lengths of utilities required for removal were estimated from the sponsor-provided utility datasets which were limited to water and wastewater lines at the time of analysis. Visual assessment of plotting positions (Figure 4-22) was completed to assign site ranks.

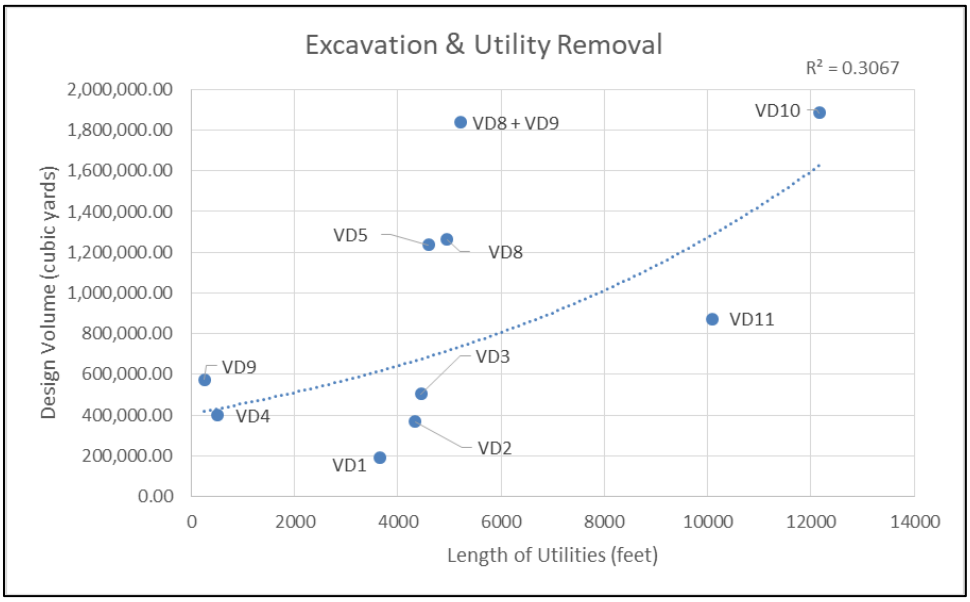

Figure 4-22: *Excavation and utility removal required for implementation of overbank detention sites.*

4.2.1.2 Site Ranking

A scoring system was developed for rank assignment based on performance and constructability. Scores for performance were based on the ratio of reduction frequency results-to-required excavation for each site as follows:

$$Score = S/\forall \qquad \text{Equation 4}$$

where S is the number of structures within the analyzed bin, and ∀ is the design volume (or storage capacity) of each site (2 ranks assigned). In this form, scores take on units of structures/ac-ft. Rank improved with increasing scores for each site (i.e., rank # decreased). Additionally, Equation 4 was applied to analyze scores for structures removed from the 0.04 AEP floodplain for each site. These scores were increased by 25% to weight importance of total removal and averaged with the performance scores from the 0-1.00-foot bin results. As mentioned, constructability ranks were determined from visual assessment of Figure 4-22, whereby individual ranks were assigned for excavation and utility removal, and excavation values were weighted by 25% as a method to account for increased costs associated with mobilization, cycle hauling, and disposal. Figure 4-23 provides the final results of site ranking for both performance and constructability. Ranks without indication of WSE reductions between 1.0 and 3.5 feet represent a lack of reduction within this bin for any parcels within the structure inventory (sites VD2, VD3, VD4, and VD11).

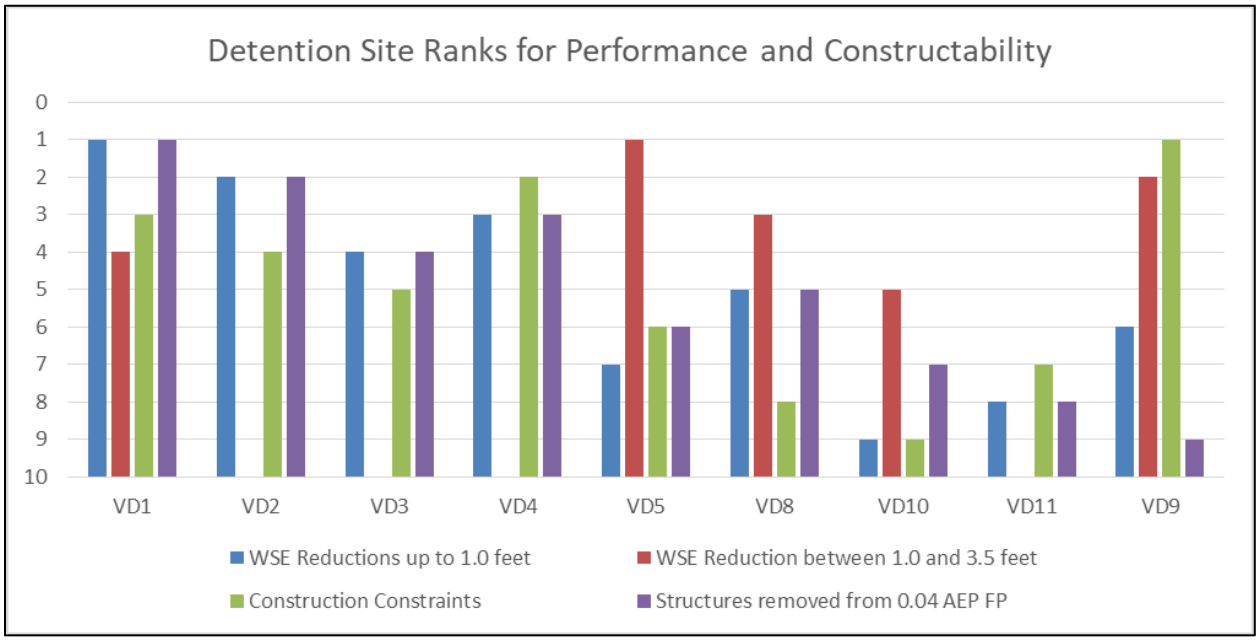

Figure 4-23: *Final overbank detention site ranks for analyzed criteria*

4.2.2 Preliminary Alternatives

The measures that remained after preliminary screening were utilized for formulation of preliminary study alternatives (Table 4-10). These initial alternatives were heavily refined based

on additional performance analysis, improved cost data, development of an economic benefit threshold, and full economic performance analysis of targeted, individual measures in the Hydrologic Engineering Center's Flood Damage Reduction Analysis (HEC-FDA) software. Final alternatives were developed based on progressive study of detention sites that utilized economic results to drive additional formulation. Some of the initially developed alternatives served as final alternatives, as they were non-detention, standalone plan-types, or combinations unaffected by additional economic results and further screening. In most cases, standalone plans employed all of the refined measures for the specific type; however, the standalone bridge modification plan excludes one structure as it was determined to be dependent on implementation of the channel modification measure (VB8 – Murphys Ln. over Valley Creek). Based on the analyses detailed in Section 4.2.1, three preliminary detention-based plans were formulated.

Table 4-10: Preliminary Structural FRM Alternatives

Type	Name	Description
Detention	D1	All Sites
	D2	VD1, VD2, VD3, & VD4
	D3	VD1, VD2, VD3, VD4, & VD5
Levee	L1	VL2 & VL3
Bridge Modification	B1	VB1, VB2, VB9, UB1, & UB2
Combination	C1	Chosen Detention plan + VC1
	C2	Chosen detention plan + L1
	C3	Chosen detention plan + B2
	C4	Chosen detention plan + B2 + VB8 + VC1
	C5	Chosen detention plan + B2 + VB8 + VC1 + L1
	C6	Chosen detention plan + B2 + VC1 + L1
	C7	L1 + B1 + VB8 + VC1
	C8	B1 + VB8 + VC1

As shown, 13 preliminary structural alternatives were developed for the study area including 8 alternative combinations and 7 stand-alone plans. D2 represents a detention alternative combining the four most effective, and lowest cost sites, while D3 represents the best overall performing detention plan based on the results of analysis presented in Section 4.2.1. Combinations 1 through 6 represent early ideas of effective combinations, where the "chosen detention plan" represents a placeholder for potential detention plan combinations. As the following section describes (4.2.3) additional work was completed to identify the most beneficial combination of detention sites, and these were tested with other measures as applicable.

4.2.3 Revised Overbank Detention Plan Formulation

With design template development for all pond sites, detailed quantities were produced, and from these, updated measure costs were provided from cost team members. Cost data were used to execute improved analysis of the early correlations that were made between site work and benefits provided by detention sites. Previously, each detention site was ranked based on

criteria of earthwork, utility removal, and derived benefits computed in terms of the number of structures that observed total removal from the 0.04 AEP floodplain, or water surface reductions of either 0 – 1.0 feet, or 1.0 – 3.5 feet. With the completion of rough-order-of-magnitude costs (ROMs) a direct correlation of site effectiveness and costs could be made for each detention measure. Figures 4-24 through 4-26 illustrate this.

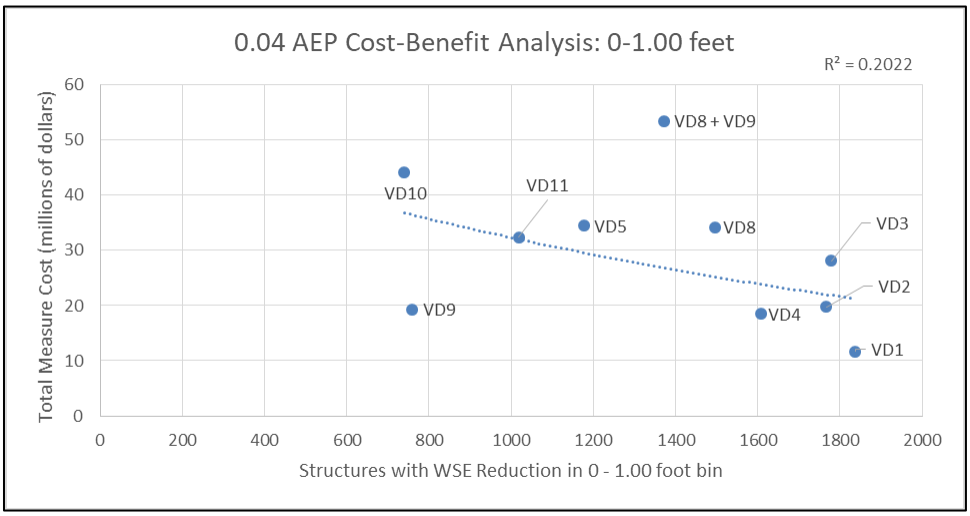

Figure 4-24: *Cost-benefit analysis for WSE reductions between 0 – 1.0 feet*

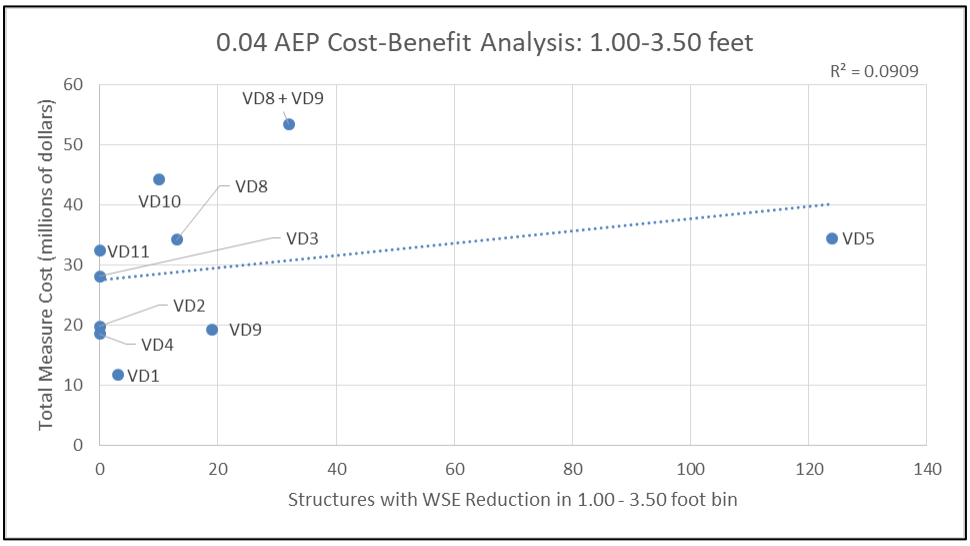

Figure 4-25: *Cost-benefit analysis for WSE reduction between 1.0 - 3.5 feet*

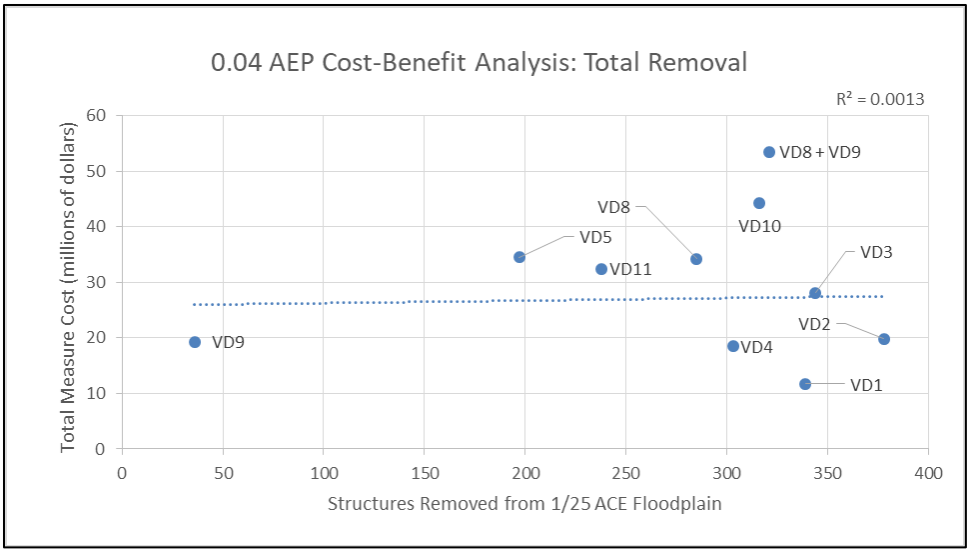

Figure 4-26: *Cost-benefit analysis for structures removed from the 0.04 AEP floodplain*

For plan formulation it was also considered desirable to understand the value associated with Figures 4-24 through 4-26. To support, additional analysis was completed to quantify the value removed from the 0.04 AEP floodplain (Figure 4-27). Only the value (depreciated structural) removed from the 0.04 AEP floodplain was quantified for each measure, as this can be executed in a relatively simple spatial workflow. Quantifying the structural value associated with water surface elevation reductions in the aforementioned bins (0 to 1.0 ft. and 1.0 to 3.5 ft.) would require much more in-depth analyses related to the function of HEC-FDA. Fortunately, the value-data associated with floodplain removal were thought to be the most critical for analysis of site performance.

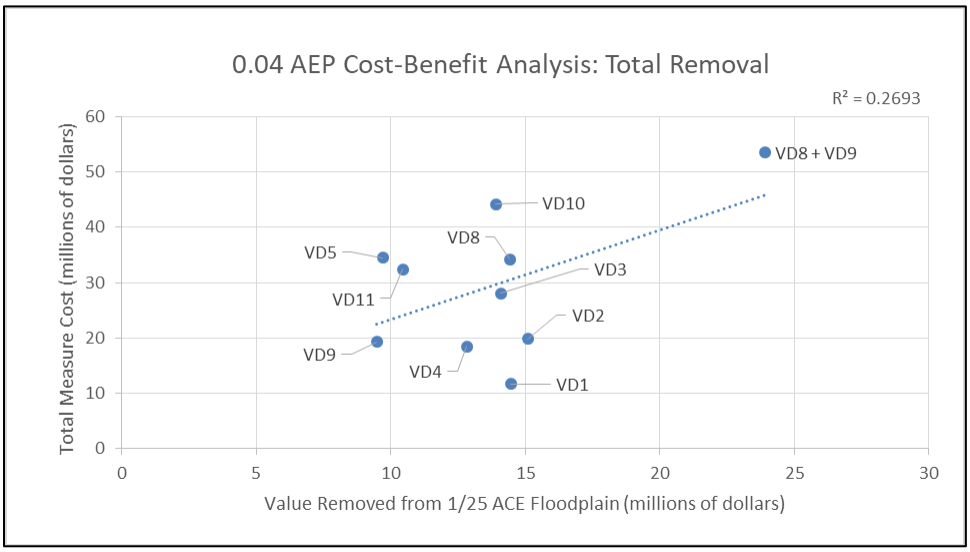

Figure 4-27: *Cost-benefit analysis for value removed from the 0.04 AEP floodplain*

These analyses worked together to provide guidance for formulation of detention-only plans, and combinations with a selection of detention sites. From Figure 4-27 it can be seen that the

most effective site in terms of total value removed from the 0.04 AEP floodplain is site VD1, followed by VD2, VD4, and subjectively, VD9 or VD3. Table 4-11 provides the data supporting Figure 4-27.

Table 4-11: Detention site performance detail

Measures	Total Cost (millions)	Structures removed (0.04 AEP FP)[1]	Value removed (0.04 AEP FP)[1]	Value-to-cost ratio
VD1	$11.70	339	14.46	1.24
VD2	$19.80	378	15.10	0.76
VD3	$28.10	344	14.09	0.50
VD4	$18.50	303	12.83	0.69
VD5	$34.50	197	9.70	0.28
VD8	$34.20	285	14.43	0.42
VD9	$19.30	36	9.49	0.49
VD10	$44.20	316	13.90	0.31
VD11	$32.40	238	10.46	0.32

[1]*FP = floodplain*

Selection of detention sites for final plans relied on the development of a plan-cost threshold in order to limit possible combinations of detention measures. Development of a cost threshold was completed with economic modeling of an alternative incorporating all final measures (referred to as A1). This methodology was pursued with the understanding that no alternative plan cost should exceed the present worth of economic benefits derived from such an alternative. Moreover, because the benefits of A1 were based on implementation of all measures with a total cost of approximately $261,000,000, the cost limit for alternatives should be much less than the present worth of benefits produced by this plan. Utilizing the computed benefit (present worth) of $92,000,000 a conservatively high cost threshold of $80,000,000 was established to create detention plans that maximized value-to-cost ratios. Plans were formulated utilizing Figures 4-24 through 4-27. As well as Table 4-11. Following this methodology, full economic analysis of a reduced number of plans was justified, as it was understood that no combinations of less efficient, more expensive sites could produce improved results over plans based on the described methodology. Figure 4-28 plots the total cost of some preliminary plans against value removed from the 0.04 AEP floodplain; the paragraph following details its use for final plan formulation.

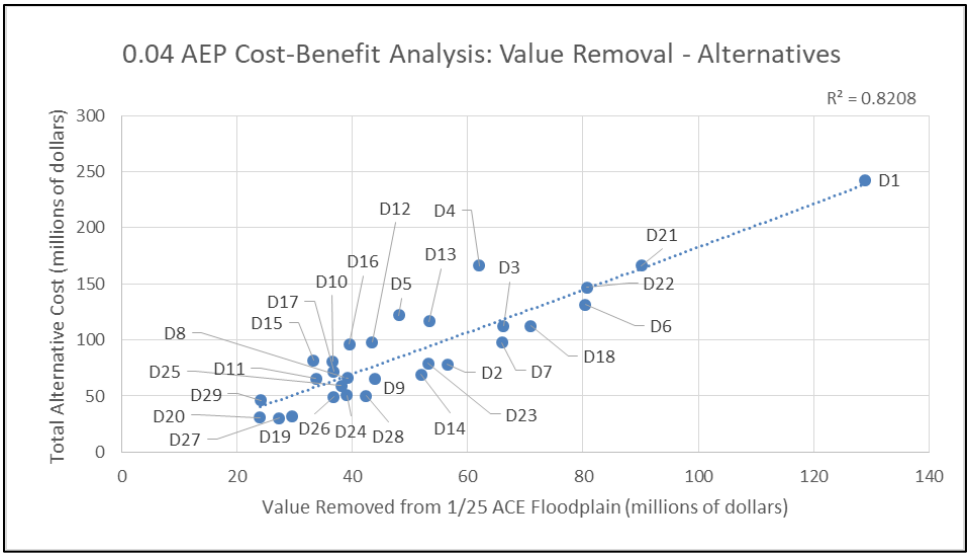

Figure 4-28: *Alternatives cost-benefit analysis for value removed from the 0.04 AEP floodplain*

The plans presented in Figure 4-28 were created with the cost data applicable to each detention site as well as the derived performance data described in Section 4.2.1. For illustrative purposes, plans both above and below the cost threshold are provided. The 29 total plans shown represent a working formulation to inform the analysis described in this section and were created as most-sensible detention site combinations based on performance and cost effectiveness (Figures 2-24 through 4-27 and Table 4-12). Individual measures within all of the depicted combinations are not provided here; the individual measures that make up plans selected for additional analysis (i.e., economic modeling) are provided in Table 4-13.

Figure 4-28 shows that detention sites plotting between (and including) **D2** and **D19** are desirable. D19 represents the lowest cost but beneficial detention plan possible from the array, while D2 represents the highest cost ($78,100,000) but beneficial plan possible from the array. These two plans were provided to economics both as final alternatives for analysis, but also to direct further formulation. By capturing the benefits of these plans, the desirability of utilizing lower cost, lower benefit plans, or higher cost, higher benefit plans was better understood (i.e., selection was projected to either include, or be located between these two plans). For example, it was assumed that D2 would likely be too expensive for this study based on the plans total cost and the economic threshold. However, by running economics on this plan, and D19, indication of the level of cost reduction from D2 was provided.

Additionally, water surface elevation reduction statistics were considered for final formulation. Interestingly, the value removed from the 0.04 AEP floodplain correlates very well with structures that observed reductions between 0 and 1 foot (Figure 4-29), so this bin was considered satisfied by the analysis completed for total removal from the floodplain. The 1.0 to 3.5-foot bin was also targeted for formulation on the basis that, despite the comparably low numbers of structures classified within this bin, these structures could have higher values than those removed from the floodplain, and the greater reductions associated with these statistics create higher benefits than the same number of reductions from 0 to 1.0 ft. Based on Figure 4-

25, it was somewhat obvious that VD5 should be utilized for this targeted plan; however, several additional plans were developed with consideration of this bin (Figure 4-30).

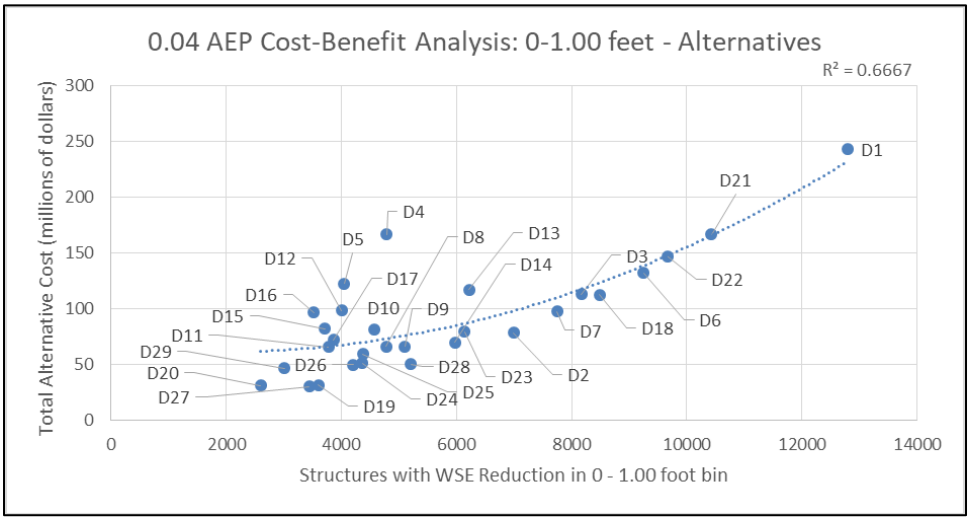

Figure 4-29: *Alternatives cost-benefit analysis for WSE reductions between 0 – 1.00 feet*

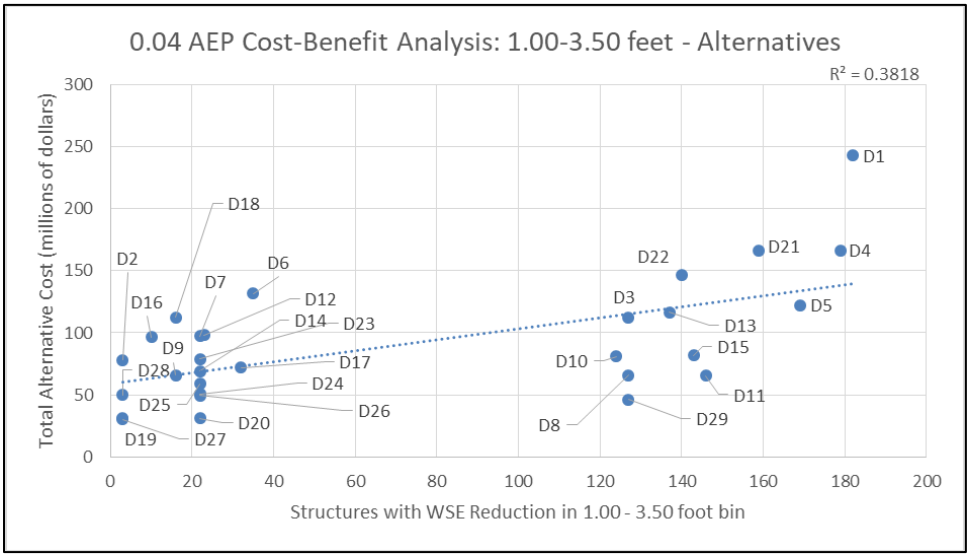

Figure 4-30: *Alternatives cost-benefit analysis for WSE reductions between 1.00 – 3.50 feet*

Based on Figure 4-30, plans **D11** and **D29** were selected as "indicator plans" for economic modeling in FDA. The confidence associated with these plans was not as high as that associated with plans D2 and D19, provided the lower value-to-cost ratios (see Table 4-12). This ratio was based only on value removed from the floodplain, however, and does not consider reductions in flood elevations on affected structures (overall "value" should increase). Trends between quantified structures with WSE reductions and value associated with WSE reductions are expected to be the same based on strong correlation between structures and value removed from the 0.04 AEP floodplain (Figure 4-31).

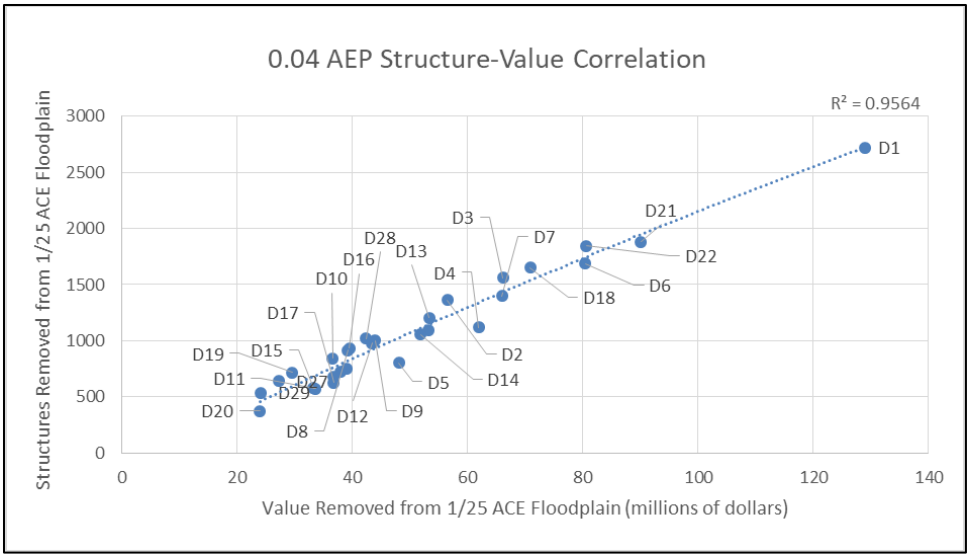

Figure 4-31: *Alternatives correlation analysis for structures and associated value removed from the 0.04 AEP floodplain*

4.2.4 Final Alternatives

The final alternatives included both standalone and combination plan-types. The previously described "indicator" detention plans as well as full FDA modeling results for individual measures of VD1, VD2, VD5, and VB9 provided valuable insight for the development of additional detention plans as well as determination of the most effective detention sites to use in measure combinations. Individual analysis was completed for the listed detention sites based on their overall performance, and for certification of combination alternatives formulation. An iterative workflow was undertaken to refine plan formulation as economic modeling was completed. Table 4-12 provides the results for costs and economic benefits for all modeled plans (individual measures included as well). Data in the table do not include any NED cost refinements.

Table 4-12: Costs and economic performance for all HEC-FDA-modeled structural study alternatives and measures[1, 2]

Type	Name	Description	Total First Cost	Annualized Cost	Mean Annual Benefit	Mean Annual Net Benefit[3]	Mean BCR[3]
Detention	D2	VD1, VD2, VD3, & VD4	$78,169	$3,075	$2,733	-$342	0.89
	D11	VD1, VD5, & VD9	$65,434	$2,569	$2,028	-$540	0.79
	D19	VD1 & VD2	$31,469	$1,244	$2,203	$959	1.77
	D27	VD1 & VD4	$30,293	$1,198	$2,021	$822	1.69
	D28	VD1, VD2, & VD4	$50,070	$1,976	$2,717	$740	1.37
	D29	VD1 & VD5	$46,143	$1,810	$1,991	$181	1.10
	VD1	-	$11,692	$466	$1,305	$839	2.80
	VD2	-	$19,777	$778	$1,220	$442	1.57
	VD5	-	$34,451	$1,344	$1,673	$329	1.24

Levee	L1	VL2 & VL3	$38,223	$1,504	$223	-$1,281	0.15
Bridge Modification	B1	VB1, VB2, VB9, UB1, & UB2	$22,880	$942	$668	-$275	0.71
	VB9	-	$1,483	$72	$555	$483	7.69
Combination	C1	VC1 + VB8	$8,457	$356	$976	$619	2.74
	C2	VC1 + VB8 & VB9	$9,940	$428	$1,008	$579	2.35
	C3	VD1, VC1 + VB8, & VB9	$21,632	$894	$1,413	$591	1.72
	C4	VD1, VD2, VC1 + VB8, & VB9	$41,409	$1,692	$2,030	$338	1.20
	C5	VD1, VC1 + VB8	$20,149	$822	$1,413	$591	1.72
	C6	VD1, VD2, & VC1 + VB8	$39,926	$1,620	$1,989	$369	1.23
	C7	VC1 + VB8, B1, L1	$69,560	$2,803	$416	-$2,387	0.15
	C8	VC1 + VB8, & B1	$31,337	$1,299	$1,007	-$292	0.78
	C9	VD1, VD2, VD4, VC1, & VB8	$58,526	$2,332	$2,865	$503	1.21

[1]*Costs and economic benefits in thousands of dollars.*
[2]*Data based on FY20 price level.*
[3]*Plans with negative net benefits shown in red.*

As described, all plans that did not include any detention sites were provided to economics for the first modeling cycle. This analysis showed that negative net benefits were associated with the levees (L1), which also drove negative net benefits for plan C7. Negative net benefits were associated with B1; however, additional investigation was carried out to isolate one structure – VB9 (18th Ave. Bridge in Bessemer) – for further analysis. Isolation of VB9 from the bridge modification plan and inclusion of this measure in subsequent plan formulation was considered desirable based on its hydraulic performance. It was understood that modifications to bridges upstream of VB9 (VB1 and VB2) were responsible for downstream increases in flood profiles that drove the negative net benefits associated with B1. The hydraulic performance of VB9 was considered strong at upstream structure locations, and isolated modeling of this site showed minimal impacts downstream. Hydraulic performance was confirmed with isolated economic modeling as well (see Table 4-12).

Results from the economic model showed that the detention plan with the greatest mean benefits overall was D2; however, overlap in the benefits of individual detention sites within this plan ultimately drove negative net benefits. D19 was considered the best overall performing detention plan with strong net benefits ($939,000/year), and a BCR of 1.74. Incremental analysis of structural and non-structural combinations was performed on a selection of structural plans to test sensitivity including C1, C5, C6, D28, and the individual measure of VD1 (based on highest performance). The non-structural measure analyzed in economic analysis was acquisitions that targeted residual 0.50 AEP floodplain risk (i.e., structures remaining in the 0.50 AEP floodplain after structural plan implementation) for all combinations. Standalone non-structural plans were also analyzed for structures subjected to flood risk from FWOP 0.50 and 0.20 AEP events. In accordance with Planning Bulletin 2016-01 (USACE, 2015a), other non-structural measures were considered within this study, but were eliminated based on feasibility

of implementation related to construction type, expected costs, or overlap with local efforts. Land-use regulations were addressed in sponsor-drafted stormwater management plans described in Section 3.1.2 but remained a consideration for measure designs in this study. Wet and dry flood-proofing were considered, though not pursued based on structural density and flow velocities and residential construction types within the basin. Basement fills were considered inapplicable based on construction types. Structural elevations were removed from the study based on feasibility and costs related to the number of structures in even very frequent floodplains. Emergency preparedness plans and flood warning systems were discussed; however, the study sponsors indicated that planning phases for local efforts to address these measures were being initiated. Reference the main study report for more information on nonstructural measures.

The NED plan was identified as D19, and this plan was selected as the recommended plan. This plan was selected as the FRM plan that maximizes net benefits on a national scale. The recommended plan provides a high level of flood risk reduction based on uniformly distributed benefits within the study area and is the study sponsor's preferred plan. All final structural, non-structural, and structural/non-structural plans considered for final plan selection are provided in Table 4-13. Data in the table do not reflect NED plan cost refinements. Information on cost refinement resulting in increased net benefits for the recommended plan is provided in the Main Report as well as Economic and Cost Appendices of this study report.

Table 4-13: Final FRM alternatives considered for plan selection[1, 2]

Description	Total First Cost	Annual O&M Cost	Annual Total Cost	Mean Annual Benefit	Mean Annual Net Benefit	Mean BCR
Structural Alternatives						
C1 = VC1, VB8	$8,457	$30	$356	$976	$619	2.74
C2 = VC1, VB8, VB9	$9,940	$45	$428	$1,008	$579	2.35
D28 = VD1, VD2, VD4	$50,070	$45	$1,976	$2,717	$740	1.37
Recommended Plan: D19 = VD1, VD2	$31,469	$30	$1,244	$2,203	$959	1.77
D27 = VD1, VD4	$30,293	$30	$1,198	$2,021	$822	1.69
C6 = C1 + D19	$39,926	$80	$1,620	$1,989	$369	1.23
C4 = C2 + D19	$41,409	$95	$1,692	$2,030	$338	1.20
C9 = C1 + D28	$58,526	$105	$2,332	$2,865	$503	1.21
Non-structural Alternatives						
0.50 AEP Structural Buyout (~ 100)	$53,685	$0	$2,071	$2,771	$700	1.34

0.20 AEP Structural Buyout (~ 300)	$92,713	$0	$3,576	$4,106	$530	1.15
Structural/Non-structural Alternatives						
C1 + VD1 + Residual 0.50 AEP Buyout	$73,833	$55	$2,903	$3,540	$638	1.22
C1 + D19 + Residual 0.50 AEP Buyout	$93,610	$80	$3,690	$3,907	$217	1.06
D28 + Residual 0.50 AEP Buyout (~ 40)	$70,761	$45	$2,774	$3,094	$320	1.12
C1 + Residual 0.50 AEP Buyout (~79)	$52,635	$30	$2,060	$3,266	$1,206	1.59

[1]*Costs and economic benefits in thousands of dollars.*
[2]*Data based on FY20 price level.*

4.3 Recommended Plan Details

The recommended plan for flood risk management selected from this study is Alternative 4 (D19). This plan consists of two overbank detention basins (VD1 and VD2). Conceptual designs of all refined measures were completed to support quantities, costs, and engineering analysis, with draft drawings completed for the recommended plan. Design details are provided in Section 4.1.2.2. Draft drawings (overview plans, sections, and lateral weir detail) of the recommended plan are included in Figures 4-32 through 4-35. Overbank drainage designs relevant to the basins have not been completed within this study but should be completed in a later project phase (i.e., Preconstruction Engineering and Design [PED]). As shown in Table 4-6, cost estimates included measures to support drainage of existing channels/swales through sites VD1 and VD4, however. Additionally, lateral inflow weirs were modeled with vertical side slope configurations; however, sheet pile to support this configuration was not explicitly considered in cost estimates. Refinement within PED phase may modify weir designs to incorporate trapezoidal weir templates, which would negate the need for lateral sheet pile support. The costs associated with these changes are not expected to exceed the contingency associated with estimates. An assessment of structural classification, operations and maintenance considerations, and Phase I geotechnical investigation details are provided in the sections following.

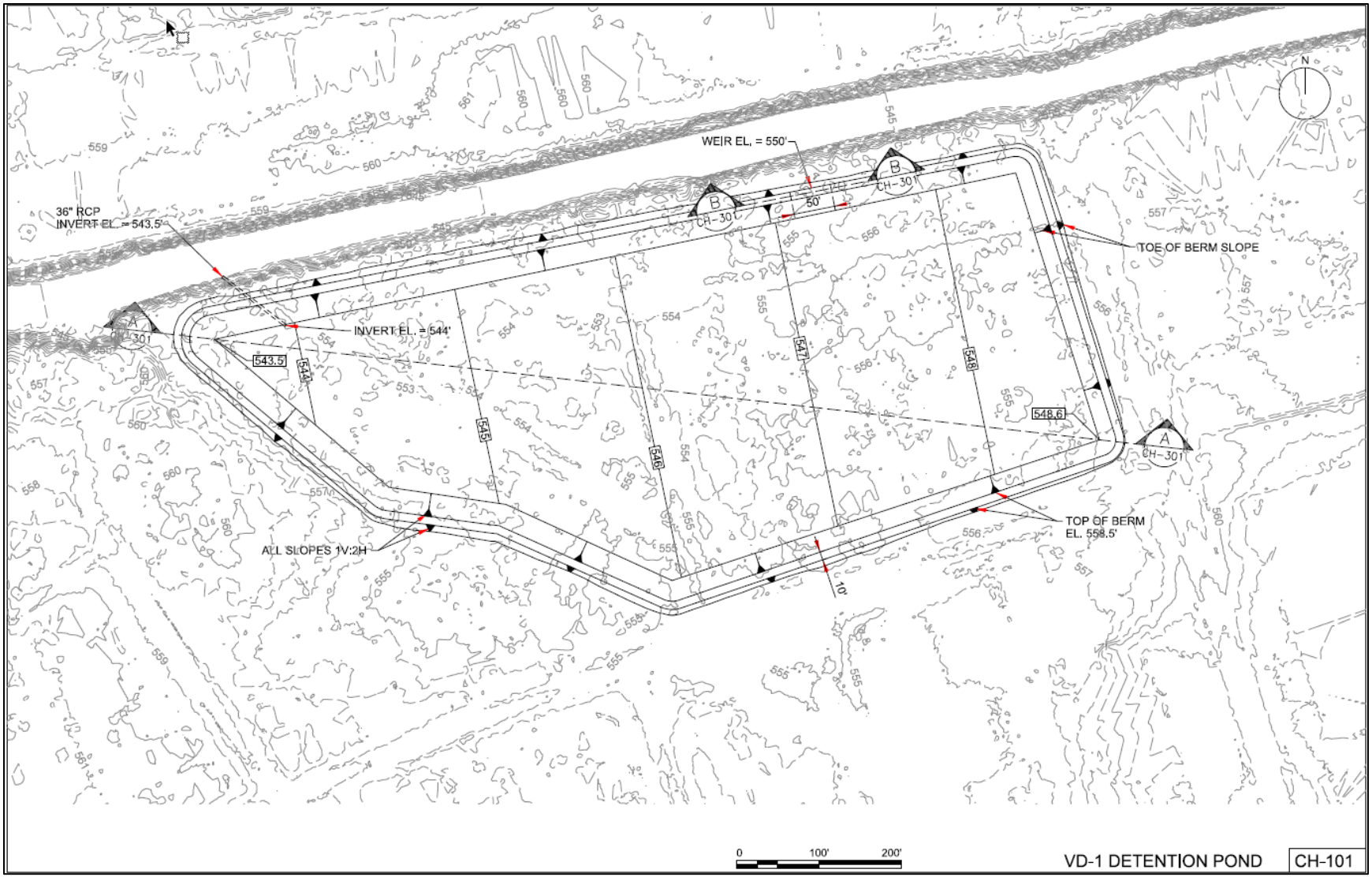

Figure 4-32: *Conceptual plan of overbank detention basin and levee VD1.*

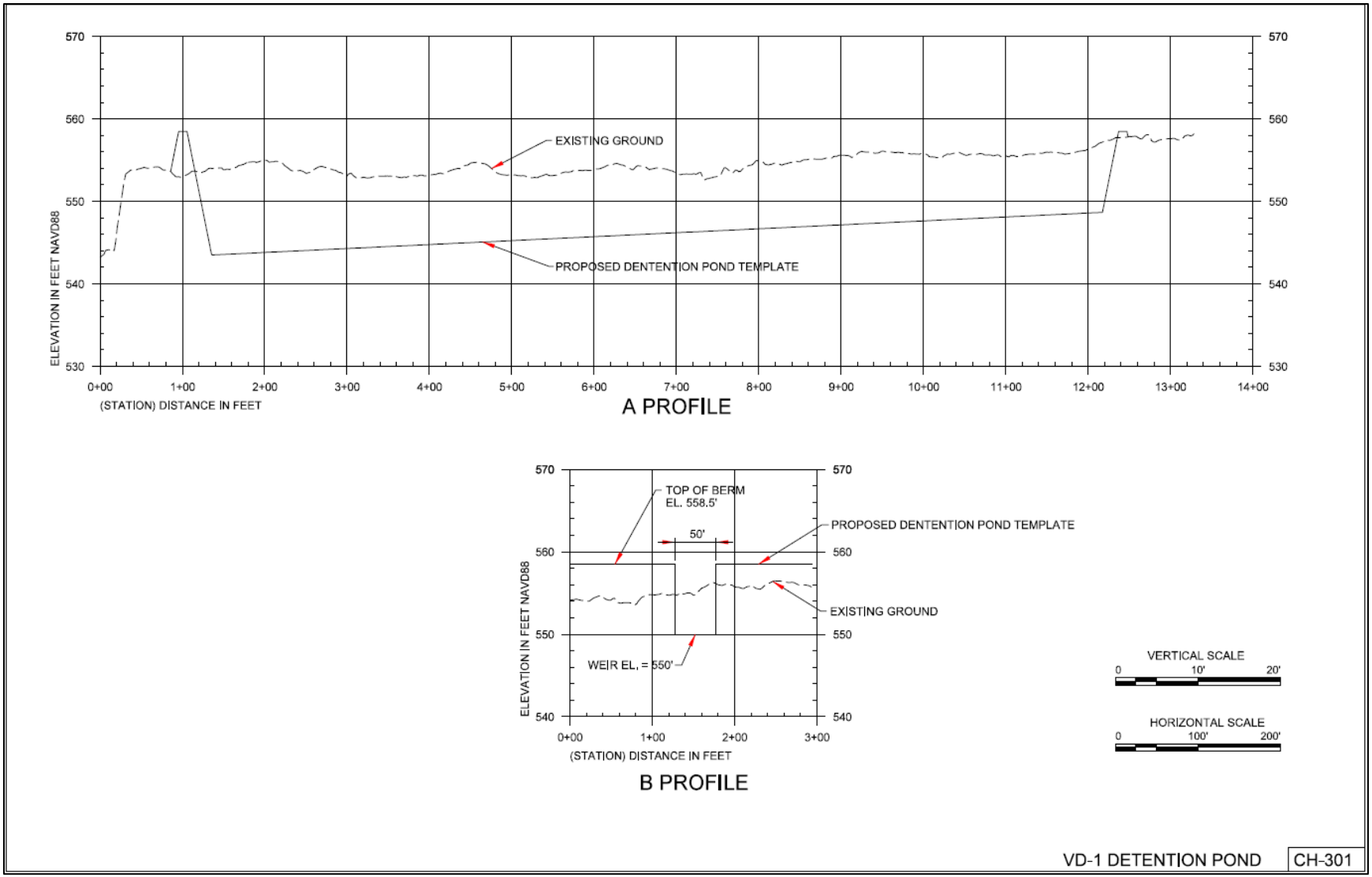

Figure 4-33: *Conceptual profile and section detail of basin and lateral inflow weir through levee at VD1, respectively.*

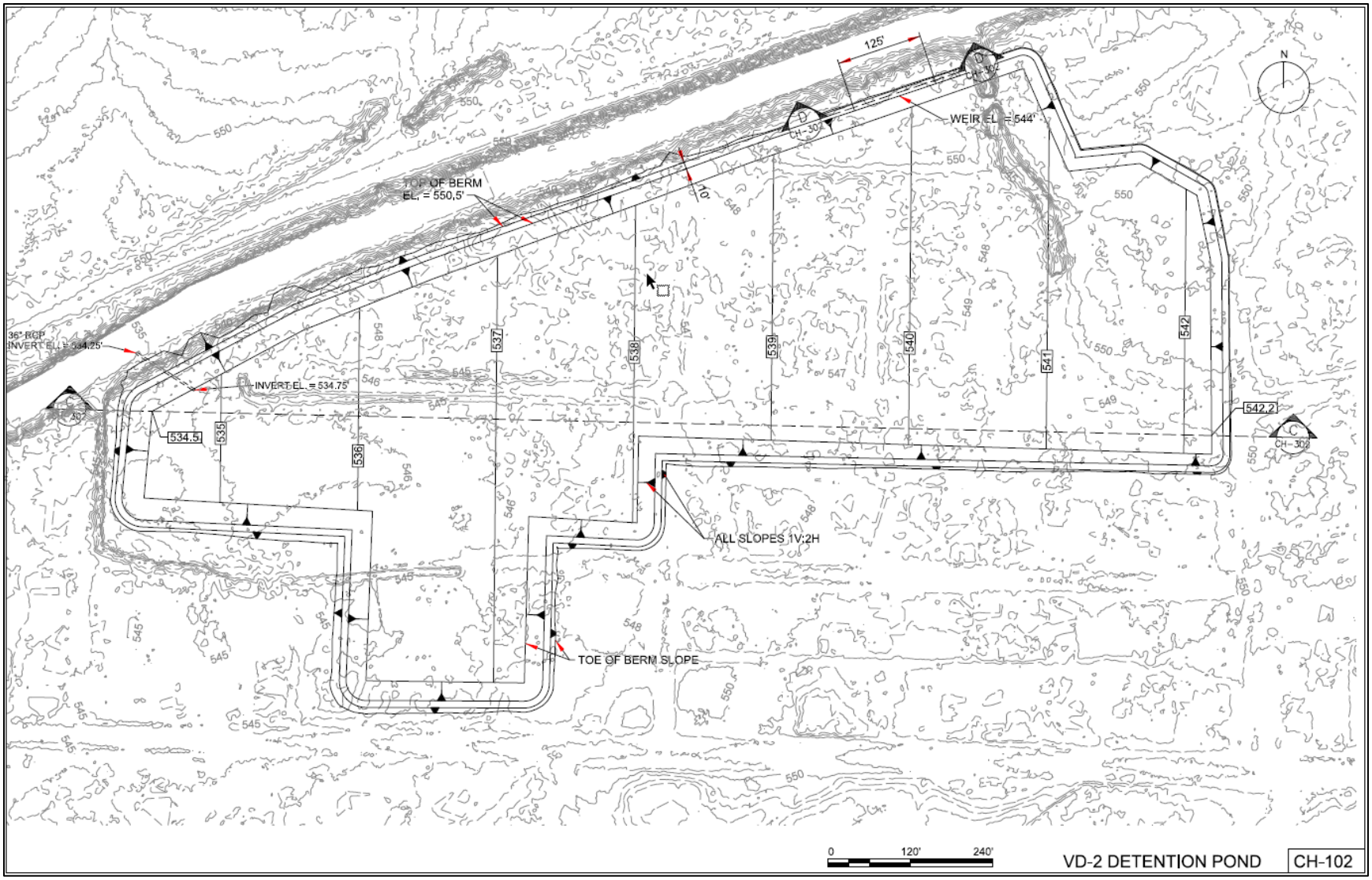

Figure 4-34: *Conceptual plan of overbank detention basin and levee VD2.*

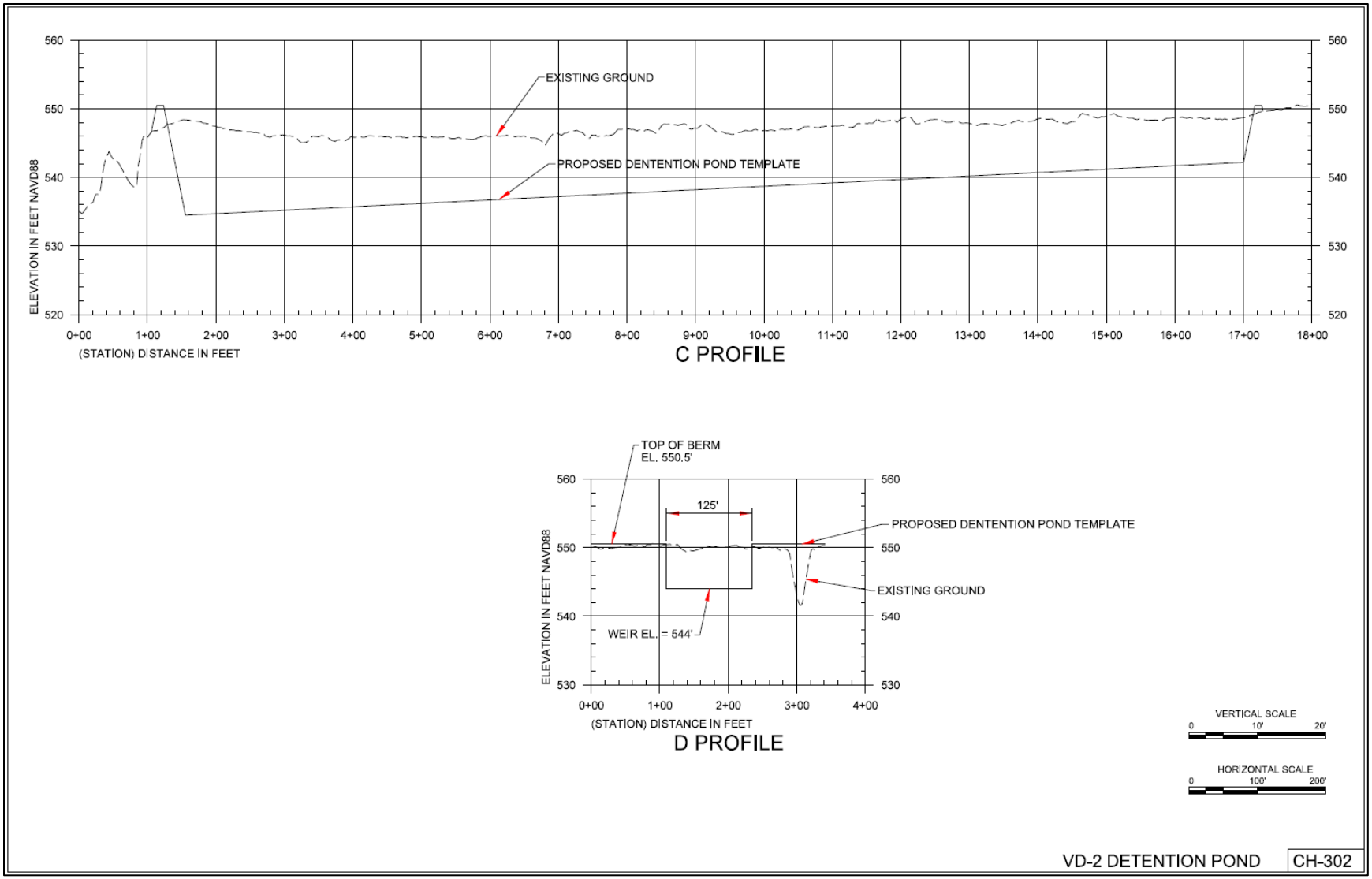

Figure 4-35: *Conceptual profile and section detail of basin and lateral inflow weir through levee at VD2, respectively.*

4.3.1 Structural Classification

The potential for dam or levee classification of the overbank detention sites was recognized early on in this study. Based on geometric parameters, neither of the proposed plan measures meet the definition of a dam as provided in ER 1110-2-1156 (USACE, 2014). Table 4-14 provides the geometric parameters of the recommended plan measures. Values for storage above adjacent ground and maximum berm height were based on the lowest continuous elevation adjacent to the toe of the pond berms.

Table 4-14: Detention basin storage details

Location	Total storage (ac-ft.)	Storage above adjacent ground (ac-ft.)	Max. berm height above adjacent ground (ft.)
VD1	98	40	4.5
VD2	184	90	5.5

As a result of policy review and vertical team coordination leading up to the Agency Decision Milestone, it was decided that the recommended plan measures would be classified as levees based on project performance, to communicate potential project risk, and for prioritization within the Inspection of Completed Works (ICW) program. The storage areas and the surrounding elevated berms act to divert water from the river, lowering water surface elevations in the floodplain during high flow events. As these berm structures will act to divert some water from the floodplain to reduce flooding to the area outside of the storage area, they are classified as levees.

However, due to the low maximum head differential and interpretation of the results of the life safety analysis (Section 5.2.4), failure of any part of these structures does not cause incremental life loss or additional damage to critical infrastructure. This assessment supported cost refinements for the recommended plan within this study's cost and schedule risk analysis (CSRA). Refinement included removal of ACB protection from the levees (excluding spillways) within the recommended plan. For consistency in reporting, and because designated levee measures were analyzed early on this study, terminology of reference to the recommended plan measures including "detention basins," "basins," or "ponds" is used in subsequent sections of this appendix.

4.3.2 Operations and Maintenance

Successful operation of the detention basins proposed within the recommended plan depends on sponsor-execution of specific maintenance activities. At The non-federal project sponsors have expressed their commitment to supporting operation of the recommended plan through maintenance activities over the project life cycle. It is expected that development of an Operations and Maintenance (O&M) manual will occur in the PED phase to detail these activities, their expected schedule, and responsible parties. At present, the activities described herein and within the Main Report (see Section 7.4) are understood to be requirements of the non-federal project sponsors. Expected activities include the following:

- removal of trees, brush, and animal burrows from embankments;
- structural repairs of damaged inlets, outlets, or spillways;
- embankment slope repairs;
- trash and debris removal from the detention areas and disposal;
- sediment removal from the detention areas and disposal;
- debris removal from outlet culvert trash-racks; and
- bottom-grade mowing.

Of pertinent consideration are repairs to damaged components (i.e., embankments, spillways, and inlet and outlet works), which should be conducted on an as-needed basis. Trash and debris removal should also occur on an as-needed basis, following observations of clogged/constricted inlet works, and may follow post-storm inspections where inflows were known to occur (i.e., ≤ 0.50 AEP by design). It is expected that annual inspections will be conducted to certify the condition of the project with scheduled maintenance to vary by activity (LFUCG, 2009). More frequent inspections should occur following storm events, and the frequency of such inspections as well as a checklist of activities to be performed should be detailed in an O&M Manual.

Expected sediment removal frequency is not fully understood at this time. While highly variable, the EPA reports values for stormwater systems between 25 and 50 years (WMI, 1997). Maintenance of trash and debris will work to prevent damage to inlet/outlet culverts, while removal of accumulated sediment will work to ensure storage capacities are maintained. Sediment deposition is expected to occur and was considered as a life-cycle cost measure in estimates. As a maintenance reduction strategy, micropool construction near the pond outlet points can aid in the capture of deposited sediments, while decreasing the frequency of removal from the basins. The EPA suggests clean-out of these areas should occur at 5 to 7 years (WMI, 1997), though the actual frequency of sediment removal will be based on project performance.

4.3.3 Phase I Geotechnical Investigation (March 2021)

4.3.3.1 Core Drill Investigation

The U.S. Army Corps of Engineers (USACE) Mobile District Core Drill team performed a more focused subsurface investigation at pond sites VD1 and VD2 in March of 2021. The investigation consisted of performing the following procedures/tests in general accordance with the methods listed and at the quantities specified:

- Performing seventeen (17) Standard Penetration Test (SPT) borings) advanced to depths ranging from 6 feet to 19.5 feet below ground surface (bgs) in the proposed pond bottom areas. The borings were sampled continuously to the boring termination depth.

- Performing one (1) manual auger boring at boring location VD2-07-21. This test boring was not appropriately cleared by Alabama 811 so a manual auger boring was performed in lieu of the SPT boring. VD2-07-21 was advanced to a depth of 7.3 feet bgs.

- Performing three (3) rock core samples at boring locations VD1-02-21, VD1-09-21, and VD2-03-21.

SPT borings were performed with a truck-mounted drill rig and advanced using the auger drilling techniques. SPT sampling was performed continuously using a 1-3/8-inch I.D. (2 inch O.D.) split-barrel sampler, in which the sampler is driven at 1.5 foot intervals into the soil by repetitive blows of a 140 pound hammer dropped from a height of 30 inches. The number of blows necessary to advance the sampler for each 6-inch interval is recorded. The standard penetration resistance, or "N" value, is the sum of the blows required for the second and third drives. The hole is then cleaned or reamed to the top of the next interval to be sampled and the procedure is repeated. SPT sampling was performed in general accordance with ASTM D1586 (2018). Split-barrel samples were visually classified in the field then placed into plastic jars which were sealed with a Teflon-lined cap.

Rock cores were performed in general accordance with ASTM D2113 (2014). Rock is core-drilled using special core bits set with carbide steel or diamond, depending upon the rock texture. The bit is fitted onto a double tube swivel-type core barrel on which an exterior tube and the bit rotate, and an interior barrel remains stationary to receive the rock core. Drill fluid is circulated between the barrels and across the bit face to provide cooling and to flush away cuttings. See boring logs attached for rock core details.

The table below summarizes the test boring locations, depths, ground surface elevations, groundwater elevations, and top of rock elevations. Ground surface elevations displayed below were obtained from the model DEM, whereas elevations shown in appended borings logs (see Appendix A-1) were based on rounded values from a contour map. As such, groundwater and top of rock elevations in Table 4-15 differ slightly from those provided in boring logs, with tabulated elevations considered more accurate. A boring location plan illustrating the locations of all test borings is also provided in Appendix A-1 of this report.

Table 4-15: Summary of Boring Location Data

Boring #	Latitude	Longitude	Depth, ft-bgs	Ground Surface Elev. ft-NAVD88	Ground Water Elev. ft-NAVD88[1, 2]	Top of Rock Elev. ft-NAVD88[1]
VD1-01-21	33.505364°	-86.836971°	11.2	556.2	546.7	545.0
VD1-02-21	33.504751°	-86.836436°	9.4	555.9	*NE	546.5
VD1-03-21	33.504560°	-86.837352°	6.1	555.5	553.7	549.4
VD1-04-21	33.505231°	-86.838039°	6.9	554.1	NE	547.2
VD1-05-21	33.504874°	-86.837004°	9.7	554.3	NE	544.6
VD1-06-21	33.504127°	-86.838184°	8.4	554.8	NE	546.4
VD1-07-21	33.504417°	-86.838905°	9.6	553.8	545.5	544.2
VD1-08-21	33.504904°	-86.839491°	8.6	554.9	NE	546.3
VD1-09-21	33.504703°	-86.838230°	9.4	554.1	546.6	544.7
VD2-01-21	33.500557°	-86.852204°	7.7	545.7	543.0	538.0

VD2-02-21	33.501241°	-86.850714°	9.6	547.0	542.2	537.4
VD2-03-21	33.501204°	-86.849415°	9.6	548.8	545.4	539.2
VD2-07-21	33.501968°	-86.851215°	7.3	547.1	540.0	539.8
VD2-08-21	33.501768°	-86.852909°	10.0	547.4	543.2	537.4
VD2-09-21	33.501127°	-86.853688°	19.5	548.5	541.9	NE
VD2-10-21	33.501270°	-86.852220°	19.5	545.6	543.0	NE
VD2-11-21	33.501631°	-86.849827°	19.5	549.0	545.5	NE
VD2-12-21	33.501967°	-86.850254°	89.9	548.0	NE	538.1

[1]NE = Not Encountered
[2]Provided elevation is post-drill elevation (at equilibrium; see *Groundwater Conditions*).

Bedrock elevations were analyzed with respect to the design templates for each site (see Figures 4-32 through 4-35) to understand bedrock infringement on required excavation. A cut-fill analysis was completed for each basin using a raster surface produced from reported bedrock elevations and a surface reflecting the design template. Results of the cut-fill analysis show that 6.4% and 4.3% of design excavation could be within bedrock for VD1 and VD2, respectively. These results are subject to uncertainty in bedrock surface interpolation.

Subsurface conditions

The following subsurface description is of a generalized nature, provided to highlight the major soil strata encountered. The boring logs located in Appendix A-1 of this report should be reviewed for specific information at individual test locations. The stratifications shown on the boring logs represent the conditions at the actual test locations. Variations may occur and should be expected between test boring locations. The stratifications represent the approximate boundary between subsurface materials and the transition may be gradual.

Based on the March 2021 subsurface investigation, the surface conditions at the VD1 pond location generally consists of about 6 inches of silty sandy topsoil [SM], with traces of concrete debris and varying amounts of limestone rock and coal fragments. Below the initial surficial zone, soils generally consisted of very silty clayey fine sands and sandy clays [SC-SM, CL-ML] to a depth ranging between 3 to 4.5 feet, followed by lean sandy silty clays with varying amounts of coarse sands and limestone rock fragments to refusal depths ranging from 6.1 feet to 11.5 feet bgs.

Surface conditions at the VD2 boring location generally consists of about 6 inches of silty sandy topsoil [SM], with varying amounts of concrete debris and buried organics. Below the initial surficial zone, soils generally consisted of very silty clayey sands, with varying amounts of limestone rock fragments, coal fragments, and construction debris [SM, SC-SM, SM], to depths ranging from about 1.5 to 3 feet bgs. Below 3 feet soils generally consisted of silty sandy clays, with traces of limestone rock fragments [CL-ML, CL], to depths of about 6 feet, underlain by clayey silts [ML, CL-ML] to the boring termination depth. Borings were typically terminated at rock refusal except for boring locations VD2-9-21, VD2-10-21, and VD2-11-21 which were drilled to 19.5 feet.

Three (3) rock cores were performed at boring locations VD1-2-21, VD1-9-21, and VD2-2-21. From the rock core results, the underlying bedrock generally consists of moderate to good quality dolomite limestone with styolite seams running across the samples. Joint fractures generally occurred horizontally along the styolite seams. Some longitudinal cracks were observed along the upper 1.5 feet at the VD2-3-21 core location. RDQ values of the rock ranged from 67% to 83% across the three core locations. Rock core results and pictures are provided in Appendix A-1.

No laboratory tests were conducted at the time of this investigation. General properties and material classifications shown above and in the boring logs attached are based on field classifications made at the time of the field investigation.

Groundwater Considerations

The groundwater table will fluctuate seasonally depending upon local rainfall. The typical wet season groundwater level is defined as the highest groundwater level sustained for a period of 2 to 4 weeks during the "wet" season of the year, for existing site conditions, in a year with average normal rainfall amounts. At the time of this field exploration, groundwater was encountered at depths ranging from 1.7 feet to 9.8 feet bgs.

Delayed water table readings were taken following the field procedures. At boring locations VD1-03-21, VD2-01-21, and VD2-03-21 water levels increased several feet following completion of the field work. This could be caused by a localized confined aquifer which may be under pressure. Confined aquifers develop when groundwater is separated from atmospheric pressure by two relatively impermeable soil layers (Figure 4-36). If the top confining unit is penetrated, groundwater below the unit will rise through the hole/well until it equalizes with the groundwaters unconfined source.

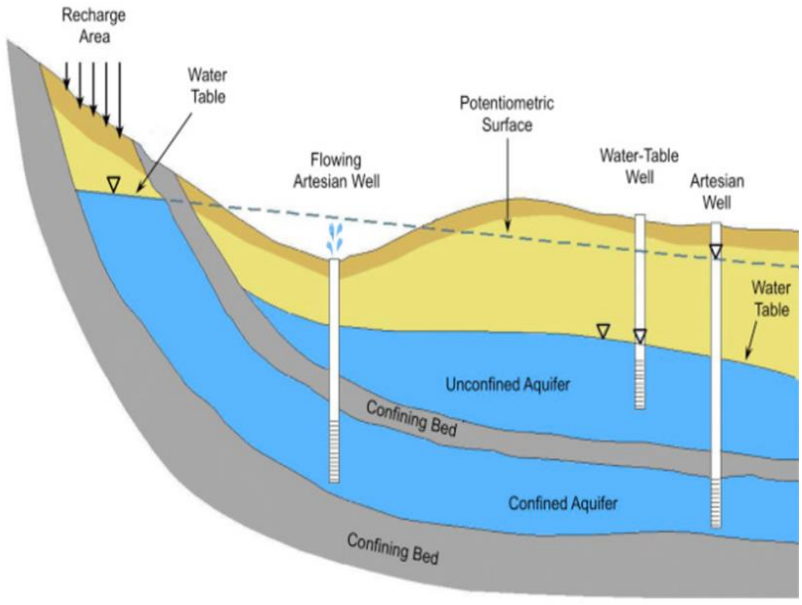

Figure 4-36: *Confined and unconfined groundwater conditions.*

Another possibility is a transient (perched) groundwater table above a confining soil stratum percolated into the borehole following completion of the field test. Transient perched groundwater typically develops above shallow deposits of hydraulically restrictive soils, especially following periods of heavy rainfall and/or irrigation. It should be noted that undercutting into the hydraulically restrictive materials will impact the depth of the transient perched groundwater zone. Additionally, it should be noted that groundwater was observed in a drainage swale located between boring locations VD2-10-21 and VD2-1-21. About 0.5 to 1 foot of water was observed in the berm at the time of the field investigation in March 2021. The dimensions of the swale were not evaluated, however the water level appeared to coincide with the groundwater table measurements at boring locations VD2-1-21 and VD2-10-21. A picture of the drainage swale taken at the time of this field investigation is shown below.

Figure 4-37: *Drainage swale located between boring locations VD2-1-21 and VD2-10-21.*

Based on existing LiDAR data, the drainage swale appears to extend west about 530 feet then turn north to connect with Valley Creek. Proposed pond bottoms at VD2 are anticipated to be between 535.0 ft-NAVD88 and 542.0 ft-NAVD88 from east to west respectively, and proposed pond bottom elevations at VD1 are anticipated to be between 544.0 ft-NAVD88 to 548.0 ft-NAVD88. Excavations to these elevations may encounter either perched or stabilized groundwater tables. Mitigation in construction utilizing controlled drainage should be expected if the collected groundwater data are representative of at-site conditions. If seepage relief is needed following construction of the basins, the existing outlet works, or new and existing drainage channels, may be utilized. It is recommended that piezometers be installed prior to PED to evaluate the groundwater conditions across both sites prior to final pond design.

Geotechnical Assessment

From the rock cores obtained during the field investigation, the bedrock encountered across both pond sites generally consists of Limestone Dolomite with a RQD range from 61 to 83. This is considered to be a fair to good quality moderately hard-to-hard rock with unconfined compression strengths ranging from 285 tsf to 725 tsf. Furthermore, excavating this quality of rock by use of excavator and shank is not feasible. Traditional methods of drilling and blasting should be used to reach design elevations along the pond bottom. Blasted rock is considered suitable for reuse as rip rap, so long as the size requirements are met.

No laboratory tests were performed following this investigation. Based on visual observations made at the time of the investigation the cohesive layers encountered between depths ranging from about 3 to 8 feet appear to be suitable for reuse as levee berm material. However, laboratory tests are required to confirm field observations made during the investigations. Soils must meet classifications requirements described in EM 1110-2-1913 (USACE, 2000).

Additional investigations within PED should be conducted in the proposed berm areas to allow for the slope stability design and seepage analysis. The sampling, testing and selection of drained and undrained soil shear strength parameters shall comply with the guidance provide in EM 1110-2-1902 – Slope Stability (USACE, 2003) and EM 1110-2-1913 – Design and Construction of Levees (USACE, 2000). Piezometers should also be installed to evaluated groundwater conditions at both sites to determine stabilized groundwater conditions.

4.3.1.2 Geophysical Investigation

The Geosciences Branch of the U.S. Army Corps of Engineers Huntsville Center conducted a seismic refraction survey in support of the recommended plan. The objective of the study was to map the top of bedrock, and to provide seismic velocities which could be used to determine the rippability of the bedrock.

The geophysical survey was conducted between February 1 and 5, 2021. Data was collected along a total of twelve (12) seismic lines totaling 1701.5 meters in length. Four lines of seismic data totaling 737.5 meters were collected at VD-1 and eight (8) lines of seismic data totaling 964 meters was collected at VD-2. The refraction survey was successful in providing data to assist in mapping the depth to bedrock as well as delineating the depth to saturated soils, which would represent the approximate water table. The following section provides a summary and description of the site background, the seismic refraction methodology, field investigation activities, and interpretation of results from the geophysical surveys. Maps showing seismic lines and results from the refraction survey are provided in Appendix A-1.

Approach and Geophysical Methods

Seismic refraction requires the generation of a sound wave into the subsurface of the earth and instrumentation to measure and record the refracted waves. This is accomplished using a seismic source (hammer and plate, shotgun, explosive, etc.), seismograph, and a length of cable with multiple geophones. The seismograph measures the travel times of elastic waves generated by the source through the subsurface. Geophones sense the seismic vibrations and convert this mechanical signal or energy into electrical impulses that are measured and recorded by the seismograph.

The refraction method measures the compressional wave (p-wave) velocity to image the subsurface. Refraction waves or ray paths cross boundaries between materials in a way that energy travels from source-to-receiver in the shortest possible time. Source-to-receiver travel time and the corresponding geometry of the geophone spread are then used to calculate layer velocities and layer depth/thickness based on first arrivals of the refracted p-wave. The seismic velocities are characteristic of the type and density of the unconsolidated material and/or rock represented.

The seismic refraction data is interpreted using software for selecting first arrival times and calculating the seismic velocities for each unit and the depth to rock. This process provides high-resolution seismic refraction interpretations by providing depth information under each geophone to various geologic layers. Tomographic processing algorithms can also be used with multiple shot data and provide a higher resolution interpretation of spatial changes in subsurface velocities. Seismic data are typically presented in two-dimensional (2-D) cross section showing changes in velocity with depth. Certain site-specific conditions, if present, can limit the resolution of the seismic refraction interpretation. Examples may include cultural noise (automobiles, machinery, etc.), the presence of thin layers and/or slow velocity zones at depth, which can create erroneous depths in the interpretation of the data.

Field Investigation Activities

The seismic data were collected utilizing a Geometrics Geode 24-channel seismograph for shorter lines or combining two Geometrics Geode seismographs together to create a 48-channel system for longer lines, 4.5 Hz geophones and a 16-pound hammer as a seismic source. The geophone spacing was set at 2.5 meters for all lines.

Shots were performed at the following locations along each seismic line as follows: one off-end shot located 7.5 meters from the first and last geophones, one shot at the first and last geophones and one shot every third geophone. Data from each shot were recorded at 0.5 millisecond intervals for one second and stored on a laptop computer connected to the Geode seismograph. The autostacking feature of the seismograph was used to stack multiple hammer blows at each location to increase the signal-to-noise ratio of the data.

Data Interpretation

All of the data were analyzed using Geometrics' SeisImager program. P-wave data were analyzed using the Pickwin module of SeisImager to select first arrival times. These p-wave first arrivals were then input into SeisImager's Plotrefa module and used with tomographic modeling algorithms to create comparative 2-D cross sections of p-wave velocities. Reciprocal travel time errors were then calculated, and where travel time errors exceeded 5% in any portion of the seismic line, the computer program was used to automatically correct the data by iteratively shifting the travel time curves to spread the reciprocity error out as evenly as possible. These tomographic seismic sections were then converted into three-layer seismic sections in SeisImager. The interpreted three-layer seismic cross sections and corresponding tomographic cross sections are found in Appendix A-1 (Figures 4 - 27). Typically, tomographic data provides interpretation of gradational changes in spatial p-wave velocities, while layered seismic sections, created from refraction first arrivals, provides both interpretation of distinct changes at depth and identification of specific layers.

Materials with three distinct ranges in seismic velocities were detected in the seismic survey. The uppermost material with velocities of 300 – 1,350 m/s is interpreted to be unsaturated sediments, an intermediate layer with velocities of 1,500 – 2,250 m/s, is interpreted to be saturated sediments, and the deepest layer with velocities ranging from 2,400 - 3,000 m/s is interpreted to be competent bedrock of limestone. The velocity range for bedrock might indicate variations in the degree of weathering. Seismic velocities are bulk measurements and variations in velocity reflect broad changes in properties that cannot be interpreted on a fine scale.

An average p-wave velocity of 900 m/s was assigned to layer one of the 3-layer model to represent dry unconsolidated soils, 1,500 m/s was assigned as layer two of the 3-layer model to represent saturated unconsolidated sediments, and 3,000 m/s was assigned as layer 3 for bedrock. Based on the results of the three-layer models, thickness of the unsaturated soil horizon is approximately 1 - 5 meters, and the depth to competent bedrock is 4 – 9 meters for both VD1 and VD2. These ranges agree with data obtained from the core drill investigation.

5.0 Plan Performance

5.1 Plan Benefits

The flood risk reduction performance of the recommended plan is strong throughout the developed portion of the Valley Creek study area. Other studied reaches (Halls Creek, Halls Tributary, and Opossum Creek) are mostly unaffected by implementation of the recommended plan; however, there are some changes from FWOP conditions at and near their confluences with Valley Creek. No structural benefits were derived from these locations, however. Water surface elevation reductions from FWOP conditions on Valley Creek vary by location and frequency, but average approximately 1.5 feet from the location of VD1 (upstream most pond in plan) to just below Murphys Ln. for 0.50, 0.20, 0.10, and 0.04 AEP events (0.50 and 0.04 AEPs shown in Figures 5-1 through 5-6). Benefits were observed for less frequent events as well (0.01 AEP profiles shown in Figures 5-4 through 5-6); however, optimization of pond

performance for the 0.04 AEP event drove increased benefits for more frequent events. For reference, average profile elevation reductions (along development of Valley Creek reach) are approximately 0.4 feet for both 0.005 and 0.002 AEP events.

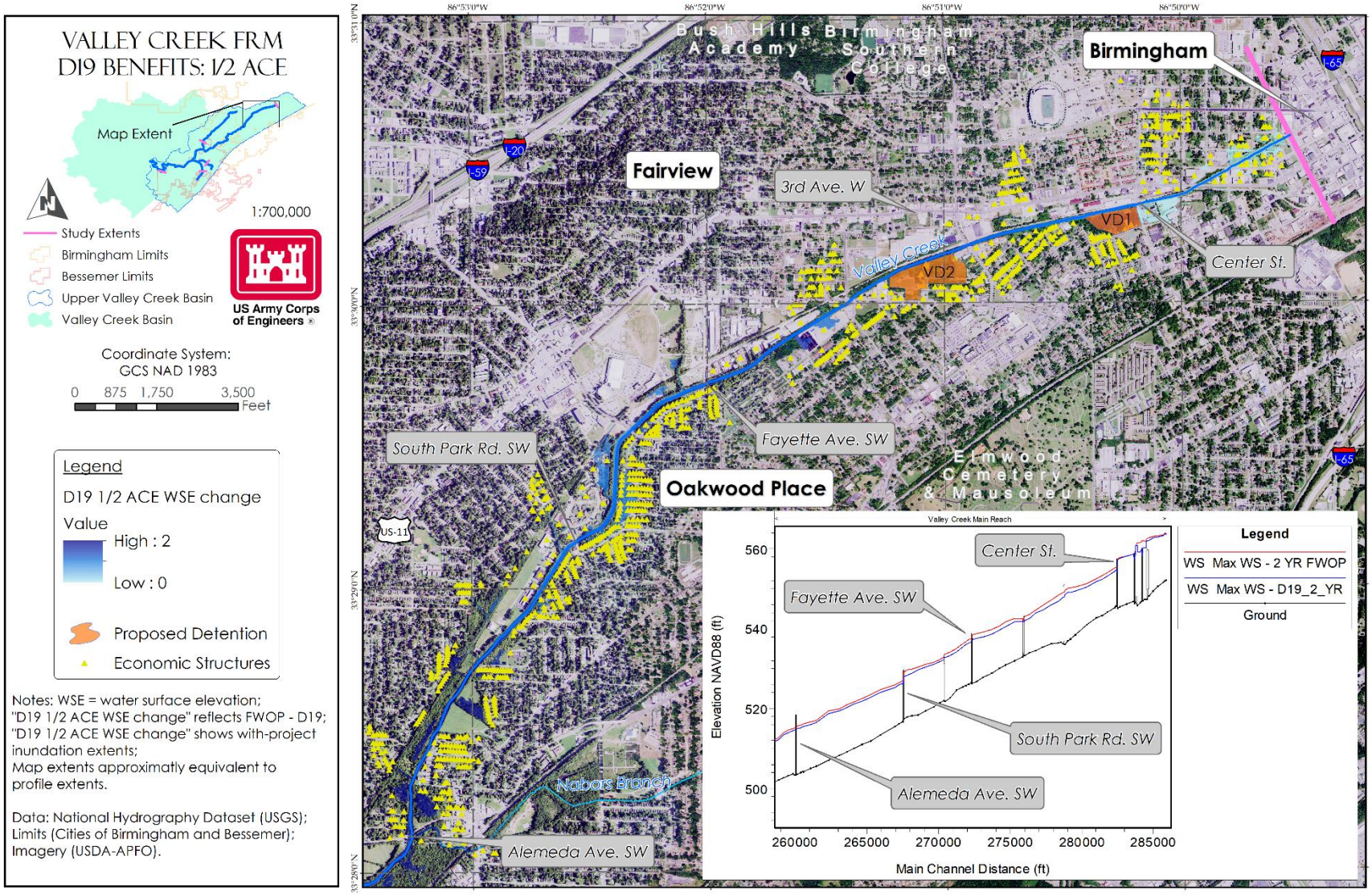

Figure 5-1: *D19 benefits (0.50 AEP event) in the upper extent of Valley Creek.*

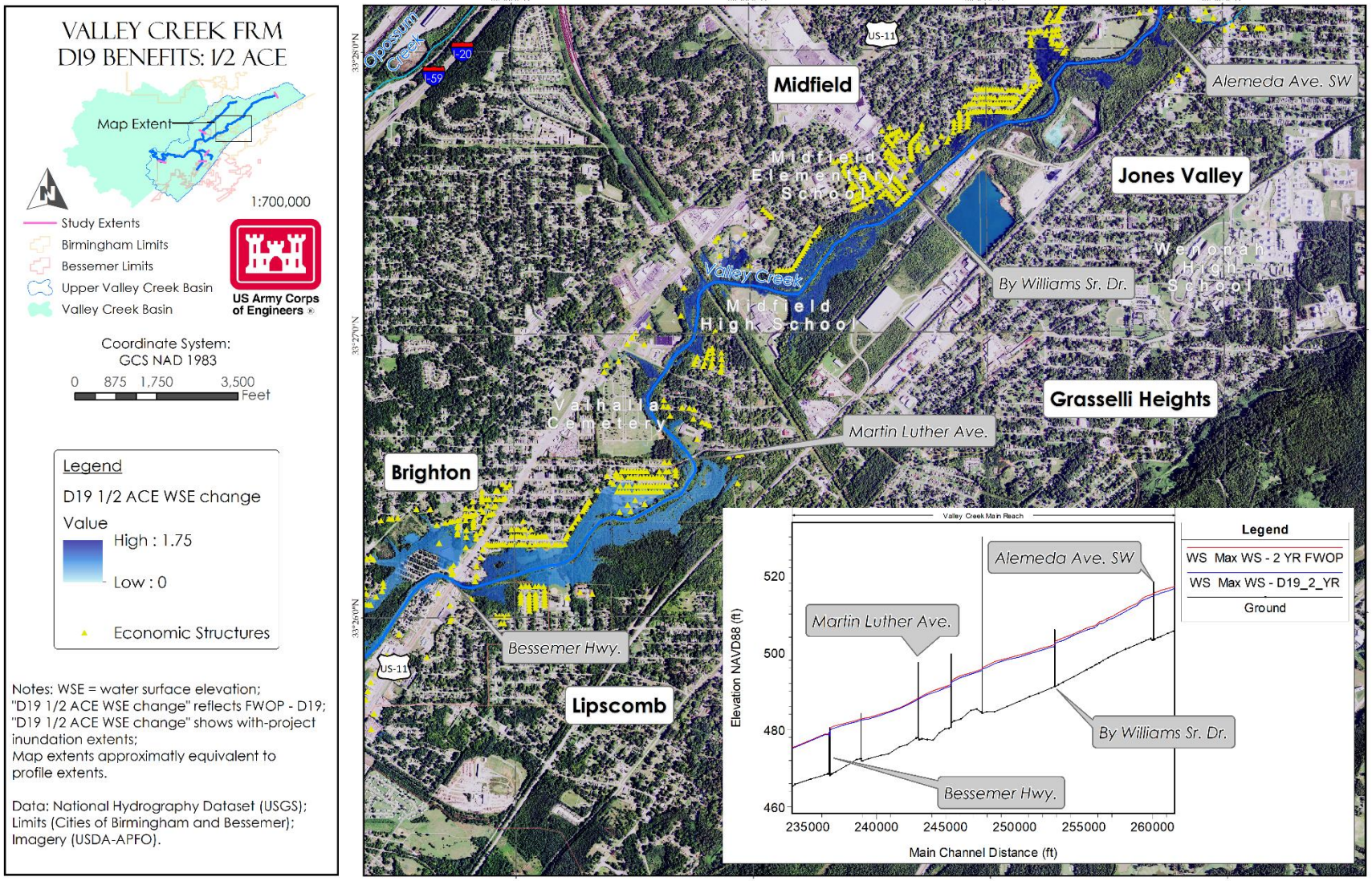

Figure 5-2: *D19 benefits (0.50 AEP event) within the middle extent of Valley Creek.*

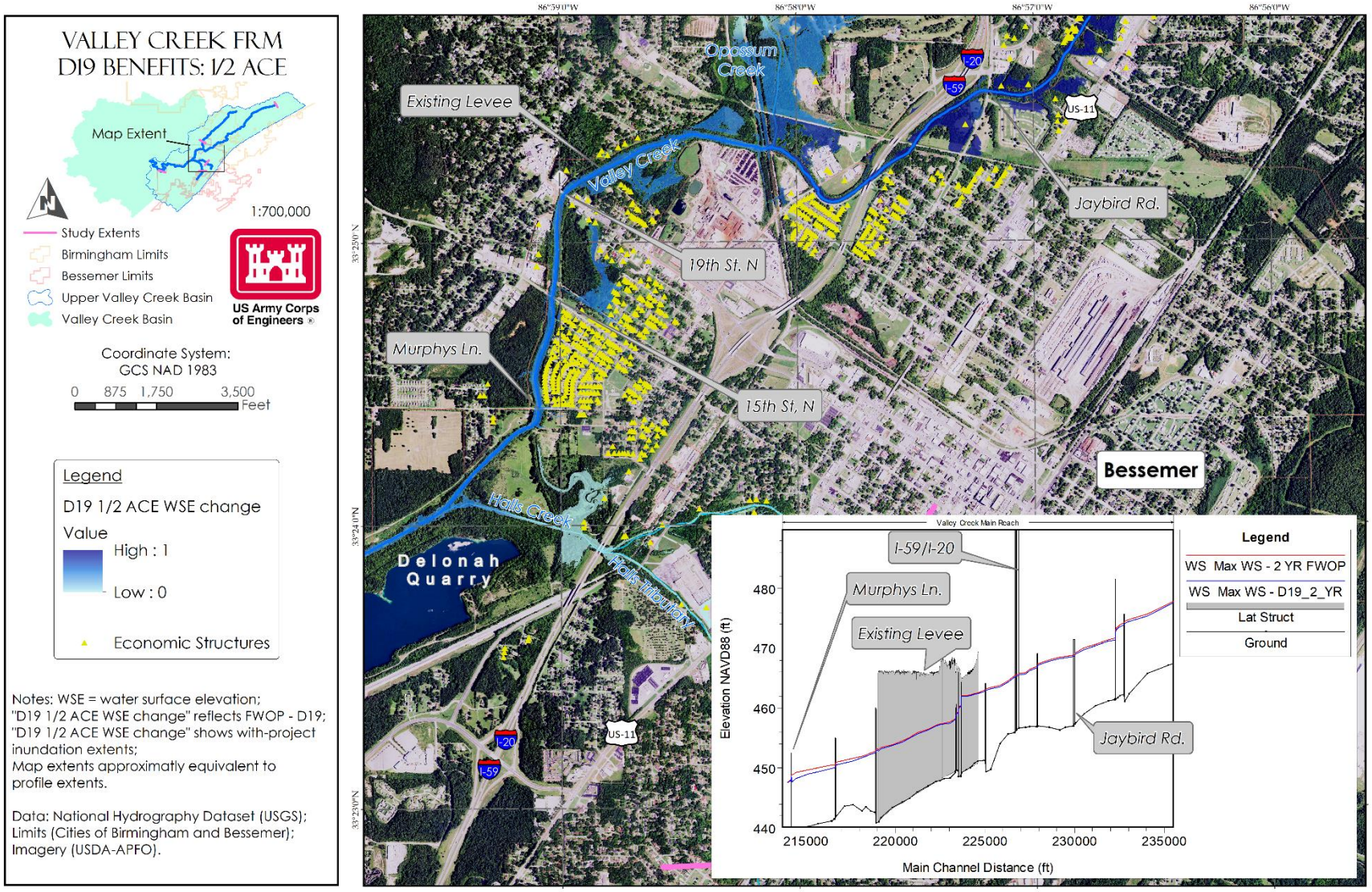

Figure 5-3: *D19 benefits (0.50 AEP event) in the lower extent of the Valley Creek study reach.*

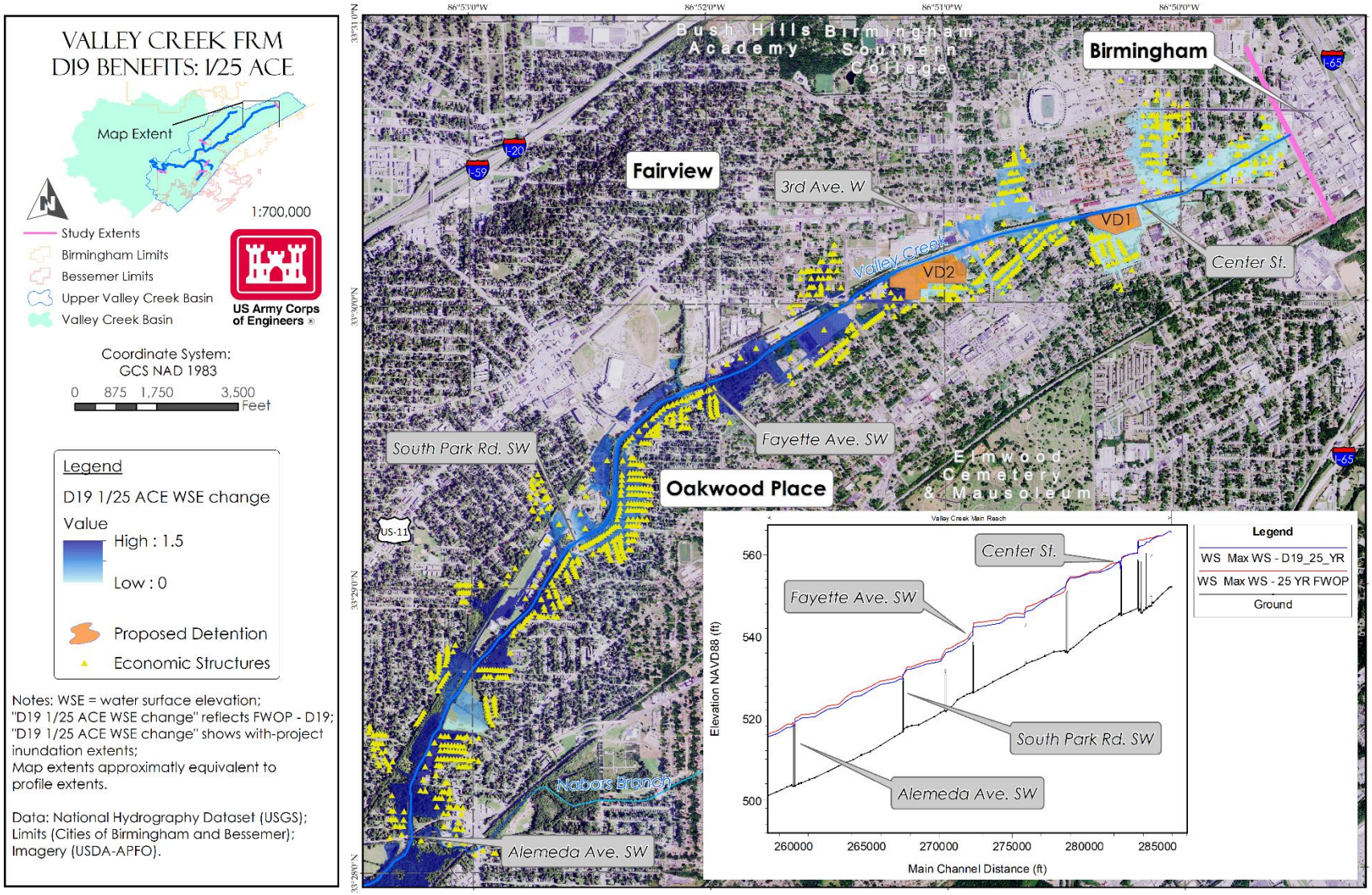

Figure 5-4: *D19 benefits (0.04 AEP event) in the upper extent of Valley Creek.*

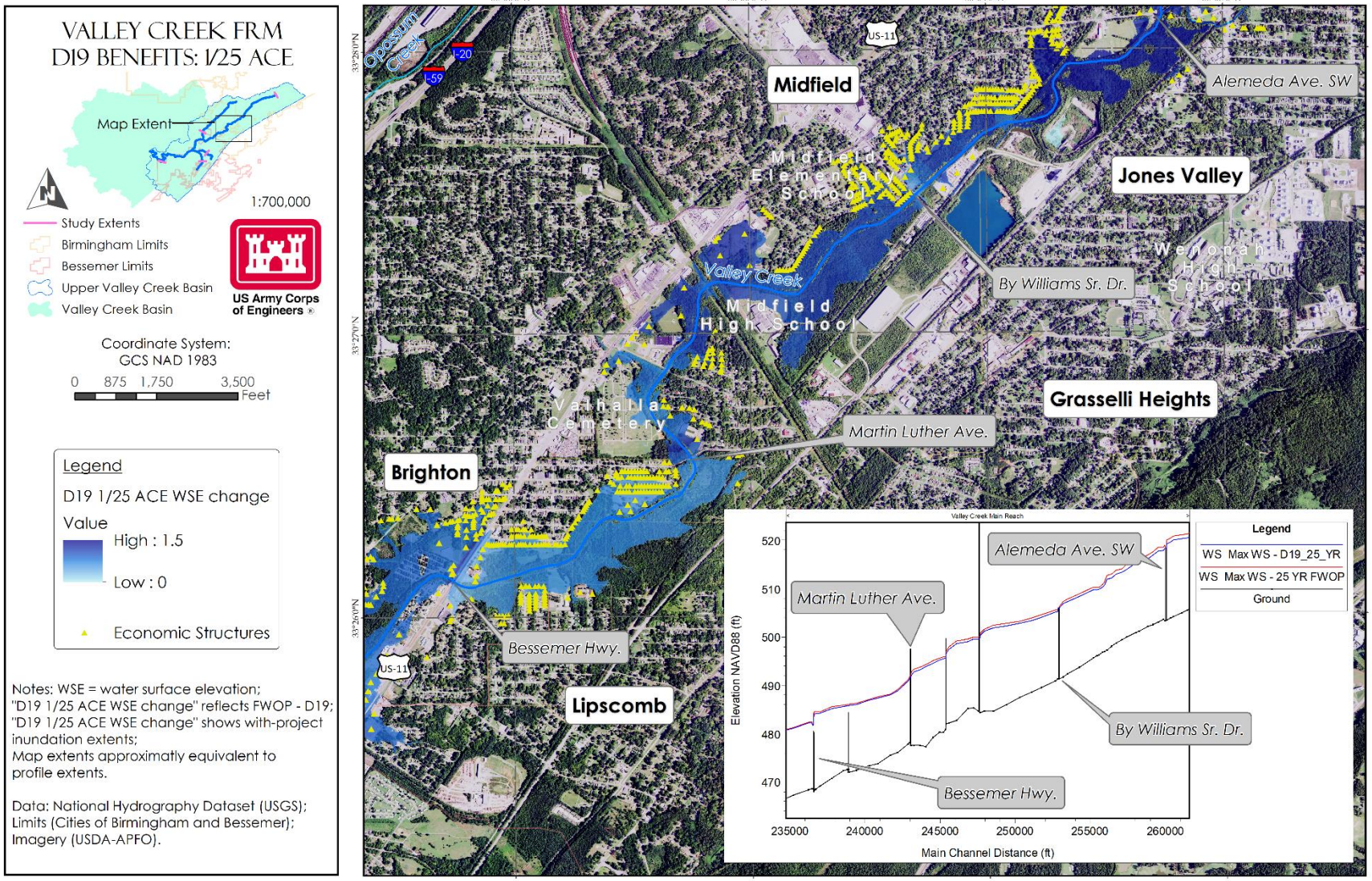

Figure 5-5: *D19 benefits (0.04 AEP event) within the middle extent of the Valley Creek study reach.*

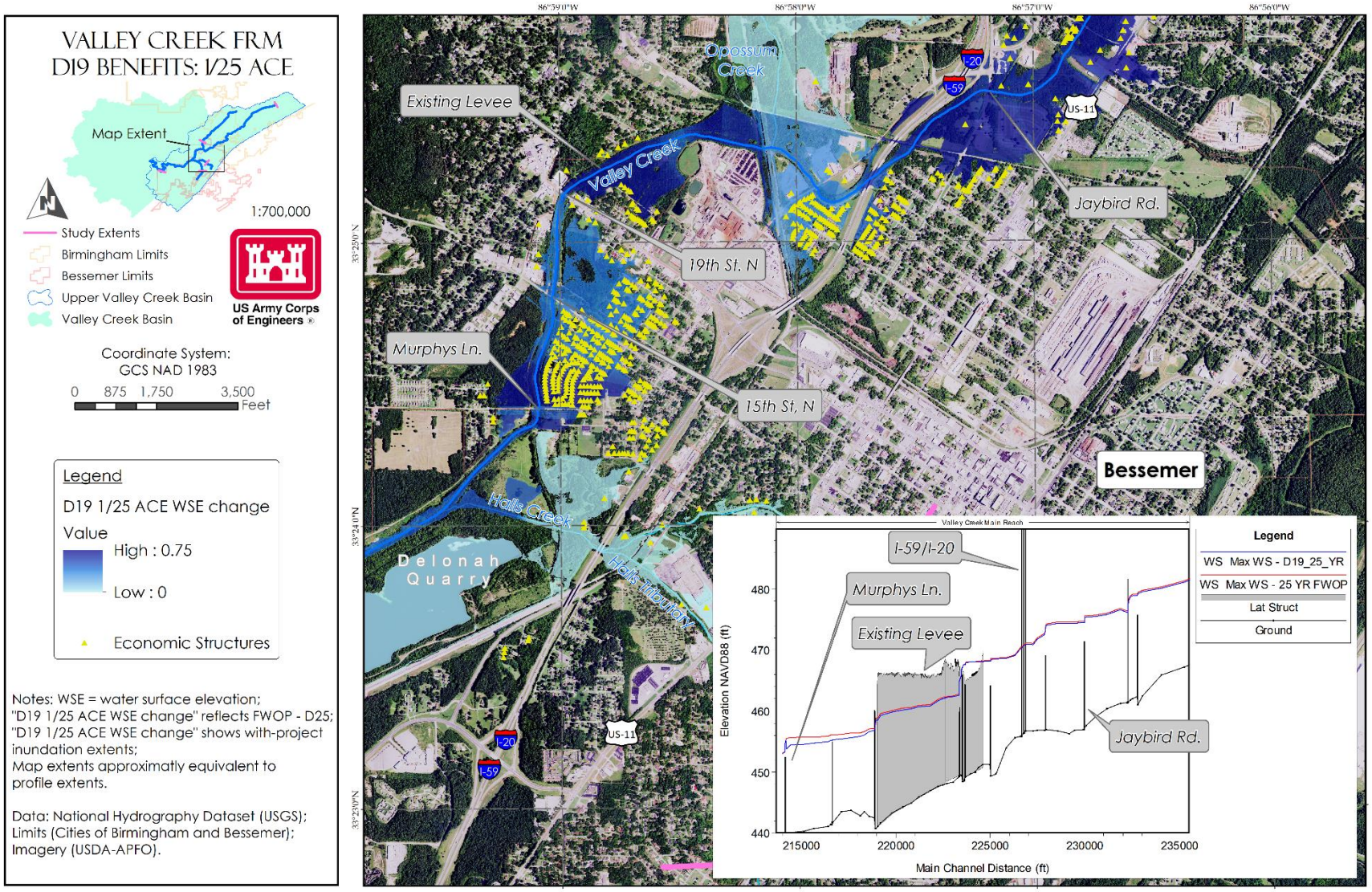

Figure 5-6: *D19 benefits (0.04 AEP event) in the lower extent of the Valley Creek study reach.*

Structural benefits for the selected plan were quantified based on relative water surface reduction statistics (Figure 5-7). Similar analysis as described in Section 4.2.1.1 was completed (Figure 5-8); however, additional work was carried out to ensure bin values included only those structures that observed flood reductions above their first-floor elevations (as determined in this study). Table 5-1 provides the results from the analysis.

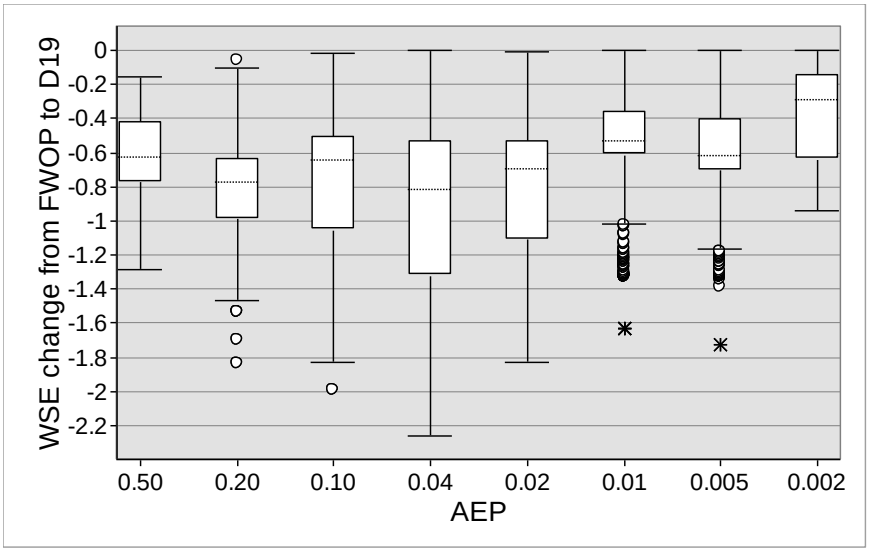

Figure 5-7: *Box plots of recommended plan WSE reductions from FWOP conditions by AEP.*

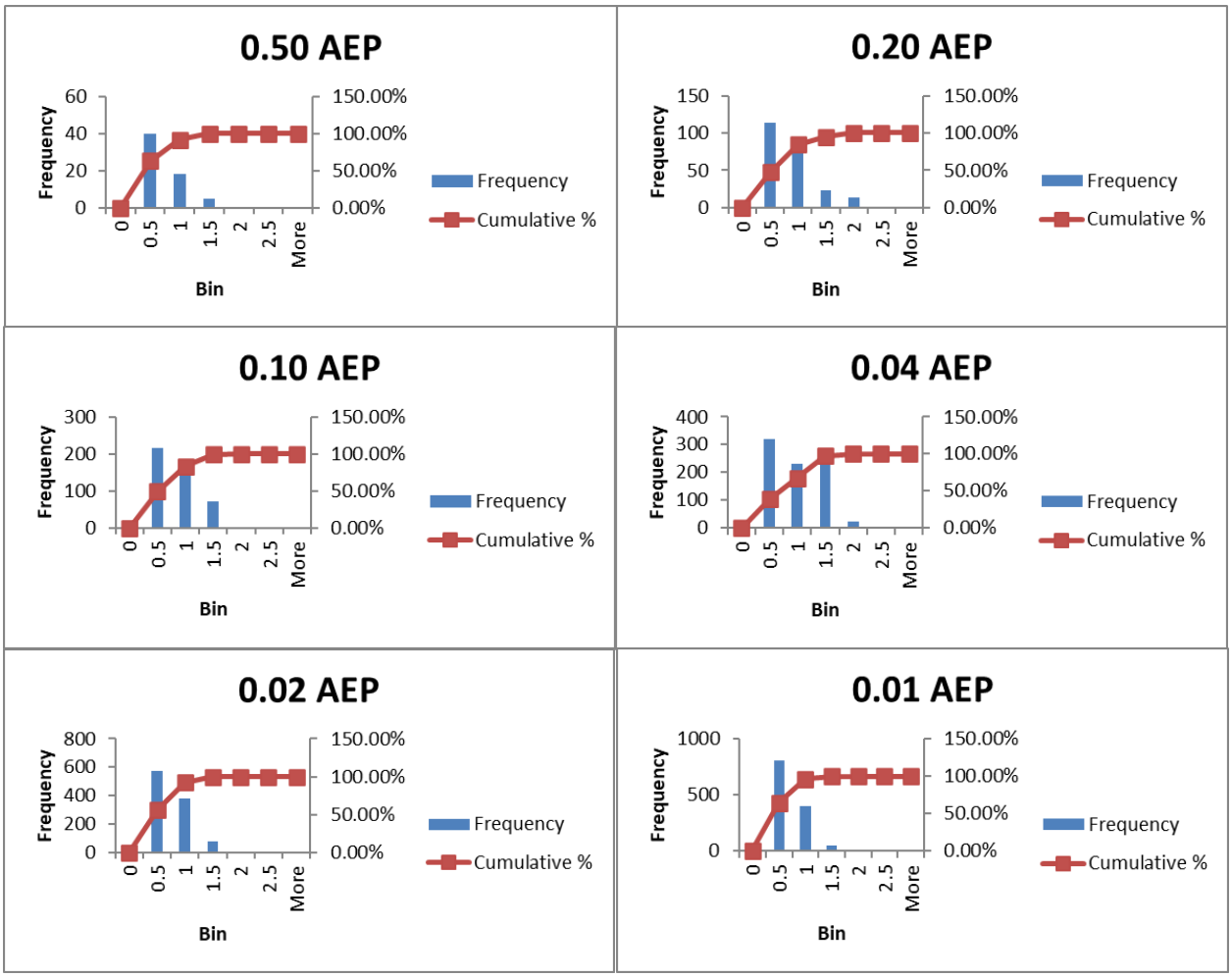

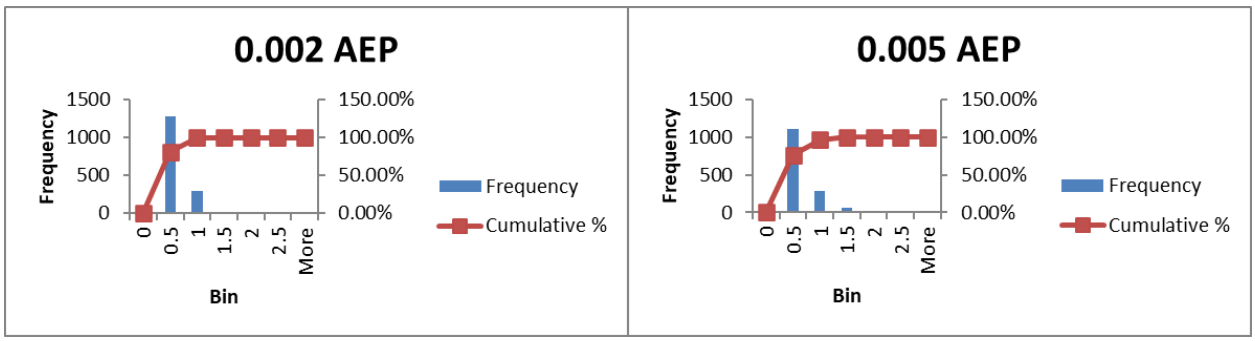

Figure 5-8: *Histograms of D19 performance by AEP. Note: frequency shows number of structures in bin (WSE reduction).*

Table 5-1: Recommended Plan Structural Benefits[1]

AEP	Structures Removed	WSE Bin Reductions (# of structures)				
		0 – 0.5 ft.	0.5 – 1.0 ft.	1.0 – 1.5 ft.	1.5 – 2.0 ft.	2.0 – 2.5 ft.
0.50 AEP	13	40	18	5	0	0
0.20 AEP	38	113	88	23	13	0
0.10 AEP	24	216	149	72	2	0
0.04 AEP	23	319	229	247	21	0
0.02 AEP	22	573	378	76	1	0
0.01 AEP	11	803	402	44	1	1
0.005 AEP	8	1107	287	55	0	0
0.002 AEP	7	1281	297	0	0	0

[1]*All data based on estimated first floor elevations.*

5.2 Risk Assessment

5.2.1 FRM Uncertainty

There are many sources of uncertainty contributing to the analyses involved in flood risk management studies. Fuguitt and Wilcox (1999) distinguish between the two types of uncertainty: future unknowns and data inaccuracy/measurement error. Future unknowns, in the case of this study, may be encountered in forecasting future watershed development, future storm water management, meteorology supporting synthetic storm development, or the effect of climate change on local hydrology. Measurement uncertainty may be encountered in supporting data (i.e., topography) and model calibrations, whereby error may be associated with reported data (i.e., stage and discharge). As flood risk management analyses deal with natural systems, the frequency and severity of risk drivers warranting investigation are most often random. Flood events can be examined as the results of a meteorological risk-driver, basin development, storm water management practices, and hydraulic characteristics. In the area of study, the meteorological risk driver is considered heavy rainfall produced from frontal or dissipating tropical events. Both, the frequency and severity of the risk driver and its response (flooding in this case) have associated uncertainties.

Previous methods of accounting for the consideration of uncertainty (and associated risk) included freeboard and safety factor application, over-designing, and analyzing long-term performance (USACE, 1996a). In response to such practice, USACE developed a risk-based analysis approach to flood risk analyses by analytically incorporating the consideration of risk and uncertainty in evaluations and decision making (USACE, 1996b). In practice these considerations are made through modeling flood damages with the Hydrologic Engineering Center Flood Damage Analysis (HEC-FDA) system, whereby expected probability distributions for critical study decision tools are developed from extensive sample-testing. The use of HEC-FDA to assess damage-frequency in combination with calibrated hydraulic inputs works to reduce uncertainties associated with flood risk analyses and overall plan performance. In this section, additional results from risk analyses supporting a comprehensive FRM risk assessment mandated by ER-1105-2-101 (USACE, 2019b) are presented. The risk and uncertainty associated with climate change in and around the study area, and its effect on the selected plan, are assessed in the following section (Section 6.0).

5.2.2 Recommended Plan Model Refinement

Uncertainty in plan performance was reduced with model refinement. Refinement of the hydraulic model geometry supporting the selected plan (D19) was considered necessary to improve simulation of hydrodynamics in the vicinity of the detention ponds, and to analyze residual and incremental risk. Section 4.1.1.1 describes the model approach that was employed for initial measure screening, and for production of FDA inputs. This approach was limited in its ability to appropriately describe backflows – or conveyance behind detention sites – as well as approaching flows and the full effect of pond berms on floodplain stage computations. To account for this, model refinement that incorporated 2D flow areas, and appropriate 1D/2D hydraulic connections was employed. An updated model terrain based on preliminary design data was created to reflect the ponds and their berms, and to support 2D modeling of the areas. Constructed two-dimensional flow areas included pond areas, backflow areas, and upstream and downstream areas.

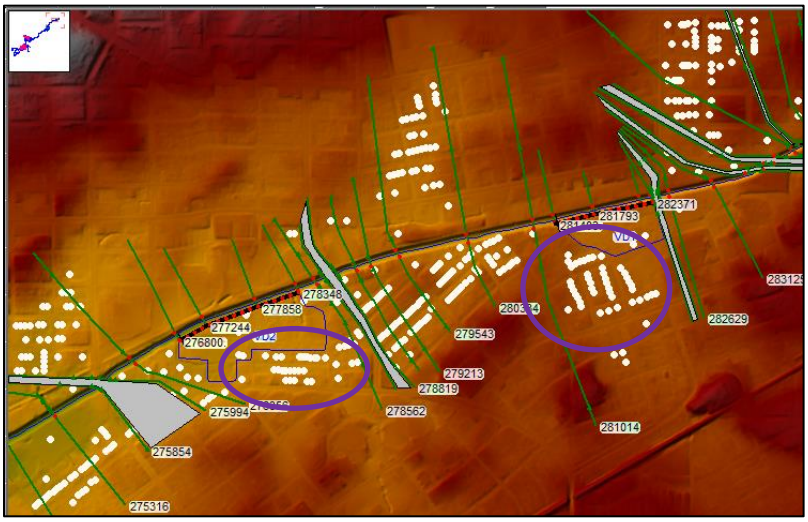

Figure 5-9: *RAS schematic showing original modeling approach at VD1 and VD2. Structures (only) from the structure inventory are shown in white. The purple areas represent locations where profile elevations were transposed, but no actual inundation would be depicted in these areas (see Figures 5-6). Schematic notes: north is oriented up and scale is 1:8,000.*

Because the ponds overtop, and because they are overbank features, it is not easy to describe the hydrodynamics that occur around these features during high-flow events. This is why, for screening purposes, the sites were modeled as simple storage areas, and calculations

ignored the backwater flows that may or may not occur (not applicable to all of the initially identified sites). The previous modeling approach (Figure 5-9) was considered acceptable for economics, however. The cross sections associated with the structures/vehicles around pond locations observed increased water surface elevations in the FDA model as a result of the previous modeling approach (Figure 5-10). Although Figure 5-9 shows cross sections terminating at the embankment of the pond, the structural allocations were never reorganized, so the raised water surface profiles in the cross sections were transposed onto the structures behind (or south of) the pond locations. This applies to pond VD4 as well. The updated modeling approach (Figure 5-11) provided a much better understanding of the water surface elevations that occur on these structures. The necessity of re-running the economics with the modified results for D28 was considered, but comparison of original and modified results at multiple model cross sections in and around the pond locations showed that profiles are generally lower for the modified version (Figure 5-12). So, less damage to the previously mentioned structures/vehicles should be expected with the modified approach. Additionally, modified flood profiles downstream of pond locations are slightly lower than original profiles (suggesting improved benefits).

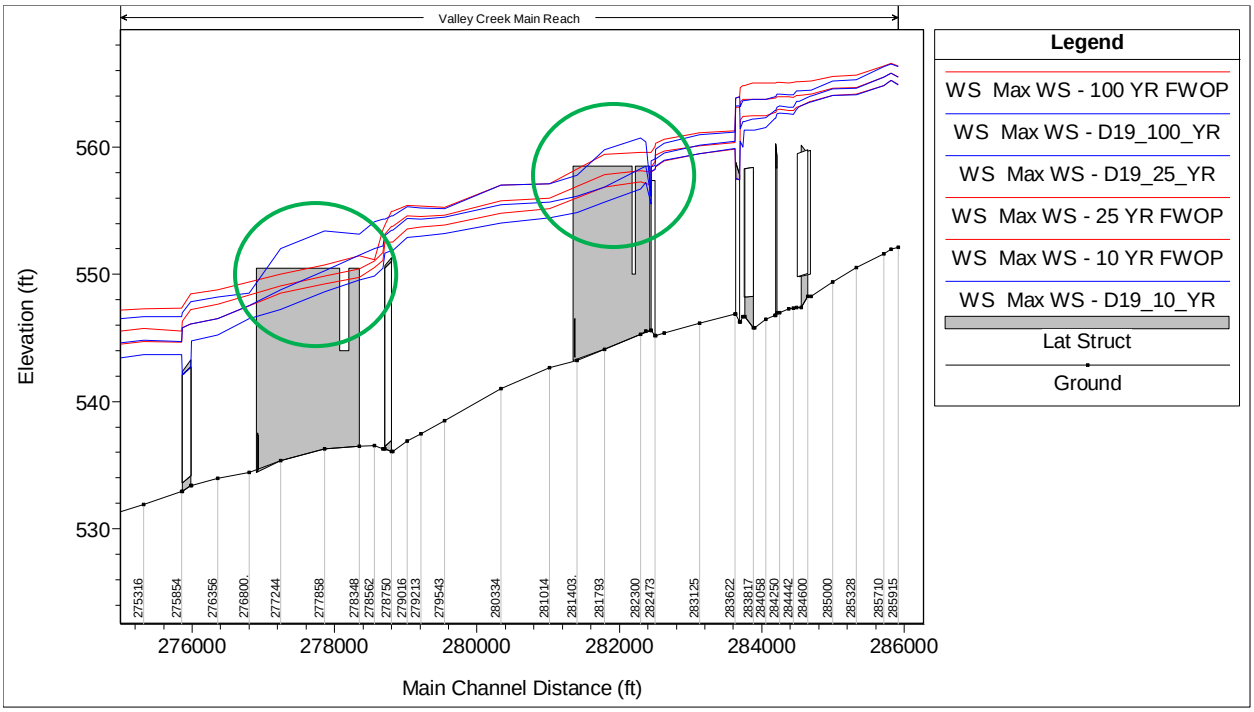

Figure 5-10: *Original modeling approach water surface profiles (0.10, 0.04, and 0.01 AEPs shown) in the vicinity of VD1 and VD2 with cross section station names shown. Areas of increases in water surface profiles associated with the recommended plan are circled in green.*

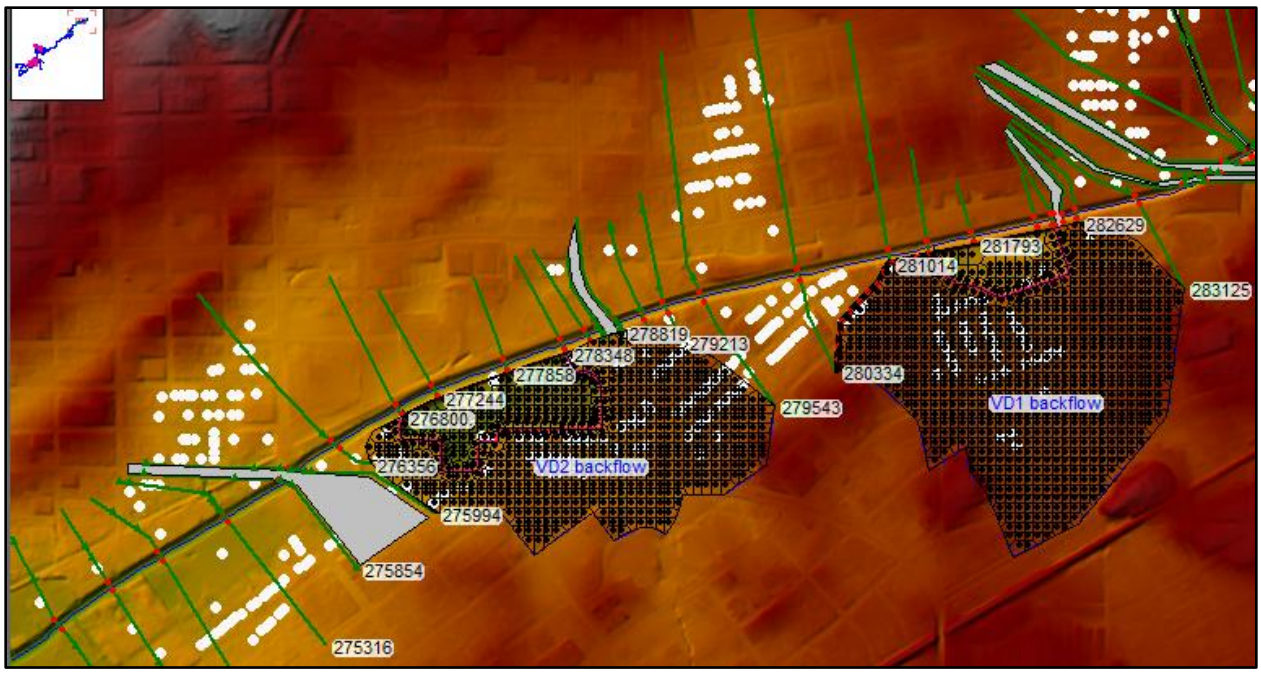

Figure 5-11: *RAS schematic showing updated modeling approach in the vicinity of VD1 and VD2. Note that the 2D areas model both the ponds and their backflow areas. The pond berms are physically represented in the terrain. The same inflow weirs are utilized in the updated configuration; however, additional connections are used to properly transfer the left overbank flows from cross sections to the backflow areas, and vice-versa. The set-up of VD4 is similar. Schematic notes: north is oriented up and scale is 1:8,000.*

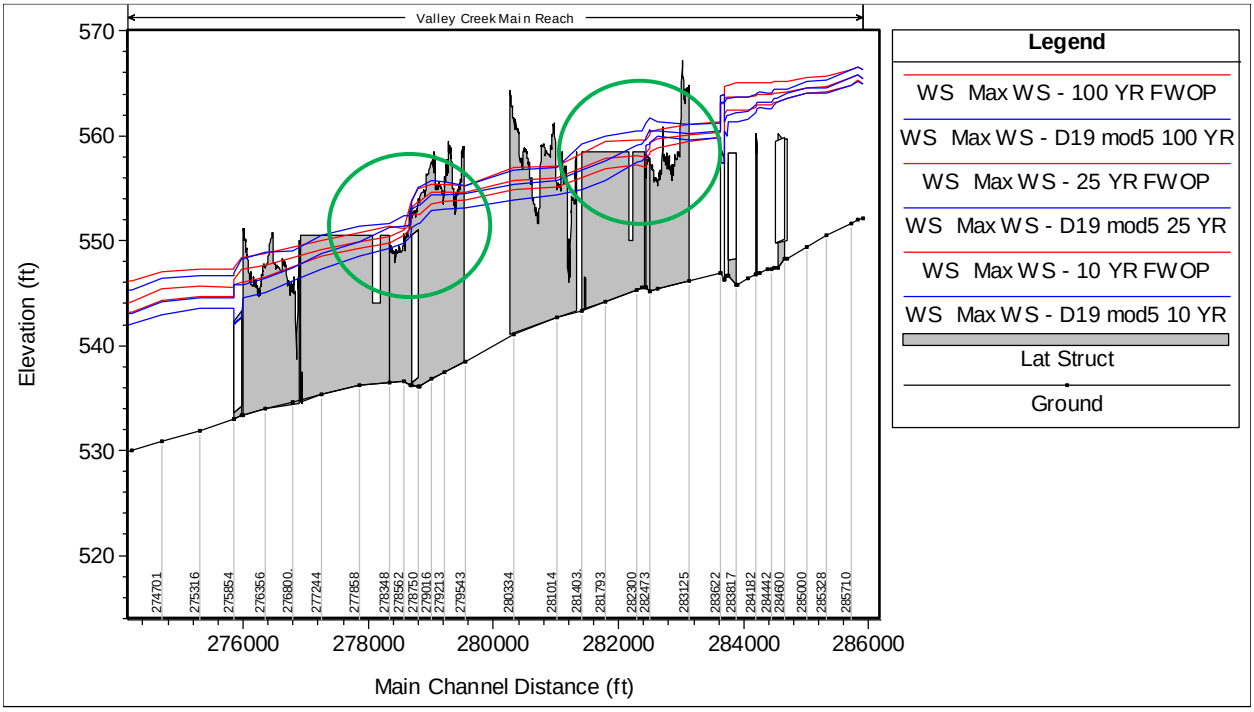

Figure 5-12: *Updated modeling approach water surface profiles (0.10, 0.04, and 0.01 AEPs shown) in the vicinity of VD1 and VD2 with cross section station names shown. Areas of increases in water surface profiles associated with the recommended plan are circled in green. Note decreased severity associated*

with updated profiles. The additional grey structures shown represent overbank connections required to properly transfer the left overbank flows from cross sections to the backflow areas, and vice-versa.

5.2.2.1 Model Refinement Results

Initial comparison of outputs from the modified D19 geometry with the FWOP conditions geometry showed measurable impacts in the backflow areas of VD1 and VD2. These impacts were initially thought to be the result of floodplain constraint created by pond berms; however, it was discovered that impacts were over-exaggerated from comparison of 1D and 2D modeling approaches, despite with- or without project conditions.

To address, additional model simulations were run with a modified FWOP geometry that included the same 2D and 1D/2D connection components described in Section 5.2.2. This geometry referenced the original project DEM (i.e., no detention basins included) to appropriately reflect FWOP conditions. Analysis of outputs from these simulations showed that, in general, overbank WSEs in the 2D areas were higher than the original 1D-based FWOP simulations. Figures 5-13 through 5-15 show inundation extents of FWOP, original D19, and modified D19 profiles around pond locations, and describe changes in WSEs within the backflow areas. Emphasis was placed on impact significance for frequency selection in map development. As shown in Figure 5-14, only a small group of structures is subjected to increased flood depths outside of model uncertainty (see Section 1.4.1) for the 0.01 AEP event. This area and others surrounding the recommended plan measures were analyzed in detail through quantitative methods to support a plan risk assessment (see Section 5.2.4).

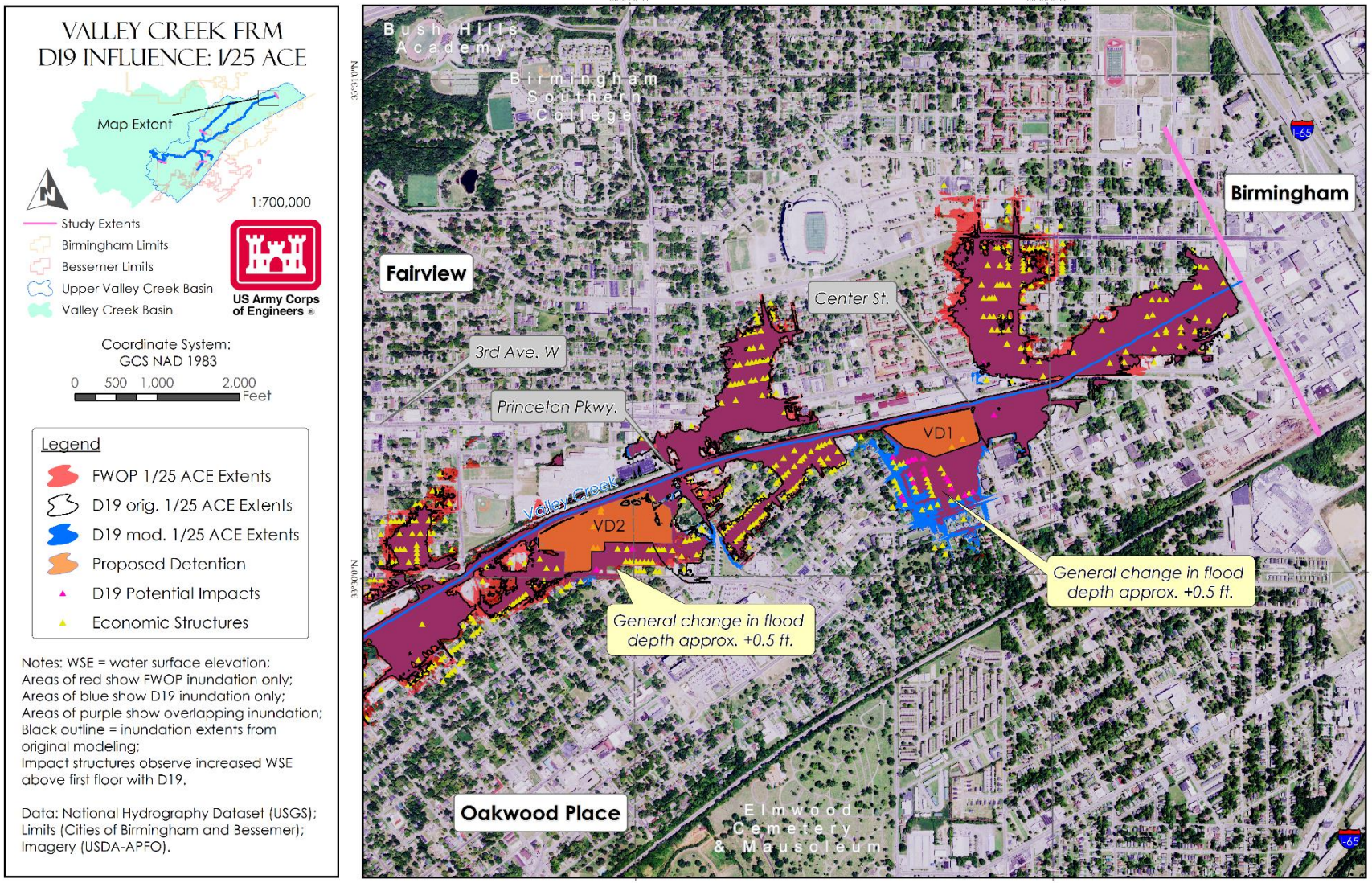

Figure 5-13: *Inundation extents of original and updated D19 models as well as FWOP conditions (original, 1D-based) for the 0.04 AEP event in the vicinity of VD1 and VD2 (in Birmingham extents). Structures in the inventory as well as structures that observe an increase in WSE above their first-floor elevation with implementation of D19 are shown.*

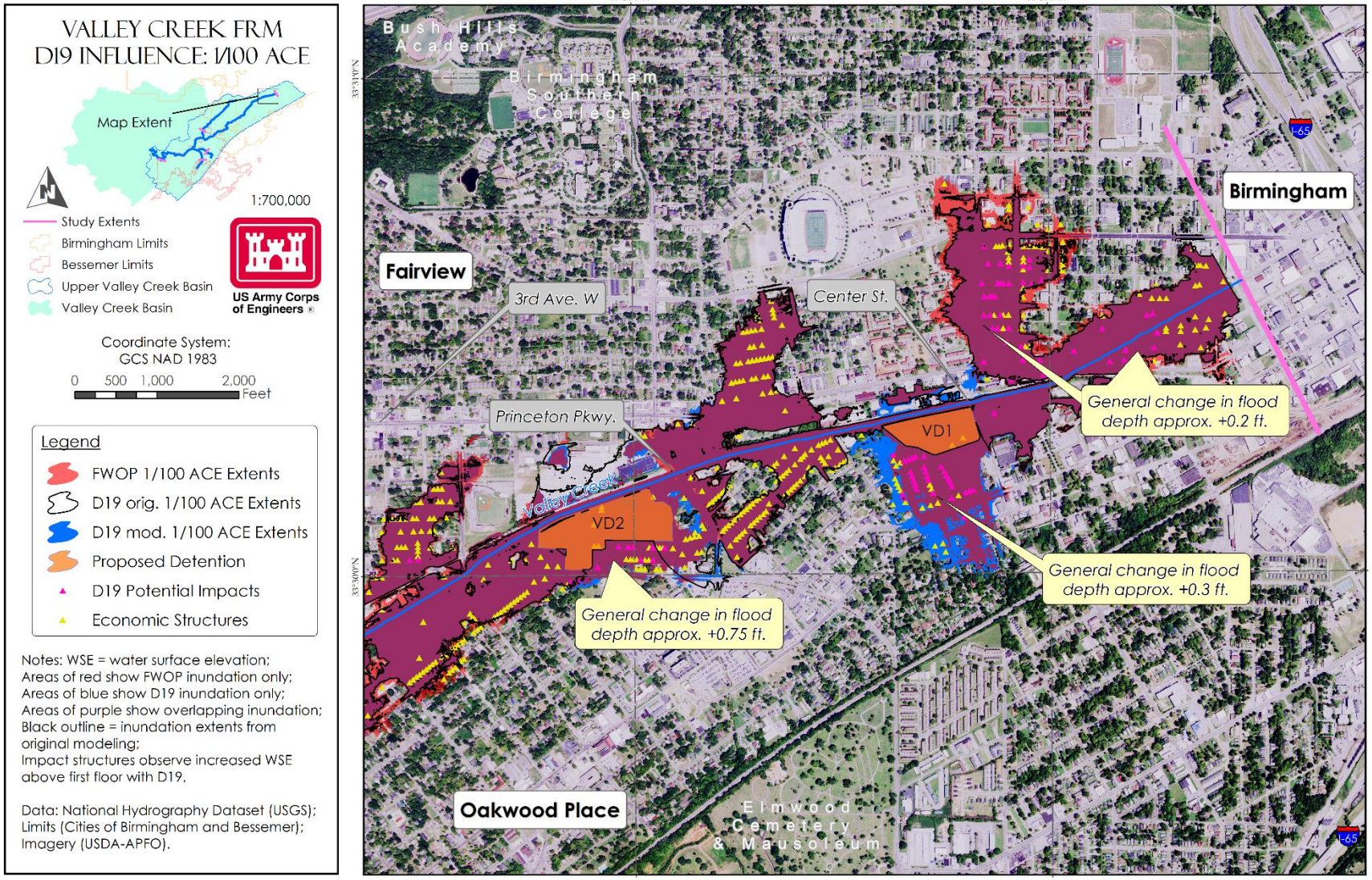

Figure 5-14: *Inundation extents of original and updated D19 models as well as FWOP conditions (original, 1D-based) for the 0.01 AEP event in the vicinity of VD1 and VD2 (in Birmingham extents). Structures in the inventory as well as structures that observe an increase in WSE above their first-floor elevation with implementation of D19 are shown.*

5.2.3 Risk-Informed Planning and Design

Per USACE guidelines, risk should be considered throughout the planning and design processes (USACE, 2019b) in order to ensure population and infrastructure risk is not increased with any proposed plan, life safety is prioritized, and facilitation of risk-informed decision making. In this study, a comprehensive hazard analysis was completed to assess the residual and incremental risks to life and infrastructure potentially associated with the proposed plan. This analysis was considered applicable by referenced guidance (USACE, 2019b) as features of the proposed measures are designated as levees by EM 1110-2-1913 (USACE, 2000). In designs, robust features were considered to increase measure resiliency, decreasing hazard risk (i.e., life or infrastructure), and decrease cost risk. The hazard analysis completed for this assessment shows that a low hazard designation likely applies to the measures of the proposed plan.

In accordance with the USACE risk framework, the tolerable risk guidelines (TRGs) were evaluated with respect to recommended plan performance. The TRGs defined by USACE (2019b) include the following:

> TRG 1 – Understanding the Risk. The first tolerable risk guideline involves considering whether society is willing to live with the risk associated with the dam or levee to secure the benefits provided by the dam or levee.
>
> TRG 2 – Building Risk Awareness. The second tolerable risk guideline involves determining that there is a continuation of recognition and communication of the risk associated with a dam or levee, because the risk associated with the dam or levee are not broadly acceptable and cannot be ignored.
>
> TRG 3 – Fulfilling Daily Responsibilities. The third tolerable risk guideline involves determining that the risks associated with the dam or levee are being properly monitored and managed by those responsible for managing the risk.
>
> TRG 4 – Actions to Reduce Risk. The fourth guideline is determining if there are cost effective, socially acceptable, or environmentally acceptable ways to reduce risks from an individual or societal risk perspective.

As shown, the first step in addressing the TRGs is to gain an understanding of the risk associated with a recommended plan. Specifically, life safety, societal, and environmental risks should be evaluated. Evaluation of life safety risk with respect to TRG 1 is guided by a risk matrix (Figure 5-15) and includes components of societal life risk and individual life risk. To address TRG 1, a comprehensive hazard analysis was completed. The hazard analysis is not equivalent to a semi-quantitative risk assessment (SQRA); however, the analysis leveraged quantitative assessment methods to inform risk understanding. Through this phase of the project development process, TRG 2 has been addressed through communication of plan performance, risk, and best available information with the Non-Federal Sponsor. TRG 3 is expected to be met through O&M and monitoring activities as well as emergency action plan

development, which are understood to be local responsibilities by the non-federal sponsors. Finally, TRG 4 has been satisfied by plan design and quantitative assessment of life and infrastructure safety; however, there may be precedent for further analysis of life safety to reduce uncertainty in results.

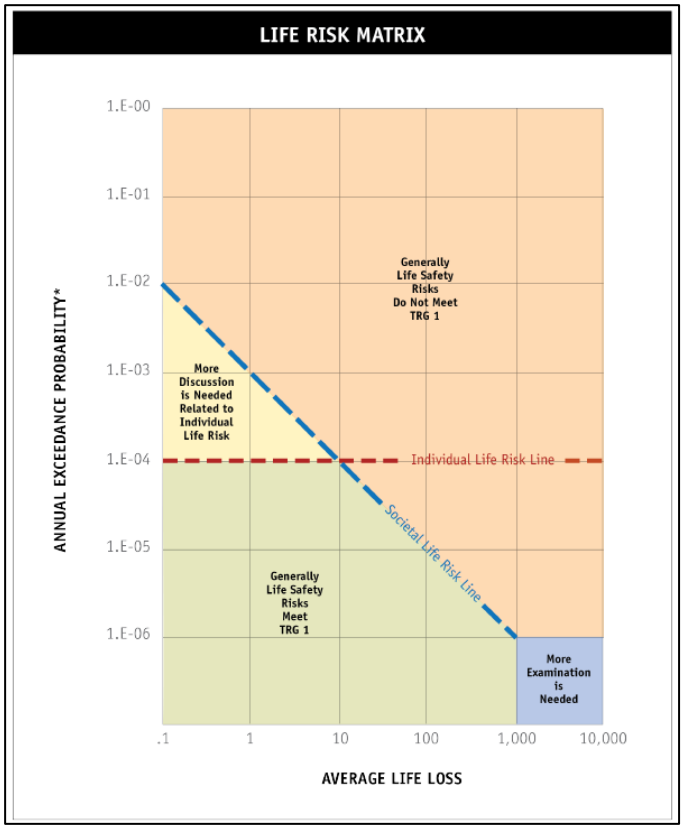

Figure 5-15: *Life Safety Risk Matrix (from USACE, 2019b)*

5.2.4 Hazard Analysis

The H&H analyses supporting this study were supplemented with a hazard analysis that included life and infrastructure safety assessments. Both with-project and breach conditions were assessed against FWOP conditions to gain a comprehensive understanding of residual and incremental risk-potential associated with the recommended plan. A life loss and direct damage estimation model (HEC-LifeSim) was constructed to assess life risk in the study area, while a hydrodynamic assessment was used to assess potential impacts to critical infrastructure and the environment. Breach simulations included individual pond sites as well as combined scenarios. Table 5-2 summarizes the breach simulations, loading parameters, and geometric breach data.

Table 5-2: Breach Scenarios, Loading Parameters, and Geometric Breach Data

Scenario	Peak WSE at VD1 (ft-NAVD88)	Peak WSE at VD2 (ft-NAVD88)	Failure Mode[1]	VD1 Breach Bottom Elev. (ft-NAVD88)	VD1 Final Breach Width (ft.)	VD2 Breach Bottom Elev. (ft-NAVD88)	VD2 Final Breach Width (ft.)
0.50 AEP	551.95	N/A	Piping	543.4	1.82	N/A	N/A
0.20 AEP	555.35	546.20	Piping	543.4	2.81	542.5	1.00
0.10 AEP	557.53	548.72	Piping	543.4	3.60	542.5	1.00
0.04 AEP	559.17	550.63	Piping	543.4	4.79	542.5	1.39
0.02 AEP	559.82	550.89	Piping	543.4	5.51	542.5	1.60
0.01 AEP	560.39	551.13	Piping	543.4	6.17	542.5	1.78
0.005 AEP	560.90	551.37	Piping	543.4	6.80	542.5	1.92
0.002 AEP	561.53	551.67	Piping	543.4	7.46	542.5	2.01

[1]*Failure mode applies to VD1 and VD2.*

Breach parameters for the basin levees were simulated with physical erosion rates as per USACE guidance (Lewis and Barto, 2020). Overtopping failure modes were tested for

applicable frequencies but did not produce breaches due to the lack of head differential (between interior and exterior WSEs) and resulting breach velocities, even with exaggerated erosion rates (erosion rates described in the following paragraph). As a conservative approach for analysis, piping failure modes were utilized in the locations of maximum head differential for all assessed frequencies. This location was not the lowest toe loading (LTL) location for VD1. At the VD1 LTL, no head differential is present for any analyzed frequency. Test simulations were run to assess breach potential in this location; however, breaches did not develop after initiation. A 0.50 AEP breach at VD2 was not applicable because there is no head differential above adjacent grade (i.e., toe elevation) along any portion of the basin levee.

Rates for downward and widening erosion were developed by the Engineer Research and Development Center (ERDC; Wibowo, 2016; Table 5-3). For sensitivity, both ERDC-Moderately Resistant and ERDC-Erodible erosion rates were tested for both VD1 and VD2 levee failures. Because the basin levees will be engineered features, the ERDC-Resistant rates are considered the best representation of erosion potential based on published data. All erosion rate data were obtained from Modeling Mapping and Consequences (MMC) Production Center Technical Manual for Levees, Appendix 3.1.4 (Lewis and Barto, 2020).

Table 5-3: Breach Erosion Rates[1]

Velocity (ft/s)	*ERDC-Erodible*	*ERDC-Mod. Resistant*	*VD1*	*VD2*
	Rate (ft/hr)	Rate (ft/hr)	Rate (ft/hr)	Rate (ft/hr)
0	0	0	0	0
1.5	0	0	0	0
2	0	0	0	0
3	0	0	0	0
4	0	0	0	0
6	3.6	0	0	0
8	18.9	0	0	0
10	37.4	0	0	0
15	99.6	3	3	3
20	179	15.1	15.1	15.1
25	270	34.9	34.9	34.9
30	425.1	56.7	56.7	56.7

[1]*Erosion rates apply to both downcutting and widening.*

5.2.4.1 LifeSim Model Background

The life safety model was created using version 1.0.1 of LifeSim (Flood Risk Management Center of Expertise for Flood Risk Management Studies certified version). Mapping Modeling and Consequences (MMC) standards for levee modeling were used in the creation of the model. A study area outline shapefile was received from the FDA modeler. This polygon was in turn buffered to increase the area that would be modeled. This buffered study area polygon was used to extract the model's structure inventory from the National Structure Inventory version 2. The model's structure inventory was then reviewed in GIS and adjusted to increase the accuracy of the placement of the structures.

The buffered study area polygon was also used to extract the road network that is necessary to simulate evacuation. Once the network was extracted, it was reviewed and scrubbed to remove any issues in the road network such as intersections that are not completed. Also, elevations of roads and bridges over water and drainage areas were adjusted so that they did not present an elevation of 0 (being on the ground) which would suggest flooding in any event. After the road network was completed, a layer for the destinations (also used in evacuation simulations) was created. The destination layer contains points that the evacuated population will mobilize toward. Once they arrive at a destination point, LifeSim will consider then cleared and they are removed from that simulation iteration. Since this model is a relatively small geographical area, there is a single emergency planning zone (EPZ) for Jefferson County.

After all of the previously mentioned components were created and the hydraulic data was imported, the alternatives to be simulated were created. Each hydraulic event has 2 alternatives, one for ample warning and one for minimal warning. Following MMC standards, the minimum warning alternatives have a hazard identification time of 3 hours prior to 0.5 hours after the event with uniform uncertainty. The ample warning alternatives have a hazard identification time of 24 hours prior to the event with no uncertainty. All other uncertainty curves (Warning Issuance Delay, Daytime First Alert, Nighttime First Alert and Protective Action Initiation) were left at their default settings of “Unknown”. Alternative simulations were set to run for 1000 iterations with the imminent hazard times of day set for 2 AM and 2PM. The 2 AM time is representative of nighttime and the 2 PM time is representative of daytime.

5.2.4.2 Hazard Analysis Results

Results of the hazard analysis were plotted with respect to the SQRA methodology outlined by O’Leary (2018). In this form, average (day and night) order-of-magnitude life loss estimates and annual probability of failure are plotted in a risk matrix as the geometric mean of the applicable order-of-magnitude (based on log space; Figure 5-16). Additionally, the risk matrices include the individual risk limit of 1E-04 and the societal tolerable risk limit for average annual life loss of 1E-03.

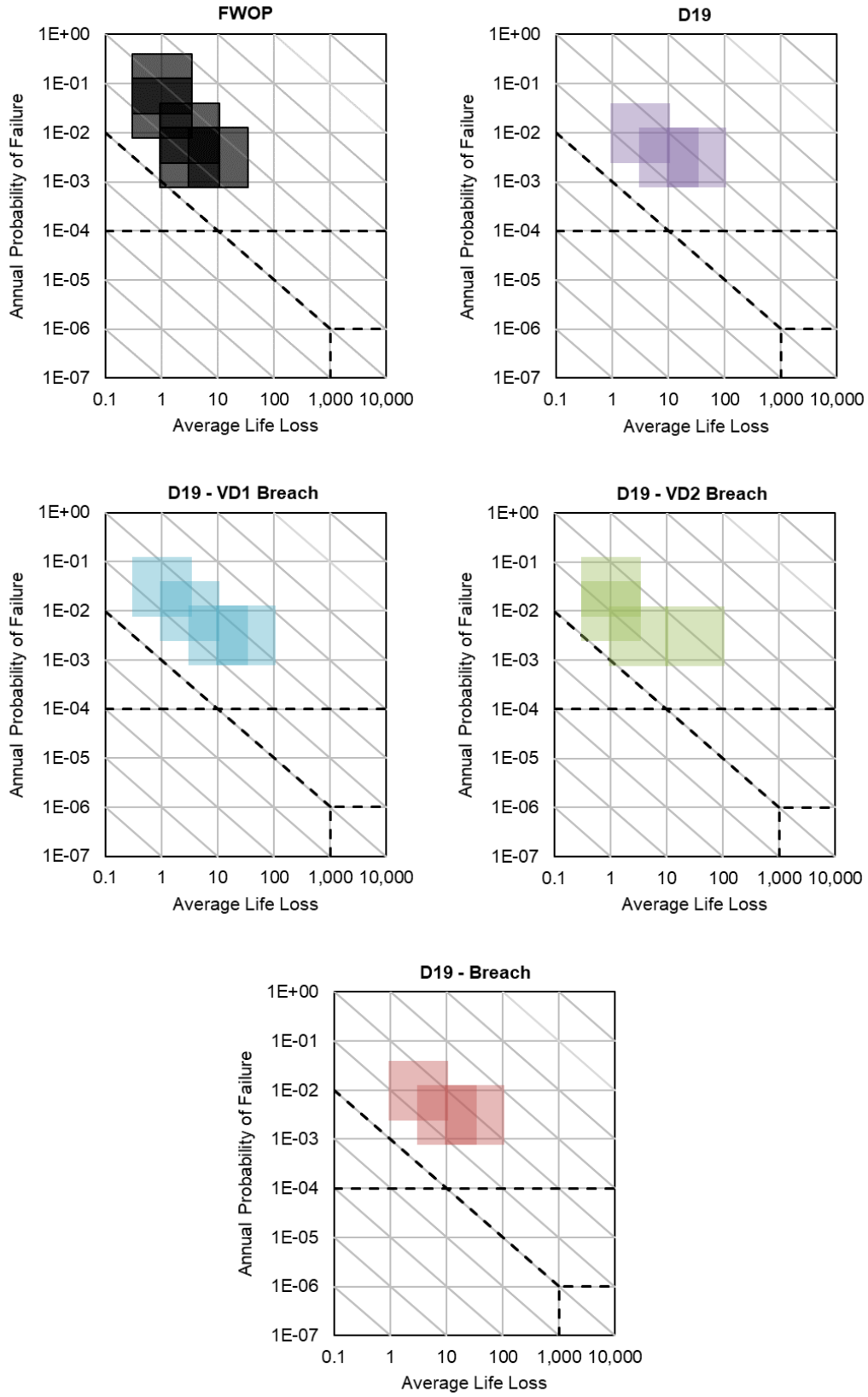

Figure 5-16: *Total Life Risk Matrices for Minimal Warning Scenario*

Model results show that life safety benefits are realized for the with-project condition, and preserved during failures; however, the order-of-magnitude total life loss for breach simulations increases slightly for the largest analyzed events (0.005 and 0.002 AEPs). Additionally, for individual levee failures, there is an increase of 1 in order-of-magnitude total life loss for 0.02 AEP. This increase is not observed in the D19 breach results, however. Increases in order-of-magnitude average life loss are not considered an accurate representation of the risk, rather an artifact of statistical uncertainty. This assessment is based on a thorough review of LifeSim outputs, breach and with-project hydrodynamics, and general hydraulic performance of the basins.

Spatial results were reviewed in LifeSim for FWOP, non-breach, and breach scenarios. Careful attention was paid in analyzing both median and extreme LifeSim iterations, with several outputs for each scenario generated. Results showed incremental losses (between both FWOP/with-project and breach/non-breach) downstream of the basin locations. In general, hydraulic model outputs do not agree with the computed losses at these locations. Compared to FWOP, these locations observe a reduced flooding hazard in the with-project condition. For example, Figure 5-17 provides a representative loss output from LifeSim for D19 and FWOP 0.002 AEP simulations. For the loss cluster location identified, stage and flow hydrographs are provided from a model cross section in the area (Figure 5-18). Model results at this location show hydraulic benefits throughout the simulation, suggesting the median increase in life loss is the result of statistical sampling and variation in other LifeSim parameters (i.e., human mobilization and evacuation response).

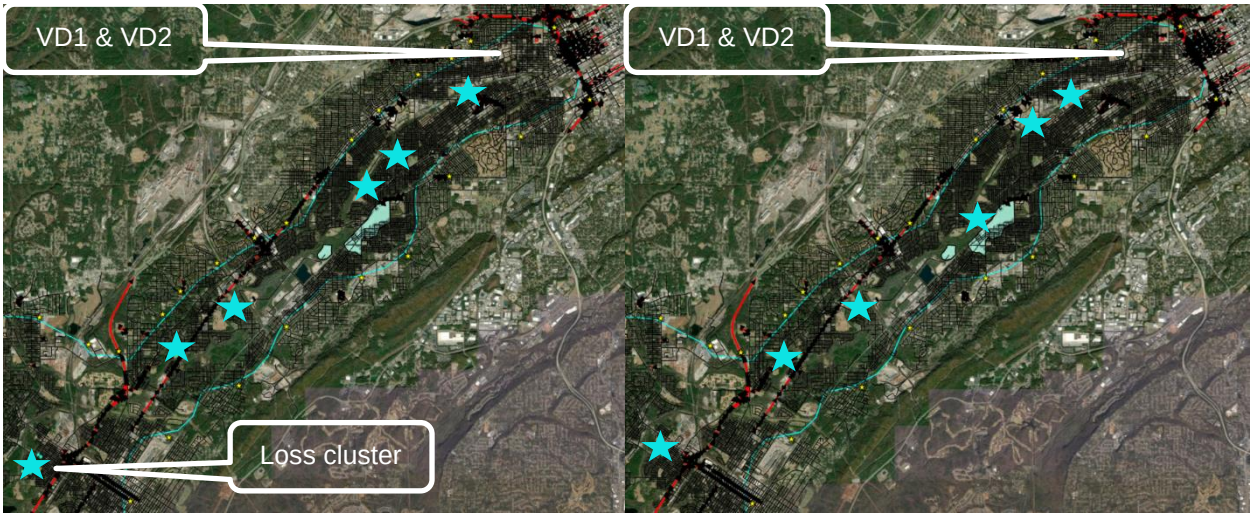

Figure 5-17: *Representative 0.002 AEP LifeSim Results for D19 (left) and FWOP conditions (right).*

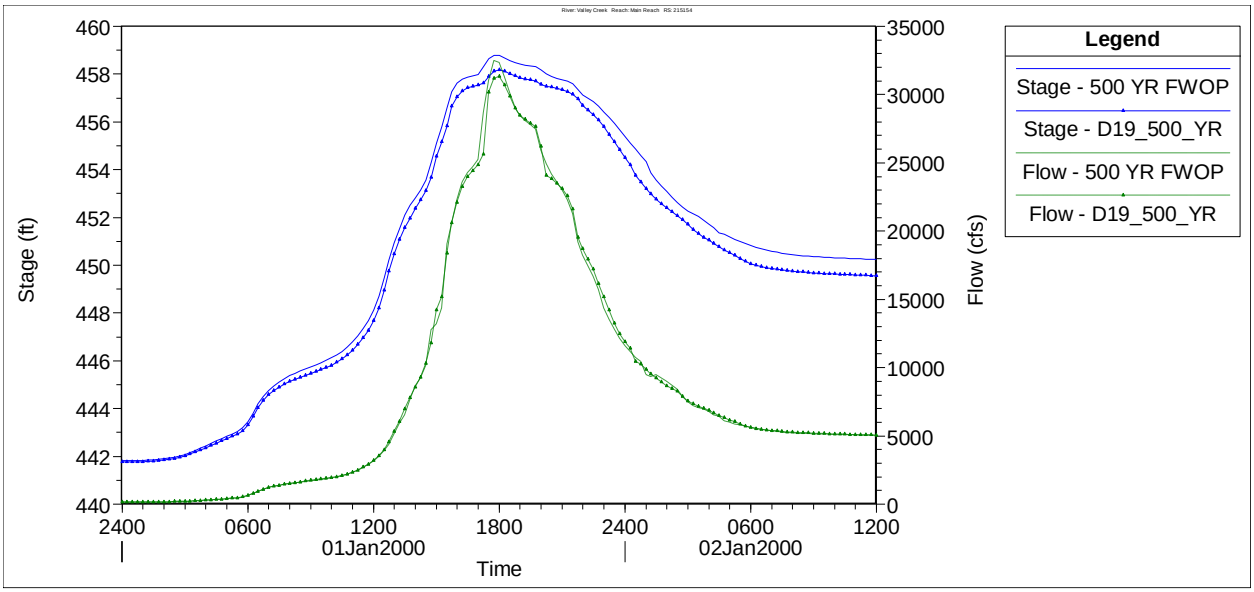

Figure 5-18: *Stage and flow hydrographs for 0.002 AEP at 2151+54 showing significant stage reduction for with-project condition and lack of timing differential throughout simulation.*

Figure. 5-19 provides representative outputs for 0.002 AEP D19 breach/non-breach simulations. In all displayed locations, hydraulic outputs are identical between scenarios. Even immediately downstream of breach locations, no significant differences are observed for singular or combined breaches (Figure 5-20). For singular breaches at both VD1 and VD2, a single incremental loss was identified in the residential area upstream of the Delonah Quarry. Similar to other analyzed events, hydraulic outputs between breach and non-breach scenarios are identical in this location (Figure 5-21), suggesting that the loss is a product of statistical sampling, and not physical results.

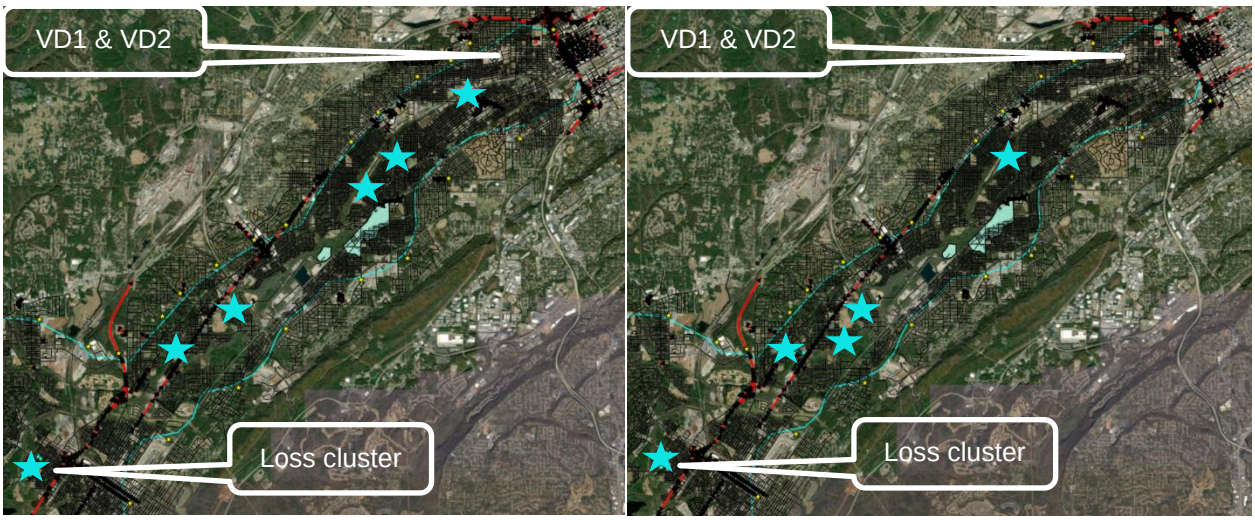

Figure 5-19: *Representative 0.002 AEP LifeSim Results for D19 non-breach (left) and D19 breach (right).*

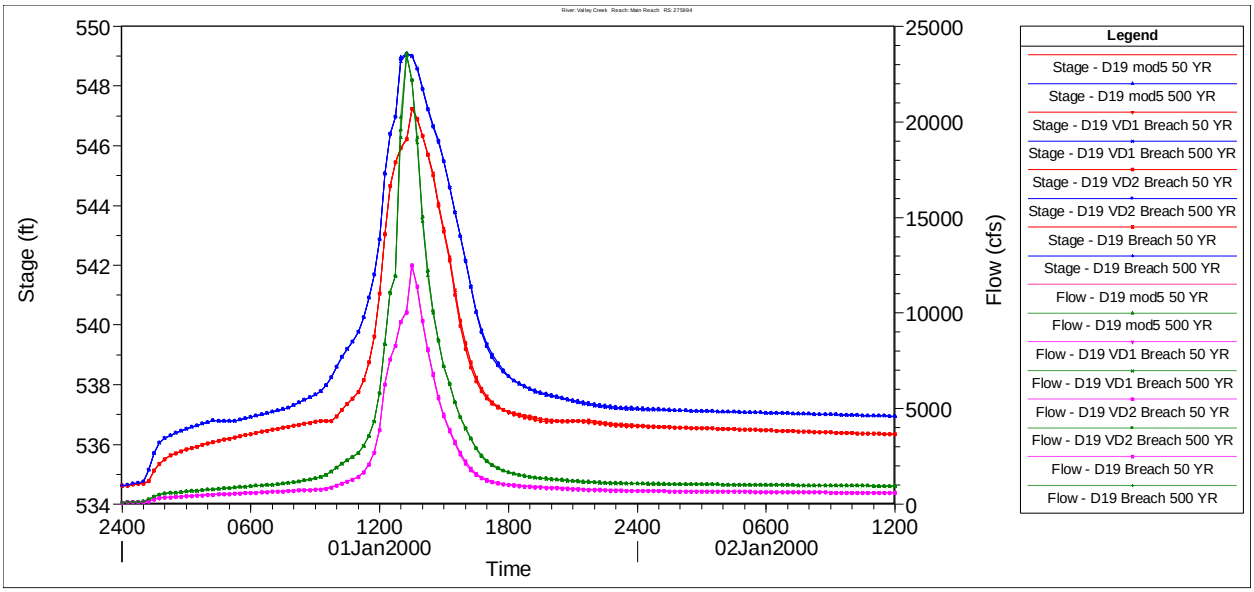

Figure 5-20: *Stage and flow hydrographs for 0.002 AEP event (blue and green, respectively) and 0.02 AEP event (red and pink, respectively) at first cross section downstream of VD2 (2759+94; at 12th St. SW). Results show no change in hydraulics between non-breach, VD1 breach, VD2 breach, or combined breach simulations.*

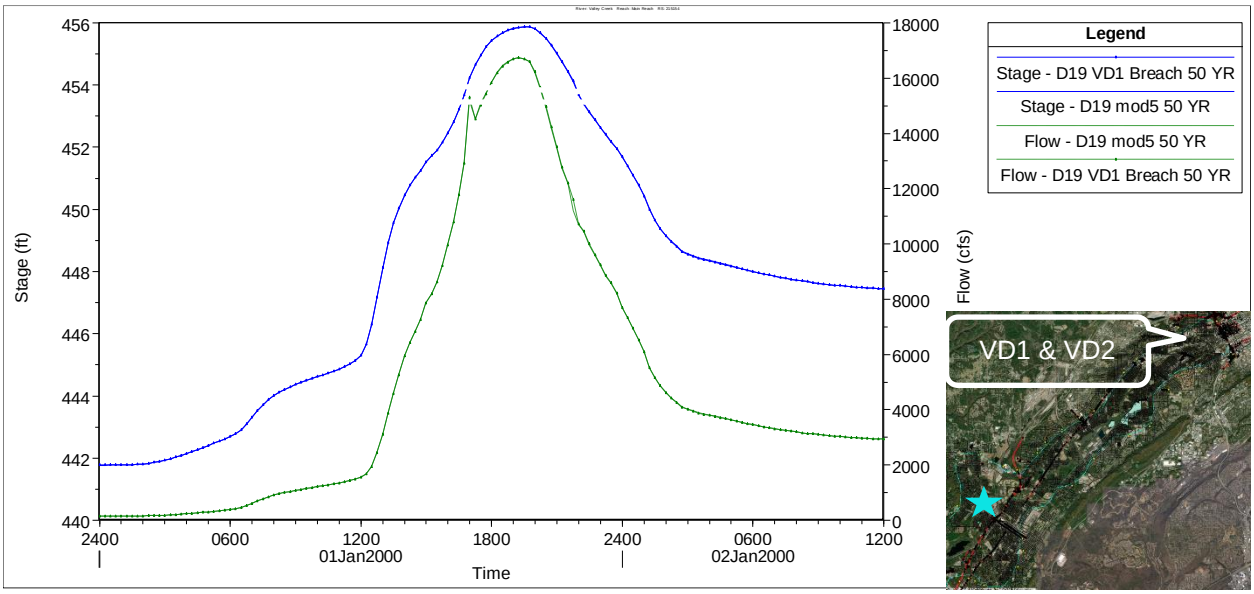

Figure 5-21: *Stage and flow hydrographs for 0.02 AEP at 2151+54 showing no change between breach/non-breach simulations at loss location.*

Incremental critical infrastructure and environmental risk can be inferred from the data provided to support assessment of the life safety results (see, e.g., Figure 5-20). Velocities in the vicinity and downstream of each basin were also assessed between breach/non-breach scenarios with only negligible variations observed across frequencies. Within the 2D backflow areas, no distinguishable differences to inundation extents or WSEs were observed across frequencies.

5.2.4.3 Hazard Analysis Discussion and Conclusions

Because of low hydraulic detention times, geotechnical design to reduce piping risk, and expected overtopping, the more likely failure mode for the proposed basin levees is considered overtopping. However, as described, overtopping failure risk is considered very low based on the hydraulic performance of the recommended plan measures. Failures were initiated with piping failure modes such that the largest practical breach could develop. The locations of maximum head differential for each site were selected for breaching (along channel at VD1; southwest corner of VD2), although stages capable of overtopping the pond levees do not outlast the recession of similar exterior water surface elevations at any site. As a result, surrounding inundation would significantly mitigate the effect of berm failure, resulting in a negligible influence of the breach on exterior floodplain conditions. As previously described, it was not possible to develop overtopping breaches with exaggerated parameters, even at locations of maximum head differential.

The risk of an overtopping breach within the basin spillways is considered very low based on the proposed design features. As shown in Section 4.1.2.2, armoring in the form of ACB/ACM was included in basin cost estimates for the spillways (not removed following CSRA). Generally, the performance of ACBs/ACMs is considered strong for overtopping velocities less than 15-20 ft/s (see, e.g., Hewlett et al., 1987; Clopper, 1989; Clopper, 1991; Abt et al., 2001; and Cox et al., 2014). USACE project performance has also shown that ACB and ACM products can serve as successful lateral spillway revetments for medium-sized spillways with heads between 5 and 10 feet (Gambucci, 2009). Maximum velocities over the design spillways are on the order of 4-5 ft/s. While not expected, future design efforts (in PED) should highlight any potential high-velocity areas along pond berms and assess protection needs. Assessment should be completed with detailed 2-D hydraulic analysis.

The results of the LifeSim analysis do not agree with the physical performance of the proposed plan in both breach and non-breach scenarios. The life safety analysis is valuable in assessing uncertainty in project performance; however, it is understood that the hydraulic model results suggest that no incremental risk is associated with the project. Based on the provided model information, uncertainty in the statistical life loss model, and increased confidence in engineering models supported by calibration to physical data, the recommended plan hazard potential is considered low, though additional life safety analysis may be warranted to fully address TRG 4 (USACE, 2019b). Additionally, as described, breach scenarios supporting incremental risk assessment were simulated with less likely parameters, which increases confidence in the plan performance.

5.2.5 Stage Uncertainty

To better understand recommended plan (and other final alternatives) performance and risk, efforts were made to establish upper and lower bounds on the uncertainty sourced from critical study parameters and assess their effect on plan performance. This analysis included model testing to establish sensitivity associated with channel and overbank roughness (Manning's n-

values), which generally serve as the greatest source of uncertainty in hydraulic stage calculations. Additionally, this parameter is a highly influential factor in assessing watershed flood risk (Lie et al., 2019). Provided the importance of baseline and with-project stage (or WSE) values in FDA damage-frequency assessment (and resulting benefit calculations) as well as applicable gage datum uncertainty described in this report (see Section 1.4.1), analysis of this influential parameter was considered desirable. Manning's n-values were scaled at +/-19% to reflect the uncertainty associated with estimated gage datums in locations of high-density development. Because these estimates were based on standard instrumentation practice (see, e.g., Carter and Davidian, 1968; Sauer and Turnipseed, 2010; Kenney, 2010), datum elevation uncertainty was equated to topographic uncertainty (approximately 6.5 inches; see Table 1-2). The scaling factor was determined from the change in roughness required to increase computed depths by 6.5 inches at cross sections in the hydraulic model corresponding to applicable USGS gage locations (USGS 02461130 and USGS 02461192). Analysis was completed for flows applicable to both channel and overbank stages; however, overbank change was considered preferential for assessing stage uncertainty.

Simulations for all modeled frequencies were run with the applicable roughness adjustments applied to the FWOP conditions project geometry (16 simulations total). The resulting range of stages models the margin of error associated with computations at an estimated 95% confidence interval (CI). Using these data, bounded stages of importance were developed at high-density development locations and recommended plan measures. Locations were selected to assess confidence in overtopping frequency for all final measures, and benefit frequency at some critical locations that observe significant profile reductions from implementation of the final plan. Stage ranges were computed as ± 2 standard deviations (SD) from the expected stage modeled at critical locations. The event assessed at each location was either the highest frequency event for overtopping (at measure locations) or derived benefits (at high-density development locations). These data are provided in Table 5-4. Standard deviations about the calibrated mean, or expected stages at select locations were computed as:

$$SD = (max.\ stage - min.stage)/4 \qquad \text{Equation 5}$$

Sensitivity simulations were not made for with-project conditions; confidence and associated standard deviation for overtopping exceedance (or exceedance of capacity) of project features were applied from FWOP simulations to compute with-project stage limits. Expected stage values and SDs (based on calibrated baseline model) for cross sections at, and near, plan features differ for without- and with-project conditions. However, the uncertainty associated with roughness is considered independent of basin conditions, as it was directly related to gage datum uncertainty.

Table 5-4 reports new AEPs (as applicable) for detention basin locations that are associated with stages at the upper limit of confidence bounds for the next greatest AEP, if that stage falls in the 95% confidence limits of the stage associated with the expected AEP of exceedance. In this manner, a new AEP is reported if the lower stage within the limits of confidence is equaled or exceeded by the upper stage of a greater AEP at the analyzed location. This required re-

computation and reference of the SD from the next-greatest AEP to the appropriate location. For analyzed benefit locations, the new AEPs (as applicable) represent the next-lesser AEP in order to describe the risk associated with realizing benefits less frequently than observed. Similarly, the SD was re-computed based on roughness sensitivity from the next-lesser AEP at the cross sections shown.

Table 5-4: Stage uncertainty at critical locations[1]

River Station (feet)	Location Purpose	AEP of Exceedance	Expected Stage (ft.)	Stage Lower Limit (95% CI; ft.)	Stage Upper Limit (95% CI; ft.)	SD (ft.)	New AEP[2]
2824+43	Backflow at VD1	0.10	558.29	557.33	559.25	0.48	0.20
2823+00	Overtopping at VD1	0.04	559.17	558.51	559.83	0.33	0.04
2785+62	Backflow at VD2	0.02	550.65	550.17	551.13	0.24	0.02
2783+48	Overtopping at VD2	0.04	550.63	549.75	551.51	0.44	0.04
2691+02	D19 benefits	0.20	531.94	531.74	532.14	0.10	0.20
2542+62	D19 benefits	0.10	507.70	507.30	508.10	0.20	0.10
2416+73	D19 benefits	0.10	487.20	486.92	487.54	0.14	0.10
2151+54	C1 benefits	0.20	449.69	449.59	449.79	0.05	0.20
2151+54	D19 benefits	0.20	450.71	450.61	450.81	0.05	0.20
2151+54	C9 benefits	0.20	449.27	449.17	449.37	0.05	0.20

[1]*Stage (WSE) values reference NAVD88.*

[2]*AEPs with change shown in red.*

The data show that, overall, the risk of AEP exceedance related to structural impacts is relatively low. The only analyzed scenario that drove an increase in AEP was backflow at VD1. No decreases to AEPs associated with benefits were identified by this analysis. For this assessment, special attention was paid to the detention basins, whereby SD was computed at cross sections where the risk of overtopping pond berms, or flood-wave influence originated. For example, 2D modeling upstream and behind VD1 shows that flooding behind the site originates from upstream of the pond (just upstream of Center St.), and that the risk is driven by left overbank flows approaching the pond berm (and consequently being influenced by the berm). Therefore, RS 2825+09 (first cross section downstream of Center St. Bridge) was utilized to develop the SD for stage limit analysis of the VD1 backflow area, as variations in stage at this location would ultimately drive flood risk at the structures of interest, slightly downstream (reference upstream circled structures in Figure 5-9). In this manner, the frequency at which overbank flows are influenced by the presence of the pond was chosen for computation of SD. For this site and VD2, the resulting upper and lower stage limits were determined by applying the computed SD to the expected stage at backflow structure locations.

Additionally, stage limits were developed for general overtopping of pond berms. Both upstream and back-berm hydrographs were analyzed (VD1 examples shown in Figures 5-22 and 5-23) to determine the greatest AEP associated with outward overtopping (i.e., overtopping from the pond, to adjacent low-lying areas). Analysis of two profile lines representing these berm

sections was required due to the flow exchange differences between upstream and back-berms. Standard deviations for stage limit computations were obtained from the cross sections nearest the inflow weirs in order to best represent the roughness sensitivity pertinent to pond inflows. Computed SD was applied to the pond elevations to assess uncertainty in the AEP of overtopping.

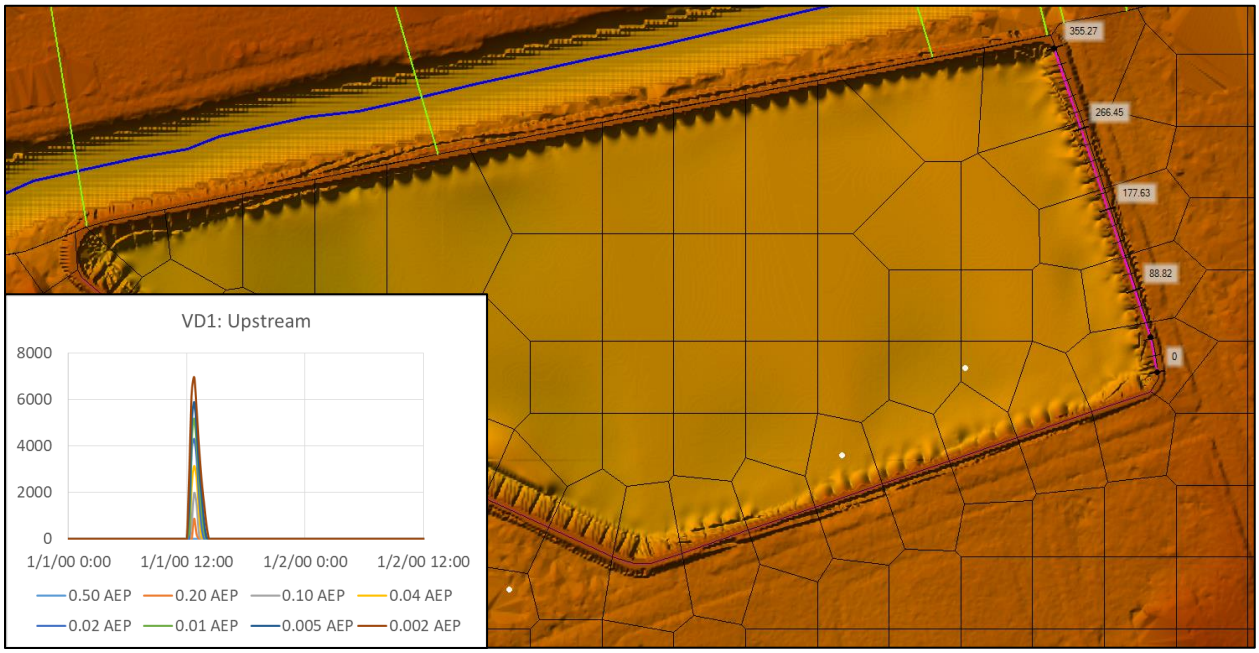

Figure 5-22: *Schematic from RASMapper with plot of upstream berm hydrographs at VD1 (all analyzed AEPs shown). Profile line from which hydrographs were produced is shown in pink. Note all flow is positive; overbank flows overtop the upstream berm profile line and enter the detention basin. No outward overtopping risk associated with the analyzed berm exists. Map notes: flow is east-to-west, north is up, and scale is approximately 1:1,250.*

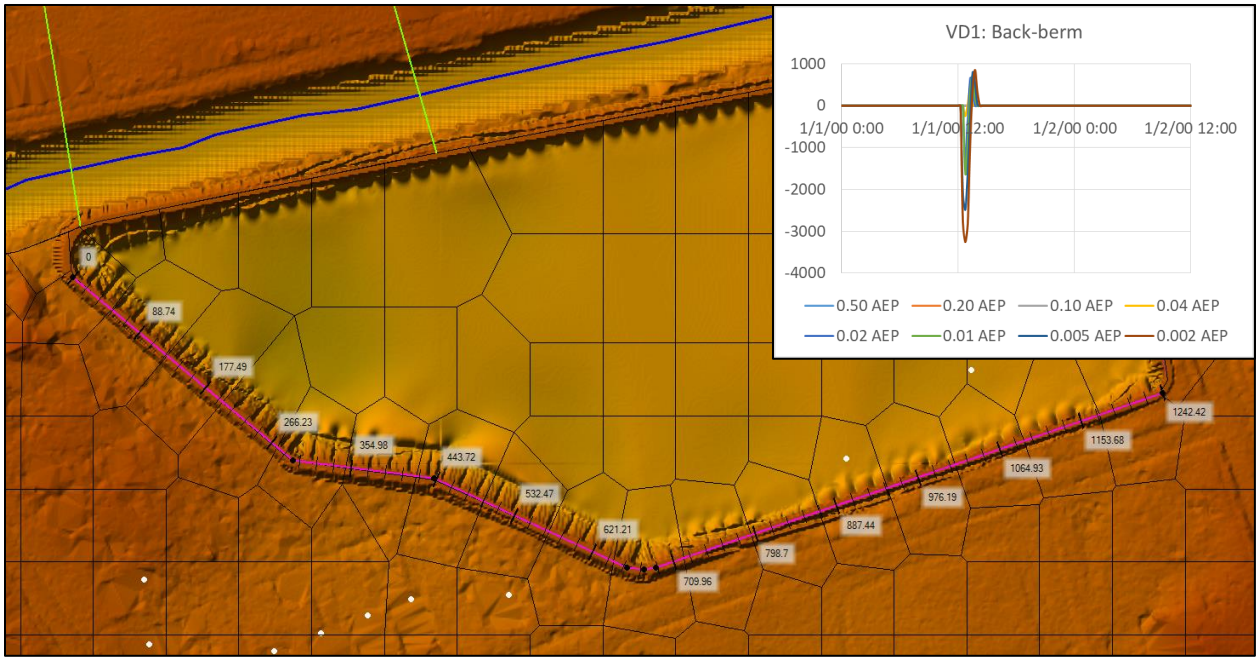

Figure 5-23: *Schematic from RASMapper with plot of back-berm hydrographs at VD1 (all analyzed AEPs shown). Profile line from which hydrographs were produced is shown in pink. Note flow is both positive and negative; overbank flows overtop the upstream extent of the back-berm profile line and enter the detention basin, and flows leave the basin and inundate the backflow area. Outward overtopping risk associated with the analyzed berm exists. Greatest AEP that produces overtopping risk determined as 0.04 for this site. Map notes: flow is east-to-west, north is up, and scale is approximately 1:1,250.*

Upper and lower limit stages for all other cross sections were determined directly from the roughness-scaled model results. Stages reported correspond to the maximums from respective simulations (based on the falling limb of looped rating curves; see Figure 5-24) to align with economic benefit analyses which consider the maximum flood profile associated with each analyzed frequency. In reality, the risk of feature exceedance, or flooding impacts, would be perceived at the onset of flooding, which could be realized in the rising limb of a passing hydrograph. However, it was necessary to analyze the falling limb only, in order to prevent applying confidence calculations across model time-steps. Utilization of the falling limb associates a lesser discharge than that of the rising limb; however, in most cases, the expected stage associated with exceedance of a measure was only reached during the falling limb of the hydrograph.

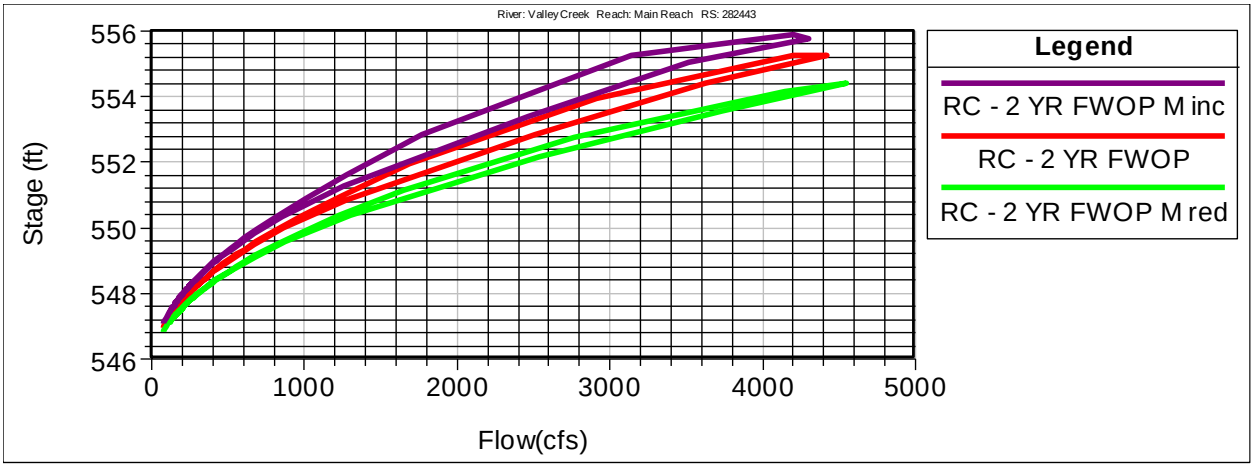

Figure 5-24: *Rating curves with hysteresis for the 0.50 AEP event at River Station 2824+43 on Valley Creek (at measure VD1).*

Measure performance was also analyzed in terms of long-term exceedance probabilities (LTEPs; Table 5-5). LTEPs are useful risk communication tools, and work to express the risk of occurrence over a select period of time. Berm height exceedance (overtopping) was analyzed for the detention basins over periods of 10, 30, and 50 years. Additionally, channel capacity exceedance and overtopping of the proposed bridge modification relevant to the NED plan were analyzed. LTEPs were based on the mean (or expected) AEPs derived from model results.

Table 5-5: Measure performance described by AEP and LTEP

Measure	Mean AEP[1]	LTEP		
		10 Years	30 Years	50 Years
VD1	0.04	0.34	0.71	0.87
VD2	0.04	0.34	0.71	0.87

[1]*AEP references overtopping.*

5.2.6 Cost Uncertainty

Three components of cost uncertainty specifically related to geotechnical engineering analysis of the recommended plan were identified. Bedrock conditions, groundwater conditions, and suitability of excavated material were considered potential risks to computed plan costs and contingency. Geotechnical investigations described in Section 4.1.1.3 highlight the work performed to develop at-site bedrock and groundwater conditions prior to finalization of the recommended plan in November 2020. As of March 2021, advanced geotechnical investigations (borings and geophysical surveys) were completed with results summarized in this report (see Section 4.3.3). Cost contingencies were initially factored at 35% for all plans, which provides a conservative amount of adjustment in the costs utilized to determine the net annual benefits and BCR associated with the recommended plan. The refined cost contingency to support the recommended plan is lower than the baseline estimate of 35% (see Cost Appendix for details). Following the CSRA, the refined contingency was not lowered any further based on the potential to encounter bedrock for some portion of excavation, or the need for groundwater mitigation.

Additionally, as described in Section 4.3.3.1, laboratory testing has not been completed to confirm suitability of material, which also factored into contingency decisions. However, field observation of material suggests design compatibility is likely, and given the small volume of required fill relative to required cut per site, risk of contingency exceedance associated with additional fill requirements is considered very low.

5.2.7 Bessemer Gardens Levee

Stage uncertainty at the Bessemer Gardens Levee (location shown in Figure 1-2) was not assessed, as flood conditions are improved in the vicinity of the project for all analyzed frequencies. In general, maximum water surface profile reductions decrease approximately 0.5 foot with implementation of the recommended plan. Figures 5-3 and 5-6 show the 0.50 and 0.04 AEP profiles in the vicinity of the levee as well as the depth-difference rasters (from FWOP conditions) for these events. As described in Section 2.2.2, interior drainage through the levee's floodgate was not modeled; however, overtopping flows are represented in the hydraulic model with a lateral structure and 2-D flow area. A coincidental frequency analysis of interior flooding and main-stem flood-wave timing was not completed; however, this analysis was not considered necessary based on negligible timing differences in without- and with-project flood-waves (Figure 5-25) and the reduction in maximum WSEs associated with recommended plan implementation.

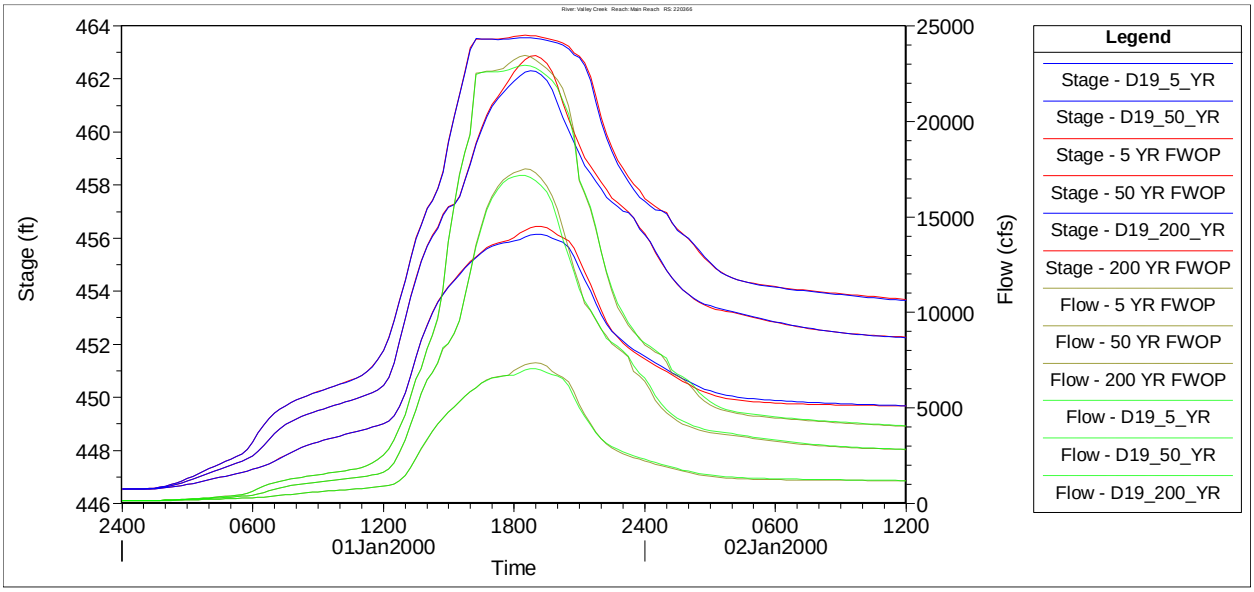

Figure 5-25: *Stage and flow hydrographs for 0.50, 0.02, and 0.005 AEP events at RS 2203+66 (middle extent of Bessemer Gardens Levee, approximately).*

6.0 Climate Change Assessment for Valley Creek

6.1 Introduction

In 2016, USACE issued Engineering and Construction Bulletin No. 2016-25 (USACE, 2016) (hereafter, ECB 2016-25), which mandated that climate change be considered for all federally funded projects in planning stages. This guidance was updated with ECB 2018-14 (USACE, 2018). A qualitative analysis of historical climate trends, as well as assessment of future projections was provisioned by ECB 2018-14. Even if climate change does not appear to be an impact for a particular region of interest, the formal analyses outlined in the guidance result in better-informed planning and engineering decisions.

6.2 Literature Review

A literature review was performed to summarize climate change literature relevant to the study area and highlight both observed and projected assessments of relevant climate change variables. As this is a flood risk management project, the primary relevant variable is streamflow. This variable is also affected by precipitation and air temperature. Therefore, this review focuses on observed and projected changes in precipitation, air temperature, and hydrology.

6.2.1 Temperature

The Fourth National Climate Assessment (USGCRP, 2017) states that observed temperatures in the United States have increased up to 1.9 degrees Fahrenheit since 1895, with the increase in temperatures accelerating since the 1970s. The National Climate Assessment goes on to say that warming is projected for all parts of the United States through the 21st century (USGCRP, 2017). The 2015 review conducted by the USACE Institute for Water Resources (IWR) summarizes the available literature on climate change for the South Atlantic-Gulf Region, which includes the Valley Creek Basin (USACE, 2015b). In general, studies have shown that, over the last century, a period of warming in the region has been observed since a transition point in the 1970s that was precluded by an observed cooling period (see Patterson et al., 2012; Laseter et al., 2012; and Dai et al., 2011). However, the overall warming trend is fairly inconsistent for the region overall since the early 1900s. The consensus from the IWR report (USACE, 2015b) indicates only mild increases in annual temperature in the region over the past century with significant variability; however, there is a clear consensus in general warming since the early 1970s.

The project area itself has seen similar results. The longest running gage in the area, the NOAA gage located at the Birmingham, Alabama airport (KBHM), has continuous records of precipitation and temperature going back to the early 1900s and is located only a few miles northeast of the headwaters of the study area (see Figure 1-5). As mentioned, this gage was previously located within the Valley Creek Basin (relocated in 1990). Since the early 1900s

there was a gradual decrease in annual average temperatures, transitioning to a consistent increase in the early 1970s.

A statistical analysis was performed on the entire dataset from the airport gage as shown in Figure 6-1 with associated p-value. The alternative hypothesis of an apparent trend, is accepted to be true at the 0.05 significance level, meaning that p-values less than 0.05 are indicative of statistical significance. This is a threshold commonly adopted within statistical references, but consideration should also be given to trends whose p-values are close to this reference threshold. In this case, the period of record data produces a high p value of 0.82303 and therefore is not considered to have a significant increasing or decreasing trend. However, performing the same test of average annual temperatures from 1970 – 2018, seen in Figure 6-2, produces a p-value of 0.00000029. This would be considered very indicative of a statistically significant upward trend in temperatures.

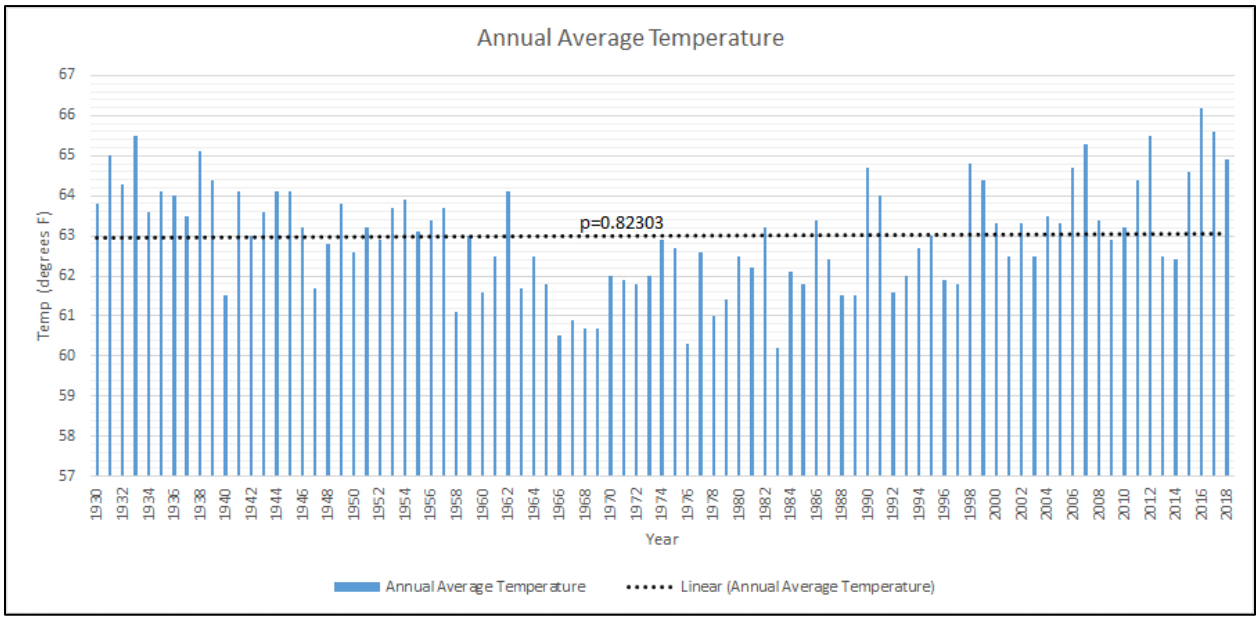

Figure 6-1: *Annual average temperature and p-value from 1930 - 2018*

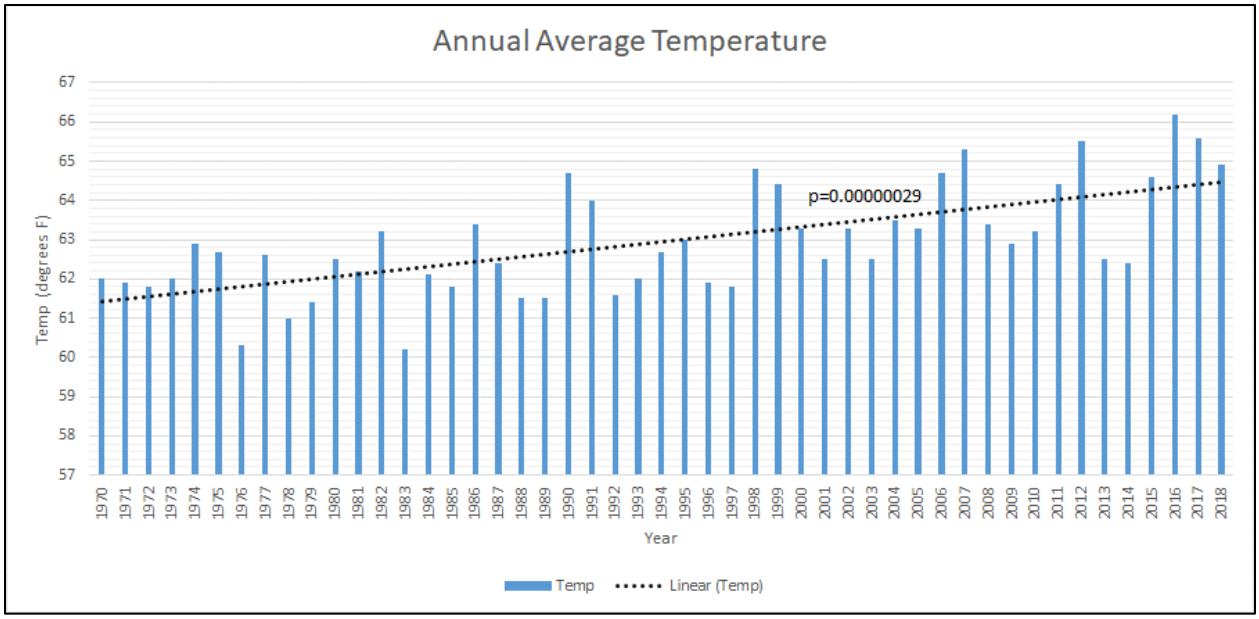

Figure 6-2: *Annual average temperature and p-value from 1970 - 2018*

Global Circulation/Climate Models (GCMs) have been used to project future climate conditions in the U.S. including the southeast regions. Results show a significant warming trend at a national and regional scale. Figure 6-3 shows the projected changes in seasonal maximum air temperatures based a report by Liu et al. (2013) assuming a “worst case” greenhouse gas emissions scenario. This shows that, overall, there is a projected warming trend of about 2 degrees in the winter months up to 3.5 degrees in the summer by 2070 for the southeast.

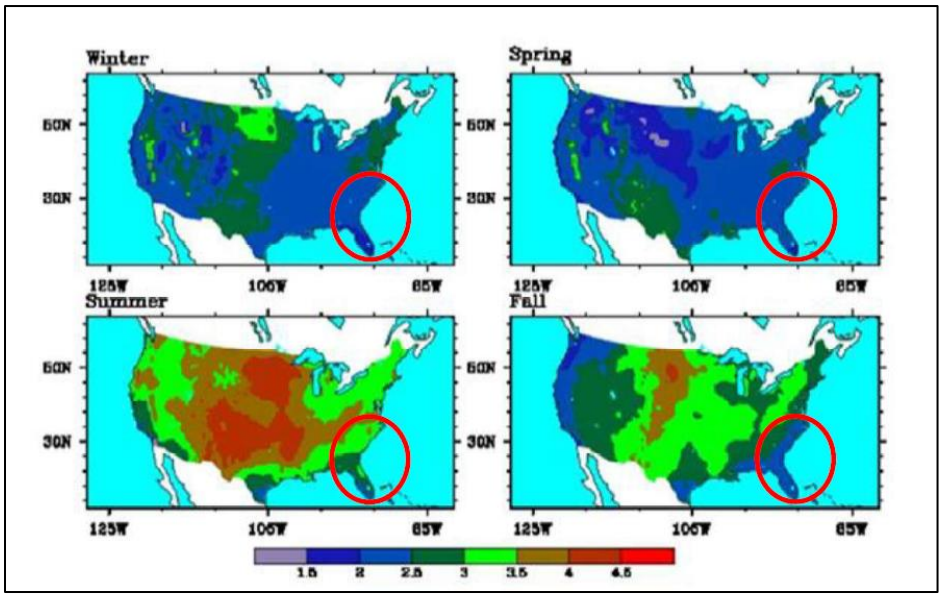

Figure 6-3: *Projected changes in seasonal maximum air temperature, ºC, 2041 – 2070 vs. 1971 – 2000. The South Atlantic-Gulf Region is within the red oval (Liu et al., 2013; reprinted from USACE, 2015b).*

6.2.2 Precipitation

Observed Average Precipitation

The IWR report (USACE, 2015b) shows that there is a general increase in precipitation for the southeast region; however, it is highly variable for the region. Analysis of gridded data including years 1950 -2000 showed that winter precipitation has consistently increased over the last century (Wang et al., 2009). Other seasons, however, have shown increases in precipitation in some area, decreases in some areas, and some areas with little change in precipitation.

A study by Patterson et al. (2012) did not identify patterns of precipitation change utilizing monthly and annual trend analysis (data included 1934 – 2005) for a number of climate and streamflow stations within the South Atlantic-Gulf Region. The study did find, however, that more sites exhibited mild increases in precipitation than those that exhibited decreases.

The NOAA Birmingham Airport gage (KBHM) shows fairly variable annual average precipitation since 1930 (Figure 6-4 and Figure 6-5) with no statistically significant upward trend based on a high p value of 0.270996 and 0.5963 respectively.

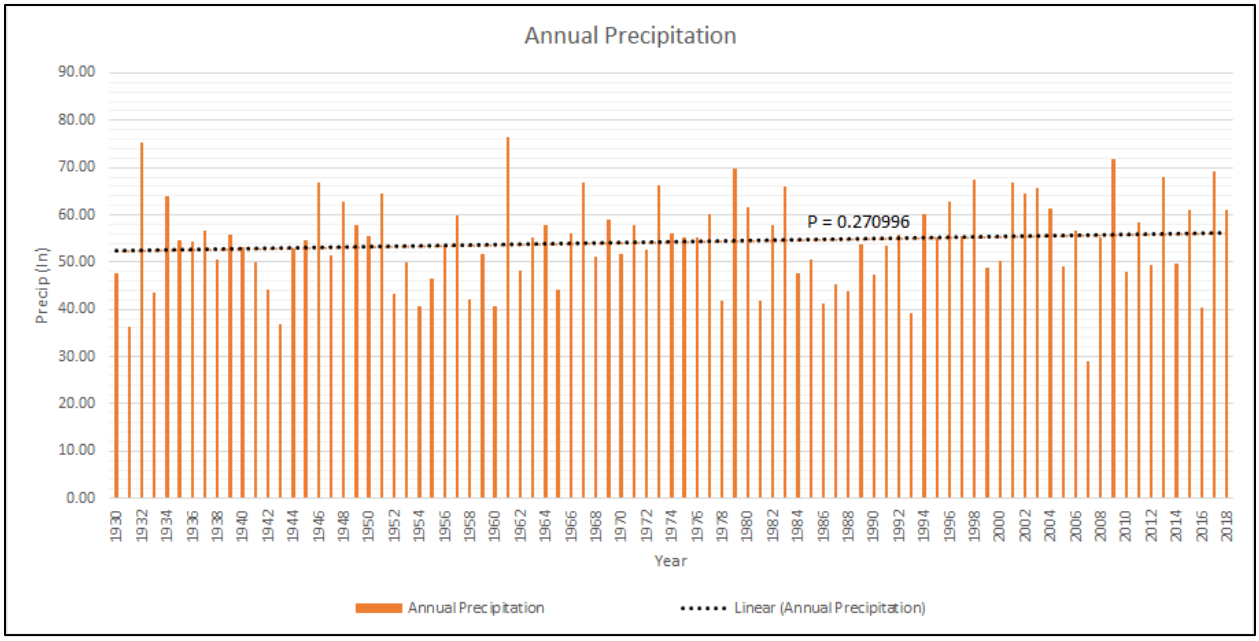

Figure 6-4: *Annual total precipitation and p-value from 1970 – 2018*

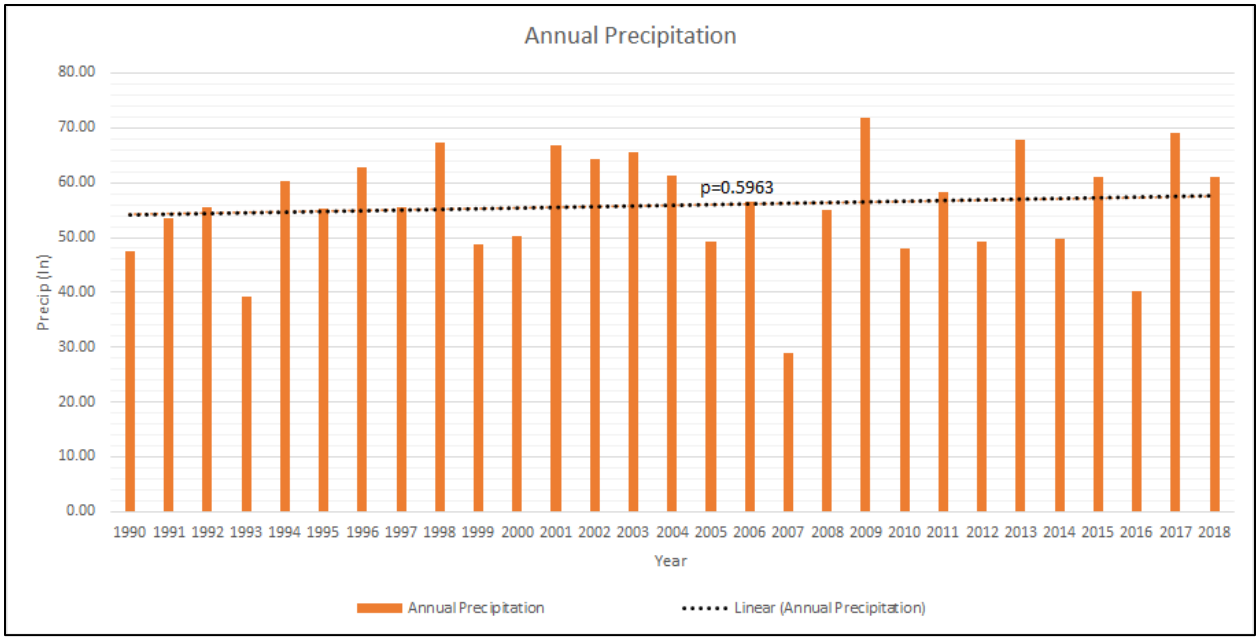

Figure 6-5: *Annual total precipitation and p-value from 1990 – 2018*

Observed Extreme Precipitation

The Fourth National Climate Assessment shows that extreme events in the southeast are increasing. Days with 3 or more inches of precipitation have generally increased in the southeast in the past 25 years. Many precipitation gages show upward trends since 1950; however, some gages show downward trends in areas near the Appalachian Mountains and Florida, with some localized decreases in other areas. Figure 6-6 (left) shows the change in annual number of days with precipitation greater than 3 inches in the southeast averaged over the recording locations (right). This distribution shows a general increase; however, looking at the location of the study area, there is minimal change, or a small decrease in days with 3 inches of precipitation since 1950 (USGCRP, 2017).

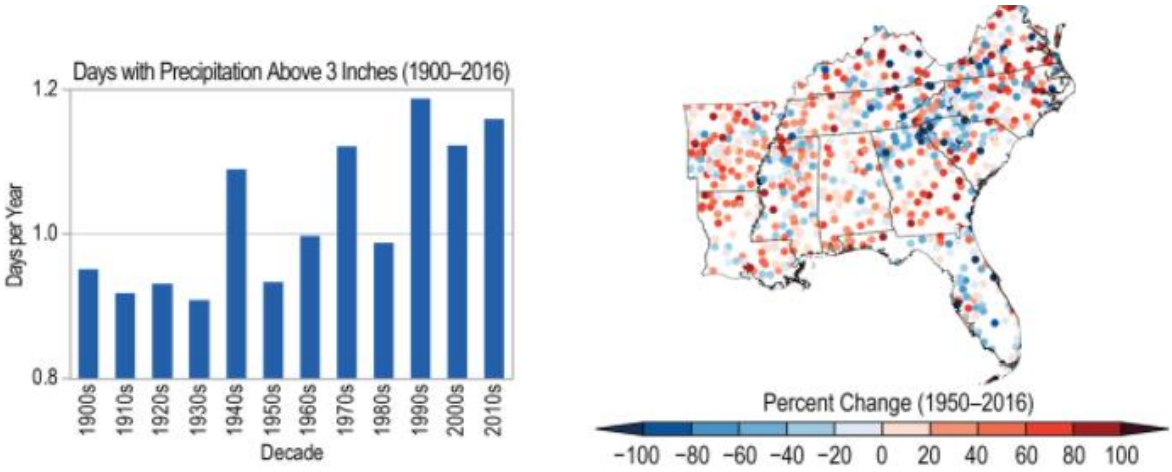

Figure 6-6. ***(****Left) change in annual number of days with precipitation greater than 3 inches in the southeast averaged over the recording locations (right) (reprinted from USGCRP, 2017).*

Projected Average Precipitation

Projection of future changes in average precipitation for the southeast region are variable and lack consensus. The Liu et al. study (2013) quantified significant increases in winter and spring precipitation associated with a 2055 future condition for the South Atlantic Region. However, other seasons showed almost no increase or a slight decrease in precipitation. Figure 6-7 illustrates the projected change in seasonal precipitation. The authors also project increases in the severity of future droughts for the region, leading to projected temperature and evapotranspiration (ET) impacts that can offset the increases in precipitation (Liu et al., 2013).

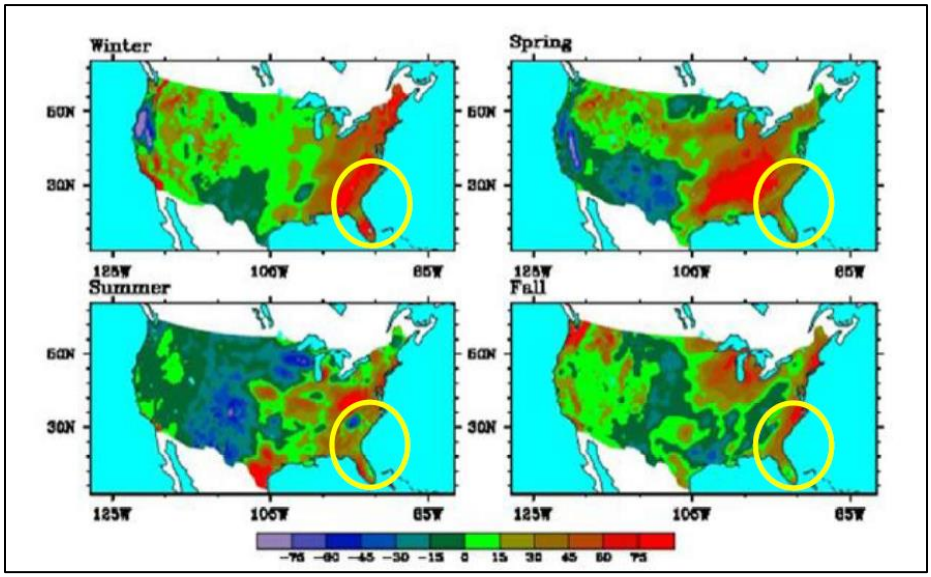

Figure 6-7: *Projected changes in seasonal precipitation, 2055 vs. 1985, mm. The South Atlantic-Gulf Region is within the yellow oval (Liu et al., 2013; reprinted from USACE, 2015b).*

Projected Extreme Precipitation

Studies reviewed by the IWR (USACE, 2015b) suggest that there is no consensus in trends indicating a shift in precipitation (severity and frequency). However, some analyzed literature shows mild increasing trends in extreme precipitation severity and frequency. For instance, Li et al. (2011) investigated anomalous precipitation (based on deviation from the mean) in summer months in the southeastern U.S., and found that a greater number of climate stations within the region did not exhibit increasing trends in frequency of occurrence of heavy rainfall than those that did. Increases were shown by Wang and others (2013), who found that 20% of sites analyzed within 56 southeastern watersheds exhibited increasing trends for 90th quantile precipitation months. The Fourth National Climate Assessment does indicate a moderate consensus across climate models for an increase in extreme precipitation throughout the United States (USGCRP, 2017). As there is some consensus regarding trends in extreme precipitation events in the United States, it is important to remain mindful of the identified increasing and decreasing trends in intensity and frequency of rainfall within the region. Consensus on increasing trends in extreme precipitation severity and frequency in the Southeast is low and an increase in extreme storms has not been seen in the immediate study area as will be discussed in future sections of this assessment.

6.2.3 Hydrology

Observed Hydrology

Generalized observations of streamflow trends in the southeast lack a clear consensus, with some models showing positive trends in some areas and others showing negative trends for areas in the southeast. Generally, most studies in the southeast showed no trend in streamflow in either direction or a negative trend. Most notably, studies have shown that the negative trend in streamflow being more consistent for the region since the 1970s (Kalra et al., 2008; and Patterson et al., 2012). Observed streamflow data presented in the nonstationarity assessment in the next section strongly reflects this trend. While there were multiple large floods in the 1960s- 1980s, there have been very few significant streamflow events in the region since the early 1980s.

Projected Hydrology

Review of projected hydrology for the southeast region show that there is very low consensus in in projected changes. This is in part due to the additional uncertainties that are added when coupling climate models to hydrologic models, both of which carry their own uncertainties. Overall, there are little indications of an increasing or decreasing trend in hydrology based on the reviewed literature presented in IWR report (USACE, 2015b).

6.2.4. Summary

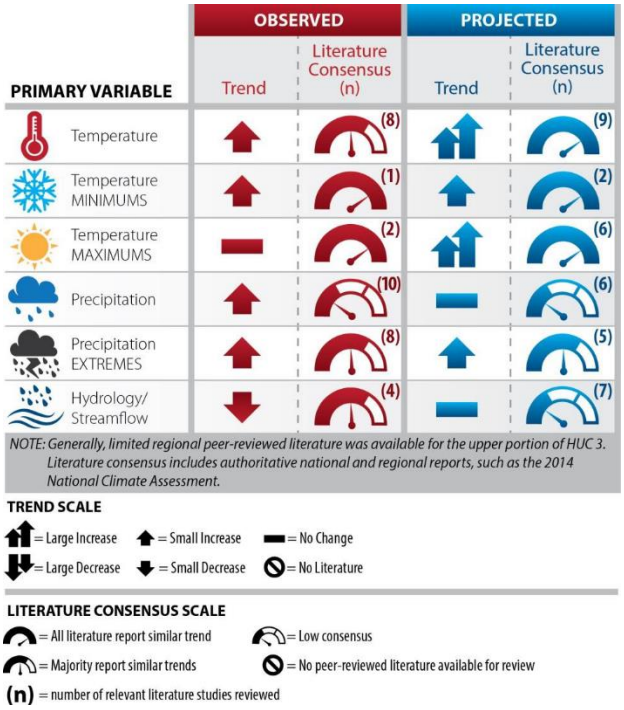

Figure 6-8: *Summary matrix of observed and projected climate trends and literary consensus (reprinted from USACE, 2015b).*

Figure 6-8 shows the discussed variables and their overall consensus in trends for both observed and projected scenarios based on the findings of the 2015 USACE IWR literature synthesis. There is strong evidence of increasing trends in projected, future temperatures. Based on model projections, the study area can anticipate increases from 2-4 degrees Celsius by the late 21st century. There exists some consensus in the observed record that temperatures are increasing, as well. Overall, there is low consensus from observed precipitation records that total precipitation is changing. There is some evidence that there might be an increase in extreme precipitation events. However, there is a lot of variation in precipitation trends throughout the southeast region with some areas seeing a drop in average precipitation and extreme events. There is some consensus that there will be an increase in extreme precipitation events across the United States in the future, but a low consensus for an increase in the southeast. It is unclear if indications of an increase in extreme precipitation result in higher peak flows and increased flooding. Some effects of projected increases in extreme precipitation events could be offset by increasing temperatures prolonged droughts. Very few conclusions can be drawn regarding future hydrology in the region largely due to the substantial amount of uncertainly in these projections when coupling climate models with hydrology models.

6.3 Nonstationarity Assessment

In accordance with ECB 2018-14 (USACE, 2018), a stationarity analysis was performed to determine if there are long-term changes in peak streamflow statistics within the Valley Creek basin and its vicinity. Assessing trends in peak streamflow is considered appropriate as one of the primary purposes of this feasibility study is to assess and reduce flooding in the Valley Creek Basin. Measures being considered, including off-channel storage, inline storage, and channel and bridge modifications, are significantly affected by changes in peak streamflow.

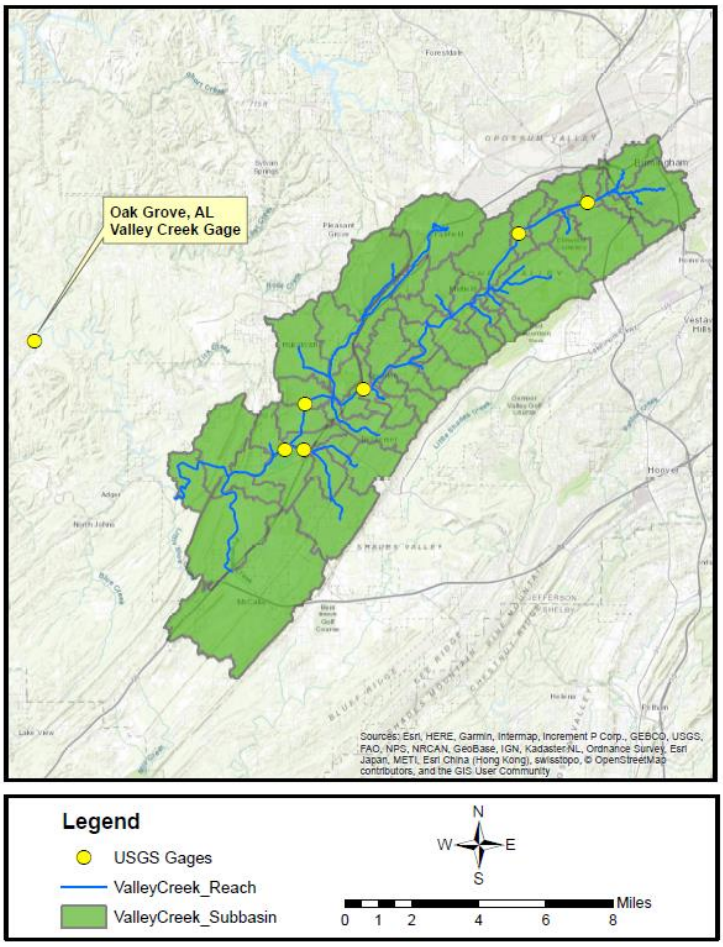

Figure 6-9: *Study area and location of the Oak Grove gage used in this analysis*

The USACE NonStationarity Tool was used to assess possible trends and change points in peak streamflow in the region. The following analysis for the detection of nonstationarities was performed in accordance with ETL 1100-2-3 (USACE, 2017b) which provides guidance for the detection of nonstationarities in annual maximum streamflow. USGS 02462000 was used for the analysis (Figure 6-9). The green area encompasses the study area within the larger Valley Creek Basin. The gage in this analysis is located on Valley Creek, but approximately 14 miles downstream of the study area, and has the longest continuous streamflow record for any site on Valley Creek. Additionally, this gage is the only site with at least 30 continuous years of record which is the minimum recommended years for this tool to detect nonstationarities. Figure 6-10 shows the time series of Annual Peak

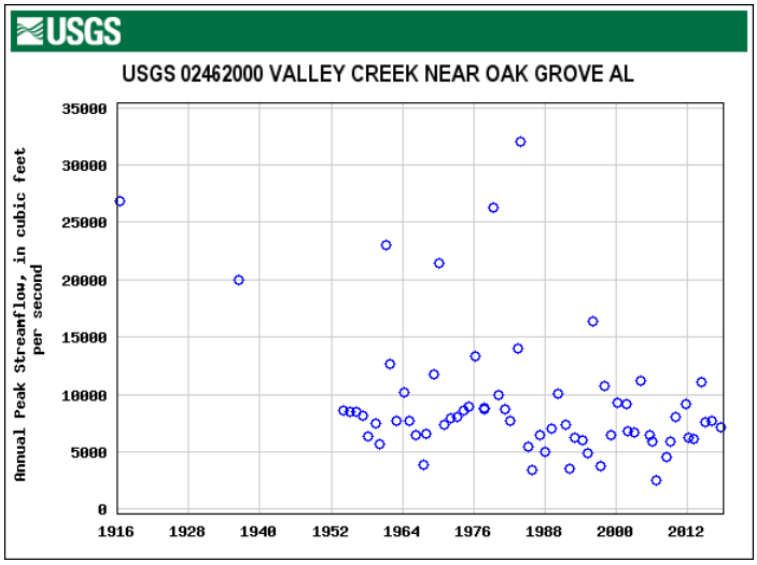

Figure 6-10: *APF at USGS 02462000 Valley Creek Near Oak Grove, AL.*

Streamflow (APF). The continuous period of record of 1954-2014 was used for this analysis.

The following 16 statistical tests were conducted on the APF time series shown in Figure 6-9 using the NonStationarity Tool:

1. Cramer-von-Mises distribution
2. Kolmogorov-Smirnov distribution
3. LePage distribution
4. Energy Divisive distribution
5. Lombard (Wilcoxon) abrupt mean
6. Pettitt mean
7. Mann-Whitney mean
8. Bayesian mean
9. Lombard (Mood) abrupt variance
10. Mood variance
11. Lombard (Wilcoxon) smooth mean
12. Lombard (Mood) smooth variance
13. Mann-Kendall trend
14. Spearman rank trend
15. Parametric trend
16. Sen's slope trend

Tests 1-12 are used to detect change points in the distribution, mean, and variance of the time series. These nonstationarity tests can be useful in detecting changes in annual instantaneous streamflow peaks driven by natural and human driven changes in the climate, addition/removal of water control structures, changes in land cover, as well as any other drivers of nonstationarity. Meanwhile, tests 13-16 are used to analyze long term trends. The variety of tests is essential for increasing confidence in the overall stationarity analysis. Significant findings in one or two tests are generally not enough to declare nonstationarity.

For this analysis the continuous period of water years 1954 – 2014 was analyzed. All sensitivity parameters were left in their default positions. Figure 6-11 shows the results of tests 1-12. Of all the 16 tests, seven produced results that indicated nonstationarity at the gage. The five tests that indicated nonstationarity detected a change point in the mean and overall statistical distribution of annual peak flows occurring in 1984. In this case, several abrupt statistical methods detected statistically significant nonstationarities within five years of one another, and therefore these tests can be considered a single nonstationarity in the flow record. The detection of these multiple nonstationarities within such a short span is partly due to differences between how each method detects and identifies change point years. Some methods detect the last year of a homogeneous period, while others identify the first year of a subsequent homogeneous period. Tests 13-16 (shown in Figures 6-12 and 6-13) showed an increasing monotonic trend in the period before the nonstationarities in 1984, but no trend in the post 1984 subset.

The nonstationarty identified in the annual peak streamflow time series is considered strong and robust. Four tests indicate a nonstationarity in overall statistical distribution and three additional tests show a nonstationarity in mean. A nonstationarity is considered robust if tests targeting changes in two or more different statistical properties show nonstationarity. Therefore, based on the results showing that there are nonstationarities in both mean and overall statistical distribution, this nonstationarity is robust. In terms of magnitude, the change in mean peak annual streamflow is significant. There is a near 30% decrease in mean peak annual streamflow after the 1984 nonstationarity compared to the period of record before it.

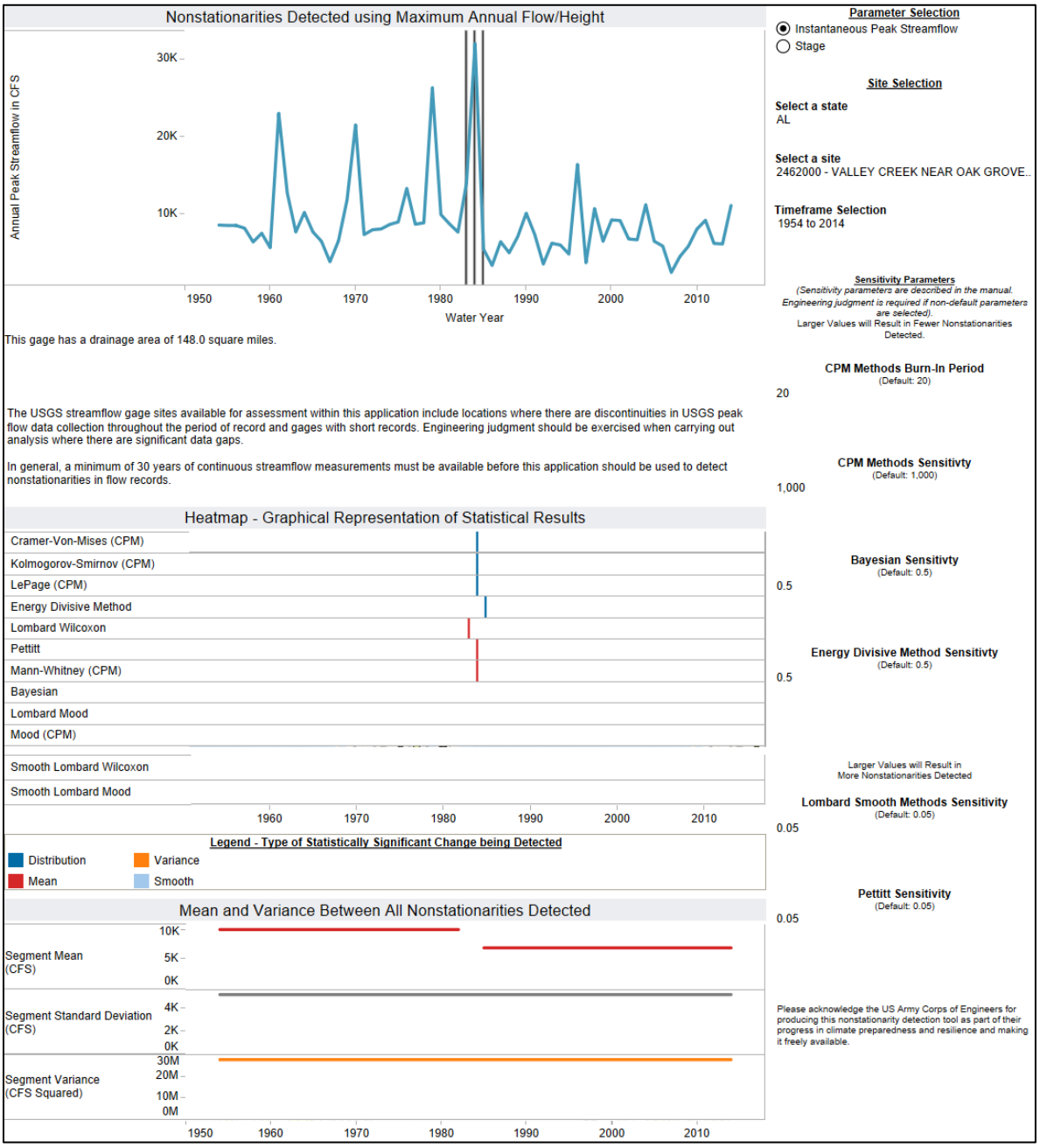

Figure 6-11: *Results of the nonstationarity assessment for USGS 02462000 Valley Creek Near Oak Grove, AL.*

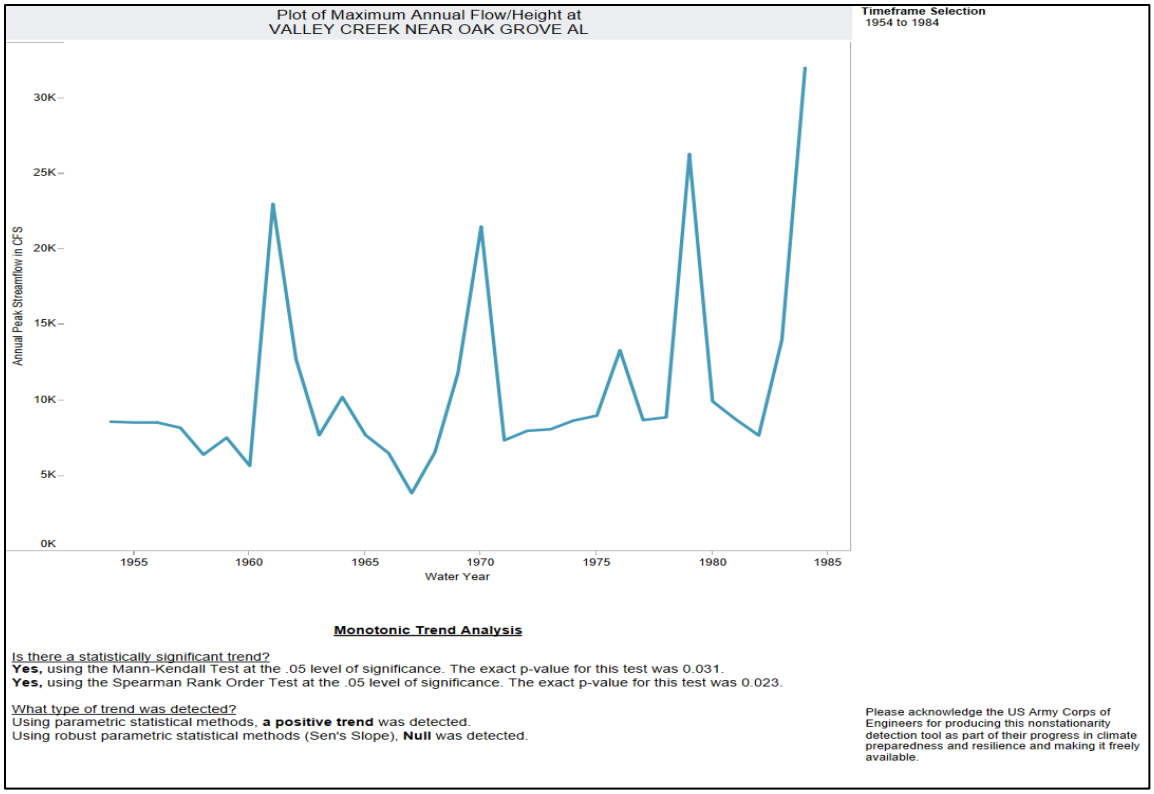

Figure 6-12: *Monotonic trend analysis for the POR before the nonstationarity.*

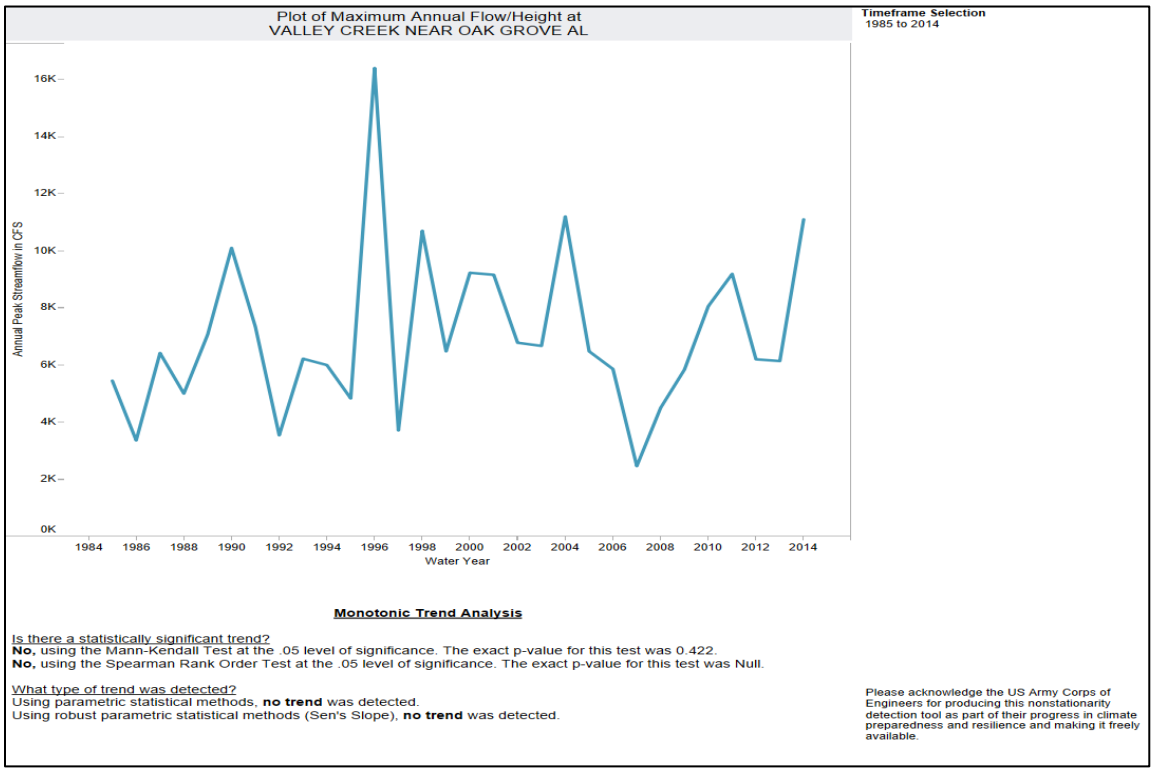

Figure 6-13: *Monotonic trend analysis for the POR after the nonstationarity.*

In addition to the stationarity assessment, the USACE Climate Hydrology Assessment Tool (CHAT) was used to assist in the determination of future streamflow conditions. For this assessment, the continuous period of record of 1954 – 2014 for USGS 02462000 was used. Figure 6-14 shows the Climate Hydrology Assessment Tool output for this gage. This analysis indicated no statistical trend for annual peak instantaneous streamflow for Valley Creek. The monotonic trend tab in the Nonstationarity Assessment Tool was applied to the entire period of record and also indicated that there is no statistically significant trend in the annual peak streamflow record from 1954-2014.

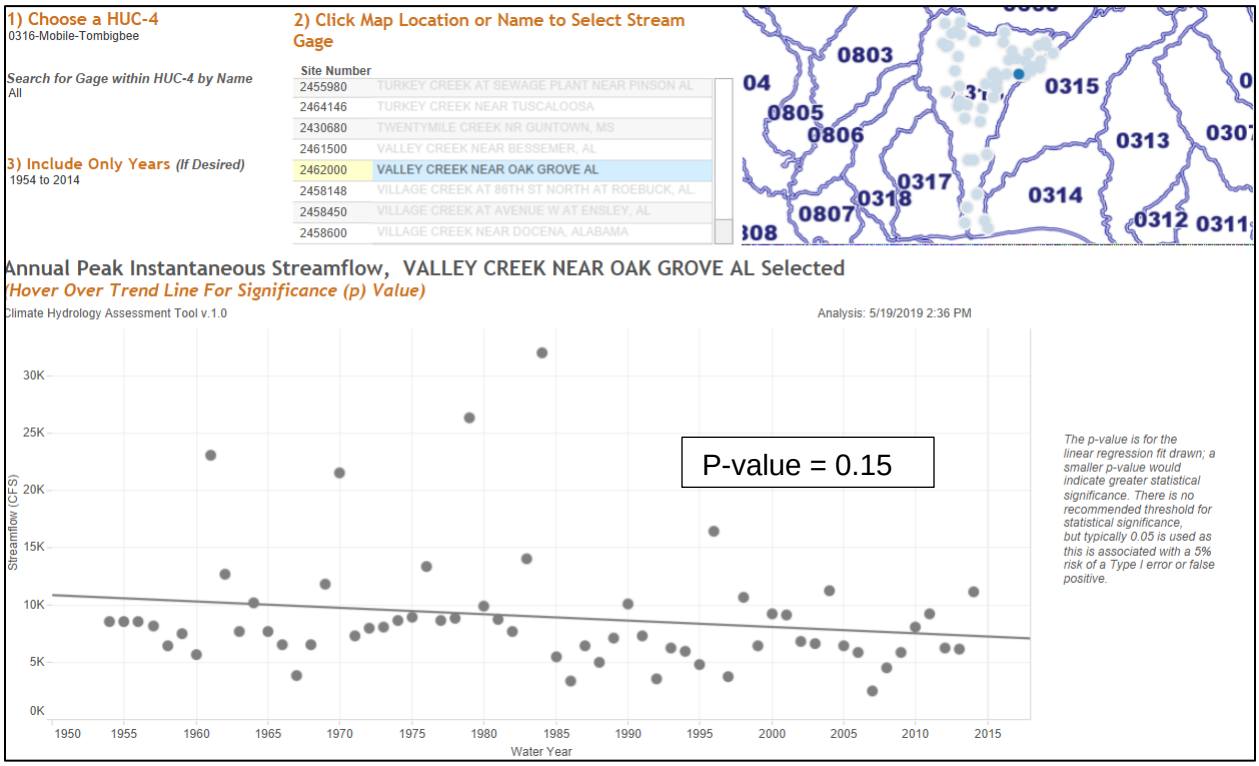

Figure 6-14: *CHAT output for USGS 02462000 Valley Creek Near Oak Grove, AL.*

USGS water year summaries where checked and do not reveal any information that would indicate gage errors or issue with flow recording or a change in location. Investigations into changes in the basin showed that stormwater management plans have been implemented as well as some channel improvements upstream; however, these were likely implemented gradually by applicable municipalities, and do not fully explain the abrupt change in peak annual streamflow. No flood control structures other than minor stormwater detention features have been identified in the basin above the study area. Urbanization in the basin has been gradually increasing, through the period considered, and should indicate an increase in runoff during extreme events.

Inspection of the record shows that there were significant hydrologic events that occurring in 1961, 1970, 1979 and 1983. Three of these events are well known events that caused flooding on a regional scale, affecting basins hundreds of miles away as far as north Georgia and south Florida. Many of the Mobile District's flood control projects have the events of 1961, 1979 and

1983 as either the record peak event at the project or within the top five largest events within their period of record. In the larger HUC-4 basin in which Valley Creek resides there has been little flooding of this magnitude since the 1983 event, with the exception of some moderate to major flooding affecting the lower end of the basin below Valley Creek in 1990.

An analysis of the peak 24-hour and 48-hour annual maximum precipitation shown in Figures 6-15 and 6-16 was performed to determine if this drop in peak annual streamflow could be attributed to a drop in precipitation. The NOAA Birmingham Airport gage (KBHM) was used for this analysis. The statistical analysis shows that there is no statistically significant trend in the data. However, another important aspect to consider is the effects of seasonality on large hydrologic events in the area. For this region, the dry season is considered from mid-May to mid-November. This period is associated with overall less rainfall, higher temperatures and an increase in vegetation growth and canopy. The wet season is considered from mid-November to mid-May. This period is associated with cold temperatures, consistent rainfall and low vegetation growth and canopy. Rainfall events occurring in the dry season require much more rainfall to initiate a basin runoff response compared to the wet season. Sometimes this is on the order of a few inches, depending on duration and intensity of the event. What can be seen from Figures 6-13 and 6-14 is that while there appears to be homogeneous distribution of extreme events through the period of record, they are more recently occurring during the dry season. Prior to the mid-1980's all extreme events occurred during the wet seasons. After the mid-1980s, extreme events occurred during the dry season. This shows a shift in the seasonality of events, rather than intensity. It should be noted this is not universally true for all events such as the January 2003 event, and this is only a small sample of events considering the largest events on record. This alone is a possible contributor to the downward shift in peak annual streamflow. However, more analysis would be needed on both the occurrence of less extreme events and streamflow response to state with confidence that the nonstationarity is the result of a seasonal shift in floods.

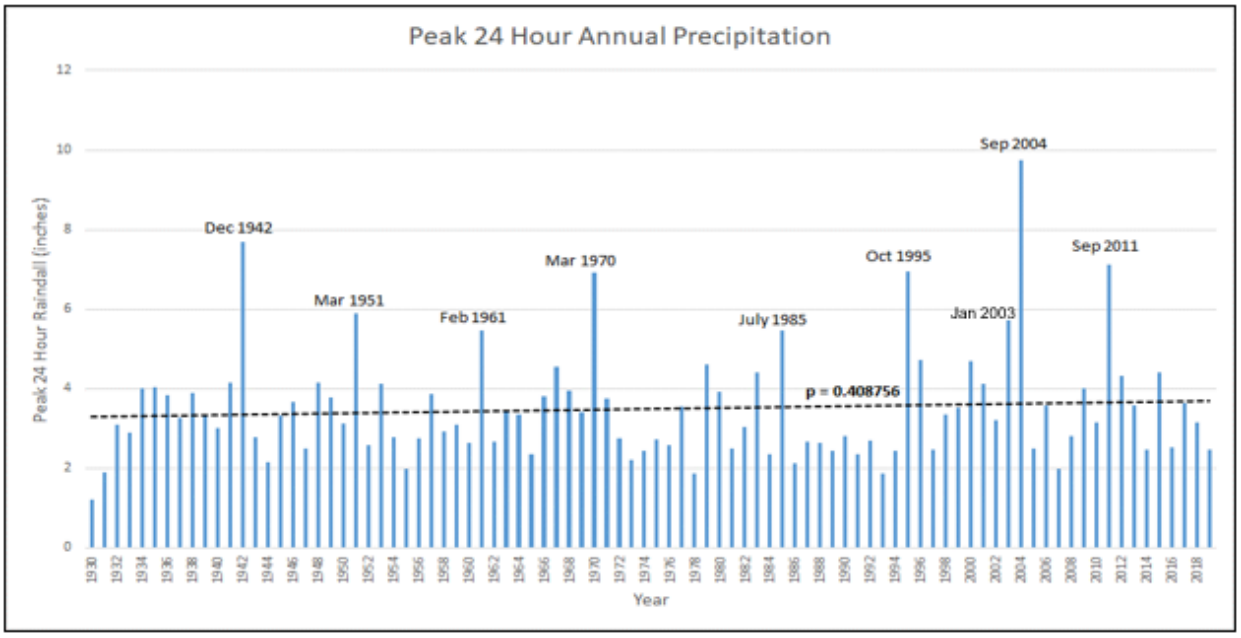

Figure 6-15: *Peak 24-hour annual precipitation at the Birmingham Airport gage.*

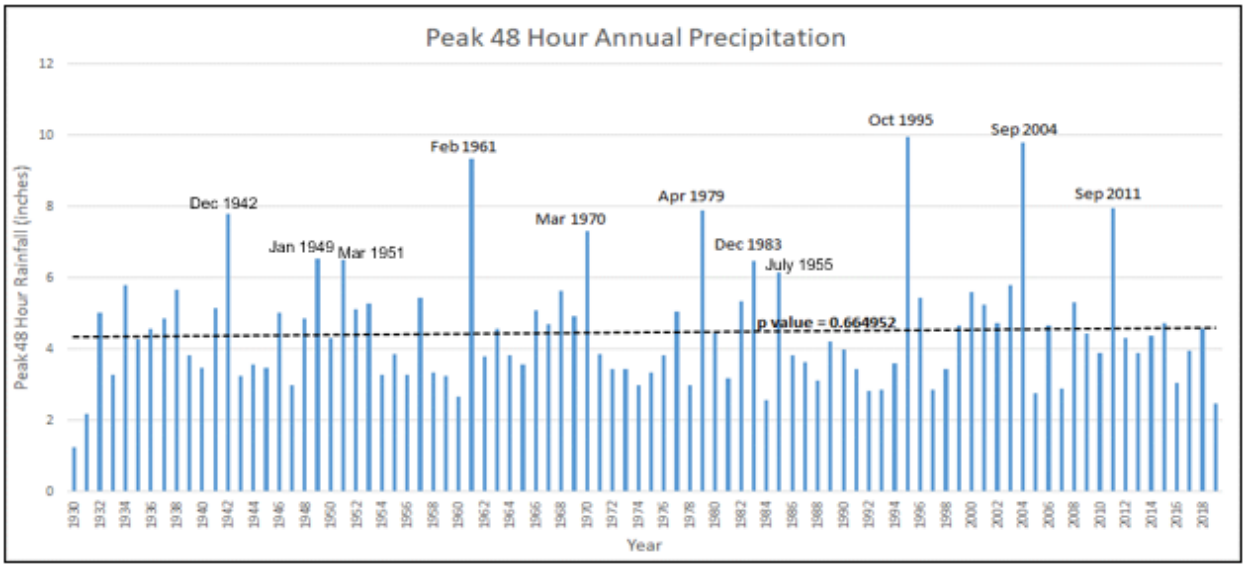

Figure 6-16: *Peak 48-hour annual precipitation at the Birmingham Airport gage.*

A Hydrologic Unit Code 4 (HUC-4) level analysis for mean projected annual maximum monthly streamflow was also performed. The trends in mean projected annual maximum monthly streamflow or “Later” period (2000-2099) presented in this analysis represent outputs from the Global Climate Models (GCMs) using representative concentration pathways (RCPs) of greenhouse gasses that are then translated into a hydrologic response using the United States Bureau of Reclamation (USBR) Variable Infiltration Capacity (VIC) model. The “Earlier” (1950-1999) period uses GCM outputs simulated to mimic present-day conditions the VIC model. The VIC model, forced with GCM meteorological outputs, is used to produce a streamflow response for both the earlier period (1950-1999) and the later period (2000-2099). This dataset is

unregulated and does not account for the many flood control structures located on the mainstem rivers within this HUC-4 basin.

These data represent flow near the downstream end of the larger Mobile-Tombigbee HUC-4 basin, of which Valley Creek is a small tributary to the mainstem rivers. There is not a statistically significant trend in this data as shown in Figure 6-17 (p-value of 0.098). However, this p-value is very close to the threshold of 0.05 for statistical significance and should not be discounted completely. While there has been no significant source of regulation within the Valley Creek watershed, there have been numerous changes to regulation along mainstem Black Warrior and Tombigbee Rivers within the larger Mobile-Tombigbee HUC-4 since the 1950s. As this dataset is comprised of unregulated flow, it does not reflect these changes in regulation that have occurred along the mainstem rivers in the Mobile-Tombigbee watershed.

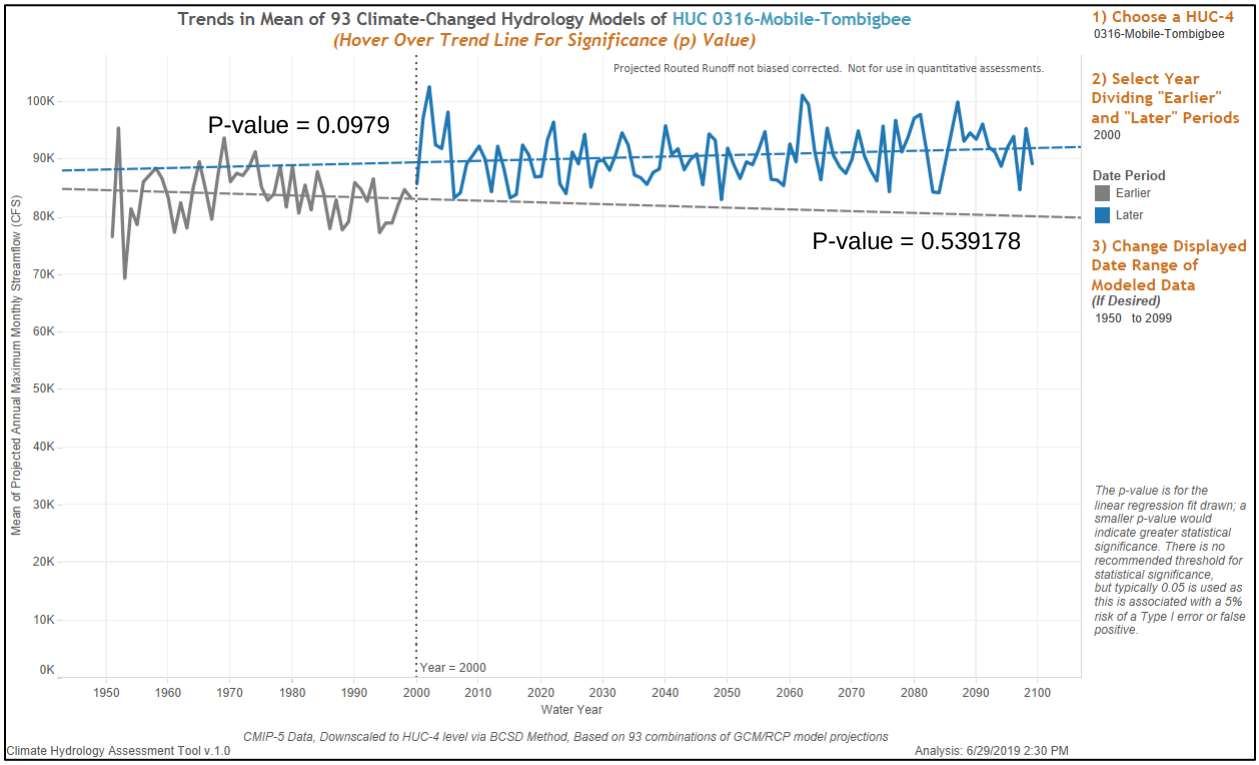

Figure 6-17: *Mean projected annual maximum monthly streamflow for the Mobile-Tombigbee HUC-4.*

Figure 6-18 provides the projected climate data of both the maximum and minimum values for the watershed along with the mean value for 93 climate ensembles through the year 2099. There is an increase in the range of projections around the year 2000. This would be expected as the USBR VIC hydrology model forced with GCM outputs only use the RCPs in the “Later” 2000 - 2099 period. Overall, the variability of the spread is fairly consistent through time after the year 2000. Furthermore, the mean has a very slight trend upward, accounting for only about a 5,000 cfs increase from the year 2000 to 2099.

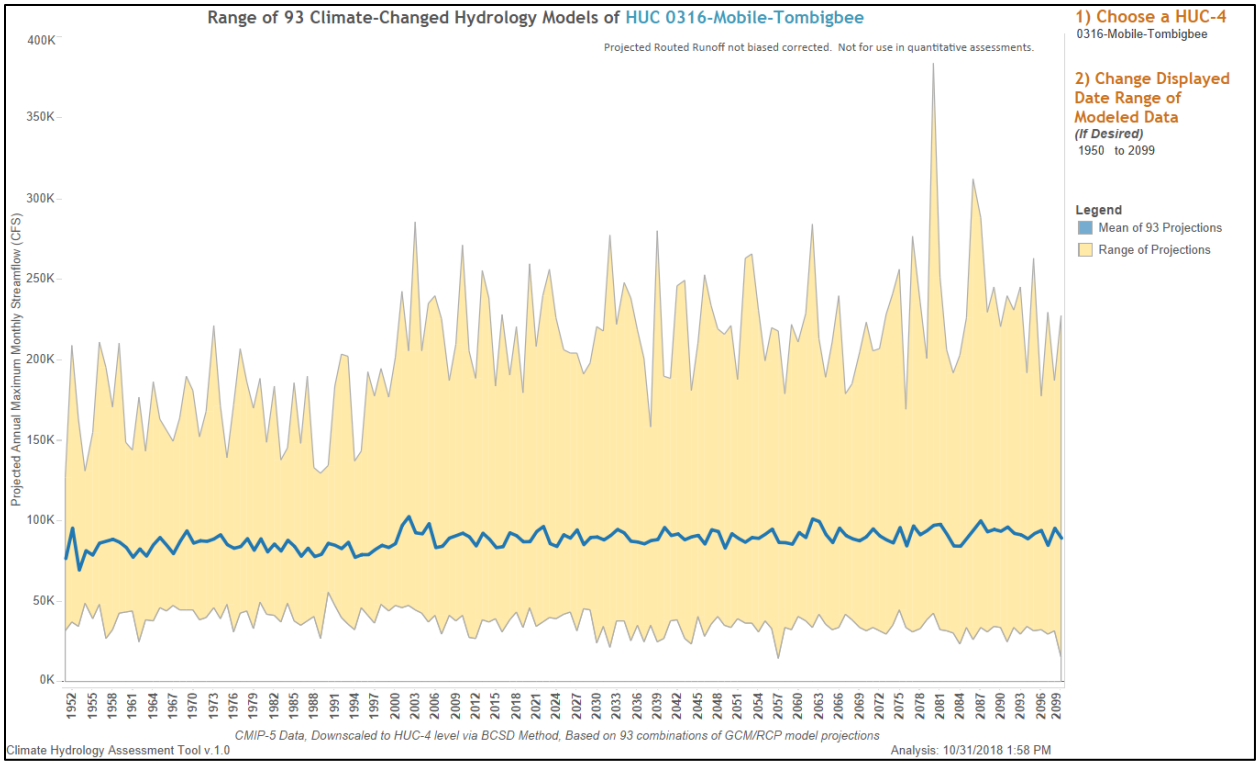

Figure 6-18: *Projected hydrology for the Mobile-Tombigbee HUC-4 base on the output from 93 projections of climate changed hydrology.*

It can be seen in Figure 6-18 above that there is significant uncertainty in projections. It is important to understand that this uncertainty comes from each of the model sources that are used to develop the spread of streamflow datasets. Global climate models generate results with significant uncertainties associated with their meteorological outputs. Additional uncertainty is generated when these climate models are combined with hydrologic models that carry their own uncertainty. For these reasons, this quantitative analysis should be used with caution, with an understanding that this data should only be considered within the large uncertainly bounds of the analysis.

6.4 Vulnerability Assessment

To understand potential climate change effects and to increase resilience/decrease vulnerability of flood risk management alternatives to climate change, the relative vulnerability of the basin to such factors was analyzed. In accordance with ECB 2018-14 (USACE, 2018), the USACE Watershed Climate Vulnerability Assessment tool was used to identify vulnerabilities to climate change on a HUC-4 watershed scale relative to other HUC-4 basins across the nation. As this study is an assessment of flood risk management alternatives, vulnerability with respect to the Flood Risk Reduction business line is presented.

To address vulnerabilities due to climate change, the Vulnerability Assessment tool utilizes two 30-year epochs centered on 2050 (2035-2064) and 2085 (2070-2099) as well as a base epoch. These epochs line up well with other climate change assessments. For each epoch, the tool

utilizes the results of 100 combinations of Global Circulation/Climate Models (GCM) run using different Representative Concentration Pathways of greenhouse gas emission. The results of the GCMs are translated into flow and are then sorted by cumulative runoff projections. Traces of the highest 50% of cumulative runoff are categorized as wet and traces with the lowest 50% of cumulative runoff are categorized as dry. This provides two scenarios (wet and dry) for each of the two epochs, excluding the base epoch. Consideration of both wet and dry scenarios reveals some of the uncertainties associated with the results produced using the climate changed hydrology and meteorology used as inputs to the vulnerability tool.

The tool uses specific indicators of vulnerability relative to the business line being considered. There are a total of 27 indicators in the tool, 5 of which are used to derive the vulnerability score in the Mobile-Tombigbee HUC 4 with respect to the Flood Damage Reduction business line. Table 6-1 lists the indicators and their descriptions.

Table 6-1: Indicator Variables used to derive the flood risk management Vulnerability score for the Mobile-Tombigbee Basin as determined by the Vulnerability Assessment tool.

Indicator Short Name	Indicator Full Name	Description
175C_ANNUAL_COV	Annual CV of unregulated runoff (cumulative)	Long-term variability in hydrology: ratio of the standard deviation of annual runoff to the annual runoff mean. Includes upstream freshwater inputs (cumulative).
277_RUNOFF_PRECIP	% change in runoff divided by % change in precipitation	Median of: deviation of runoff from monthly mean times average monthly runoff divided by deviation of precipitation from monthly mean times average monthly precipitation.
568L_FLOOD_MAGNIFICATION	Flood magnification factor (local)	Change in flood runoff: Ratio of indicator 571L (monthly runoff exceeded 10% of the time, excluding upstream freshwater inputs) to 571L in base period.
568C_FLOOD_MAGNIFICATION	Flood magnification factor (cumulative)	Change in flood runoff: ratio of indicator 571C (monthly runoff exceeded 10% of the time, including upstream freshwater inputs) to 571C in base period.
590_URBAN_500YRFLOODPLAIN_	Acres of urban area within 500-year floodplain	Acres of urban area within the 500-year floodplain.

Figures 6-19 and 6-20 show a comparison of WOWA scores for HUC-4 watersheds nationally, and for the South Atlantic Division only, respectively, for the wet and dry scenarios as well as the 2050 and 2085 epochs. The analysis parameters were left at the National Standard and a threshold of 20% was used. This means, only HUC-4s that have a vulnerability, or Weighted Ordered Weighted Average (WOWA), score in the top 20% nationally will be considered vulnerable relative to the rest of the country. The Flood Risk Management WOWA scores range from the 42.25 for the dry 2050 epoch to 47.62 for the wet 2085 epoch. In no scenario or epoch does the Mobile-Tombigbee basin fall within the 20% threshold for identification as being vulnerable under the Flood Risk Reduction busines line with respect to other basins in the nation. In SAD, for the wet subset of traces (corresponding to both epochs), there are only two HUC-4 watersheds, and for the dry subset of traces, there are three HUC-4 watersheds that are considered relatively vulnerable to climate change for the Flood Risk Reduction business line. All three watersheds in question are in Florida.

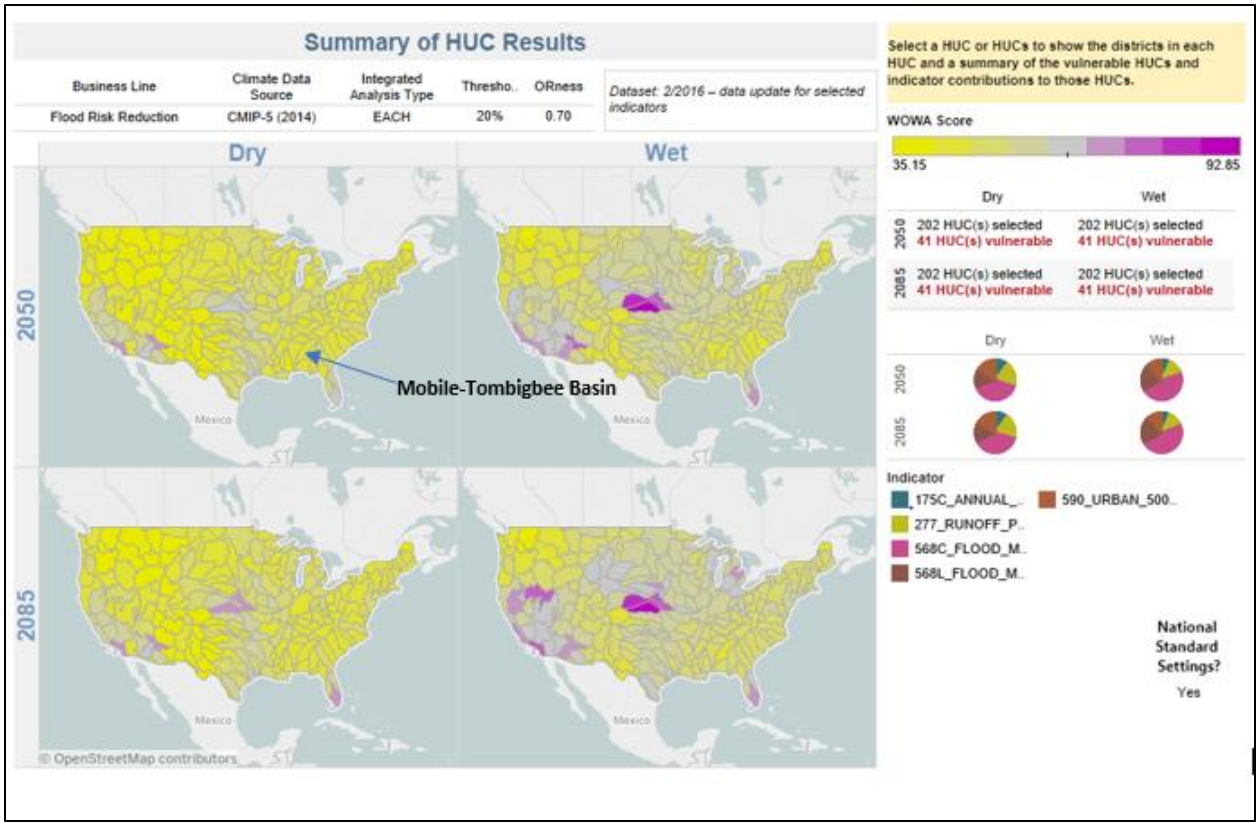

Figure 6-19: *Comparison of national vulnerability scores for CONUS HUC-4s.*

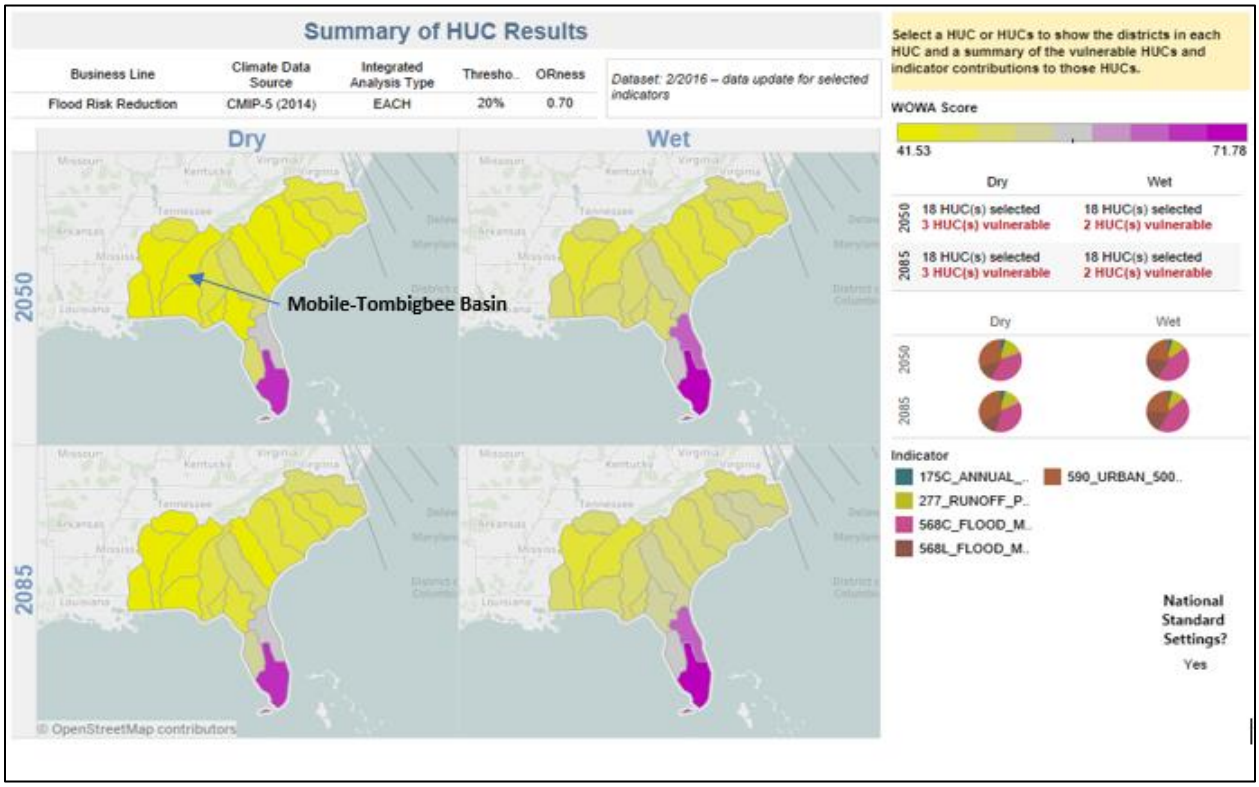

Figure 6-20: *Comparison of national vulnerability scores for South Atlantic Division HUC-4s.*

It is important to note that the vulnerability assessment only indicates vulnerability relative to the rest of the nation. It does not state that the basin itself is invulnerable to impacts of climate change on the Flood Risk Reduction business line. Therefore, it is beneficial to understand the composition of the relevant HUC04's vulnerability score in terms of how much each flood risk reduction indicator variable contributes to the vulnerability score for each subset of traces and for both epochs of time. Figures 6-21 and 6-22 below show the dominant indicators relative to Flood Risk Reduction. These both show that cumulative flood magnification is the prevailing indicator driving vulnerability relative to Flood Risk Reduction followed by urbanization in the 500-year floodplain in the dry scenario and local flood magnification in the wet scenario. This aligns with the literature review that indicates the potential for more frequent and more severe storms in the southeast.

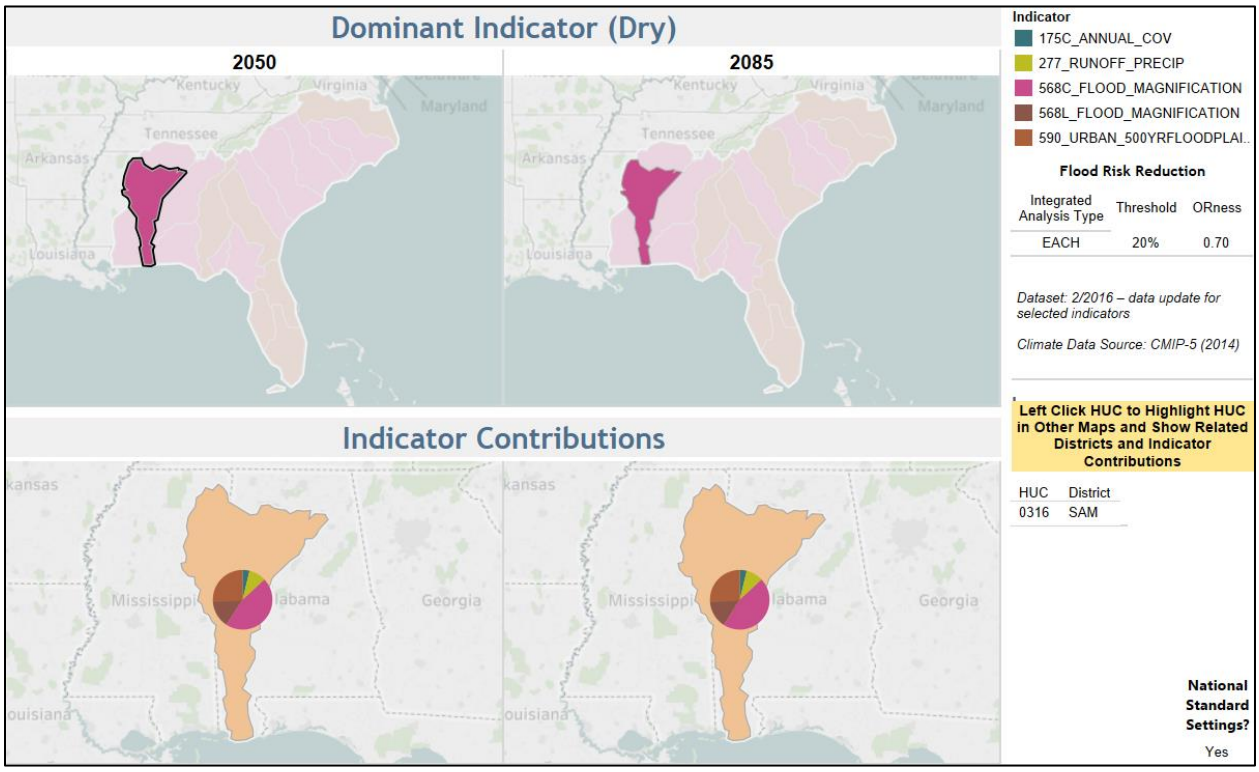

Figure 6-21: *Dominate indicators for the Flood Risk Reduction Business Line for the Dry Scenario.*

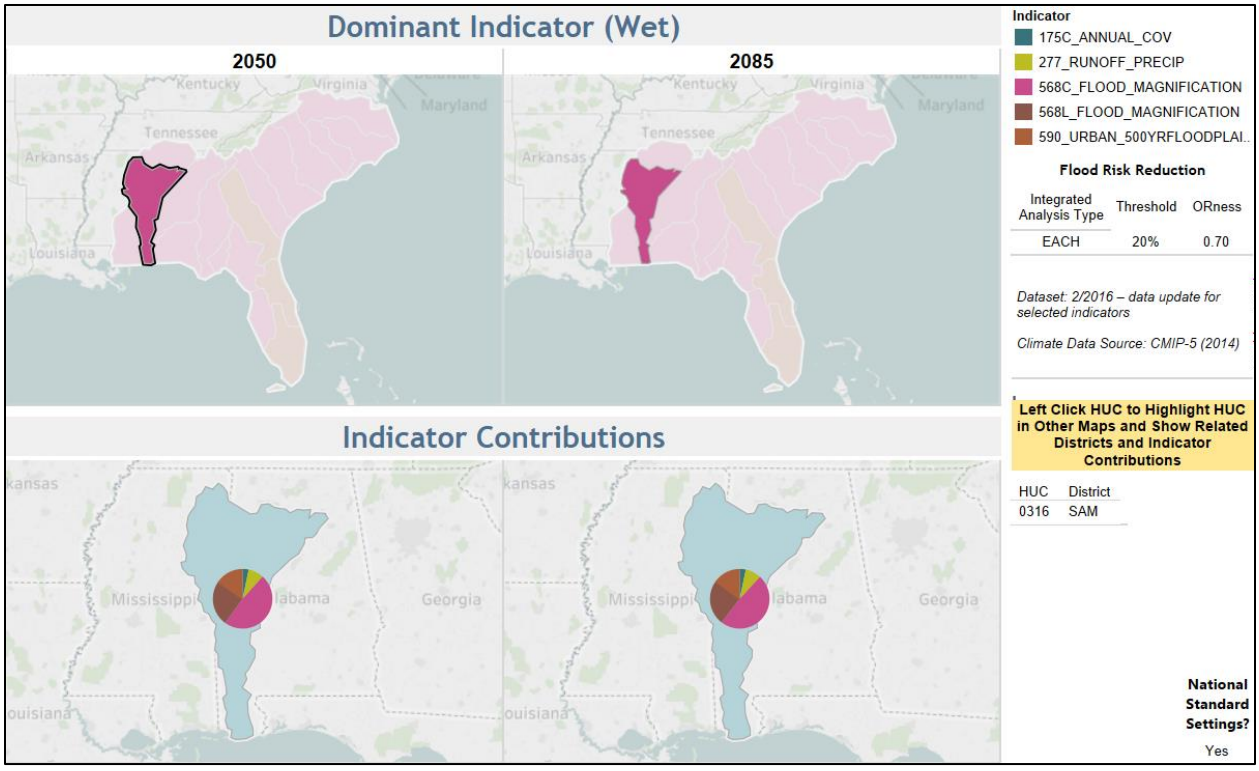

Figure 6-22: *Dominate indicators for the Flood Risk Reduction Business Line for the Wet Scenario.*

6.5 Climate change and Impacts on Recommended Plan

As discussed, the recommended plan for this study consists of three overbank detention areas in the northern end of the basin. These detention basins were optimized to reduce floods of magnitude less than 0.01 AEP (specifically, 0.04 AEP). The trigger of a change in hydrology could have an impact on the effectiveness of these structures where an increase in the intensity and frequency of precipitation could lead to increased flood volumes for all analyzed frequencies. In this scenario, the ponds will still produce benefits across the range of analyzed frequencies (as documented in Section 5.0); however, benefits associated with lesser AEPs may be realized more frequently. Beyond the 0.04 AEP event, this could be perceived as a negative occurrence.

The hazard of more frequent, higher flood volumes would lead to pond berms overtopping more frequently than the expected AEPs presented in Appendix A. Additionally, berm-influenced backflows discussed in Section 5.2.3 of Appendix A could occur more frequently. This could result in more frequent incremental risk associated with the selected plan, as impacts were shown to increase as the magnitude of analyzed events increased (Appendix A: Table 5-2). However, an increase in overtopping frequency is not considered an increase to incremental risk as equivalent flooding occurs in areas adjacent the ponds for all events. Section 5.2.4 of Appendix A details the negligible risk associated with berm overtopping as well as piping failure. Additionally, it is considered unlikely that the trigger of increased precipitation would be realized based on the results of this climate change assessment. The assessment shows that there is

little consensus that there will be an increase in peak streamflow from rain events. Furthermore, historical evidence has shown a drop peak streamflow in the local area occurring after 1983. The trigger of increased streamflow is also driven by the intensity and duration of storms. There is some consensus that there will be a small increase in intense and slower moving storms in the southeast region, but still, the recent hydrologic record, and the results of the CHAT tool assessment, do not provide evidence that a change in peak hydrology is expected.

The overall qualitative likelihood of the harm occurring is considered is highly unlikely. Without more solid evidence of increasing peak flows and volumes of floods, it cannot be said that the area is likely to see this change. Furthermore, there is an expectation by design that the pond berms will overtop for an infrequent flood. Therefore, the likelihood of the trigger occurring, leading to a hazard, and resulting in the harm of an increase in economic damages or threat to life safety are considered highly unlikely. Table 6-2 provides a summary of the climate change risks and likelihood for the individual measures of the recommended plan.

Table 6-2: Climate change risks and likelihood for the recommended plan measures

Feature or Measure	Trigger	Hazard	Harm	Qualitative Likelihood
Overbank Detention-VD1	Increase in peak precipitation leading to increased peak streamflow	Larger, more frequent future flood volumes	More frequent overtopping of berms and surrounding overbank flooding with adjacent damage to structures surrounding the berms as well as a threat to loss of life.	Highly Unlikely
Overbank Detention-VD2	Increase in peak precipitation leading to increased peak streamflow	Larger, more frequent future flood volumes	More frequent overtopping of berms and surrounding overbank flooding with adjacent damage to structures surrounding the berms as well as a threat to loss of life.	Highly Unlikely
Overbank Detention-VD4	Increase in peak precipitation leading to increased peak streamflow	Larger, more frequent future flood volumes	More frequent overtopping of berms and surrounding overbank flooding with adjacent damage to structures surrounding the berms as well as a threat to loss of life.	Highly Unlikely

6.6 Conclusions

Based on a literature review of relevant climate data, there is a clear consensus that temperatures will rise over the next century. Furthermore, there is some consensus of a small increase in the frequency and intensity of extreme precipitation events. However, there is no consensus on future changes in hydrology. Observed data from near the study area show temperatures have been gradually rising since the 1970s after a cooling period in the earlier part of the century. Annual precipitation seems to be variable since the 1930s however, peak annual streamflow at USGS gages within the study area has decreased since the 1980s.

The nonstationarity assessment on the Valley Creek watershed shows multiple significant nonstationarities around 1984 at USGS 02462000. There appears to be a sudden drop in peak streamflow after a 1983 extreme event with no major events occurring after 1983. A monotonic trend analysis performed using the subsets before and after the nonstationarities detected around 1984 show a small, statistically significant upward trend before 1984 and no general trend in the period after. The USACE CHAT tool indicates that there is no statistically significant trend in the dataset between 1954 and 2014. These analyses provide almost no indication that there will be significant changes in peak annual streamflow in the future as a result of climate change. However, caution should be used in making any definitive statements on potential future hydrology as there is substantial uncertainty in both the climate and hydrologic models that drive these analyses. The vulnerability assessment helps to further reinforce a lack of evidence in increasing streamflow. Findings of the vulnerability assessment show that the Mobile-Tombigbee HUC-4 basin is not considered vulnerable with respect to other HUC-4s in the nation.

Based on the results of this assessment, including considerations of observed precipitation and streamflow in the basin, there is not strong evidence suggesting increasing peak annual streamflow will occur in the future within the region. However, based on the literature review, there is some consensus that the region will see more frequent and more extreme storms. This would typically translate to larger flood events in the small, urban Valley Creek Basin, as flooding in the basin is strongly driven by short-duration extreme precipitation events. However, a combination of increasing temperatures in the region as well as a shift in the time of year in which the extreme precipitation events have occurred could be responsible for offsetting increases in peak streamflow to some degree. It is unclear if the shift in extreme precipitation events to the dry season is an anomaly or a consistent trend that will continue in the region. Furthermore, additional analysis on the hydrologic response would be needed to determine if this seasonal change was the driver of the decrease in annual peak streamflow. Based on the lack of clear evidence showing an increase in streamflow, the effects of climate change can be considered within the standard uncertainty bounds associated with the hydrologic/hydraulic analysis being conducted as part of this study.

7.0 Summary

This appendix details the engineering analysis required to support the Valley Creek FRM study initiated in 2018, which covered approximately 20 miles of Valley Creek (a Black Warrior River tributary located in the Valley Creek Basin and in Jefferson County, AL) and several pertinent tributaries within the city limits of Birmingham, AL and Bessemer, AL as well as several other municipalities. The study basin is subject to frequent flooding, driven by intense rainfall, and poor hydrologic conditions including significant impervious area and direct run-off connectivity. Federal interest was driven by dense development throughout study reach corridors subject to economic damage and life safety risks from fluvial flooding.

Hydrologic and hydraulic models were developed and calibrated for existing conditions and utilized to forecast synthetic 0.50, 0.20, 0.10, 0.04, 0.02, 0.01, 0.005, and 0.002 AEP flood events with consideration of FWOP conditions. Future basin conditions were based on local stormwater management information and land-use forecasts driven by national climate and land-use scenarios. To support flood risk management within the study basin, a total of 35 measures were developed from which a screened array of 17 measures was derived. Using these measures, 16 structural FRM plans were formulated. Economic modeling for derivation of benefits associated with the plans was completed for all 16 plans as well as 4 individual measures. Ultimately, a total of 13 alternatives (including 8 structural, 2 non-structural, and 3 combined structural/non-structural) were considered for selection of the recommended plan.

A structural plan was identified as the NED plan, and selected as the recommended plan. This structural plan includes 2 overbank detention basins, has an estimated first cost of $31,469,000, estimated annual operations and maintenance costs of $50,000, and produces mean annual net benefits of $939,000 (BCR of 1.66). The benefits of the recommended plan were quantified and provided on a structural basis. Additionally, risk (residual and incremental) associated with implementation of the recommended plan was analyzed with respect to USACE guidance. The hazard analysis considered life, infrastructure, and environmental safety, and was supported by hydraulic and life safety models. Results showed that the project's hazard potential should be considered low. Additionally, this assessment showed that the expected probability for overtopping of basin levees and/or observing incremental risk in areas adjacent to the measure locations is not likely to increase based on model sensitivity. Furthermore, the AEPs associated with observed benefits are unlikely to decrease based on model sensitivity. Climate change assessments of the study basin and the recommended plan were completed with data ultimately suggesting that increases to peak streamflow are unlikely, despite the regional consensus that frequency and severity of storms will increase.

References

Abt, S. R., Leech, J. R., Thornton, C. I., and Lipscomb, C. M., 2001. Articulated concrete block stability testing. J. Am. Water Resources Assoc., 37(1), 27–34.

ASTM International, 2018. D1586/D1586M-18 Standard Test Method for Standard Penetration Test (SPT) and Split-Barrel Sampling of Soils.

ASTM International, 2014. D2113-14 Standard Practice for Rock Core Drilling and Sampling of Rock for Site Exploration.

Atlantic, 2013. Aerial Lidar Report: Jefferson County, Alabama. *Atlantic Group, LLC.*

Burkham, D.E., and Dawdy, D.R., 1976. Resistance equation for alluvial-channel flow: Proceedings American Society of Civil Engineers, Journal of the Hydraulic Division. v. 102. no. HY10.

Carter, R.W., and Davidian, J., 1968. General Procedure for Gaging Streams. Techniques of Water-Resources Investigations of the United Stated Geological Survey. Chapter A6. Book 3: Applications of Hydraulics. *U.S. Geological Survey.*

Center for Watershed Protection (CWP), Unified Stream Assessment: A User's Manual, Ellicott City, MD: CWP, 2004), chapter 3.

Champion, J. EEFS Company. Personal communication via email. 28 May 2019.

Chow, V.T., 1959, Open-channel hydraulics: New York, McGraw-Hill, 680 p.

Clopper, P. E., 1989. Hydraulic stability of articulated concrete block revetment systems during overtopping flow. Rep. No. FHWA-RD-89-199, Federal Highway Administration, McLean, VA.

Clopper, P. E., 1991. Protecting embankment dams with concrete block systems. Hydro Rev.10 (2): 54–67

Cowan, W.L., 1956. Estimating hydraulic roughness coefficients. Agricultural Engineering, 37(7).

Cox, A. L., Thornton, C.I., Abt, S.R., 2014. Articulated Concrete Block Stability Assessment for Embankment-Overtopping Conditions. Journal of Hydraulic Engineering, 104(5) American Society of Civil Engineers.

Cox, A. L., Thornton, C.I., Abt, S.R., 2019. Articulated Concrete Block Stability Assessment for Channelized Flow. Journal of Hydraulic Engineering, 145(4) American Society of Civil Engineers.

Dai, Z., Amatya, D.M., Sun, G., Trettin, C.C., Li, C., Li, H. (2011) Climate variability and its impact on forest hydrology on South Carolina coastal plain, USA. Atmosphere 2, 330-357.

Edelen, G. W. Jr., Wlison, K.V., Harkins, J.R., Miller, J.F., and Chin, E. H. 1986. Floods of April 1979, Mississippi, Alabama, and Georgia. Survey Professional Paper 1319. *U.S. Geological Survey and the National Oceanic and Atmospheric Administration.*

England et al., 2017. Guidelines for Determining Flood Flow Frequency Bulletin 17C. Ch. 5. Sec. B, Surface Water. Book 4, Hydrologic Analysis and Interpretation. *U.S. Geological Survey.*

EPA, 2014. Estimating Change in Impervious Area (IA) and Directly Connected Impervious Areas (DCIA) for New Hampshire Small MS4 Permit.

EPA, 2017. Updates to the Demographic and Spatial Allocation Models to Produce Integrated Climate and Land-Use Scenarios (ICLUS). Version 2. Environmental Protection Agency. January.

FEMA, 2019. Effective Flood Insurance Study. Jefferson County, Alabama. 01073CV003C.

FHWA, 1979. Design of Urban Highway Drainage, The State of the Art. *Federal Highway Administration.*

Freeman, F. City of Bessemer. Personal communication: USACE FRM Planning Charette. 6 November 2018.

Fry, J., Xian, G., Jin, S., Dewitz, J., Homer, C., Yang, L., Barnes, C., Herold, N., and Wickham, J., 2011. Completion of the 2006 National Land Cover Database for the Conterminous United States, *PE&RS*, Vol. 77(9):858-864.

Fuguitt D., S.J. Wilcox. 1999. Cost-benefit analysis for public sector decision makers. Quorum Books, Westport, CT

Gilbert, R. EEFS Company. Personal communication via email. 6 December 2018.

Hains, C.F., 1973, Floods in Alabama, magnitude and frequency: Alabama Highway Department Special Report, 174 p.

Hedgecock, T.S., and Feaster, T.D., 2007. Magnitude and Frequency of Floods in Alabama, 2003. *U.S. Geological Survey*.

Hedgecock, T.S., and Lee, K.G., 2010. Magnitude and Frequency of Floods for Urban Streams in Alabama, 2007. *U.S. Geological Survey*.

Heidemann, H.K. 2018. Lidar Base Specification. Chapter 4 of Section B, U.S. Geological Survey Standards. Book 11, Collection and Delineation of Spatial Data. *Geological Survey. U.S. Department of the Interior.* v. 1.3. February 2018.

Hewlett, H. W. M., L. A. Borman, and M. E. Bramley. 1987.Design of reinforced grass waterways. Rep. No. 116. London: Construction Industry Research and Information Association.

Hicks, D.M., and Mason, P.D., 1998. Roughness characteristics of New Zealand rivers: National Institute of Water and Atmospheric Research Ltd., Water Resources Publications, LLC, 329 p.

Homer, C.G., Dewitz, J.A., Yang, L., Jin, S., Danielson, P., Xian, G., Coulston, J., Herold, N.D., Wickham, J.D., and Megown, K., 2015, Completion of the 2011 National Land Cover Database for the conterminous United States-Representing a decade of land cover change information. *Photogrammetric Engineering and Remote Sensing*, v. 81, no. 5, p. 345-354.

ICLUS, 2017a. Integrated Climate and Land-Use Scenarios. ICLUS v2.1 Land Use Projections (SSP2 and SSP5). *Environmental Protection Agency.*

ICLUS, 2017b. Integrated Climate and Land-Use Scenarios. ICLUS v2.1 Percent Impervious Surface Projections (A1, A2, B1, and B2). *Environmental Protection Agency.*

Kenney, T.A., 2010. Levels at Gaging Stations. Techniques and Methods 3-A19. *U.S. Geological Survey.*

Konrad, C.E. II and Perry L.B., 2010. Relationships between tropical cyclones and heavy rainfall in the Carolina region of the USA. Int. J. Climatol.30: 522 – 534 (2010).

Laseter, S.H., Ford, C.R., Vose, J.M., Swift, L.W. (2012) Long-term temperature and precipitation trends at the Coweeta Hydrologic Laboratory, Otto, North Carolina, USA. Hydrology Research 43, 890-901.

Lewis, C. and Barto, T., 2020. Technical Manual for Levee, Appendix 3.1.4: Application of Simplified Physical Breach Method in HEC-RAS. Modeling Mapping and Consequence Production Center. *U.S. Army Corps of Engineers.*

Li, W., Li, L., Fu, R., Deng, Y., Wang, H., 2011. Changes to the North Atlantic subtropical high and its role in the intensification of summer rainfall variability in the southeastern United States. Journal of Climate 24:1499-1506.

Li, X. Yan, D., Wang, K., Weng, B., Qin, T., Liu, S., 2019. Flood Risk Assessment of Global Watersheds Based on Multiple Machine Learning Models. *MDPI: Water* 2019, 11, 1654.

Liu Y, Goodrick SL, Stanturf JA (2013) Future U.S. wildfire potential trends projected using a dynamically downscaled climate change scenario. Forest Ecology and Management 294:120-135.

Lexington-Fayette Urban County Government (LFUCG), 2009. *Lexington-Fayette Urban County Government Stormwater Manual*.

Merkel, W.H., Moody, H.F., Quan, Q.D. 2015. Design Rainfall Distributions based on NOAA Atlas 14 Rainfall Depths and Durations. *Natural Resources Conservation Service.*

Municipality SWMPs, 2019. Storm Water Management Plans for Birmingham, Bessemer, Midfield, Brighton, and Hueytown. Personal Correspondence with the City of Bessemer and City of Birmingham. January 2019.

NOAA, 2013. Atlas 14: Precipitation-Frequency Atlas of the United States. Vol. 9 Version 2.0: Southeastern States. *National Oceanic and Atmospheric Administration.*

NRCS, 1986. Urban Hydrology for Small Watersheds. Technical Report 55. *Natural Resources Conservation Service.* June 1986.

NWS Birmingham Southeastern Forecast Office. n.d. Remnants of Tropical Storm Lee – September 4-6, 2011. *National Weather Service.* https://www.weather.gov/bmx/event_lee2011.

O'Leary, T.M., 2018. Semi-Quantitative Risk Calculation Methodology. RMC-TN-2018-01. *Army Corps of Engineers.*

O'Neill, B.C., Kriegler, E., Ebi, K.L., Kemp-Benedict, E., Riahi, K., Rothman, D.S., van Ruijven, B.J., van Vuuren, D.P., Birkmann, J., Kok, K., Levy, M., Solecki, W., 2016a. The roads ahead: narratives for Shared Socioeconomic Pathways describing world futures in the 21st century. Global Environ. Change.

Patterson, L.A., Lutz, B., Doyle, M.W. (2012) Streamflow Changes in the South Atlantic, United States During the Mid- and Late 20th Century. Journal of the American Water Resources Association 48, 1126-1138.

Public Law 113-121, 2014. Water Resources Reform and Development Act of 2014. 128 Stat. 1193. *113th United States Congress.*

Rouse, H., 1965. Critical analysis of open-channel resistance. Journal of Hydraulic Engineering, American Society of Civil Engineers, v. 91, no. 4, p. 1–25.

Sauer, V.B., 1986. New Studies of Urban Flood Frequency in the Southeastern United States. Transportation Research Record 1073. *U.S. Geological Survey.*

Sauer, V.B., and Turnipseed, D.P., 2010. Stage Measurement at Gaging Stations. Techniques and Methods 3-A7. *U.S. Geological Survey.*

Soil Survey Staff, Natural Resources Conservation Service, *United States Department of Agriculture.* Soil Survey Geographic (SSURGO) Database for Valley Creek Basin, Alabama. Accessed 2019.

Stricklin, V. USGS. Personal communication via email. 21 September 2018.

Sutherland, R. C. (1995). "Methodology for estimating the effective impervious area of urban watersheds." *Watershed Protection Techniques*, *2*(1), 282-284.

USACE, 1980. Flood Damage Reduction Measures in Urban Areas. Engineer Regulation ER 1165-2-21. *U.S. Army Corps of Engineers.*

USACE, 1986. Warrior River and Tributaries Interim Reconnaissance Report, Valley Creek, Jefferson Co., AL. *U.S. Army Corps of Engineers, Mobile District.* January.

USACE, 1996a. Risk-based analysis for evaluation of hydrology/hydraulics, geotechnical stability, and economics in flood damage reduction studies. Engineer Regulation ER 1105-2-101. US Army Corps of Engineers, Washington, DC

USACE, 1996b. Risk-based analysis for flood damage reduction studies. Engineer Manual EM 1110-2-1619. US Army Corps of Engineers, Washington, DC USACE (US Army Corps of Engineers). 1998. HEC-FDA flood damage reduction analysis: User's manual, Version 1.0. CPD-72. US Army Corps of Engineers, Davis, CA

USACE, 1999. Engineering and Design for Civil Works Projects. Engineer Regulation ER 1110-2-1150.

USACE, 2000. Design and Construction of Levees. Engineer Manual EM 1110-2-1913. *U.S. Army Corps of Engineers.*

USACE, 2003. Slope Stability. Engineer Manual EM 1110-2-1902. *U.S. Army Corps of Engineers.*

USACE, 2014. Safety of Dams – Policy and Procedures. Engineer Regulation ER 1110-2-1156. *U.S. Army Corps of Engineers.*

USACE, 2015a. Planning Bulletin 2016-01. *U.S. Army Corps of Engineers.*

USACE, 2015b. Recent US Climate Change and Hydrology Literature Applicable to US Army Corps of Engineers Missions –South Atlantic-Gulf Region 03. Civil Works Technical Report, CWTS 2015-03, USACE, Washington, DC

USACE, 2016. Engineering and Construction Bulletin: Guidance for Incorporating Climate Change Impacts to Inland Hydrology in Civil Works Studies, Designs, and Projects. ECB 2016-25. *U.S. Army Corps of Engineers.*

USACE, 2017a. Flood Risk Management Draft Feasibility Report, Village Creek, Jefferson Co., AL. *U.S. Army Corps of Engineers, Mobile District.*

USACE, 2017b. Engineering Technical Letter; Guidance for Detection of Nonstationarities in Annual Maximum Discharges. ETL 1100-2-3. *U.S. Army Corps of Engineers.*

USACE, 2018. Engineering and Construction Bulletin: Guidance for Incorporating Climate Change Impacts to Inland Hydrology in Civil Works Studies, Designs, and Projects. ECB 2018-14. *U.S. Army Corps of Engineers.*

USACE, 2019a. Engineering and Construction Bulletin: Interim Approach for Risk-Informed Designs for Dam and Levee Projects. ECB2019-15. *U.S. Army Corps of Engineers.*

USACE, 2019b. Engineer Regulation: Risk Assessment for Flood Risk Management Studies. ER 1105-2-101. *U.S. Army Corps of Engineers.*

USGCRP, 2017: Climate Science Special Report: Fourth National Climate Assessment, Volume I [Wuebbles, D.J., D.W. Fahey, K.A. Hibbard, D.J. Dokken, B.C. Stewart, and T.K. Maycock (eds.)]. U.S. Global Change Research Program, Washington, DC, USA, 470 pp., doi: 10.7930/J0J964J6.

USGS, 2017. StreamStats Version 4. Web. 18 December 2017.

Von Thun, Lawrence, J., and Gillete, D.R., 1990. Guidance on Breach Parameters, unpublished internal document. *U.S. Bureau of Reclamation.* Denver, Colorado 17 p.

Wang H, Schubert S, Suarez M, Chen J, Hoerling M, Kumar A, Pegion P (2009) Attribution of the seasonality and regionality in climate trends over the United States during 1950-2000. Journal of Climate 22:2571-2590.

Wang, H., Killick, R., Fu, X., 2013. Distributional change of monthly precipitation due to climate change: Comprehensive examination of dataset in southeastern United States. Hydrological Processes, in press.

Watershed Management Institute (WMI), 1997. Operation, Maintenance, and Management of Stormwater Management Systems. Prepared for U.S. Environmental Protection Agency, Office of Water. Washington, DC.

Wibowo, Johannes. 2016. Estimating Levee Erosion Widening Rates (Draft). *Engineering Research and Development Center–U.S. Army Corps of Engineers.*

Xian, G., Homer, C., Dewitz, J., Fry, J., Hossain, N., and Wickham, J., 2011. The change of impervious surface area between 2001 and 2006 in the conterminous United States. *Photogrammetric Engineering and Remote Sensing*, Vol. 77(8): 758-762.

Yen, B.C. 1991. Hydraulic resistance in open channels, in Yen, B.C., ed., Channel flow: centennial of Manning's formula: Water Resources Publications, Littleton, Colo. p. 1–135.